A Proteomic and Functional Study of the *Schistosoma mansoni* Egg

William Mathieson

Submitted for the Degree
of
Doctor of Philosophy

The University of York
Department of Biology

September 2007

Abstract

Newly released eggs of the parasitic worm *Schistosoma mansoni* either pass through the gut wall to escape from the host or are washed away in the host's bloodstream. In the latter scenario most eggs become lodged in the host's liver, where they become the focus of a granulomatous response which can have severe pathological consequences. In this study, the *S. mansoni* soluble egg proteome is described and characterised for the first time. Mature eggs were separated from immature eggs and then fractionated into their morphological components: the miracidia, the hatch fluid (which bathes the miracidia) and the egg-secreted proteins. Each egg preparation was subjected to two-dimensional electrophoresis and tandem mass spectrometry. Developmental proteomic changes were then described in terms of the egg's morphology so insights into the egg's natural history were gained. For example, acquisition of aerobic respiratory enzymes by the miracidium was seen, but nevertheless the miracidium still favours the use of energy-efficient heat shock proteins. Western blotting was used to show that the immature egg adopts the ubiquitin-proteasome pathway to degrade its nutritive vitelline cells. The hatch fluid contains host proteins but it also has a defensive role, although its most abundant constituent (a large, acidic glycoprotein) is of unknown function. The egg-secreted proteins consist of different variants of just four proteins, one of which has a pro-protein convertase domain and another of which appears to be a general purpose binding protein. A protocol is devised to purify each variant, so further functional studies into the individual secreted proteins can be carried out in the future. The secreted proteins induce a profound proliferative response in lymphocytes from acutely infected mice, indicating that they may work by activating granuloma T cells to secrete pro-proteases that are subsequently activated, enabling the egg to cross the gut wall.

Contents

List of Figures and Tables

Acknowledgements

I would like to extend my thanks to the following people who were generous with their time and help:

Dr. Peter Ashton for his help with the laboratory work early in the project and later for his assistance with the bioinformatics.

Dr. Jared Cartright for teaching me HPLC.

Dr. William Castro-Borges for his help with the work on the ubiquitin-proteasome pathway.

Dr. Rachel Curwen for her help with the proteomics.

Dr. Adrian Mountford for his help with the immunological aspects of the project and also for his role as a member of my Training Committee.

Prof. Jenny Southgate for her role as a member of my Training Committee.

All members of the Schistosome Research Group, whether past or present.

I would especially like to thank Alan for his input, guidance and enthusiasm throughout the project.

On a personal level I would like to thank my friends and family, particularly Stella, whose support made it all possible.

Author's Declaration

I declare that all of the work in this thesis is my own, with the following exceptions:

The illustration of the female reproductive system (Figure 1.1) is from Spence & Silk (1971).

The transmission electron micrographs of the egg (Figure 1.2) were taken from Neill *et al.*, (1988).

The illustration of the possible fragmentation points of a peptide (Figure 1.3) is from Johnson *et al.*, (1987).

The gel illustrating the ESP nomenclature (Figure 2.1) is taken from Ashton (2001).

The gel-image of the 20S proteasome subunits of *S. mansoni* (Figure 4.2) is from Castro-Borges *et al.*, (2007).

The perfusion of mice (described in Section 2.2.6) was carried out by Dr. William Borges

The cercarial secreted protein preparation used in Figure 4.5C was a gift from Dr. Rachel Curwen.

The proteomic data relating to *Mesocricetus auratus* albumin (Chapter 2, Section 2.3.6 and Appendix 2) has already been published (DeMarco *et al.*, 2007), as has the gel of ESP in Figure 2.7 of Chapter 2 (Jang-Lee *et al.*, 2007).

Abbreviations used in the text

1-DE	one-dimensional electrophoresis
2-DE	two-dimensional electrophoresis
AAA	agarose-bound *Aleuria aurantia* lectin
ACN	acetonitrile
ADAM	A disintegrin and metalloproteases
ADAMT	A disintegrin and metalloproteases with thrombospondin domains
APC	antigen presenting cell
ATP	adenosine triphosphate
BSA	bovine serum albumin
CD	cluster of differentiation
CEF	Cation Exchange Fractions
CHIP	C-terminus of HSP70-interacting protein
Con A	concanavalin-A
cpm	counts per minute
cv	column-volumes
DC	dendritic cell
DC-SIGN	DC-specific intercellular adhesion molecule 3-grabbing nonintegrin
dd H_2O	doubly-distilled water
DTT	dithiothreitol
ECL	Enhanced Chemiluminescent
EDTA	Ethylene Diamine Tetraacetic Acid
ELISA	Enzyme-Linked ImmunoSorbent Assay
ER	endoplasmic reticulum
ERAD	endoplasmic reticulum-associated degradation
ESP(s)	Egg Secreted Protein(s)
FCS	foetal calf serum
FRET	fluorescence resonance energy transfer
HPLC	high performance liquid chromatography

HSP	heat shock protein
IEF	isoelectric focussing
IFN	interferon
IL	interleukin
IPG	immobilized pH gradient
IPSE	Interleukin-4-inducing principle of *S. mansoni* eggs
LPS	lipopolysaccharide
MALDI	matrix-assisted laser desorption-ionisation
MHC	Major Histocompatibility Complex
MMP	matrix metalloproteinase
MS	mass spectrometry
MSMS	tandem mass spectrometry
MSA	Major Serologic Antigen
m/z	mass to charge ratio
PAGE	polyacrylamide gel electrophoresis
PBS	phosphate buffered saline
PCR	polymerase chain reaction
PEC	peritoneal exudate cells
pI	isoelectric point
PI	propidium iodide
PIC	protease inhibitor cocktail (Sigma P1860)
PMA	phorbitol 12-myristate 13 acetate
PMB	polymyxin B
PMF	peptide mass fingerprint
PRR	pattern-recognition receptor
RT-PCR	reverse transcription-polymerase chain reaction
PVDF	polyvinylidenefluoride
SDS	sodium dodecyl sulphate
SEA	Soluble Egg Antigen
sHSP	small Heat Shock Protein
SmCKBP	*S. mansoni* chemokine binding protein (also ESP 3-6)
SmEP25	*S. mansoni* egg protein of 25kDa (also ESP 3-6)

SmPEPCK	*S. mansoni* phosphoenolpyruvate carboxykinase (also ESP 3-6)
Sm-TPx	*S. mansoni* thioredoxin peroxidase
TCA	tricarboxylic acid
TEM	transmission electron microscopy
TFA	trifluoroacetic acid
Th	T-helper
TNF	tumour necrosis factor
ToF	time of flight
TLR	toll-like receptor
UPP	ubiquitin-proteasome pathway
WHO	World Health Organisation

Chapter 1

General Introduction

Part 1: Schistosomiasis and *Schistosoma mansoni*

1.1.1 Disease Burden

Schistosomiasis is a tropical parasitic disease caused by trematode worms of the genus *Schistosoma*. Five species of schistosomes infect man (*S. mansoni*, *S. haematobium*, *S. japonicum*, *S. intercalatum* and *S. mekongi*), but *S. mansoni*, *S. haematobium* and *S. japonicum* account for the vast majority of infections. It is one of the world's most prevalent diseases, infecting over 200 million people, most of whom live in sub-Saharan Africa (WHO, 2002).

The impact of schistosomiasis has been assessed in terms of its public health burden at 4.5 million disability-adjusted life years (WHO, 2002). This was calculated by applying a "disability weighting" factor to the estimated prevalence of infection. The disability weighting was too low however, because its criteria did not include clinical sequelae - only the mortality directly attributable to schistosomiasis. An attempt was therefore made to better quantify the relationship between the clinical morbidity of schistosomiasis and the prevalence and intensity of infection (Van der Werf *et al.*, 2003). The Van der Werf study concluded that 245 million people in sub-Saharan Africa had clinical symptoms that were consistent with a schistosome infection, 166 million were definitely infected and 280,000 deaths per year were attributable to this disease.

The paper by Van der Werf *et al.*, (2003) was restricted in its geographical remit and didn't take more subtle morbidities into account, so the disability weighting factor for schistosomiasis was recalculated on a worldwide basis and included factors such as nutritional impairment and reduced working productivity (King *et al.*, 2005). In King *et al.*, (2005), meta-analysis of the data from 135 earlier papers was carried out and it was concluded that the disability weighting needed to be drastically increased from the WHO estimate of 0.5% to between 2 and 15%. Although the overall disease burden of schistosomiasis is clearly underestimated, the true impact of the disease is still unknown. It cannot be assessed because it is very difficult to tease apart the pathological consequences

of schistosomiasis from other concurrent factors that are prejudicial to health, such as access to a safe water supply and co-infections.

1.1.2 The Schistosome Life Cycle

Schistosomes infect two hosts during their life cycle - a mammalian definitive host and an aquatic snail intermediate host. For the snail to become infected it must be penetrated by a free-swimming miracidium. A period of asexual reproduction occurs in the snail (reviewed in Jourdane & Theron, 1987). Each miracidium transforms into a mother sporocyst, within which germinal cells multiply to produce many daughter sporocysts. Further replication occurs in each of these daughter sporocysts to produce germ balls, each of which develops into a cercaria. Thousands of free-living cercariae emerge from the snail each day on stimulation by light, most of which die, but those that are able to locate a suitable mammalian host penetrate it.

The infection of and migration in the definitive host has been reviewed (e.g. see Wilson, 1987). Penetration of the host skin is achieved by a combination of muscular contractions and the secretion of cercarial proteases from three sets of glands contained within the cercarial body. After penetration, the cercaria migrates through to the base of the epidermis within 30 minutes, losing its glycocalyx and tail as it transforms into a schistosomulum. The epidermal basement membrane appears to impede the progress of the parasite, because there is a delay of hours/days before it enters the vasculature, through which it migrates to reach the lungs. Here it elongates (presumably to traverse the lung capillaries) and continues its migration (via the heart) until it arrives in the hepatic portal vasculature. The transit time of this migration depends upon the host and how many circuits of the vasculature are required, but in the mouse model parasites are accumulating in the hepatic portal system 6 – 21 days after skin penetration. Once established in the hepatic portal system the schistosomulum differentiates into a blood-feeding form. It matures, pairs and then the paired worms migrate (against the blood flow) to their final location in the host. The final location is the veins of the gut wall in *S. mansoni* and *S. japonicum* infections or the veins of the bladder wall in the case of *S. haematobium.*

Eggs are then released by the female, some of which penetrate the venous endothelium, cross the gut wall (or bladder wall in *S. haematobium* infections) to be voided with the faeces (or urine). If an egg emerges into fresh water it hatches and a single, motile miracidium emerges. The miracidium will actively seek out a suitable snail, penetrate it and thereby complete the life cycle. Only a proportion of the eggs are voided form the host in this way. Many are washed away by the blood stream to become lodged in other organs (particularly the liver) where they can induce an inappropriate host immune response. It is this immune response to trapped eggs that is responsible for the most severe forms of pathology.

1.1.3 The Pathogenesis in *S. mansoni* Infections

Schistosomiasis mansoni manifests itself in humans as a generally non-specific complex of acute and chronic sequelae, usually involving the gastrointestinal tract and liver. Although penetration of the skin by cercariae can cause dermatitis (Gonzalez, 1989), the initial onset of pathogenesis usually corresponds with parasite migration and the start of egg deposition. Also termed acute schistosomiasis or Katayama fever, these symptoms are generally a feature of individuals who have had no previous exposure to schistosomiasis. Acute schistosomiasis is caused by the immune system responding to worm and/or egg antigens, and produces a myriad of sequelae including fever, sweating, headache, cough, myalgia, lymphadenopathy, hepatomegaly, diarrhoea and blood in the stool (Rabello, 1995).

The pathology associated with chronic infection manifests itself some time after the worms have become established. It is caused by the ongoing deposition of eggs that induce cellular foci and can lead to further complications, ranging in severity from scattered granulomata to gross hepatic periportal fibrosis. Clinical features are restricted to a small proportion of infected individuals and can include blood in the stool, diarrhoea, cramps and secondary symptoms such as cachexia (Savioli *et al.*, 2004).

Although egg-induced granulomata can occur in any part of the intestinal tract (Cheever *et al.*, 1977), the major complication in chronic infection is periportal hepatic fibrosis. This occurs when eggs become lodged in the venules of the liver, initially causing cellular

infiltration and the formation of a granuloma. The granulomatous infiltration can spread to the connective tissue, causing the affected portal tracts to become distorted by inflammation and fibrosis, leading to portal enlargement and hypertension (Andrade, 2004). Hepatic fibrosis results from an increase in cellular, cytokine-induced collagen production, probably in conjunction with a reduction/imbalance in the secretion of matrix metalloproteases (Boros & Whitfield, 1999; Singh *et al.*, 2004). Over time, portal hypertension can induce gastro-oesophageal varices which can haemorrhage, causing potentially fatal haematemesis.

1.1.4 The *S. mansoni* Egg and the Immunopathology of the Granuloma

A proportion of the eggs released by the female worms in the mesenteric vasculature are washed away by the blood stream. They travel along the superior or inferior mesenteric veins (depending upon whether the worm is located in the small or large intestine respectively). The inferior mesenteric vein and the superior mesenteric vein join, forming the hepatic portal vein, and from here it is a short distance to the liver. The liver sinusoids are smaller than the eggs, so the vast majority of incoming eggs become lodged in the pre-sinusoidal vessels, where they form the foci around which the granulomata develop.

The granuloma is the cellular response to the lodged egg, principally comprising $CD4^+$ T cells, macrophages and eosinophils (Iacomini *et al.*, 1995; Warren & Domingo, 1970; Swartz *et al.*, 2006). The $CD4^+$ cells comprise both Th2 (T-helper) cells (capable of secreting interleukin (IL)-4, IL-5, IL-10 and IL-13) as well as a smaller proportion of $CD25^+CD4^+$ regulatory T cells that are capable of ameliorating cytokine production (Hesse *et al.*, 2004; Baumgart *et al.*, 2006). The Th2 response generated by the $CD4^+$ cells of the granuloma is in stark contrast to the Th1 response that dominated the infection up to this point, and its induction results in a more balanced and mixed Th1/Th2 response overall (Pearce *et al.*, 1991). In the murine model, granulomata appear about two weeks after egg production commences, peaking in size 2-4 weeks later and then declining in an IL-10-dependent manner during chronic infection (Boros *et al.*, 1975; Sadler *et al.*, 2003). This pattern of a peak followed by a down-modulation is mirrored by the levels of cytokine production and proliferative capabilities of granuloma cells when stimulated with egg antigen (King, 2001).

The Th2 response to egg deposition is IL-4-dependent and has a host-protective function. In the mouse model, 20% of $CD4^+$ cells in the lymph nodes that are closest to the site of egg deposition expressed the IL-4 gene 7-days after the injection of eggs (Taylor *et al.*, 2006a). A Th2 response fails to develop in IL-4 knockout mice, resulting in increased iNOS and O_2^- expression in the liver, causing an inhibition of hepatocyte proliferation, smaller granulomata, a failure of the liver to enlarge, leading eventually to cachexia and death (La Flamme *et al.*, 2001; Brunet *et al.*, 1997). In T-cell deficient mice granulomata fail to develop and fatal hepatotoxic reactions to egg proteins occur (Doenhoff *et al.*, 1981). It is therefore possible that by encapsulating the egg, the cells of the granuloma may be protecting the host by providing a physical barrier to localise hepatotoxic egg proteins prior to their detoxification. Balanced against these beneficial effects however is the pathological consequences of IL-13-induced collagen production as discussed in 1.1.3.

There is no doubt that *S. mansoni* eggs can cause the pronounced Th2 response in the host because it is induced when live or dead eggs are injected via the intravenous, intraperitoneal or subcutaneous route (Pearce & MacDonald, 2002). Attempts to identify the egg antigens responsible for the Th2 induction indicate that glycans and lipids may be important. Deglycosylated egg antigens fail to induce a Th2 response, whilst unglycosylated, non-schistosome proteins modified with the schistosome egg glycan lacto-*N*-fucopentose III (LNFPIII) do (Okano *et al.*, 1999; Okano *et al.*, 2001). The *S. mansoni* egg version of the lipid lysophosphatidylserine can activate Toll-like receptor 2 (TLR 2) in dendritic cells (DCs), which in turn can induce the development of $CD25^+CD4^+$ T regulatory cells, whose secretory IL-10 potentially could induce hyporesponsiveness to the existing Th1 response (Van der Kleij *et al.*, 2002). The TLR 2-activating motif of the *S. mansoni* lysophosphatidylserine appears to relate to the structure of the acyl group in its (uniquely single) tail as well as the phosphoserine head group.

The mechanism that causes the general down-regulation of the granulomatous response when the infection becomes chronic is unknown, but it correlates with the reduced expression of CD80/CD86 co-stimulatory molecules on macrophages/DCs, prostaglandins and increases in the concentration of IL-10 and the soluble IL-13R (Rathore *et al.*, 1996;

Chensue *et al.*, 1983; Mentink-Kane *et al.*, 2004; Sadler *et al.*, 2003). IL-10 can control the growth and differentiation of several effector cells via different mechanisms and so is the prime contender for inducing hyporesponsiveness. It can inhibit the ability of antigen presenting cells to interact with both Th1 and Th2 $CD4^+$ cells by down-regulating both the Major Histocompatibility Complex II (MHCII) and its co-stimulatory molecules CD80 and CD86 (de Waal Malefyt *et al.*, 1991; Flores Villanueva *et al.*, 1994).

Part 2: The *S. mansoni* Egg: Development to Escape/Sequestration

1.2.1 The Female Reproductive System and the Development of the Egg

Both the ovum and its nutrients are produced in the ovary in most animals. Trematodes differ fundamentally in that the nutrient-containing vitelline cells are produced in an entirely separate organ called the vitellaria (Smyth & Halton, 1983). The reproductive system of the female schistosome must therefore be capable of packaging the oocyte and vitelline cells together. Studies utilizing transmission electron microscopy (TEM) and confocal laser scanning microscopy have been able to explain how this happens, and show how glandular secretions, physical moulding and sperm form the male are used in egg production (Spence & Silk, 1971; Erasmus, 1973; Neves *et al.*, 2005).

A diagram of the female *S. mansoni* reproductive tract is reproduced overleaf as Figure 1.1, and it can be seen that in terms of volume, the vitellaria are by far the largest of the reproductive organs, occupying the posterior two thirds of the worm. The vitellaria consist of a single vitelline duct from which many much smaller ducts are linked to numerous vitelline follicles. These vitelline follicles produce the vitelline cells, which enter the vitelline duct once they have fully developed. There are four maturational stages in the development of a vitelline cell (Erasmus, 1975). Stage 1 consists of a small, undifferentiated cell, containing ribosomes and a nucleus. The endoplasmic reticulum appears in Stage 2 and Golgi complexes in Stage 3. Abundant protein synthesis is now apparent and vitelline droplets are starting to form in the cytosol, having budded from the Golgi. The vitelline droplets consist of membrane bound vesicles, inside which are many

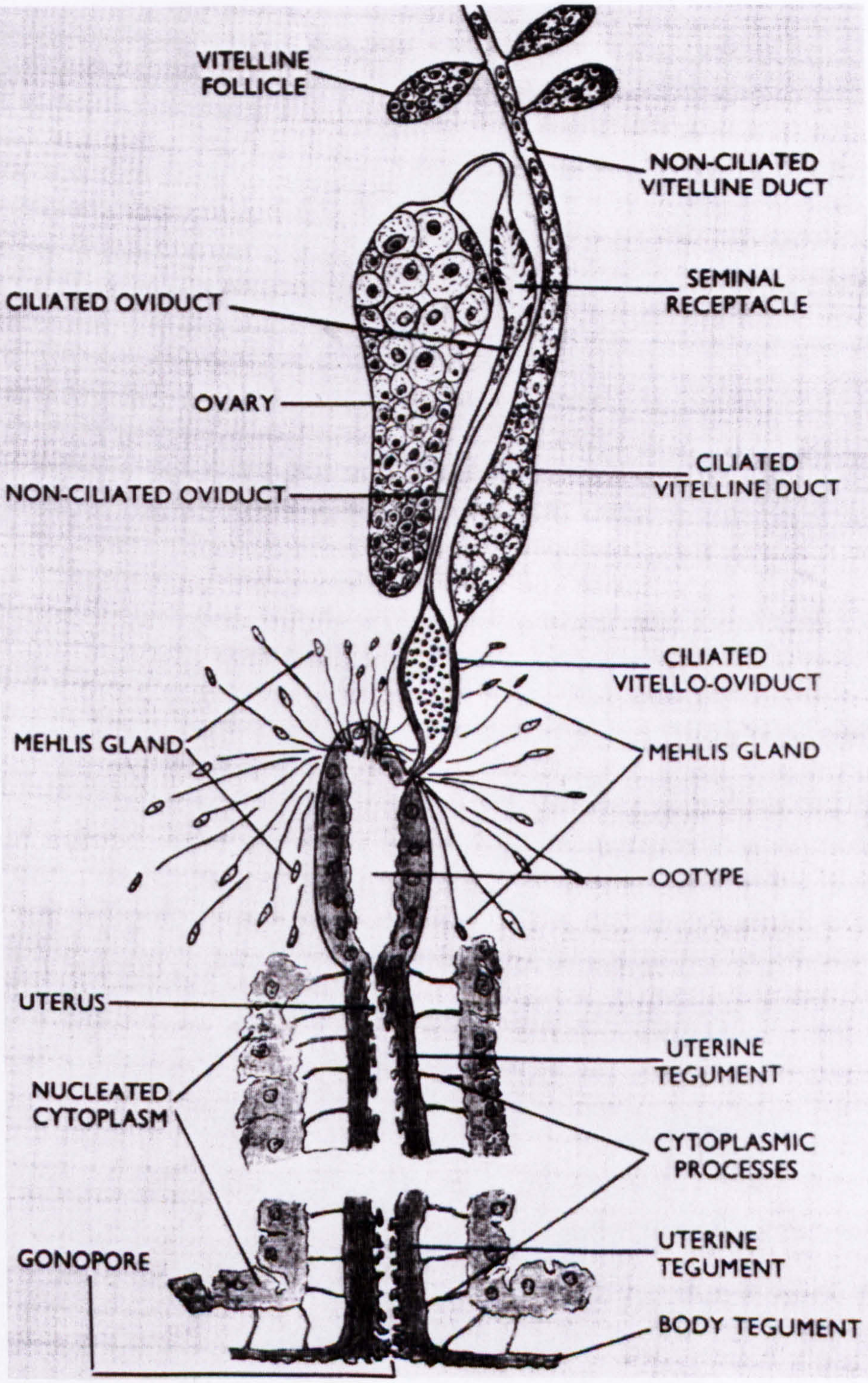

Figure 1.1 The female reproductive system (from Spence & Silk, 1971). The vitellaria at the top of the diagram (comprising vitelline follicles and the non-ciliated vitelline duct) occupy the posterior two-thirds of the worm.

electron-dense granules that contain eggshell precursor proteins (Erasmus, 1973; Cordingley, 1987; Koster *et al.*, 1988; Wells & Cordingley, 1991). Stage 4 vitelline cells are fully mature, with larger vitelline droplets and abundant lipid material (Erasmus, 1975).

The vitellaria have a high production rate, so it is not surprising that they occupy such a large proportion of the volume of the female worm. Each egg contains 30-40 vitelline cells (Erasmus, 1987), and if (as discussed below) a female worm produces 300 eggs per day, it can be calculated that the vitellaria must produce 9,000 - 12,000 cells per day (i.e. 6 - 8 cells/minute). Once mature, the vitelline cells pass along the vitelline duct towards the anterior of the worm, where the vitelline duct narrows to form a valve which regulates entry into the vitello-oviduct. The vitello-oviduct is where the vitelline duct joins the oviduct.

The sole purpose of ovary is the production of the haploid ovum. It is an elongated organ situated centrally in the worm, adjacent to the vitelline duct and between the branches of the gut. The schistosome ovary is unusual in that it consists of a single organ (most trematodes have paired ovaries). The ovary consists of an epithelium, thinner at the (open) posterior end, surrounded by a fibrous inner layer and then a layer of muscle (Erasmus, 1987). Its surface is covered with developing oocytes. A gradient of oocyte development can be seen, with the smaller undeveloped oocytes at the anterior end of the ovary and mature oocytes at the posterior end, nearest to the oviduct (Neves *et al.*, 2005).

The mature oocyte exits the ovary, travels along the oviduct and enters the seminal receptacle, which is a specialized area for the storage of sperm. Here it associates with spermatozoa from the male worm. It is not known at exactly what point the sperm penetrates the oocyte in *S. mansoni*. Erasmus (1987) assumed that fertilization occurs in the seminal receptacle itself, but fertilization was subsequently found to occur in the oviduct adjacent to the seminal receptacle in *S. japonicum* (Yang *et al.*, 2003). In *Schistosomatium douthitti*, penetration of the oocyte by the sperm also takes place in the oviduct adjacent to the seminal receptacle, but nuclear fusion was not seen to occur until the egg had been released (Nez & Short, 1957).

The route that the sperm take to arrive in the seminal receptacle is not known either. In the schistosome genera *Heterobilharzia, Dendritobilharzia, Trichobilharzia, Schistosomatium* and *Ornithobilharzia* sperm travel through the Laurer's canal which provides a direct link between the tegument and the vitello-oviduct (Lee, 1962; Ulmer & van de Vusse, 1970; McMullen & Beaver, 1945; El-Gindy, 1951; Price, 1929). However, a Laurer's canal has not been found in *Schistosoma*, despite *S. mansoni*, *S. japonicum* and *S. haematobium* being the subject of more numerous and more detailed morphological studies (Faust *et al.*, 1934; Sakamoto & Ishii, 1977; Irie *et al.*, 1987; Moczon & Swiderski, 1983; Leitch & Probert, 1984; Yang *et al.*, 2003; Neves *et al.*, 2005; Erasmus, 1987; Erasmus, 1973; Spence & Silk, 1971). So in *S. mansoni*, either the Laurer's canal remains to be discovered or the sperm must enter the female through the gonopore and swim through the reproductive tract (via the uterus, ootype, vitello-oviduct and oviduct) in the opposite direction to the exiting eggs.

Both the oviduct and the vitelline duct unite to form the vitello-oviduct, so this is the point at which the oocyte, sperm and vitelline cells are packaged together, before passing into the adjacent ootype. The ootype is a specialized muscular chamber that reflects the size and shape of the egg, to include the very prominent, lateral spine. The ootype is surrounded by a network of unicellular gland cells called the Mehlis gland, which appear to discharge into it but whose function is unknown (Spence & Silk, 1971; Erasmus, 1973). It is in the ootype that the oocyte and vitelline cells are moulded to form the distinctive egg shape and where the eggshell is formed.

As mentioned above, the eggshell is made from the precursor proteins that have been stored in the granules of the vitelline droplets. In *S. mansoni*, the shell precursors have not been fully characterized, but they are comprised of numerous proteins from three families, two of which are genus specific and the third shared with other trematodes (Ebersberger *et al.*, 2005). They have similar staining properties to the eggshell precursors of *Fasciola*, which have undergone a post-translational modification in which an intracellular tyrosine hydrolase has oxidized the majority of the tyrosine residues to 3, 4-dihydroxyphenyl-$_L$-alanine, producing "presclerotized" proteins (Waite & Rice-Ficht, 1987; 1989; Wells & Cordingley, 1991). These presclerotized precursor proteins later form the "sclerotized" or

"quinnone-tanned" eggshell of *Fasciola*, and consequently often the *S. mansoni* eggshell is also described in the same terms. Although formed in the vitellaria, the eggshell precursors are not activated until the cell mass enters the ootype. The regulatory mechanism preventing premature eggshell formation involves maintaining both a low pH within the vitelline droplet and also the integrity of the droplet membrane. Raising the pH inside the droplet causes fusion of the droplet's granules resulting in the formation of intra-droplet eggshell, and treatment with a calcium ionophore causes the granules to be exocytosed intact from the cell where they coalesce to form extracellular eggshell (Wells & Cordingley, 1991). The purpose of the Mehlis glad could therefore be to secrete ionophore-like factors that induce the vesicles within the vitelline droplets to exocytose their contents such that they fuse together around the cell mass to form the eggshell at the appropriate moment (i.e. in the ooytye). The newly completed egg then passes along the uterus and exits the worm through the gonopore. No developmental processes have been reported to occur during its transit along the uterus, but only one egg at a time is present in this organ (Bruckner & Schiller, 1974).

Although the described features of the *S. mansoni* reproductive tract are the same in Erasmus (1973), Neves *et al.* (2005) and Spence & Silk (1971), differences in their interpretations are evident. Erasmus (1973) and Neves *et al* (1995) both describe the various organs as being clearly demarcated from one another, so that the reproductive tract can be divided into three distinct regions: vitellaria/vitelline duct, ovary/oviduct and the remainder. The paper by Spence & Silk (1971) differs in that the transition from one region to the next is considered to be more gradual, so that no such demarcations can be made.

Various attempts have been made to establish the daily output of eggs per female worm, as summarised overleaf in Table 1.1. Calculating fecundity is difficult because it is necessary to accurately determine the number of pairs of gravid worms, pinpoint the time at which egg production commences and account for all of the eggs produced, whether they be lodged in the organs of the host, excreted in the faeces or destroyed by the host. Each of the studies detailed below account for a different selection of these criteria but none have accounted for them all, and furthermore, differences in *S. mansoni* isolates, host species and the intensity/duration of infection between the studies add another layer of complexity.

Table 1.1 The estimated fecundity of *S. mansoni* in seven studies.

Study	Host	Host Sample Size	Fecundity (mean eggs/female/day)
Koura, 1970	Albino mice	24	362
Pellegrino & Coelho, 1978	Albino mice	4	300
Kloetzel, 1967	CF1 mice	94	257
Moore & Sandground, 1956	Hamster	6	291
Nelson & Saoud, 1966	Rhesus monkey	2	211
Damian & Chapman, 1983	Baboon	12	1107
Cheever & Duvall, 1974	Grivet monkey	40	598

It is therefore not surprising that there is such a wide variation in estimates of fecundity between the studies. However, this collection of data suggests that fecundity may be host dependent and the often-quoted figure of 300 eggs per female per day is probably an underestimation.

1.2.2 The Physiology of the Egg

TEMs of the *S. mansoni* egg in both its immature and mature state have been published by Neill *et al.*, (1988) and are reproduced overleaf as Figure 1.2. When it is first released by the female, the *S. mansoni* egg consists of an ovum plus 30-40 vitelline cells, surrounded by the cross-linked shell. In addition to the (diagnostic) lateral spine, the outer surface of the shell is covered by microspines (Race *et al.*, 1971; Neill *et al.*, 1988; Ashton *et al.*, 2001). The mean dimensions of the immature, newly-released egg are 112µm x 44µm (Ashton *et al.*, 2001). At an early point in its development one or two peripheral cells detach from the embryo and spread out as an epithelium around the inside of the shell, forming an envelope. As the egg matures, it increases greatly in size and acelluar material appears between the envelope and the shell. This material is secreted by the envelope (Ashton *et al.*, 2001; Schramm *et al.*, 2006), which by now is thicker and contains abundant rough endoplasmic reticulum, indicative of protein synthesis. Once fully mature, the average egg has increased in size to149µm x 69µm, equivalent to an increase in volume in excess of 300% (Ashton *et al.*, 2001). The viable miracidium can be seen, bathed in liquid, which also incorporates large vacuoles. The eggshell must be permeable because the proteins synthesised in the envelope of mature eggs are actively secreted through the shell (Ashton *et al.*, 2001). Pores in the shell have been reported, either taking the form of direct inner-outer perforations of 100nm in diameter (Race *et al.*, 1969; Race *et al.*, 1971) or oblique, branching channels of 34nm in diameter (Neill *et al.*, 1988). However, it is possible that the "pores" described by Race *et al.* and Neill *et al.* are actually artefacts, resulting from the respective sectioning and slam freezing processes carried out during the preparation for TEM. In the study by Ashton *et al.*, (2001) the fixative was allowed to penetrate the eggshell before sectioning was carried out and no pores could be seen, so it remains unclear exactly how material passes through the eggshell.

1.2.3 Egg Escape from the Host: the Parasite's Requirement

It is an absolute requirement for the schistosome that some of its eggs are excreted from the host in a viable state, so that the miracidia can infect a snail to continue the parasite's life cycle. The eggs are released into the bloodstream, so each egg must incorporate some kind

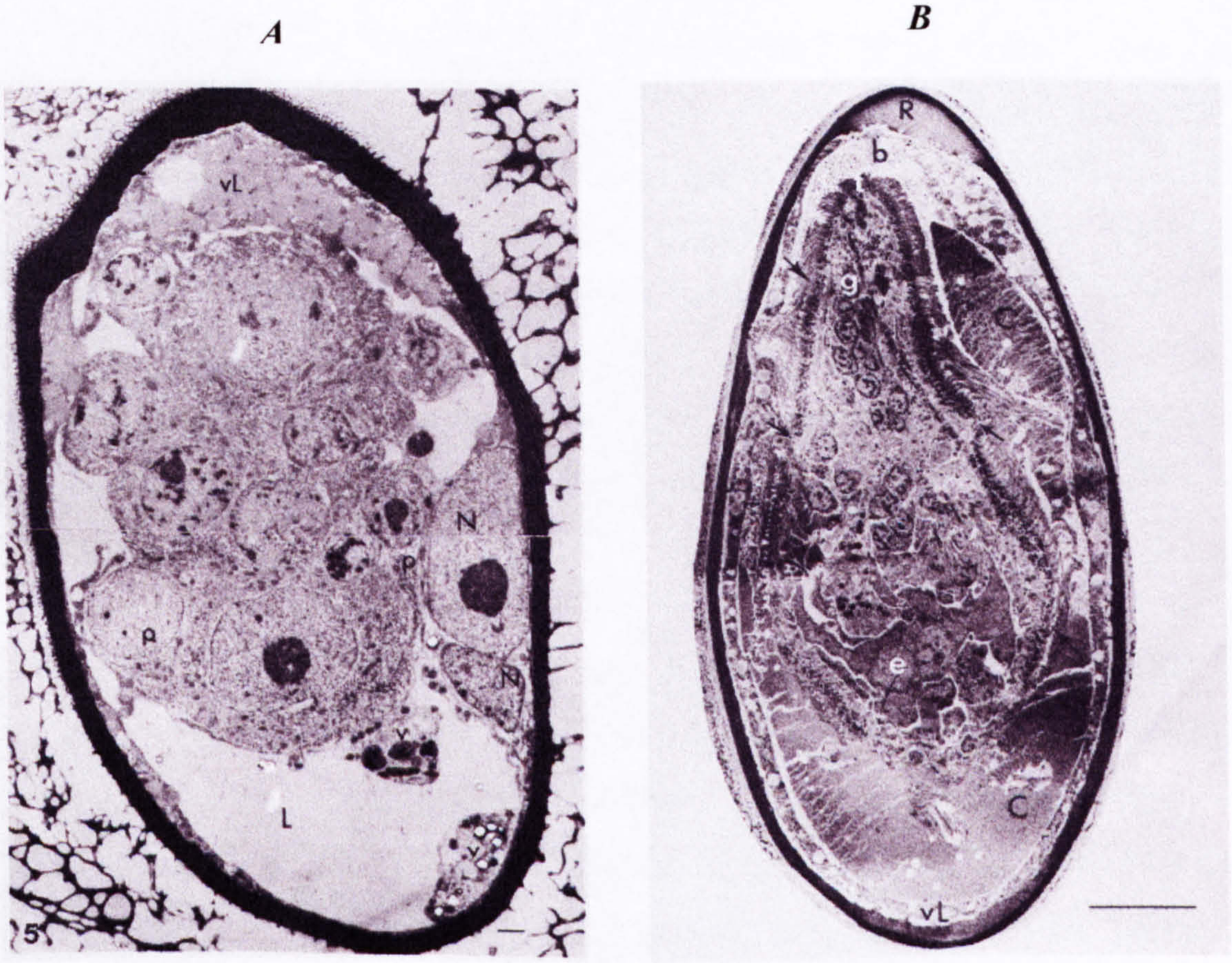

Figure 1.2 Transmission electron micrographs of the immature and mature egg. **A:** In the immature egg, the envelope (vL) forms adjacent to the inside of the shell from parent cells that have become detached from the embryo. The nucleus (N) of the parent cell is large. The developing embryo contains micro-nucleated cells (p) and is bathed in a liquid, sometimes called Lehman's lacuna (L). A residual vitelline cell (v) contains lipid droplets. **B:** In the mature egg, another layer of material (sometimes called Reynolds layer) can be seen (R), sandwiched between the envelope (vL) and the shell. Large vacuoles (C) are present. The miracidium is now fully developed. The images are from Neill *et al.*, (1988).

of escape mechanism, enabling it to adhere to the wall of the blood vessel (to prevent it being washed away) and then to transport it through the tissues of the gut wall into the gut lumen. There are inherent difficulties in this because even if the physical distance is small, the egg must negotiate the various different tissues of the gut wall - namely the venous endothelium, the connective material that makes up the submucosa and lamina propria, the smooth muscle layer of the muscularis mucosae and the intestinal epithelium. The egg's escape must be timed such that the embryo has fully developed into a viable miracidium during its transit. Indeed, it takes eight days for an *S. mansoni* egg to cross the gut wall and emerge in the faeces (Cheever & Anderson, 1971), which is one day longer than its *in vitro* maturation time and three to five after egg-secretion commences (Ashton *et al.*, 2001; Hang *et al.*, 1974).

Inevitably, many eggs are washed away, and the experiments aimed at assessing the proportion of eggs that do so have suffered with the same logistical problems associated with fecundity studies. The results of such studies vary, but it is estimated that in *S. mansoni,* between 3% and 27% of eggs released by females are excreted in the host faeces (Koura, 1970; Kloetzel, 1967; Moore & Sandground, 1956; Nelson & Saoud, 1966; Damian & Chapman, 1983; Cheever & Duvall, 1974).

1.2.4 The Escaping Egg: Parasite-Derived Factors

It has been known for some time that eggs actively secrete proteins through their shell (Oliver-González, 1954; von Lichtenberg, 1964; Boros & Warren, 1970; Ashton *et al.*, 2001). This led to the hypothesis that these secretions had proteolytic activity which enabled the eggs to degrade host tissue and escape from the host (Kloetzel, 1967; 1968). Protease activity has been attributed to the egg secretions, initially in studies that failed to eliminate the possibility that the proteases were from bacterial contaminants or had leaked from dead eggs (Kloetzel, 1968; Curtis, 1991), and then in a study that did account for these factors (Ashton *et al.*, 2001). Ashton *et al.*, (2001) also established that proteins were only secreted by mature eggs. This is an important discovery, because if proteases secreted by the egg are responsible for enabling the egg to cross the gut wall and escape the host, then by tying the onset of protease secretion to a particular point in the egg's maturation process the parasite ensures that eggs will not emerge from the host prematurely. The

failure of immature eggs to secrete proteins also explains why intact, immature eggs are immunologically inert (Hang *et al.*, 1974).

As egg secretions are only produced by mature eggs, then it follows that they cannot be involved in any mechanism that enables immature eggs to adhere to the venous epithelium as they are released by the female worm. It has been suggested that the egg's spine impales the endothelium and secures the egg (Jourdane & Theron, 1987; Whitfield, 1993), but this theory is undermined to some extent by the morphology of *S. japonicum* eggs, which possess a small knob rather than a spine. However, the higher fecundity of *S. japonicum* compared to *S. mansoni* possibly allows for a less efficient egg attachment method in the former.

1.2.5 The Escaping Egg: Host-Derived Factors

A series of experiments have indicated that platelets could be involved in the egg-excretion process. Ngaiza & Doenhoff (1990) used mice whose platelet activity had been suppressed with anti-platelet drugs and/or anti-platelet serum. These mice were found to have an impaired ability to excrete eggs, which could be reversed if platelets were injected into the mice. Several experiments followed that intended to find out whether platelets caused the eggs to adhere to the venous epithelium, and if so what the mechanism of attachment was. Adherence was initially thought to involve the release of platelet products such as platelet factor 4 or eicosanoids which went on to activate other cells (Ngaiza & Doenhoff, 1990). Other, more direct binding mechanisms were also thought to be involved, such as endothelial P-selectin binding to the platelet's von Willibrand receptor complex or endothelial integrins binding to β_3 integrins on the platelets (Gawaz *et al.*, 2005). An *in vitro* assay was carried out in which the extent of egg adherence to human umbilical vein endothelial cells was monitored, with and without the presence of serum and platelet-release products (Ngaiza *et al.*, 1993). Although both serum and (particularly) the platelet-release products both enhanced the ability of eggs to adhere to the epithelial cells, the value of the experiment was undermined because less than 10% of the eggs used in the experiment were in the immature state in which they would be released by the female. The maturation status of the adherent eggs was not noted either, so the platelet-enhanced egg attachment to the epithelial cells could have been restricted to the population of mature

eggs, via the proteins they secrete. This would not be relevant to the process that occurs *in vivo* in which immature rather than mature eggs would need to adhere to the vascular endothelium. In a later experiment, the ability of newly-released eggs to adhere to endothelial cells was studied by allowing paired worms to deposit eggs onto to human umbilical cord vein cells cultured in the presence of foetal calf serum (FCS), but not platelets (File, 1995). It was found that the endothelial cells started to migrate over the newly-released eggs, apparently as they were deposited, causing the eggs to be retained by the endothelium and then to be completely engulfed by it, such that the integrity of the endothelium was completely reinstated within four hours of egg deposition. However, gentle agitation of the culture plate severely impaired egg retention, so it remains questionable whether venous endothelial cells alone offer a high degree of retentive action *in vivo*.

Scanning electron microscopy has been used to show eggs in the vascular endothelium with platelets adhering to their surface before a cellular inflammatory reaction has formed, thereby demonstrating the likely involvement of platelets in the very early stages of egg excretion (Doenhoff *et al.*, 1986). Platelets have also been observed binding to immature eggs (Doenhoff, 2005 *pers comm.*) and vascular endothelium (Gawaz *et al.*, 2005), so the cascade of events leading to egg escape could commence with the egg adhering to the endothelium in a platelet-mediated or platelet-augmented manner. The eggshell itself is not immunogenic (Oliver-González, 1954; Boros & Warren, 1970), so a different immunogenic mechanism must induce this platelet adhesion. This could consist of adult schistosome proteins, accumulated on the surface of the eggshell as it passes through the uterus. As explained in Section 1.2.2, the outer surface of the egg is covered with microspines as well as the large terminal spine (Race *et al.*, 1969). It is easy to envisage this combination of spines scraping surface proteins from the uterus during the egg's passage through this organ, and perhaps these adult schistosome proteins could mediate the adherence of the egg to the endothelium, either directly or via platelets. This would explain the rapid response that File (1995) noticed when eggs were deposited onto umbilical vein endothelial cells.

$CD4^+$ cells have also been implicated in the escape of the egg from the host. Doenhoff *et al.* (1986) found that thymectomised mice failed to excrete eggs unless they were reconstituted

with a population of $CD4^+$ cells. Ten years later a fieldwork-based study found that HIV positive individuals had fewer eggs in their stools compared to HIV negative individuals, despite a similar intensity of infection, as assessed by the concentration of circulating cathodic antigen in the serum (Karanja *et al.*, 1997). These two papers are often quoted together as evidence that host $CD4^+$ cells facilitate the egg's passage across the gut wall, although neither research group thought that sufficient experimental evidence had accumulated to be able to speculate as to the mechanism by which the $CD4^+$ cells might be operating (Karanja *et al.*, 1997: Doenhoff, 1997). It is known that $CD4^+$ cells secrete matrix metalloproteases (MMPs) that enable them to traverse basal membranes and tissue (Goetzl *et al.*, 1996), so *S. mansoni* eggs could be utilizing these host-derived MMPs to disrupt the integrity of the gut wall tissues through which they too must pass.

It is probably too simplistic to conclude that T cells are an absolute requirement for eggs to cross the gut wall though. The Karanja *et al.*, (1997) paper was based on 53 individuals with high intensities of infection, 16 of whom were HIV positive. The differences the authors found between the egg excretion rates of HIV positive and negative individuals were not supported by a subsequent study with a much larger sample size of 1545 individuals (Kallestrup *et al.*, 2005), in which no relationship was found between egg excretion rates and $CD4^+$ count. In the thymectomised mice model, Doenhoff *et al.*, (1986) found a similar number of eggs in the intestines of the thymectomised mice as were in the normal controls, although only a few eggs were excreted in the faeces of the former. Therefore, eggs may well have been in the process of crossing the gut wall in the thymectomised mice, and the phenomenon that the authors reported could have been a delay (and probably a reduction in rate) rather than a complete cessation of egg excretion. Both the thymectomised mice and the normal controls were culled at 42 days post infection, so a slower egg transit time in the former could have manifested itself as a complete failure of excretion at this time-point. A reduction in egg transit time in the thymectomised mice would also be compounded by the delay in oviposition that occurs when schistosomes infect thymectomised mice (Dunne *et al.*, 1983).

Other work using the murine model has found that T cells are an important influence on egg excretion but not an absolute requisite. Dunne *et al.*, (1983) found that although egg

excretion occurred in thymectomised mice it was delayed and the rate was slower. When the thymectomised mice were injected with serum from chronically infected mice, the egg excretion rate increased to an intermediate level rate between the thymectomised mice and normal controls. This could have been due to antibody binding to Fc receptors on macrophages and/or eosinophils, which induced protease secretion that carried out a similar role, albeit less efficiently than the MMPs derived from $CD4^+$ cells. Indeed, it has been demonstrated that plastic-adherent (i.e. macrophage-enriched) cells taken from liver granulomata in chronically infected mice secrete collagenase (Truden & Boros, 1985).

So, a likely process of egg escape would involve platelets and several classes of host cells. Platelets could mediate the initial adhesion of the immature egg to the vascular epithelium, macrophages act as antigen presenting cells and protease secretors, the protease milieu from which is augmented by those secreted by eosinophils and $CD4^+$ cells.

Part 3 The *S. mansoni* Egg Proteome

1.3.1 "Soluble Egg Antigen"

It has been evident for decades that in schistosomiasis the eggs induce the liver pathology, so it is not surprising that attempts to identify the immunogenic components of the egg stretch back to the 1970s. Boros & Warren (1970) made the first egg antigen preparation, in which intact eggs were sonicated in a 0.9% sodium chloride solution. They called the centrifuged-supernatant "Soluble Egg Antigen" (SEA) and established that small quantities could be used to sensitize mice to induce a more rapid granulomatous response following egg deposition. SEA has remained the principal egg antigen preparation ever since, although the sodium chloride solution has now been replaced with more effective buffers.

1.3.2 "Major Serologic Antigens"

The first attempt at characterising the immunogenic components of SEA was carried out when SEA was separated by electrophoresis and probed with serum from infected mice (Pelley *et al.*, 1976). Three antigens were found and called "Major Serologic Antigens"

(MSA). After purification using chromatography, MSA1 and MSA2 were found to be glycoproteins of 137 kDa and 465 kDa respectively whilst MSA3 was an unglycosylated protein of 50 – 70 kDa.

1.3.3 CEF6 and its components: α1 and ω1

Following the identification of MSA1-3, a detailed set of experiments was carried out that aimed to identify which SEA components could induce the production of protective antibodies in mice (Dunne *et al.*, 1981). As discussed in Section 1.1.4, it was already known that T cell-deprived mice suffered fatal egg-induced hepatotoxic pathology at acute infection (Doenhoff *et al.*, 1981). It was also known that this liver damage could be prevented by injecting serum taken from immunologically intact mice that were either chronically infected or had been immunized with SEA (Doenhoff *et al.*, 1981; Byram *et al.*, 1979; Doenhoff *et al.*, 1979).

In order to identify which of the SEA components were responsible for inducing the humoral protection, Dunne *et al.*, (1981) separated crude SEA using Wieme electrophoresis apparatus (Wieme, 1959). The Wieme protocol involves subjecting a crude protein mixture to electrophoresis at a fixed pH in an agar gel. The individual proteins migrate towards the anode or cathode at different rates, depending upon their charge at the chosen pH, and the electrophoresis is stopped as the most migratory proteins approach a terminal. The gel can then be stained for protein or probed with serum, and between-gel comparisons of the characteristic pattern that emerges can be made. When SEA was subjected to Wieme electrophoresis and then probed with serum from infected mice, Dunne *et al.*, (1981) identified twelve different antigens. These were named according to their charge at pH 8.6, (α1-3 migrated towards the anode, ω1-3 didn't migrate and κ1-7 migrated towards the cathode). Crude SEA was also separated by cation exchange chromatography into six fractions, named Cation Exchange Fractions (CEF) 1-6, in the order that they were eluted from the column (i.e. decreasing acidity). Each CEF was then injected into naïve mice, a humoral immune response allowed to develop and the serum used to probe Weime gels of crude SEA. This enabled the antibody responses induced by each CEF to be separately compared to that induced by crude SEA. The anti-CEF serum was then used to immunise infected, T cell-deprived mice so that the degree of protection each CEF offered against

hepatotoxic pathology could be assessed. It was found that CEF6 was the only fraction that induced a humoral response that protected T-cell deprived mice as effectively as anti-SEA serum. Anti-CEF6 serum was reactive against ω1 (as was the anti-CEF5 serum) but unlike any other CEF, it was also reactive against α1.

Although important because it implicates CEF6 and potentially α1 as inducing the hepatotoxic reaction in the host, the paper by Dunne *et al.*, (1981) has inconsistencies that make it difficult to assess the biochemical properties of α1. The electrophoresis and the chromatography appear inconsistent with one another in that α1 migrated towards the anode at pH 8.6 (it was the third most acidic component) and ω1 failed to migrate at all (indicating an isoelectric point of approx. 8.3) - yet both were eluted in the final fraction from the column (i.e. amongst the most basic SEA proteins). The seven most basic proteins (at pH 8.3) by Wieme electrophoresis (κ1-7) did not bind to the cation exchange column at all (the column was equilibrated at pH 7.2), thereby demonstrating their acidic nature.

CEF6 was also shown to be capable of diagnosing schistosomiasis mansoni. When used in an Enzyme-Linked ImmunoSorbent Assay (ELISA), CEF6 was the most reactive fraction in terms of the antibody response in chronically infected humans, with very little reactivity with serum from patients suffering with *S. haematobium* or *S. japonicum* infections (McLaren *et al.*, 1981).

Further purification and characterization of the CEF6 components followed. A protocol using cation exchange chromatography and monoclonal antibodies purified α1 and ω1 from crude SEA (Dunne *et al.*, 1991). The antigen ω1 was characterised as a 31 kDa monomeric protein of isoelectric point (*pI*) > 9.5 and α1 as comprising two subunits of 22 kDa and 18 kDa and *pI* 7.5 - 8.5. Both ω1 and α1were glycoproteins, but when de-glycosylated neither was recognised by serum from infected mice. Therefore, it was the glycans attached to these proteins that induced the humoral response. In a series of transfer experiments the paper went on to establish that the hepatocytes of T cell-deprived mice were protected if the mice had been immunised with anti-ω1 serum, but not with anti-α1 serum.

Neither α1 nor ω1 was sequenced and no further characterisation studies were done for ten years. Then both antigens resurfaced in separate studies. Fitzsimmons *et al.*, (2005) stated that they had sequenced ω1 and that it was a secreted ribonuclease and Schramm *et al.*, (2006) stated that α1 was the same protein as an IL-4-inducing factor that was secreted from eggs and had been identified three years previously. These are both discussed in Sections 1.4.2 and 1.4.1 respectively.

1.3.4 Sm-p40

Sm-p40 is a 40kDa protein of 354 amino acids, first identified when it was precipitated from SEA with sera from infected humans, cloned and sequenced (Nene *et al.*, 1986). About 10% of the total protein in SEA is Sm-p40 (Stadecker *et al.*, 2001). It is a member of the small heat shock protein (sHSP) family, consisting of two heat shock protein (HSP)20 homologues, each of which contains two alpha-crystallin domains. Sm-p40 contains three epitopes, one of which is immunodominant (Hernandez *et al.*, 1998; Chen & Boros, 1998), but all three induce a proliferative Th1 response, particularly in the C3H and CBA mice with the H-2^{K} haplotype (Hernandez & Stadecker, 1999). This Th1 response is in contrast to the Th2 response induced by crude SEA.

1.3.5 HSP70

HSP70 was identified when a recombinant cDNA expression library derived from *S. mansoni* adults was probed with serum from infected mice and reactivity to a 70kDa protein occurred (Lanar *et al.*, 1985). A blot of SEA was then probed with serum from a rabbit immunised with the recombinant protein and it was thereby established that the protein was also present in eggs. HSP70 was then sequenced (Hedstrom *et al.*, 1987) and it was at this point that the homology between the 70kDa protein and human/*Drosophila melanogaster* HSP70 became apparent. HSP70 is expressed in all stages of the *S. mansoni* lifecycle (Lanar *et al.*, 1985; Neumann *et al.*, 1993; Yuckenberg *et al.*, 1987), but expression levels vary between the stages, with the egg being the stage at which HSP70 is most highly expressed (Curwen *et al.*, 2004).

A humoral response to *S. mansoni* HSP70 has been found in mice, humans and baboons (Lanar *et al.*, 1985; Hedstrom *et al.*, 1988; Kanamura *et al.*, 2002). The baboon study

incorporated epitope mapping in which it was established that the schistosome HSP70 contains multiple epitopes, the most immunoreactive of which by far are those at the carboxyl terminal of the protein. This section of the protein has the least homology to HSP70 from other species, thereby explaining the species-specific reactivity of antibodies to *S. mansoni* HSP70 - there being no cross-reactivity to *S. japonicum* HSP70 for example (Hedstrom *et al.*, 1988).

1.3.6 Phosphoenolpyruvate Carboxykinase

S. mansoni phosphoenolpyruvate carboxykinase (SmPEPCK) was first described when $CD4^+$ cells from acutely infected C57BL/6 mice were assayed for reactivity with SEA components that had been separated by electrophoresis (Asahi *et al.*, 1999). The most reactive antigen was a 62kDa protein, which was digested and its fragments used to stimulate a T-cell hybridoma (also derived from C57BL/6 mice) known to be reactive to the native protein. The most antigenic fragment was sequenced and found to be identical to PEPCK of other species. SmPEPCK was then cloned and the extent of its antigenicity found to be strain-dependent – in CBA mice it was less immunogenic than Sm-p40 but in both B57BL/6 and CBA mice the native protein induced a mixed Th1/Th2 response, although no IL-4 was produced in response to the recombinant version (Asahi *et al.*, 2000).

1.3.7 SmE16

When the protein products of an *S. mansoni* cDNA library were probed with serum from infected humans a 16.3 kDa, 143 amino acid calcium binding protein called SmE16 was identified (Moser *et al.*, 1992). SmE16 had homology to troponin C (from chicken and frog muscle) and calmodulin (from *Caenorhabditis elegans* and *Schizosaccharomyces pombe*). Although described by the authors as an egg-specific protein it is not known what function it performs.

Part 4: Proteins Secreted by the *S. mansoni* Egg

The idea that eggs secreted factors goes back decades – long before the first papers describing SEA were published. The idea was logical, because it would provide an

explanation as to how the cellular foci that were evident in infected people and mice were formed. Thus, egg secretions were first described as a "cytolytic fluid", secreted by the *S. japonicum* miracidium, which emerged through pores in the shell and glued leukocytes to it forming an "agglomeration" (Faust, 1946). The existence of egg secretions was first proven eight years later, when the precipitation test for schistosomiasis was first described (Oliver-González, 1954). The precipitation test involved incubating serum on a slide with *S. mansoni* eggs for 24 hours. When the serum had been taken from infected humans or animals a precipitate formed around the shell. This precipitate only occurred around live eggs and the antibodies responsible for it were unreactive to lyophilized material from cercariae or adult worms. The precipitation test was subsequently repeated but with serum from acutely infected mice and cryostat liver sections rather than intact eggs (von Lichtenberg, 1964). When probed with labelled, rabbit anti-mouse globulin antibody a precipitate around the eggshell could be seen, and the egg was described as being "embedded in a glassy precipitate which fades outwards into granules".

The first experiment designed to assign a function to the egg secretions was a protease assay in which *S. mansoni* eggs were incubated in azocollagen (Kloetzel, 1968). A time-dependent and egg density-dependent increase in protease activity was seen, which was interpreted as being evidence for a secreted collagenase. However, the proportion of dead eggs at the beginning and end of the experiment was not recorded, so it is possible that the phenomenon that was seen was the rate at which eggs were dying in the phosphate buffer and leaking their proteolytic contents. The azocollagen assay was subsequently repeated but the results could not be replicated (Asch & Dresden, 1979). The secreted protease theory was pursued further when eggs were incubated on a fibrin matrix overnight and the extent of substrate degradation measured (Curtis, 1991). Although an egg-density dependent protease activity was reported, antibiotics were not used and nor was the proportion of dead eggs assessed before or after the experiment. As in the Kloetzel (1968) paper, it is impossible to eliminate dead eggs or bacterial contamination as being the source of the protease activity in the Curtis (1991) study.

A protocol for culturing eggs in sterile media (with antibiotics) to enrich for their secretions was established by Boros & Warren (1970). The authors also compared the priming

capabilities of the egg secretions with SEA. Naïve mice were primed with either the egg secretions or SEA and challenged a week later with live eggs. Eight days after challenge the size of the granulomata were measured. By way of comparison, other mice were primed with diffusion chambers containing live eggs. When the granulomata sizes were compared, it was found that those from the mice primed with egg secretions and live eggs were of a similar size, and that this size was significantly larger than those from mice primed with SEA. Although the authors stated that they used an equivalent number of eggs in each preparation, it is difficult to assign any significance to the differences in granulomata size. This is because no protein quantification assays were carried out, so equalizing the total protein content of the egg (i.e. the SEA preparation) to the quantity of protein secreted by the egg over time (i.e. the cultured egg and live egg preparations) is impossible. However, Boros & Warren (1970) remains an important paper because it is the first report of eggs being cultured *in vitro* to enrich for their secretions.

The subject then fell out of favour, in that only two papers of significance were published in the following thirty years. The first of these followed on from Boros & Warren (1970), repeated their sensitization assays and found that immature eggs were immunologically inert (Hang *et al.*, 1974). The second paper established that anti-CEF6 serum could be used in a diagnostic precipitation test (Dunne *et al.*, 1988), thereby demonstrating that immunogenic elements of CEF6 were secreted from live eggs.

Then, interest in the subject of egg secretions was revitalised after the first detailed characterization of the secreted proteins was carried out (Ashton *et al.*, 2001). In this paper, eggs were cultured using a protocol similar to Boros & Warren (1970) and their secretions subjected to one-dimensional electrophoresis (1-DE) and casein zymogram analysis. It was thereby established that the egg secretions were very different to SEA, comprising only 6 bands on the gel, two of which had proteolytic activity. The secreted proteins were called Egg Secreted Proteins (ESPs). Immunohistological and transmission electron microscopic studies were also included in the paper, and these showed that ESPs are produced not by the miracidium as had previously been thought but by the subshell envelope, once the egg has started to mature.

ESP was then subjected to 2D electrophoresis (2-DE), glycan staining, mass spectrometry (MS) and phylogenetic analysis (Ashton, 2001). ESPs were found to comprise of 21 spots on a 2D gel, which could be grouped into six phylogenetically related clusters of spots. One of these clusters contained 6 very basic spots, four of which (ESP 3-6) were glycosylated isoforms of the same protein. They also comprised the bulk of the protein in the entire gel. ESP 3-6 was sequenced and the sequences deposited on GenBank. No homology was found between ESP and any previously characterized proteins.

Most recently, a study has been published that claims to be a full proteomic characterization of the ESPs, where mass spectrometry was used to identify proteins in egg culture supernatants (Cass *et al.*, 2007). The paper lists a total of 188 proteins and states that they make up the *S. mansoni* egg "secretome". However, list includes numerous proteins that are well known to be intracellular and which do not have a secretory signal peptide (such as glycolytic enzymes and histones). Unfortunately, the large number of obviously intracellular proteins on the list makes it impossible for the reader to be confident that any particular protein on the list is truly secreted from the egg and as such, the paper adds very little to the overall knowledge about egg secretions.

1.4.1 ESP 3-6 (a.k.a. IPSE, SmEP25 and SmCKBP)

Three independent groups have subsequently published research, each attributing a different function to ESP 3-6. Human basophils, cultured with a native and recombinant protein that turned out to be ESP 3-6 were found to secrete IL-4 when stimulated by either forms of the protein (Schramm *et al.*, 2003). The protein was called IPSE (Interleukin-4-inducing principle of *S. mansoni* eggs) and the authors hypothesized that this IL-4 may be the trigger that caused the Th1/Th2 switch that occurs consequently with egg deposition. IPSE was then described as being the same protein as the CEF6 component α1 (Schramm *et al.*, 2006). This connection between IPSE and α1 was made because both proteins were basic, glycosylated heterodimers of a similar molecular mass. The connection is supported by Dunne *et al.*, (1988) who had already demonstrated that at least one CEF6 component was secreted (because anti-CEF6 serum could be used in the precipitation test). However, IPSE has a *pI* of approx 9.5 (Ashton, 2001), which is higher than the *pI* 7.5 - 8.5 of α1, as described by Dunne *et al.*, (1991). Also, the Con A-affinity chromatography used by Dunne

et al., (1991) to purify α1 was rejected by Schramm *et al.*, (2003) in the purification of IPSE because Con A is prone to non-specific binding and it only exhibits a weak affinity for the IPSE protein (Schramm, 2006 *pers comm.*). It is therefore apparent that there are differences as well as similarities between IPSE and α1, and so it may be premature to assign the same identity to both proteins at this point in time.

The second research group measured the cytokines produced by T cells after they had been stimulated with recombinant ESP3-6 (Williams *et al.*, 2005). The cells came from two different strains of mice with acute *S. mansoni* infections. A proliferative response to the antigen was seen as well as production of cytokines associated with both Th1 (interferon (IFN)γ, IL-2) and Th2 (IL-4, IL-5) responses. The authors called the protein SmEP25 (*S. mansoni* egg protein of 25kDa).

The third group carried out chemokine binding and cell migration assays to investigate the interactions between ESP 3-6 and human neutrophils (Smith *et al.*, 2005). This group found that ESP 3-6 could bind to chemokines, inactivate them and slow down the recruitment of cells to the developing granuloma. They called the protein SmCKBP (*S. mansoni* chemokine binding protein).

The role that ESP 3-6 (aka IPSE, SmEP25 and SmCKBP) plays in the biology of schistosomiasis is still unclear because there is no consensus between the research groups working on it. For the purposes of simplicity and consistency this thesis will use the original nomenclature (i.e. ESP 3-6) when describing the protein.

1.4.2 Omega-1

Omega-1 was purified from SEA, sequenced and expressed in *E. coli* (Fitzsimmons *et al.*, 2005). As the sequence was found to be homologous to a family of extracellular plant T_2 RNAses, zymography was used to demonstrate RNAse activity in the native protein. Fitzsimmons *et al.* (2005) went on to state that omega-1 was the same protein as the potentially hepatotoxic CEF6 component ω1 (which had been originally described (concurrently with α1) in Dunne *et al.*, (1991)), presumably because the same protocol was used to purify it from SEA. The fact that both the omega 1 of Fitzsimmons *et al.* and the ω1

of Dunne *et al.* are both glycoproteins of the same mass and *pI* adds weight to this conclusion. As omega-1 contains a secretory signal peptide, Fitzsimmons *et al.* (2005) hypothesise that the protein is secreted from the egg, whereupon the RNAse activity might modulate the cell-mediated response to schistosomiasis. However, the paper falls short of demonstrating such secretion.

1.4.3 Thioredoxin Peroxidase

Thioredoxin peroxidase-1 (Sm-TPx-1) was identified as a 26 kDa component of SEA, and after sequencing, homology to thioredoxin peroxidase in various other organisms was found (Williams *et al.*, 2001). The *S. mansoni* native protein (obtained by electroelution from an SEA gel) induced a proliferative Th1/Th2 response as well as a humoral response in C57BL/6 and CBA mice. Western blots were used to demonstrate that Sm-TPx-1 was secreted from cultured eggs. The authors' hypothesis that Sm-TPx-1 was actively secreted from live eggs would be more convincing if the dead eggs had been separated from the live ones prior to the culture, and if a control blot of other SEA proteins had been carried out. To date, it has not been demonstrated that the Sm-TPx-1 in the culture medium wasn't a leakage product from the dead eggs. However, subsequent research investigating the role of thioredoxin peroxidase in *F. hepatica* has found it amongst the secretory products of the adult parasite and capable inducing the alternative activation of macrophages (Donnelly *et al.*, 2005).

1.4.4 *S. mansoni* Egg-Derived Pro-Angiogenic Factor

"*S. mansoni* egg-derived pro-angiogenic factor" was described after SEA, ESP, intact eggs and soluble preparations from adults and cercariae had been placed on a fibrin matrix containing growth medium and bovine retinal endothelial cells (Kanse *et al.*, 2005). After incubation, the endothelial cells had proliferated and become re-structured in the presence of SEA, ESP and live eggs, forming a capillary-like cellular matrix. The extent of matrix formation was found to be dependent upon the concentration of SEA, ESP or the number of eggs. The authors concluded that the eggs secreted this pro-angiogenic factor and although they do not offer a reason why it would be secreted it is logical that it would contribute to the vascular remodelling of the damaged liver and gut tissue, thereby reducing disease pathology, prolonging the life of the host and benefiting the parasite.

An identity for the pro-angiogenic factor was not ascertained, but various purifications procedures were carried out. These established that the pro-angiogenic factor was a heat-stable, protease-resistant non-lipid of between 30 and 100kDa. Unfortunately, no measures of egg viability were taken during the experiment and nor were dead eggs removed prior to the matrix incubation or egg culture steps. It is therefore impossible to eliminate leakage products of dead eggs as inducers of the bioactivity in either the ESP or whole-egg assays, so the active principal could actually be an SEA component rather than an ESP one. Also, the most potent inducer of angiogenesis was SEA, so it is unlikely that the bioactive component is enriched in egg secretions. It is therefore difficult to accept that the pro-angiogenic factor is indeed secreted from live eggs.

1.4.5 Egg Glycans

Many of the SEA components are glycosylated, including some of immunological interest such as α1 and ω1 (Dunne *et al.* 1981) and ESP 3-6 (Ashton, 2001). The *S. mansoni* egg glycans are generally characterized by multifucosylated repeating units (Khoo *et al.*, 1997). Various studies involving monoclonal antibodies have established that the principal targets in the humoral response in schistosomiasis are indeed these fucosylated glycans (Eberl *et al.*, 2001b; Van Remoortere *et al.*, 2003; Robijn *et al.*, 2005). Although the glycoproteins themselves are developmentally regulated, the glycan epitopes are often shared and this means that there is a significant amount of humoral cross-reactivity between the life cycle stages. This means that when egg deposition commences, cross-reactive antibodies are already in circulation, derived from epitopes contained in the glycoproteins and glycolipids of the cercarial glycocalyx and secretions (Weiss *et al.*, 1986; Dalton *et al.*, 1987).

The best characterized egg glycan is Galβ1-4(Fucα1-3)GlcNAc (Lewis^x). This is expressed in egg glycoproteins and cercarial glycolipids, but not in egg glycolipids (Robijn *et al.*, 2005). It is the major component of the glycans present in ESP 3-6 (Wuhrer *et al.*, 2006). Lewis^x has been shown to have immunomodulatory properties because the oligosaccharide Lacto-*N*-fucopentose III (containing Lewis^x) induces IL-10 and prostaglandin E2 production in murine B cells *in vitro* whereas its nonfucosylated homologue lacto-*N*-neotetraose does not (Velupillai & Harn, 1994). Anti-Lewis^x IgM and IgG are produced by

infected mice, hamsters and chimpanzees, but in the chimpanzee model the titre is low, possibly due to a lower antigen concentration in the blood (Nyame *et al.*, 1997; Eberl *et al.*, 2001a).

Part 5: Proteomics and Studying the Proteome

Chapter 2 of this thesis is comprised of a proteomic characterization of the *S. mansoni* egg. Therefore, some background with regard to proteomics follows, in order to put this work into context.

A proteome is the entire set of proteins expressed from a genome and "proteomics" is the branch of science dedicated to its study (Wasinger *et al.*, 1995). Originally consisting of the application of 2-DE and MS to separate and identify proteins, proteomics has now broadened to include the study of protein-protein interactions (Blackstock & Weir, 1999). The techniques of 2-DE and MS have been available for some time, but it is more recently that refinements have been made to improve their sensitivity and reproducibility. These refinements, in conjunction with the exponential increase in the quantity of sequenced genomic data have made proteomics a much more powerful tool. Proteomics enables the protein complement within and between organisms to be characterized and compared in terms of its distribution, expression levels, post-translational modifications and interactions.

A proteomic study typically involves three steps. Firstly, the complex protein mixture is separated into its individual proteins. Then, each of the proteins is characterized by mass spectrometric methods and finally the proteins are identified by searching databases of sequenced genomic data.

1.5.1 Two-Dimensional Electrophoresis

2-DE is a method of separating proteins in a crude mixture by taking advantage of two of their unrelated properties - charge and size (O'Farrell, 1975; Klose, 1975). Proteins are initially separated according to their charge on an immobilised pH gradient. The original method of creating the gradient was by absorbing a liquid mixture of carrier ampholytes

(low molecular weight synthetic polyamino-polycarboxylic acids) into an agarose or polyacrylamide gel. The application of an electrical charge across the gel caused the ampholytes to arrange themselves in order of increasing *pI,* from the anode to the cathode. By using a multitude of different ampholytes a pH gradient could be generated. This liquid-ampholyte method of creating the pH gradient was improved upon when immobilized pH gradients (IPG) were introduced (Bjellqvist *et al.*, 1982). Now, instead of applying the ampholytes in liquid form to the cast gel they could be covalently bound to acrylamide monomers incorporated into the structure of the gel itself. The gel was then bound to a plastic strip, dehydrated and could be purchased by the laboratory and stored in this form. When applied to the gel, proteins are absorbed into it and migrate, driven by the electric current until each protein reaches the point at which its *pI* equals the pH of the gel and it has no net charge. If the protein then diffuses from this position it will gain a charge (positive if it diffuses towards the anode and negative if it diffuses towards the cathode). This charge will then drive the protein back to its original spot. The protein therefore cannot move from its *pI* whilst the current is running and it becomes "focussed". The IPG strip is superior to the carrier ampholyte gel because the pH gradient is more stable, more reproducible, a larger quantity of protein can be applied and the strip itself is easier to handle and store.

The principal problem with isoelectric focussing (IEF) is one of protein solubility. In order for the focussing to effectively separate the proteins, the entire protein content of the crude extract needs to be denatured and fully solubilized. However, this must be achieved without the use of strong ionic buffers because any inherent charge in the buffer will mask that of the protein itself and induce fluctuations in the current. It is difficult to solubilise proteins with large hydrophobic regions (such as membrane proteins) and therefore 2-DE is restricted to the study of the soluble proteome.

After isoelectric focussing has completed the strip is transferred to the top of a polyacrylamide gel and sodium dodecyl sulphate polyacrylamide gel electrophoresis (SDS-PAGE) is carried out, separating the focussed proteins by their molecular masses. Then, after staining the gel, thousands of separate proteins can potentially be seen as individual spots. Each spot (containing one to a few proteins depending upon the complexity of the

sample) can be accorded *x* and *y* coordinates. These coordinates enable the molecular mass and *pI* for the protein within that spot to be easily and accurately determined.

1.5.2 Mass Spectrometry

During the last decade, mass spectrometry has revolutionised the identification of proteins. Prior to this Edman Degradation was the favoured method (Edman, 1949). Edman Degradation is a somewhat laborious process involving the sequential removal of amino acids from the amino terminal of the protein and then identifying them one-by-one using High Performance Liquid Chromatography (HPLC). MS offers a faster, more sensitive procedure that can also cope with protein mixtures.

A mass spectrometer is a device that measures the mass to charge ratio (*m/z*) of a protein, or more usually its peptides. Peptides are almost always used because they are easier to ionize than intact proteins and furthermore, if the masses of several different peptides within a protein are known a much more confident identification can be made. The protein to be analysed is therefore enzymatically degraded into its peptides. The peptides must be short enough to be amenable to ionisation, long enough to contain a potentially unique amino acid sequence and must have been cleaved at a site that is predictable. Trypsin is the protease that best fits these criteria, cleaving at the carboxyl side of arginine and lysine residues (unless they are immediately followed by proline). Tryptic digestion of a protein typically results in peptides of about 10 amino acids in length – which are also amenable to ionisation because of the basic residue on the peptide's carboxyl terminus.

A mass spectrometer generates the "peptide mass fingerprint" (PMF) of a protein. A protein's PMF is the unique set of peptide masses derived following its digestion by a protease (Cottrell, 1994). Various kinds of mass spectrometers are available, all of which produce PMFs, but in this thesis almost all of the mass spectrometry has been carried out using matrix-assisted laser desorption-ionisation time of flight mass spectrometry (MALDI-ToF MS).

In a MALDI system, the tryptic peptides from each protein are mixed together in an excess of matrix and dried as a spot on a metal plate. The plate is inserted into the mass

spectrometer and a laser targeted at the spot. The energy from the laser is absorbed by the matrix and is transferred to the peptides. This causes the peptides to be desorbed from the plate as a plume. A high voltage is applied, which propels any positively charged peptide ions through a series of focussing electrostatic lenses into a mass analyser. The mass analyser separates the peptide ions according to their *m/z*. In ToF instruments the mass analyser consists of a flight tube, and the time taken for the peptide ions to travel the length of the tube is measured. Each of the peptide ions has the same kinetic energy and is singly charged, so the time taken for an ion to travel through the tube will be entirely dependent on its mass. This is shown in the equation $t=L / ({}^{2V}/_{m/q})^{1/2}$ (where t = transit time, L = flight tube length, V = voltage applied, m = peptide ion mass and q = ion charge). The peptide ions of a particular *m/z* exit the mass analyser together and strike the detector, which amplifies the signal and passes it to the data recorder. The data recorder plots the *m/z* of each ion against its intensity. This information is presented as a mass spectrum, showing the number of ions in the sample, their relative intensities and their *m/z*. This mass spectrum, incorporating all the peptide ions from the protein is the protein's PMF. The PMF is then searched against a database. The computer program carries out a theoretical digest of all the proteins in the database to produce a theoretical PMF for each one. A comparison is then made between this expected PMF and that obtained by the mass spectrometer. The results are presented as a list of the database proteins, ranked in order of the closeness of their match.

A small amount of work in Chapter 2 has been carried out using an Electrospray Quadrupole-Time-of-Flight mass spectrometer. In such a system the ions are created by injecting the peptides into the mass analyser through a small-diameter needle in the presence of a strong electric field. The charged droplets are desolvated in a countercurrent of gas and transferred into the mass analyser. Mass sorting in the analyser depends on the motion of the ion between four rods that have either a constant current or a radio frequency electric field applied to them. Scanning is accomplished by systematically changing the field strengths, thereby changing the m/z value that is transmitted through the analyzer so that only ions of a particular *m/z* will exit the quadrupole. The ions then enter a flight tube to acquire the mass spectrum.

Tandem mass spectrometry can be used to obtain structural information from a PMF. A tandem mass spectrometer has more than one mass analyser, resulting in its ability to select a precursor ion (i.e. a peptide ion), fragment it and then to go on to calculate the *m/z* of its product ions. This fragmentation takes place in a collision cell containing an inert gas, after a timed ion selector has isolated the parent ions of the chosen *m/z*. The collision usually causes most of the precursor ions to fragment at one of the amide bonds because these bonds have the lowest energy (Steen & Mann, 2004), producing a series of y ions (if the charge is retained on the C-terminus) and b ions (if the charge is retained on the N-terminus). Other ions are also produced when the peptide fragments elsewhere as illustrated below (Johnson *et al.*, 1987). The set of fragment ions produced by tandem MS (also called MSMS) of the chosen precursor ion can then be used to deduce the amino acid sequence of the precursor ion. The *m/z* of each of the fragment ions is combined into a spectrum and the distance between the y (or b) peaks represents the difference in mass between the amino acids in the precursor peptide.

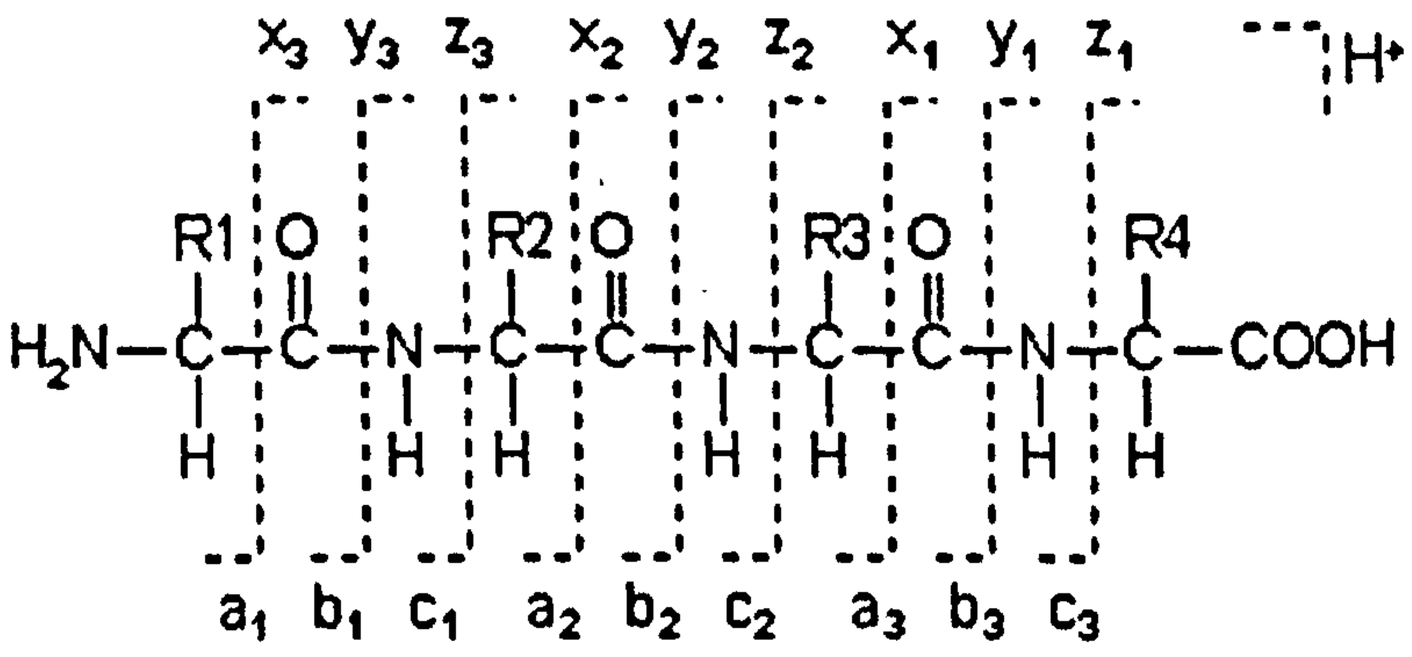

Figure 1.3 Possible fragmentation points of a peptide in tandem mass spectrometry. If the charge is retained on the carboxyl-terminal of the peptide x, y or z ions will be produced and if the charge is retained on the amino-terminal a, b and c ions are generated. The subscript number denotes the number of peptides in the ion. From Johnson *et al.*, (1987).

The set of precursor peptide ion *m/z* values can then be compared with theoretical masses obtained from protein, EST or genome databases to identify the protein. The searches of

MSMS data in this thesis used the MASCOT search engine to search against the non-redundant NCBI protein database and a database of *S. mansoni* ESTs called Schisto CDS (discussed in detail in Chapter 2). MASCOT works by carrying out a theoretical mass fragmentation of all the peptides in the database, comparing them to the observed ions and presenting the results as a list, ranked in order of decreasing scores based on the Mowse algorithm (Pappin *et al.*, 1993). The probability based Mowse score reports the result as $-10 \times \log_{10}(P)$, where P is the absolute probability that the match occurs by chance. Therefore, if an analysed protein matches a theoretically digested one from a database, and the probability of that match occurring by chance is 10^{-100}, then this becomes a Mowse score, or "total ion score" of 100.

Part 6: Regulated Protein Turnover

Although the bulk of the experimental work in this thesis relates to characterizing the proteome of the *S. mansoni* egg and its secretions, Chapter 4 differs in that it investigates the ubiquitin-proteasome pathway (UPP) of protein turnover in the egg. The introduction to Chapter 4 provides a description of the ubiquitin-proteasome pathway, so it is therefore appropriate to provide some background information below as to the other, non-proteasomal mechanisms of protein degradation.

There are many reasons why an organism must be able to degrade its proteins and recycle the amino acids. Proteins that have misfolded during their biogenesis or have been damaged whilst functioning need to be selectively destroyed. Fully-functional proteins need to be degraded if a physiological change in the cell's environment necessitates a reduction in expression levels. An ordered mechanism of protein degradation is required when cells die, so that the dying cell can collapse neatly and in a controlled manner, thereby avoiding damaging neighbouring cells and inducing an inflammatory response. Extracellular proteins taken up by endocytosis need to be broken up into their constituent amino acids for use in new protein synthesis. Although the reasons for protein degradation are varied, the mechanisms by which the process occurs can be divided into three distinct pathways – those of apoptosis, autophagy and the proteasome system.

1.6.1 Apoptosis

Apoptosis is the genetically programmed mechanism by which a multicellular organism disposes of cells that are no longer needed. Rather than bursting as occurs in necrosis following an acute injury, apoptotic cells collapse in a regulated manner, so that its remnants can be phagocytosed by a neighbouring cell. Apoptosis utilizes a special set of cytosolic cysteine proteases called caspases, which quickly degrade as much intracellular material as possible. Caspases have a wide range of substrates and are synthesised as inactive precursors called pro-caspases, which are activated by other caspases, resulting in a very rapid amplification of the initial apoptotic signal and proteolytic capability in the cell (Thornberry *et al.*, 1997). The caspase cascade is controlled by various pro and anti-apoptotic regulators, and so it is the balance between them that determines the life versus death fate of a cell (Bergmann *et al.*, 2003; Nijhawan *et al.*, 2003). There are pro-apoptotic signalling pathways that operate via cell-surface receptors and others that respond to various forms of intracellular stress.

In the intracellular stress response, members of the Bcl-2 (B-cell lymphoma 2) family are the key mediators of apoptosis. There are three Bcl-2 subfamilies: a pro-apoptotic group and a pro-survival group that are both located in the outer mitochondrial membrane plus a cytosolic sensory group called BH3-only proteins. Different BH3-only proteins respond to specific stress stimuli such as DNA damage, the accumulation of unfolded proteins in the ER or the withdrawal of growth-factors (Shibue & Taniguchi, 2006). Following their activation, the BH3 proteins translocate to the mitochondrial membrane and bind to the Bcl-2 proteins in the membrane, neutralizing the pro-survival proteins and activating the pro-apoptotic ones (Shibue & Taniguchi, 2006). The membrane-bound Bcl-2 proteins then allow leakage of material from the space between the mitochondrial membranes into the cytosol. Some of these mitochondrial proteins (such as cytochrome *c*) interact with Apaf-1, pro-caspase 9 and deoxy-adenosine triphosphate to form complexes called apoptosomes which induce the caspase cascade and start the process of apoptosis (Thorburn, 2004; Green & Evan, 2002).

There are six known cell-surface death receptors, characterized by a conserved intracellular signalling domain called a death domain (Thorburn, 2004). The death receptors are

members of the tumour necrosis factor (TNF) receptor super-family and include CD95 (APO-1/Fas), TNF receptor 1 and TRAIL. The death receptor ligands are also membrane bound (although they can be cleaved to a soluble form by extracellular metalloproteases), an important example being CD95L, which is expressed by activated T cells and tumour cells and induces apoptosis in target cells (Debatin & Krammer, 2004). Stimulation of a cell's death receptors causes them to aggregate and recruit pro-caspase 8 via an adaptor protein called FADD (Fas-Associated Death Domain), forming an intracellular protein complex called the Death Inducing Signalling Complex (DISC). The dimerization of pro-caspase 8 within DISC causes their mutual cleavage and activation. Caspase 8 then cleaves pro-caspase 3 which in turn induces the caspase cascade (Hengartner, 2000; Thorburn, 2004).

Once a cell enters apoptosis a set of cell-surface, apoptotic-specific markers are expressed. These include phosphatidylserine, intracellular adhesion molecule 3 (CD50), complement ligands, and specific glycans (Savill & Fadok, 2000). There are also a range of soluble, intermediate factors such as the first complement component C1q which create molecular bridges between receptors on apoptotic cells and phagocytic ones (Nauta *et al.*, 2003). Apoptotic cells can then be readily identified and phagocytosed, most likely by professional phagocytic cells (principally macrophages) in mammals but also by any neighbouring cell with a phagocytic capability. How macrophages are able to distinguish apoptotic cells from pathogens and are able to phagocytose the former without becoming activated and secreting pro-inflammatory cytokines is thought to relate to the range and pattern of surface markers on the apoptotic cell. These "apoptotic-cell-associated molecular patterns" may have some homology to "pathogen-associated molecular patterns" and can therefore be recognised by macrophage pattern recognition receptors (PRRs), but not by TLRs (Gregory & Devitt, 2004). Thus, TLR activation could be a key difference between pro-inflammatory activation of macrophages in response to the phagocytosis of pathogens and the non-inflammatory response seen in apoptotic phagocytosis. In support of this idea it has been demonstrated that macrophage phagocytosis is TLR 4 independent and phagocytosis of necrotic but not apoptotic cells induces expression of pro-inflammatory genes via TLR 2 (Li *et al.*, 2001; Shiratsuchi *et al.*, 2004).

After it has been phagocytosed, the remains of the apoptotic cell are contained within a large vesicle called the phagosome, which then fuses with lysosomes to form a phagolysosome. Lysosomes contain the proteases, nucleases, glycosidases, lipases, phosphatases, sulfatases and phospholipases that are collectively called acid hydrolases. Acid hydrolases are active at circa. pH5. This phagocytic pathway is distinct from the endosomal pathway. In the latter, much smaller extracellular molecules are taken up by endosomal vesicles which develop via early endosomes to form late endosomes (accompanied by a decrease in pH). The late vesicles then fuse with the acid hydrolases delivered from the Golgi to form the lysosomes. Once inside the phagolysosome the proteolysis is completed and the protein content of the apoptotic cell is degraded into its constituent amino acids.

1.6.2 Autophagy

Autophagy is a dynamic process found in eukaryotic cells that operates as an important survival mechanism in short-term starvation by recycling non-essential cytoplasmic components. It is also involved in homeostasis and in tumour suppression (Eskelinen, 2005; Gozuacik & Kimchi, 2004). The principal autophagic pathway (also called macroautophagy) begins when an induction signal induces a portion of intracellular double-membrane (called a phagophore) to undergo invagination and then complete sequestration to form a vacuole, containing portions of cytoplasm (Dunn, 1990). These vacuoles are called autophagic vacuoles in mammalian cells and autophagosomes in yeast. The autophagic vacuole then fuses with endosomes that could be at any stage of maturation from endosomal vesicles to late endosomes, forming an amphisome (sometimes called a late/degenerative autophagic vacuole). During this fusion process the outer membrane of the autophagic vesicle is incorporated into that of the endosomal membrane, thereby maintaining the integrity of the autophagic vacuole within the inner membrane. The amphisome outer membrane then fuses with a lysosome (forming an autolysosome). The released lysosomal acid hydrolases proceed to degrade the entire contents of the autolysosome so that the raw materials can be released back to the cytosol where they can be reused for metabolism (Klionsky & Emr, 2000; Eskelinen, 2005).

Three other less important autophagic routes have been described. In microautophagy the portion of cytoplasm is sequestered by an invagination of the lysosomal membrane rather than by a phagophore (Ahlberg *et al.*, 1982). Chaperone-mediated autophagy involves the chaperone-mediated transport of proteins from the cytosol into the lumen of the lysosome (Cuervo & Dice, 1996). In crinophagy secretory vesicles from the ER fuse directly with lysosomes, degrading their contents (Glaumann, 1989).

Autophagic degradation is developmentally and nutritionally regulated, so that it is induced in conditions of starvation yet inhibited in conditions of growth. The method of regulation is not fully understood but one of the major regulatory routes is via the protein kinase Tor (Target of Rapamycin). Tor inhibits the initial induction of autophagy in growth conditions, by phosphorylating the autophagic protein Atg1 and also by blocking the signal transduction cascade that controls transcription of several autophagic effector proteins (Klionsky, 2005).

Autophagy is generally considered to be a non-selective response, delivering a random supply of cytoplasmic raw materials for reuse in the cytosol. However, the process has also been implicated in the more targeted degradation of proteins such as the cytoplasmic protein Ald 6 or organelles such as damaged mitochondria or peroxisomes (Onodera & Ohsumi, 2004; Lemasters *et al.*, 1998; Hutchins *et al.*, 1999).

Part 7: Aims of the Project

This project focuses on the *S. mansoni* egg. The egg is important for two reasons – it is the means by which the parasite continues its life cycle and it is the egg proteins that are responsible for the bulk of the pathology in schistosomiasis, including the most serious sequelae.

A few of the egg proteins have been identified and papers published on these on a protein-by-protein basis. No study has been undertaken to look at the egg proteome as a whole, and so the relative abundance of each of these proteins in the egg is not known. This project

undertakes this study and characterises the egg proteome in terms of its development over time as well as its morphological constituents. Egg development over time is studied by comparing SEA preparations derived from immature and mature eggs. The immature egg is a relatively small entity consisting of a developing embryo surrounded by vitelline cells and is immunologically inert. The (much larger) mature egg is an immunogenic, protein-secreting capsule containing a viable miracidium, so significant differences were expected.

The morphological components of the mature egg consist of the miracidium, the hatch fluid (i.e. the water-soluble contents of the egg that are flushed from the egg as it ruptures at hatching) and the ESPs. Each of these have a different biological function, so they are separated, purified where necessary and the proteome of each studied independently.

By comparing the proteomes of each of these egg components a picture emerges as to how protein expression is linked to development, morphology and biological function, thereby providing a context in which to look at the previously described egg components. This is important because the pathology and immunology of schistosomiasis varies with time (changing from a Th1-dominant response to a Th2-dominant one and then subsequently down-modulating in chronic infection). An understanding of when and where proteins are expressed plus their abundance can then be accounted for in these processes. For example, exclusively miracidial proteins will not be accessible to the host's immune system until the egg has matured, died and disintegrated. This will be at a later time point than when the immune system can respond to ESPs, which are expressed when the egg is still alive but mature. Proteins present exclusively in the immature egg will not be accessible to the immune system at all, unless the eggs rupture before maturation for some reason, or the proteins are also expressed in the vitellaria of disintegrating female worms. The relative abundance of the vaccine candidates can also be assessed. This is of importance because there is a potential problem with tolerisation if a vaccine candidate is highly expressed in the mature egg, because large quantities of the antigen may be presented to the immune system as eggs degrade.

ESPs are studied in more detail, because they are of particular interest in that they are the first egg proteins that are readily accessible to the immune system. ESPs probably play a

role in egg escape across the gut wall and so are likely to be inherently immunogenic. HPLC is utilized in an attempt to purify individual components from crude ESP and some assays are carried out to assess the extent of ESP immunogenicity.

Finally, this thesis goes on to look at the proteasome/ubiquitin protein degradation pathway in the egg. It would be logical if protein degradation in the immature egg is fundamentally different from that in the mature egg, because the former requires a supply of amino acids from vitelline cells for growth and the latter needs to repair damage inflicted by the host leukocytes of the granuloma. This hypothesis is tested utilizing Western blots to compare the pattern of ubiquitination and proteasome expression in the different egg preparations. A functional assay to compare the amount of proteasome activity is also conducted.

Chapter 2

A Proteomic Analysis of the *Schistosoma mansoni* egg

2.1 Introduction

S. mansoni eggs are important because they are the means by which the parasite transmits itself between the definitive and intermediate hosts, as well as being a key contributor to the pathology of schistosomiasis when they become embolised in the liver. Describing the proteome of the egg is therefore of value because it could highlight proteins that are potentially capable of inducing pathology, which may be useful in ameliorating the disease.

As discussed in Chapter 1, the egg needs the granuloma cells to cross the gut wall and emerge into the external environment, but while doing so it must defend itself from the toxic compounds that those leukocytes secrete. Therefore, some egg proteins are likely to be involved in the recruitment and activation of the granuloma cells whilst others will be required to protect the miracidium from the damage that the host cells could potentially inflict upon it. Understanding more about the egg proteome will therefore also increase our understanding of the biology of the egg in terms of its interactions with the host.

2.1.1 Previous Work Studying the Schistosome Egg Proteome

Chapter 1 details the research carried out to date focussing on the *S. mansoni* egg, including its morphology, protein components and their immunogenicity and function. The research can be summarised as consisting of various immunological assays using crude SEA plus a series of papers that identify some of the immunogenic SEA components on a protein-by-protein basis. There are also two papers that have compared the proteomes of different life-cycle stages in *S. mansoni* and *S. japonicum* (including the egg), and these have paved the way towards the more detailed characterisation of the *S. mansoni* egg-proteome which constitutes this chapter. The first of these papers (Curwen *et al.*, 2004) compared the 2-DE pattern of spots across four *S. mansoni* life-cycle stages and then identified the forty most abundant soluble proteins in each using their PMFs. This work demonstrated that 34% of the SEA proteome was different to that of other life-cycle stages and that SEA was rich in glycolytic enzymes, structural proteins, calcium binding proteins and chaperones. The second paper is a proteomic study of *S. japonicum* that used Electrospray-MSMS to generate lists of proteins found in several life-cycle stages including the egg and the miracidium (Liu *et al.*, 2006). A total of 1440 SEA and 918 miracidial proteins were

identified, but the list is so large and diverse in terms of protein function that it is impossible to draw meaningful conclusions from it. Relative abundances of the proteins were quantified by comparing the total MASCOT ion scores for each protein. The problem with measuring protein abundance in this way is that it overestimates the abundance of larger proteins (with more peptides, each contributing to the ion score) and proteins with more ionisable peptides. Large differences in ion scores are therefore required before comparisons can be made as to levels of protein expression. Unfortunately, the ion scores in the Liu *et al* study were too similar to make between-protein comparisons of abundance, but the *S. japonicum* egg certainly contains large quantities of actin, tubulin and heat shock proteins. The glycolytic enzymes that Curwen *et al.*, (2004) found highly expressed in gels of *S. mansoni* SEA were less abundant in the *S. japonicum* egg according to Liu *et al.* (2006), but this probably reflects the highly soluble nature and intermediate size/*pI* of the glycolytic enzymes, which makes them more amenable to gel-based proteomics.

2.1.2 The Miracidium, the Hatch Fluid and their Proteomes

The miracidium hatches when the egg encounters fresh water, with the hatching rate decreasing if the salinity of the external environment is increased (Kassim & Gibertson, 1976). As discussed below, the mechanisms that cause the egg shell to rupture have been the subject of most of the research focussing on the miracidium, but miracidial morphology and miracidial-snail interactions have also received attention. Apart from the Liu *et al.*, (2006) paper discussed above, the miracidial proteome is unstudied.

There are three different theories as to the mechanism by which the egg hatches. These are that the muscular activity of the miracidium causes the shell to break (Samuelson *et al.*, 1984), that an enzyme is secreted by the miracidium, envelope or vesicles and this degrades the shell (Kusel, 1970; Xu & Dresden, 1986) and that osmotic pressure causes cushions inside the shell to expand, rupturing the shell (Kassim & Gibertson, 1976). It has been proposed and disputed that hatching is induced by light (Standen, 1951; Kassim & Gibertson, 1976) and temperature (Samuelson *et al.*, 1984; Standen, 1951). Thus, the mechanisms causing the shell to rupture remain unknown, but they certainly involve hydrostatic pressure. Only mature eggs containing fully-developed miracidia are capable of

hatching (Boros & Warren, 1970; Xu & Dresden, 1989) although one paper indicated that the miracidium does not necessarily need to be alive (Kusel, 1970).

The overall ultrastructure of the miracidium has been studied using TEM (Pan, 1980) and its musculature described using confocal fluorescence microscopy (Bahia *et al.*, 2006). Liu *et al.*, (2006), found actin, Sm-p40, tubulin and adenosine triphosphate (ATP) synthase to be highly expressed in the *S. japonicum* miracidium. Thus, the miracidium appears to be principally concerned with energy production, motor function and the maintenance of its structural integrity. The miracidial transcriptome was included in the definitive *S. mansoni* transcriptome study carried out by Verjovski-Almeida *et al.*, (2003) and more recently a microarray experiment comparing transcripts from miracidia and mother sporocysts claimed that only 6-8% of the transcriptome of these stages exhibited stage-specific expression (Vermeire *et al.*, 2006). However, as that particular microarray only contained transcripts from adult worms, cercariae and eggs, any transcripts expressed purely in miracidia or sporocysts would have been undetectable. Thus the paper has a limited value in assessing the extent to which the miracidium differs from the following stage in its life-cycle, but it is evident that the *S. mansoni* miracidial transcriptome is rich in message encoding proteins involved in energy metabolism, motility and calcium-binding proteins.

When the egg ruptures and the miracidium escapes, many other egg proteins will also be released. Some of these will be from the fluid layers found between the miracidium and the envelope and the envelope and the shell, including ESPs *en route* to secretion from the egg. The flooding of the shell with fresh water will induce an osmotic shock on the cells of the envelope, causing many to burst and release their intracellular proteins. The envelope is also torn as the miracidium emerges and can often be seen protruding from the empty shell. The vesicles, which can be seen to contain a viscous liquid under compound microscopy also regularly burst on hatching. The hatch fluid therefore represents a significant subset of egg proteins derived from several different structures in the egg, the proteome of which is likely to differ extensively from that of the miracidium. Despite its potential interest as a subset of egg proteins, hatch fluid remains relatively unstudied. Boros & Warren (1970) found hatch fluid to be capable of sensitizing naïve mice to a subsequent injection of live eggs. Xu & Dresden (1986) found leucine aminopeptidase to be enriched for in hatch fluid

compared to miracidial and SEA preparations and thought that the protease could cleave shell proteins, causing the shell to rupture. However, protein concentrations were not measured, so the differences in protease activity between the hatch fluid and the other preparations could be attributable to different quantities of protein in each preparation. Xu and Dresden's decision to assay for leucine aminopeptidase (as opposed to any other proteases) was made because leucine aminopeptidase had been found in SWAP fifteen years earlier (Coles, 1970). Coles (1970) chose the assay because it was one of the few available at the time, so no significance can be attributed to finding leucine aminopeptidase as opposed to any other protease in hatch fluid.

The only other paper relating to hatch fluid is a description of its use in diagnosing schistosomiasis (Linder, 1986). The procedure used hatch fluid from the eggs of an infected animal, adsorbed it onto nitrocellulose paper and then probed it with soybean lectin and anti-SEA antibody. As a diagnostic procedure it is completely pointless because the eggs themselves are diagnostic so there is no point in extracting hatch fluid from them. However, the paper has value in that it demonstrates that hatch fluid contains glycoproteins and it reinforces the Boros & Warren (1970) study that found hatch fluid to be immunogenic.

2.1.3 The Proteome of ESP

A general introduction to ESP forms Part 4 of Chapter 1, so the discussion that follows is restricted to its proteomic analysis. Ashton (2001) separated ESP using 2-DE and numbered the resulting gel-spots ESP1 to ESP22. A copy of the gel used to name the ESPs is reproduced as Figure 2.1. The spots were excised from the gel, subjected to tryptic digestion and MALDI-MS, but no homology to any other proteins was found when the resulting PMFs were searched against the NCBInr database.

Guiherme Oliveira from Centro de Pesquisas Rene Rachou in Belo Horizonte, Brazil then deposited sequences covering parts of ESP3-6 and ESP15 on dbEST. He then proceeded to provide the plasmids, which were amplified and completely sequenced by Peter Ashton at the University of York. The complete sequences were deposited in GenBank with Accession numbers AAM91992/gi22094805 (ESP3-6) and AAM91993/gi22094807 (ESP15).

Original in colour

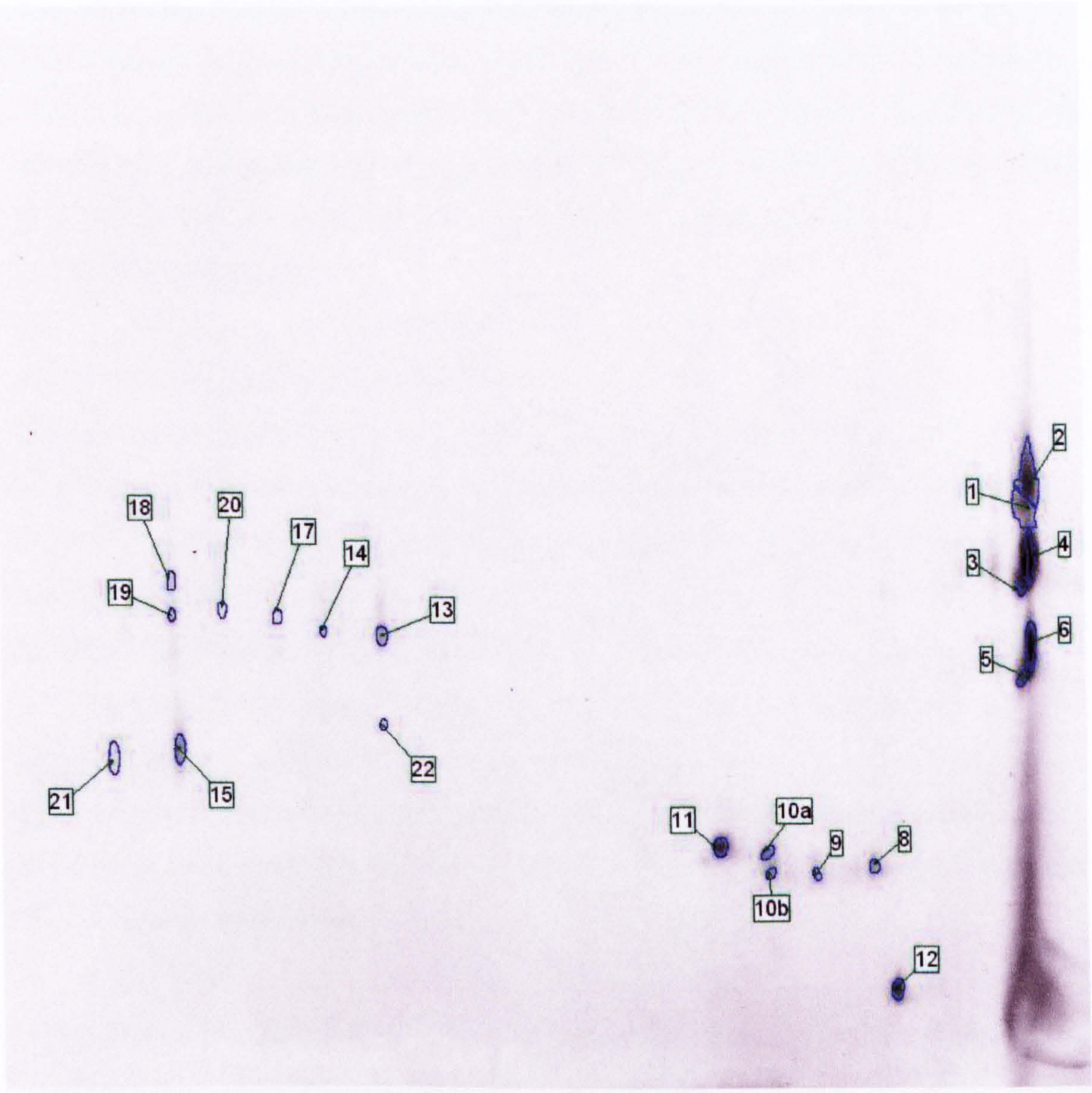

Figure 2.1. A reproduction of the gel from Ashton (2001), containing the original annotations for ESP1 – ESP22. There is no ESP7 or ESP16. MALDI-MS demonstrated that the PMFs of ESPs 3, 4, 5 and 6 were identical, as were those of ESP1 and ESP2, so in total there were sixteen different ESPs. ESP 3-6 and ESP 15 were subsequently sequenced and the sequences deposited on GenBank.

As discussed in Section 1.4.1, ESP3-6 is the same as the IPSE protein described by Schramm *et al.*, (2003), but there are small sequencing differences between them. Specifically, amino acid 29 of IPSE is leucine (it is methionine in ESP3-6), amino acid 41 of IPSE is glutamic acid (it is unidentified in ESP3-6) and amino acid 56 of IPSE is valine (it is glutamic acid in ESP3-6). These sequence differences meant that IPSE was separately deposited on GenBank as a slightly different protein (accession number AAZ85122/gi73765569).

2.1.4 Albumin and the *S. mansoni* Egg

Albumin makes up about 50% of the protein content of vertebrate serum, in which it has ligand-binding, transport, antioxidant and osmo-regulatory roles (Quinlan *et al.*, 2005). It has recently been proposed that an albumin gene has undergone lateral gene transfer from a mammalian host to *S. mansoni*, and that "*S. mansoni*-albumin" benefits the parasite by protecting the schistosomula and adult worm against oxidative damage (Sayed *et al.*, 2006; Williams *et al.*, 2006). Albumin became relevant to the *S. mansoni* egg proteome during the course of the work involved in this chapter because host albumin was found to be present inside the egg. A further experiment was therefore carried out in which the amino acid sequence of "*S. mansoni* albumin" was compared to that of albumin from another common laboratory host – the hamster.

In the Sayed *et al.*, (2006) paper "*S. mansoni* albumin" was identified by subjecting mRNA from mechanically-transformed schistosomula and adult worms (perfused from a murine host) to reverse transcription-polymerase chain reaction (RT-PCR). A schistosomal origin for the albumin was then claimed because the translated message encoded a slightly different amino acid sequence to that of albumin from the murine host. Also, the mechanically-transformed schistosomula had not been derived directly from the mammal. However, the paper did not include a Southern Blot to demonstrate hybridization between a probe generated from "*S. mansoni* albumin" cDNA and *S. mansoni* genomic DNA – an important experiment as no albumin gene has been found in the genomes of *S. mansoni* or those of any other non-vertebrates. Also, the process of lateral gene transfer in schistosomes is controversial. PCR-based studies have found murine retroviral and MHC sequences and sequences from salmonid fish in schistosome DNA (Imase *et al.*, 2003;

Melamed *et al.*, 2004), but other researchers reject these findings because contamination with host material could explain the results, bearing in mind the amplification power of PCR (Clough *et al.*, 1996; Simpson & Pena, 1991). If the amino acid sequence of "*S. mansoni* albumin" was found to be the same as that of hamster albumin (which is not a natural host for *S. mansoni*) then the prospect of a schistosomal origin for albumin is yet more unlikely.

2.1.5 The *S. mansoni* Genome and the SchistoCDS Database

The identification of *S. mansoni* proteins by mass spectrometry depends upon the extent to which its genome has been sequenced and the number of matches that can be made to sequences from other species that have been deposited on searchable databases. The *S. mansoni* genome sequencing project has been carried out by the Sanger Institute (Cambridge, UK) and The Institute for Genomic Research (Rockville, USA). It is nearing completion, with a 6-fold coverage having assembled 300Mb of DNA, encoding about 17,250 genes (Wilson *et al.*, 2007). Gene finding has been greatly assisted by a separate project that characterised an estimated 92% of the transcriptome, culminating in the release of 163,586 ESTs, including 19,077 from the egg and 18,638 from the miracidium (Verjovski-Almeida *et al.*, 2003). Thus, the searchable EST database is of sufficient size to facilitate proteomic studies of the parasite. The peptide searches in this chapter have used the nrNCBI and Schisto CDS databases. Schisto CDS is a database made up 14,000 contigs, annotated with the ESTs (generating accession numbers prefixed with Sm) and genes predicted by the programs Glimmer, Phat and Snap. Once peptides have been matched to ESTs or gene predictions, functional properties for the protein are obtained by searching the whole protein sequence for matches in other organisms, including conserved functional domains.

2.1.6 Analysing the *S. mansoni* Egg Proteome: the Approach

The characterisation of the egg proteome was based on fractionating the egg and studying the proteome of each fraction separately using 2-DE followed by MALDI-MSMS. Changes in the egg proteome over time was studied by comparing preparations made from the vitellaria-containing region of sectioned females and SEA, made either from immature or

mature eggs. The mature egg was then fractionated into its constituents – the miracidium, its secretions (ESP) and the hatch fluid and the proteomes of each studied separately.

The Phoretix Evolution software package (NonLinear Dynamics) was used to compare the 2D gels. The program matches spot patterns between the different gels and highlights those spots that are common to more than one gel. When a quantitative stain such as Sypro Ruby is used, Evolution can calculate the volume of each spot as a proportion of the total spot volume in the gel, enabling between-gel comparisons of protein expression levels. Evolution works by copying the image of the gel which contains the highest number of spots and then using it as a theoretical "reference gel". The preparative gel that is most similar to the reference gel is then superimposed on top of it and the spots in each coloured differently. Where spots overlap (i.e. have a similar *pI* and mass) they appear black and a "match" is created. Once all of the shared spots have been matched, the unmatched spots on the preparative gel are added to the reference gel. The reference gel now contains all of the spots from two preparations, and the process can be repeated for a third preparative gel. Once this process has been completed for all of the gels, every spot in the experiment can be matched, via the reference gel, to any matching spots in any of the other gels in the experiment and the relative expression levels of shared spots can be calculated.

Upon completion of the Evolution analysis, the spots of interest were chosen as per the following criteria and identities sought for them using MALDI-MSMS:

i all miracidial spots (because the proteome of the *S. mansoni* miracidium has not previously been studied).
ii all hatch fluid spots (because hatch fluid is almost completely unstudied).
iii all ESP spots (because the ESPs have not been subjected to MSMS).
iv the "top forty" spots in terms of protein volume in the vitellaria-enriched preparation, immature SEA and mature SEA (so that the most significant maturational changes in the egg proteome can be seen).
v any spots that are present in immature SEA but are not found in the mature egg (because they will be involved in the development of the egg rather than its function).

vi any spots present only in mature SEA (because they will not have been accounted for in any other preparation).

With the identities of these spots known, a picture can be constructed of the soluble egg proteome which will reflect the eggs changing priorities as it develops. Then, when the egg is fully mature its functional priorities can be mapped to its morphological components via its proteome.

2.2 Methods

2.2.1 The Infection of Mice and Recovery of Eggs

Male C57BL/6xCBA (B6CBA) mice were infected with 180 cercariae/mouse of a Puerto Rican isolate of *S. mansoni* via the shaved abdomen as described previously (Smithers & Terry, 1965). Seven weeks later their livers were removed, homogenised (MSE blender) and incubated in 3mM KH_2PO_4 plus 63mM Na_2HPO_4 buffer containing a small quantity of trypsin (Sigma T0303) for 3 hours at 37°C. The degraded liver tissue was removed by sieving the livers sequentially through sieves of 300μm and then 180μm mesh size and cleaned several times with fresh buffer.

2.2.2 Separating Eggs into Mature and Immature Populations

Eggs were separated into mature and immature populations by centrifuging them in a Percol gradient in sterile conditions. The gradient was made using 6ml Percol (Amersham), 3.4ml RPMI-1640 (Gibco) and 0.6ml of 9% saline. After centrifugation for 15-min at 250*g* the mature eggs had collected at the bottom of the centrifuge tube, the immature eggs in a layer 1cm below the surface and empty shells and other debris remained on the surface. The mature and immature eggs were then collected separately, washed seven times in sterile RPMI and the viability and their maturation status assessed using compound microscopy. Almost all (96%) of the eggs in the mature egg fraction contained a live miracidium (muscular contractions and/or flame cell activity could be seen) and 92% of the immature eggs were visibly less developed in that the embryo had not yet become a miracidium.

2.2.3 Preparing Immature and Mature SEA

Aliquots of immature or mature eggs were ground for a total of three minutes in 200μl of M3 buffer (7M urea, 2M thiourea and 4% CHAPS) containing 20μl of PIC (a general purpose protease inhibitor cocktail (Sigma P1860)). The grinding was carried out on ice with a polypropylene pestle (Sigma) attached to a Kontes motor (Fisher) in three cycles of one minute grinding followed by one minute rest on ice. This brutal treatment was needed to rupture the egg shells. Grinding rather than sonication was adopted because many eggs remained intact after repeated sonication steps and the sonication generated a considerable

amount of heat. The egg homogenate was then centrifuged at 25,000*g* and 20°C for one hour, the supernatant collected and stored at -18°C and the pellet at -80°C until required.

2.2.4 Preparing ESP

Aliquots of approx 250,000 mature eggs were incubated in 10ml of RPMI-1640 (Gibco) containing 3% penicillin/streptomycin sulphate (Invitrogen) and 0.1% gentamycin solution (Sigma) at 37°C and 5% CO_2 for 72-hours. The culture media was then replaced and a further incubation step carried out. After each period of incubation eggs hatched successfully when immersed in fresh water and 96.5% of them contained viable miracidia. The culture media, containing the ESP was gravity-filtered through a 0.2µm filter (Sartorius), concentrated in a 5kDa cut-off polyethersulphone centrifuge concentrator (Vivaspin 20) and stored at -18°C until required.

2.2.5 Making the Miracidial and Hatch Fluid Preparations

Mature eggs were hatched in a 15ml, glass test-tube containing sterile, aerated water at 25°C. Light was excluded from the bottom 12ml of the water column and a cold light source used to illuminate the top 3ml. After one hour most of the eggs had hatched and the top 5ml and bottom 3ml of water were collected. The top 5ml fraction (containing most of the miracidia) was filtered through a 0.2µm polyethersulphone filter (Millipore). As soon as the filtration was completed (retaining the miracidia in a negligible volume of water on the filter) the filter was washed with 800µl of M3 buffer containing 20µl PIC into a 1.5ml eppendorf. Aliquots of 200µl miracidia suspension were immediately ground and stored as in SEA (Section 2.2.3).

The bottom 2ml fraction of water (which contained only a few miracidia) was gently agitated to flush any material from empty shells. Then, the liquid (containing hatch fluid, empty shells, some miracidia plus a few un-hatched eggs) was gravity-filtered (to avoid rupturing any miracidia) through a sterile 0.2µm cellulose acetate filter (Sartorius). The filtrate (containing the hatch fluid) was concentrated and stored as per ESP, but with the addition of 20µl PIC.

2.2.6 Making the Female, Vitellaria-Enriched Preparation

Worms were recovered from 7-week infected B6CBA mice by portal perfusion with RPMI-1640 (Gibco) to which 10% FCS, 2.5% HEPES and 5 units heparin/ml (all Sigma) had been added. Adult, paired females were separated from the males using two fine brushes and then washed three times in RPMI-1640 to remove the FCS. The females were then severed laterally immediately below the ventral sucker. The posterior sections (containing the vitellaria) were immediately ground in M3 buffer containing PIC, centrifuged and stored as in the SEA protocol.

2.2.7 Determining Protein Concentrations

Protein concentrations in buffers other than M3 were quantified using the Coomassie Plus Bradford Assay Kit (Pierce). For m3-buffered samples (i.e. the SEA, miracidial and vitellaria-enriched preparations) the Bradford assay was found to be inappropriate because reproducible measurements could not be obtained (possibly due to the presence of urea/thiourea in the M3 buffer). The protein concentrations of these preparations were therefore assessed by separating 20µl of each sample by 1-DE in the same gel as a known quantity of *S. mansoni* soluble cercarial antigen preparation buffered in phosphate buffered saline (PBS). The gel was stained with Sypro Ruby stain (Biorad), imaged on a Molecular Imager (Bio-Rad FX) and between-lane comparisons of staining intensity used to assess protein concentrations.

2.2.8 One-Dimensional Electrophoresis

2.2.8.1 1-DE of Insoluble Egg Proteins

The pellets containing the M3-insoluble material from the SEA, miracidial and vitellaria-enriched preparations (see 2.2.3, 2.2.5 and 2.2.6) were washed twice in 40mM Tris HCl pH7.4 (30 min/wash) then solubilized for 20 min at 70°C in 12.5µl 300mM lithium dodecyl sulphate sample buffer (Invitrogen) plus 32.5µl doubly-distilled water (dd H_2O) and 5µl of 10x reducing agent (Invitrogen). After centrifugation (30 min at 25,000*g*) the supernatant was separated according to molecular mass on a NuPAGE 4-12% Bis Tris gel (Invitrogen) at 200V for 40 minutes and stained with Biosafe Coomassie (Bio-Rad)

2.2.8.2 1-DE of All Other Samples

Proteins were prepared for electrophoresis by adjusting their concentration to 750µg/ml and solubilizing them in 300mM lithium dodecyl sulphate sample buffer (Invitrogen) at a ratio of 3:1. Proteins were reduced and denatured with Reducing Agent (Invitrogen NP0004) and heating at 65°C for 5 mins. A 10µg sample of denatured protein was applied per lane to a NuPAGE 4-12% Bis Tris gel (Invitrogen) and electrophoresis performed at 200V for 40 minutes. Gels were fixed in 40% methanol/10% acetic acid solution and stained as indicated.

2.2.9 Two-Dimensional Electrophoresis

2.2.9.1 2-DE for Protein Staining

To prepare samples for 2-DE, 250µg immature SEA, mature SEA, miracidial and vitellaria-enriched preparations were adjusted to 360µl with M3 buffer, to which 3.5µg dithiothreitol (DTT) (Amersham), 2.8µl of pH3.5-10 resolytes (BDH) and 1µl bromophenol blue had been added. A 75µg sample of crude ESP was dialysed for 18 hours at 4°C into 20mM Tris HCl pH7.2 with a Slide-A-Lyzer dialysis unit (Pierce), concentrated to 35µl with an Amicon Ultrafree centrifugal concentrator (Millipore) and solubilized in 325µl of rehydration buffer (M3 containing 3.25µg DTT, 2.8µl pH3.5-10 resolytes and 1µl bromophenol blue). A 250µg sample of hatch fluid was concentrated to 50µl and then solubilized in 310µl rehydration buffer. The preparations were then separated according to their charge by IEF in an 18cm, pH 3 – 10 strip (Amersham) at 20°C, utilizing an IPGPhor system with in-gel rehydration (Amersham). After allowing 12 hours for the strip to rehydrate, the IEF protocol involved three focussing steps at a constant 50µA/strip: 3 hrs gradient to 3500V, 3 hrs at 3500V and finally 64000Vhrs. Focussed proteins were reduced (1% DL-dithiothreitol (Sigma)) and alkylated (4% iodoacetamide (Sigma)) in-gel and then the IEF strips were transferred to the top of 20cm x 24cm x 0.1cm, 9-16% SDS-PAGE gel (containing piperazine di-acrylamide (Bio-Rad) rather than bis-acrylamide). Separation in the second dimension by molecular mass was then carried out in a Protean Plus Dodeca cell system (Bio-Rad) at 200V until the dye approached the bottom of the gel (approx 7 hours). The gels were then fixed in 40% methanol/10% acetic acid solution, stained with Sypro Ruby and imaged on a Molecular Imager (Bio-Rad FX).

2.2.9.2 2-DE for Glycoprotein Staining

A 35µg sample of hatch fluid was prepared for 2-DE using the protocol described above, except a 7cm, pH 3 – 10 IEF strip (BioRad) was used. After 12 hrs strip rehydration, IEF was carried out at a constant 50µA with the following voltage changes: 30 mins at 500V, 30 mins at 1000V and finally 3 hours at 8000V. After reduction and alkylation (as described above) the strip was transferred to a precast, 7cm NuPAGE 4-12% Bis-Tris gel (Invitrogen) and protein separation by molecular mass was carried out for 40 mins at 200V. The gel was stained with Sypro Ruby, then with Pro-Q Emerald 300 glycoprotein stain (Molecular Probes) as per the manufacturers instructions and imaged on a Versadoc 3000 (BioRad).

2.2.10 Protein Digestion and Preparation for MALDI-MSMS

Sypro Ruby-stained gels were restained with Biosafe Coomassie so that the spots could be seen without an imager. All discernible spots were excised from the gels and destained with 40% methanol/10% acetic acid solution. The gel pieces containing spots selected for MALDI-MSMS were washed in 20mM ammonium bicarbonate/50% acetonitrile solution, dehydrated in 100% acetonitrile (ACN), dried in a Speedvac (Thermo Lifesciences) and then digested into peptides overnight at 37°C with 20µl of 10µg/ml sequencing grade porcine trypsin (Promega). The peptides from each spot were then absorbed onto a C_{18} ZipTip (Millipore) by repeated pipetting, desalted by three washing steps with 0.1% trifluoroacetic acid (TFA) (Fluka) and then eluted with 80% ACN/0.1% TFA solution into 5µl aliquots. The peptide solution (2µl aliquots) were then mixed with 1µl of matrix solution (α-cyano-4-hydroxycinnamic acid (Sigma)) saturated in a 50% ACN/0.1% TFA solution) and dried onto a MALDI plate. The gel spots were prepared for mass spectrometry in spot sets of 40 spots per MALDI plate, with the 16 spot sets taking ten months to complete.

2.2.11 MALDI-MSMS

An Applied Biosystems 4700 MALDI-ToF-ToF mass spectrometer operating in positive ion reflector mode was used to analyse the tryptic peptides. The mass spectrometer was calibrated using a mix of des-Arg bradykinin (*m/z* 904.4681), angiotensin (*m/z* 1296.6853), glu-fibrino-peptide B (*m/z* 1570.6774), adrenocorticotropic hormone clip 1-17 (*m/z*

2465.1989) and adrenocorticotropic hormone clip 7-38 (*m/z* 3657.9294) and its settings adjusted for optimum efficiency. Each spectrum was acquired using 1500 laser shots/spot at 2800–3500V and calibrated using tryptic autolysis peaks at *m/z* 842.510 and 2211.104. Protein identification was performed using the Mascot search engine (http://www.matrixscience.com) which uses a probability-based scoring system (discussed in Section 1.5.2). The searching parameters were set so that only MSMS fragmentation data with a tolerance < 0.2Da was used. One missed cleavage was allowed for, as were carbamidomethylation modifications to the cysteine and oxidation of the methionine residues. The searches were made against the NCBInr and SchistoCDS databases and matches only accepted if the total peptide ion score confidence intervals were >99.9%. A more recent version (v 4.0) of the *S. mansoni* genome has recently become available and so the identified proteins have also been searched against it using GeneDB (Hertz-Fowler *et al.*, 2004). Version 4.0 of the genome uses the same Sm numbers as Schisto CDS, but different gene prediction programs: Augustus, Evidence modeller (EVM3 and EVM7), Glimmer and Twinscan predictions, prefixing all the predicted gene annotations with Smp.

2.2.12 Electrospray-MSMS of *Mesocricetus auratus* Albumin

Serum from an uninfected Golden Hamster (*M. auratus*) was separated by 1-DE as described in 2.2.8.2, the gel stained with Biosafe Coomassie and the prominent 60-65kDa band excised from each lane and pooled. The gel pieces were destained with 40% methanol/10% acetic acid solution, the proteins reduced (50mM DTT at 65°C for 30 mins), alkylated (100mM iodoacetamide for 1 hour), washed and digested overnight using the protocol detailed in 2.2.10. Immediately after digestion the peptides were applied into a 100µm x 5cm Monolith nano LC column (Dionex) in 2% ACN plus 0.1% formic acid and then eluted over 15 minutes with 100% ACN plus 0.1% formic acid in a 0-50% linear gradient. The eluate was injected into an Applied Biosystems QSTAR Pulsar mass spectrometer, which carried out MS and MSMS analysis in repeated 0.5 second cycles. The entire Elecrospray-MSMS run was then repeated. Mascot was used to search the peptide fragmentation data against the nrNCBI database using 99.5% confidence limits.

2.3 Results

2.3.1 Gels of Egg Proteins

2-DE was used to separate the soluble proteins in the vitellaria-enriched preparation, immature SEA, mature SEA, miracidium, hatch fluid and ESP (Figures 2.2–2.7). Apart from in the ESP gel, spots covering a wide range of molecular masses and charges were evident in all of the gels. The ESP gel differed in that it had clusters of spots comparable to those previously described by Ashton (2001) (whose gel is reproduced as Figure 2.1 on page 61). Despite the complex nature of the gels, the immature and mature SEA preparations were quite similar with shared patterns of spots. The gel images were initially analysed by Phoretix Evolution's automatic spot-detection function, but the program incorrectly identified every pin-point of speckling as a separate protein spot (instead of ignoring them as artefacts of the staining process) and so manual spot-detection was undertaken instead. After spot detection, the automatic cross-gel spot matching function grossly warped and distorted the gels in ways that could not possibly be correct, so an extensive amount of manual intervention was required throughout the spot-matching process as well. Manual editing potentially introduces error and bias, but this could be minimised because three-dimensional imaging of small sections of the gel are possible with the software, enabling speckling to be distinguished from protein spots and for overlapping or smeared spots to be separated (see Figure 2.8). Three-dimensional imaging was also useful during cross-gel spot matching because each protein spot had a different shape, so patterns of distinctive shapes could be seen in the different gels, thus providing another parameter that could be used to match spots.

It became apparent during the spot-editing and spot-matching processes that a reasonable amount of similarity between the gels was an absolute requisite for spot-matching to be carried out with any degree of confidence. Unfortunately, the gels of the female, vitellaria-enriched preparation and ESP differed extensively from the other gels in the experiment, so their spots could not be matched. However, spots in the immature SEA, mature SEA, miracidia and hatch fluid gels could be matched with confidence. The accuracy of the spot matching was subsequently demonstrated because spots that had been matched using Evolution were then assigned the same identities following separate MALDI-MSMS runs.

Original in colour

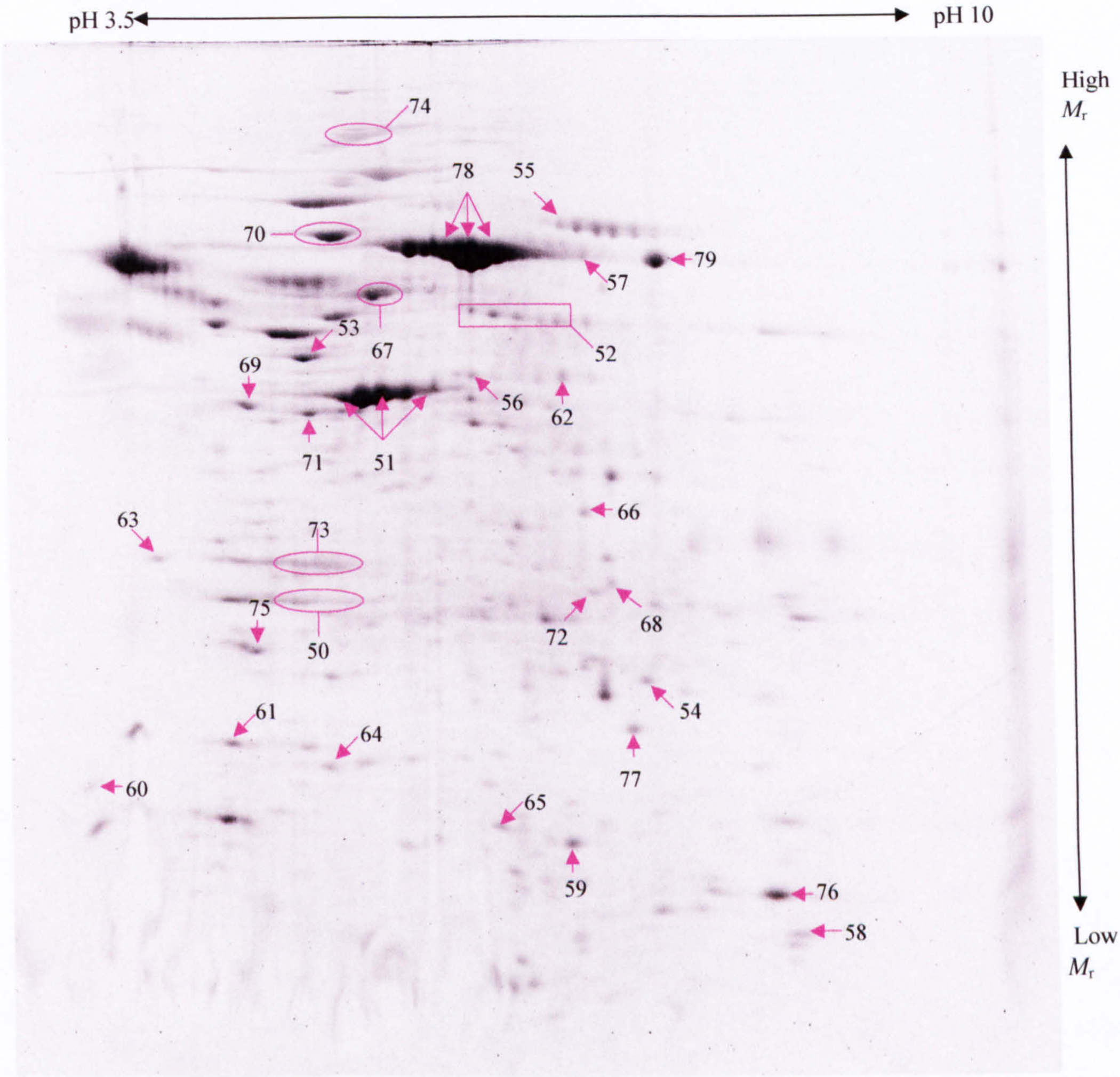

Figure 2.2. Sypro-stained gel of 250µg vitellaria-enriched protein preparation. The identities for the numbered spots are shown in Table 2.1 and the peptide fragmentation data is in Appendix 1.

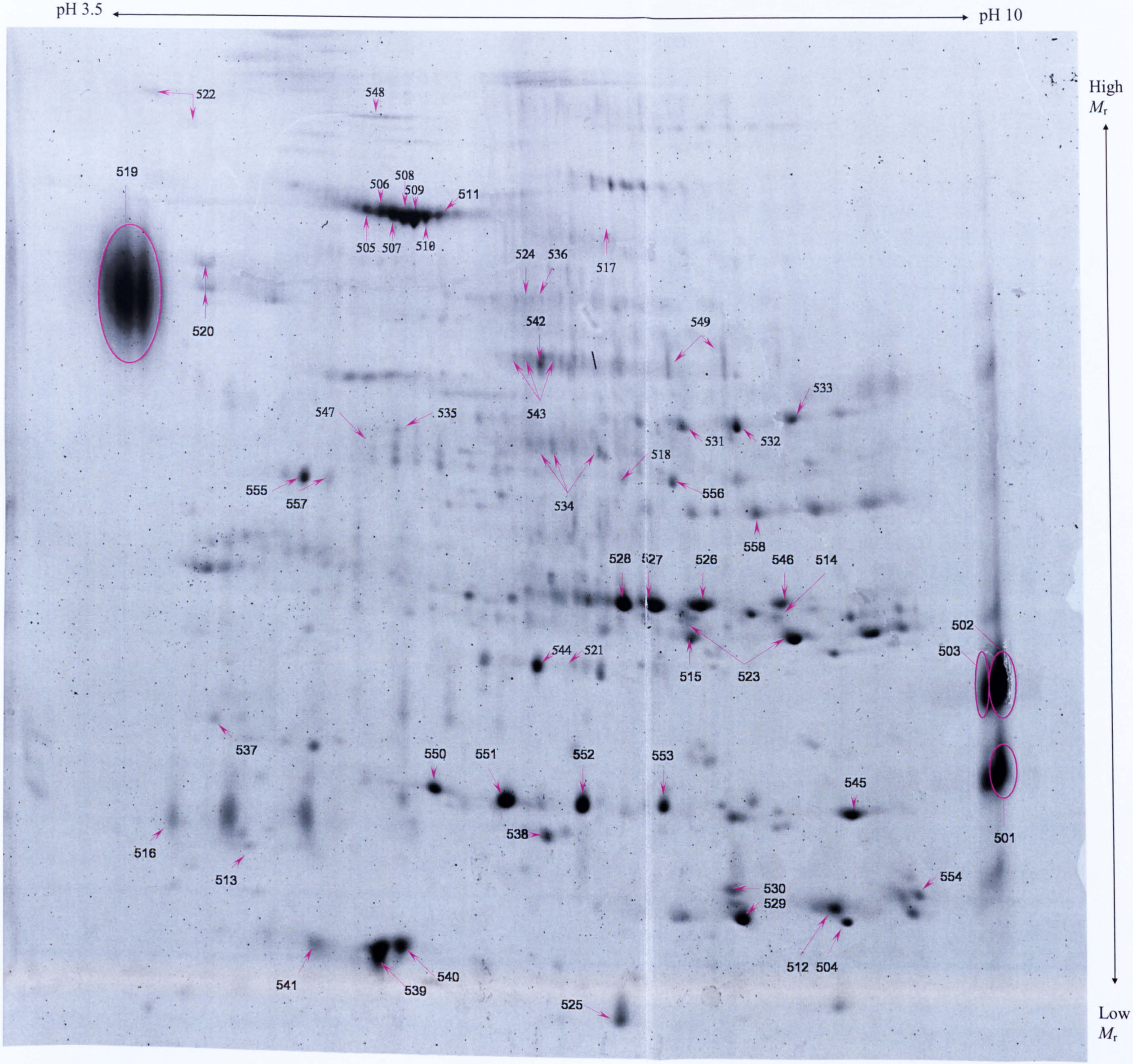

Figure 2.6. Sypro-stained 2D gel of 250µg hatch fluid. The identities for the numbered spots are shown in Table 2.2 and the peptide fragmentation data are in Appendix 1

Original in colour

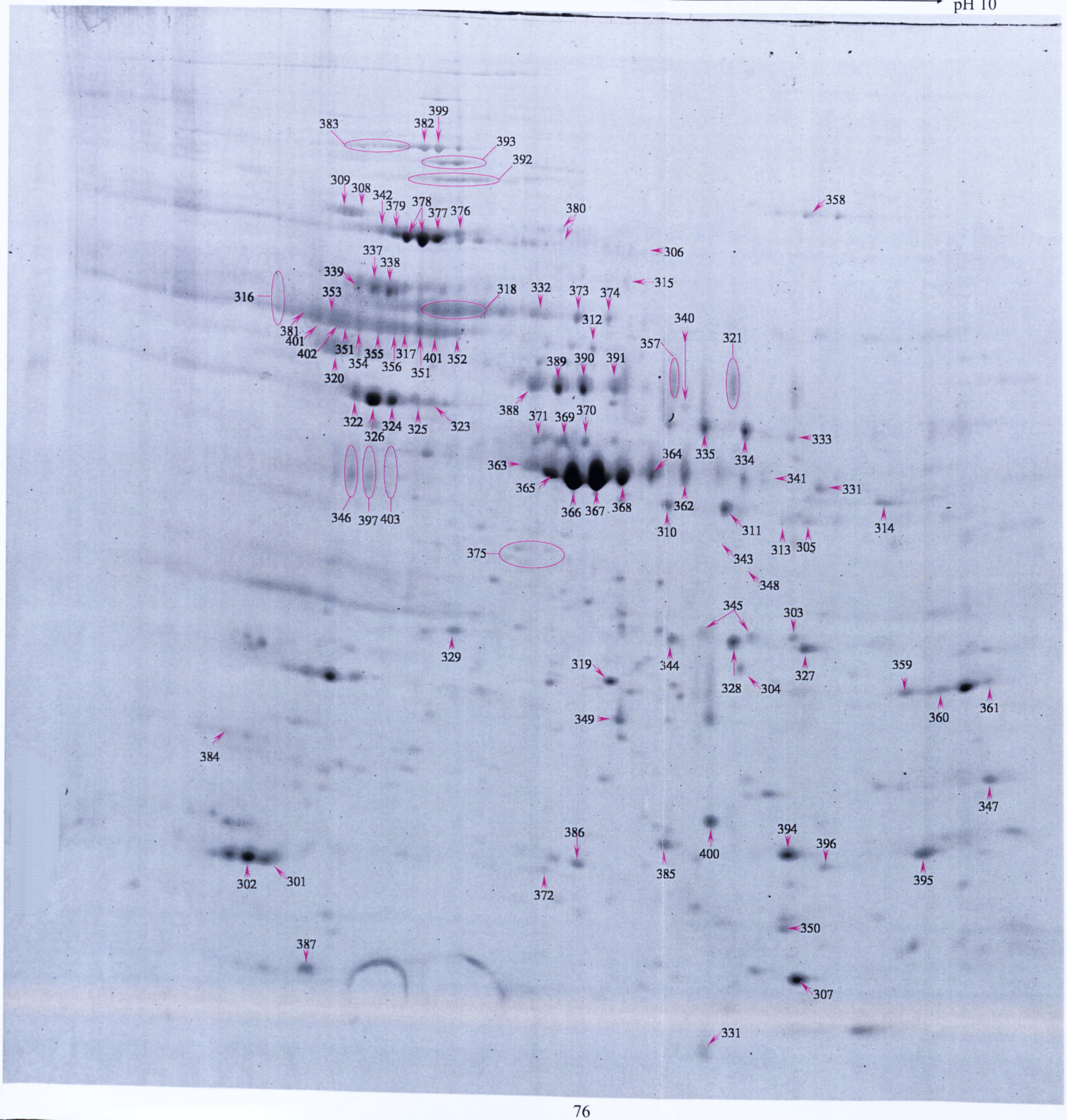

Figure 2.5. Sypro-stained gel of 250µg miracidial preparation. The identities for the numbered spots are shown in Table 2.2 and the peptide fragmentation data are in Appendix 1.

Original in colour

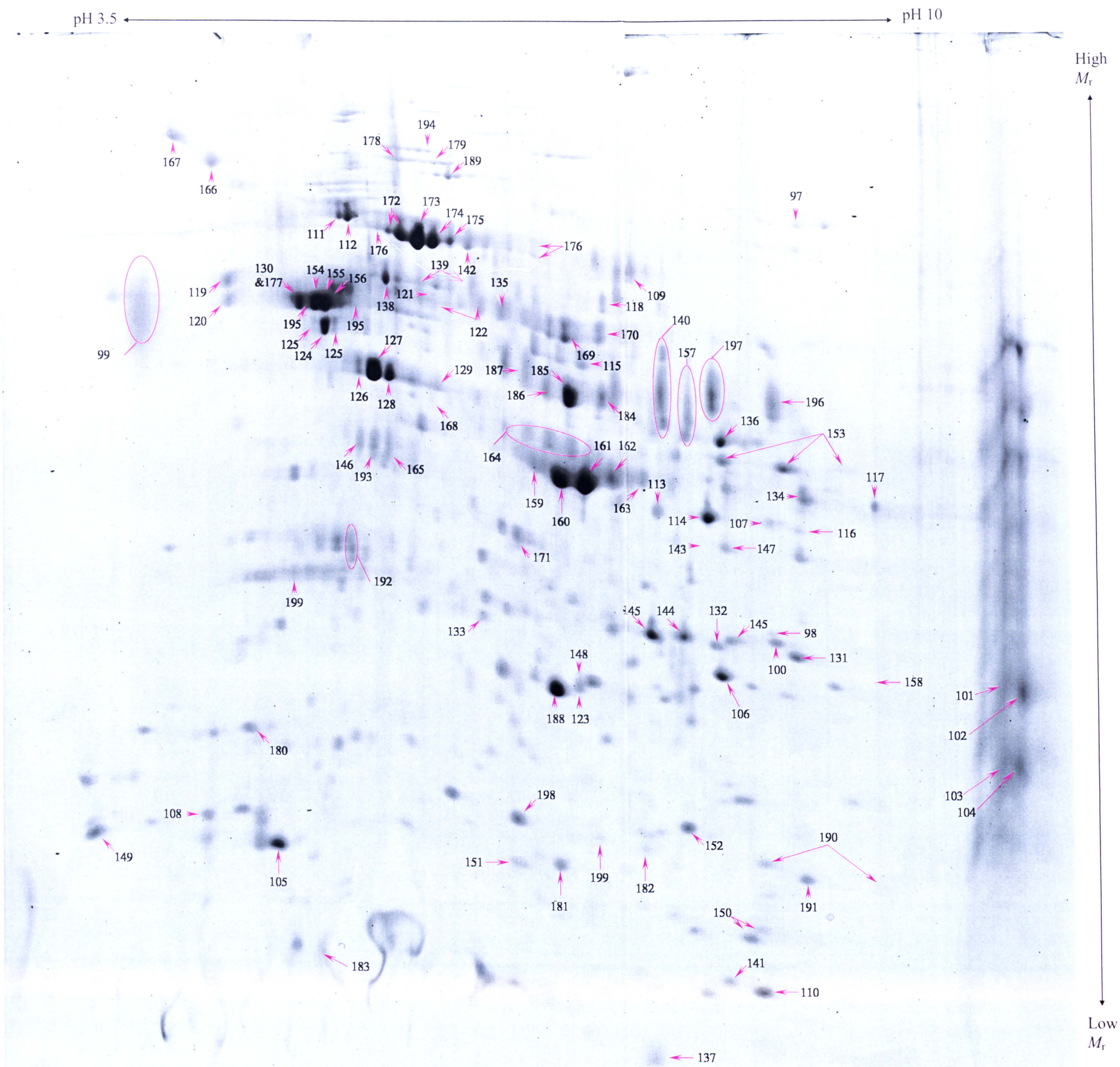

Figure 2.4. Sypro-stained gel of 250µg mature SEA. The identities for the numbered spots are shown in Table 2.2 and the peptide fragmentation data are in Appendix 1.

Original in colour

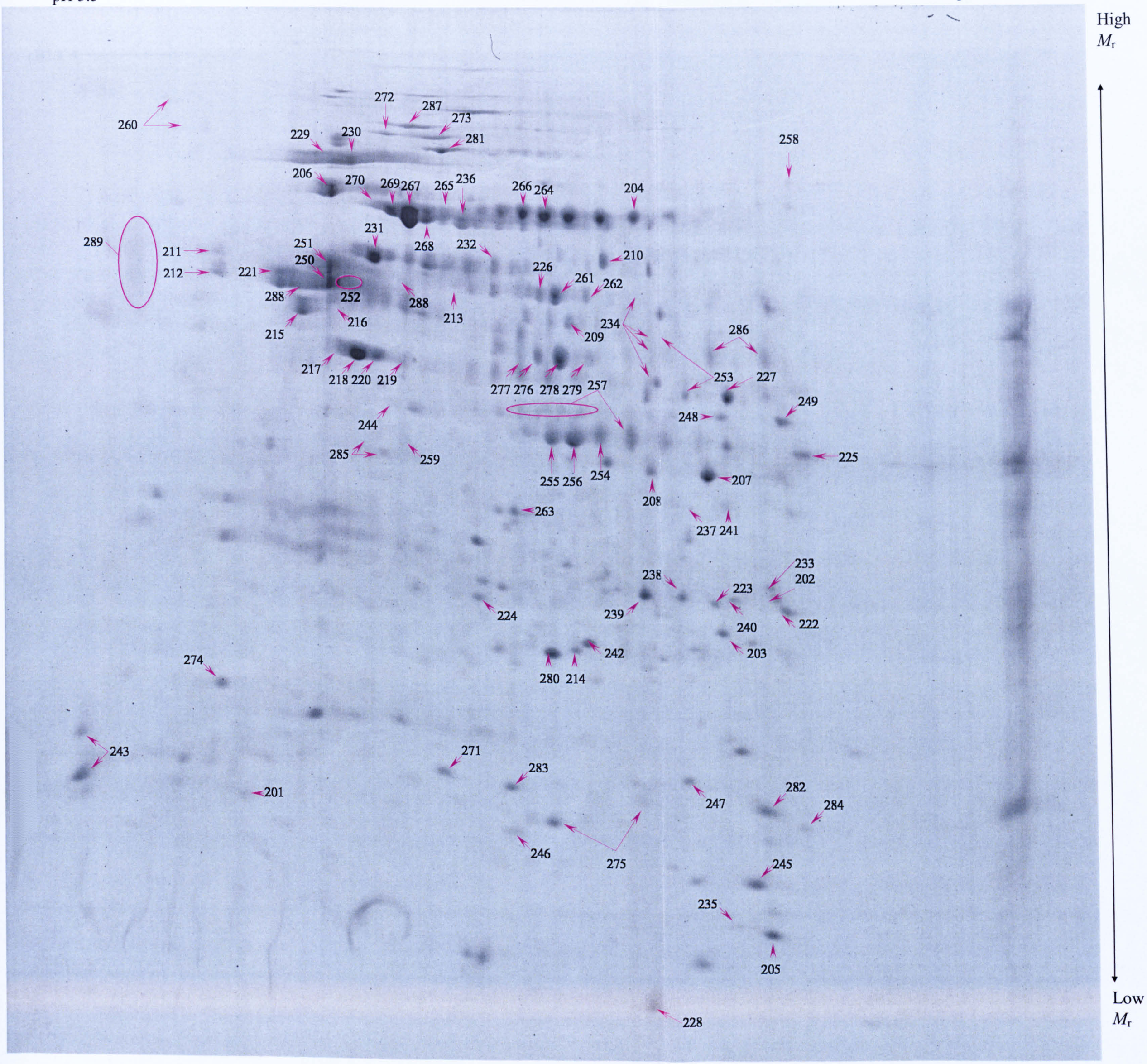

Figure 2.3. Sypro-stained gel of 250µg immature SEA. The identities for the numbered spots are shown in Table 2.2 and the peptide fragmentation data are in Appendix 1.

Original in colour

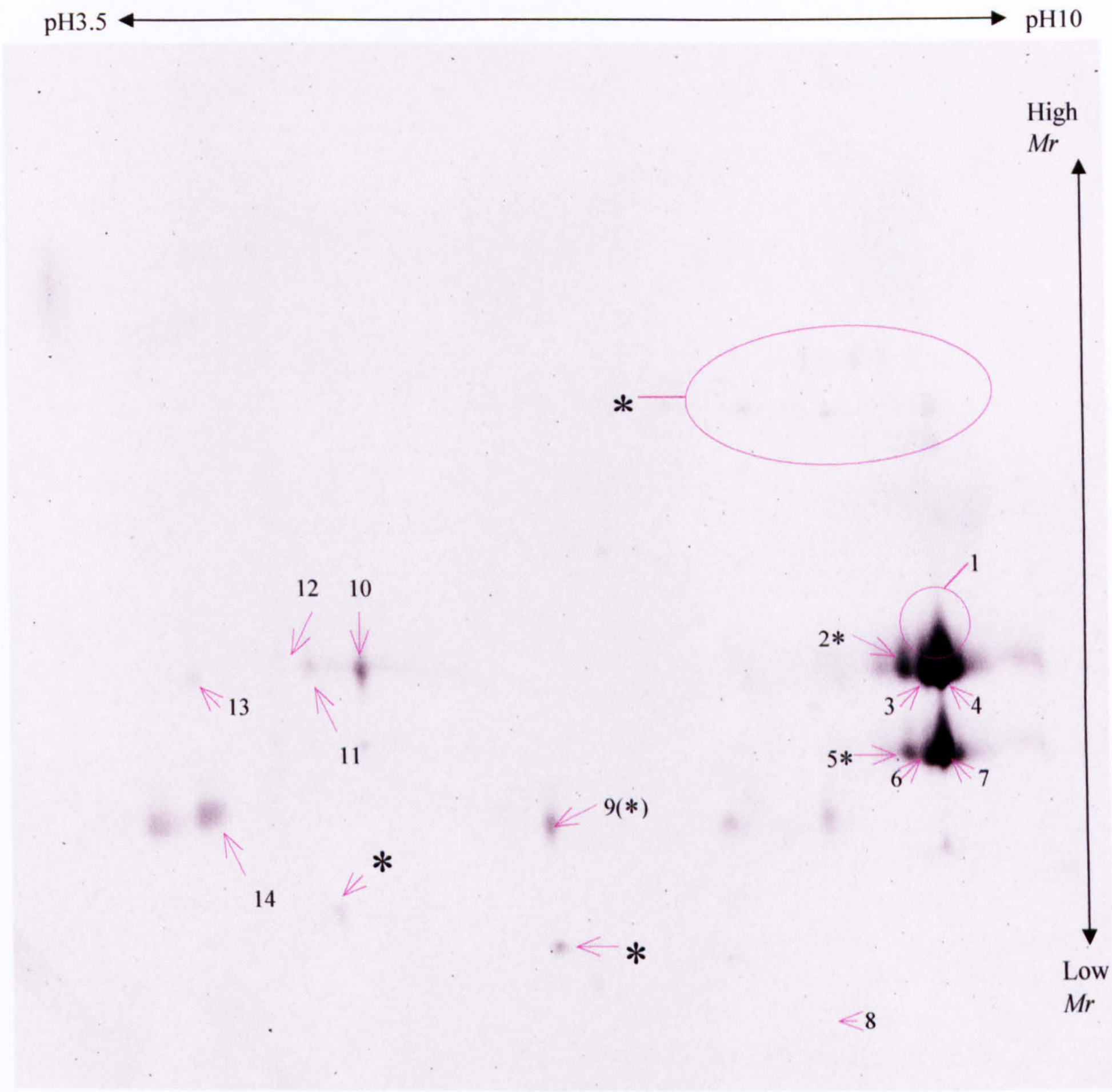

Figure 2.7. Gel of 75µg ESP stained with Sypro Ruby. The identities for the numbered spots are shown in Table 2.3 and the peptide fragmentation data is in Appendix 1. * denotes spots that do not have ESP numbers.

Original in colour

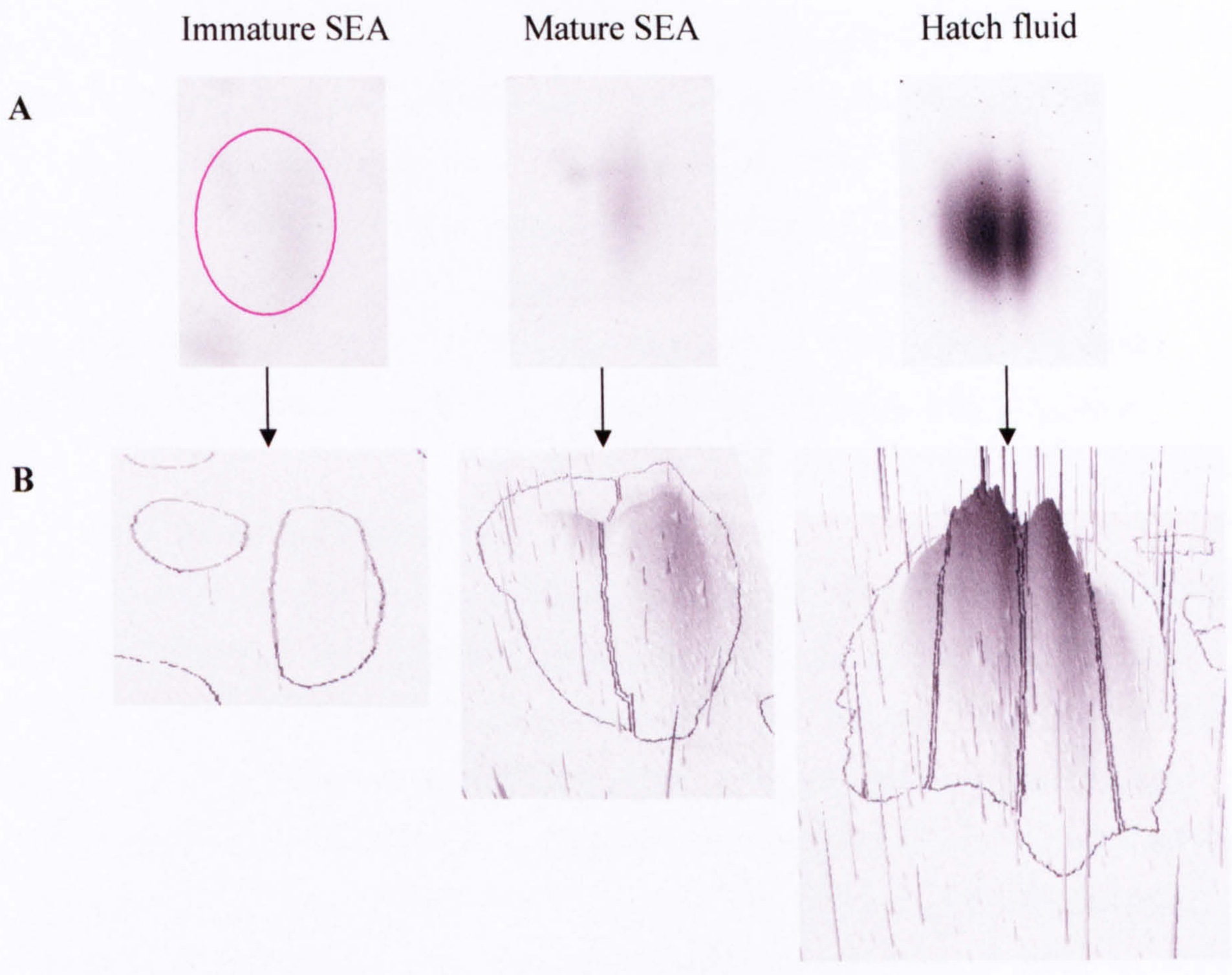

Figure 2.8. Visualising gel spots using Phoretix Evolution software. **A**: A protein (later identified as Smp170410) can be seen in Sypro Ruby-stained gels of immature SEA (Fig 2.3, spot 289), mature SEA (Fig 2.4, spot 99) and hatch fluid (Fig 2.6, spot 519). **B:** 3D images of the spots from A. Mature SEA has increased expression of Smp170410 compared to immature SEA. Significant enrichment can be seen in hatch fluid, allowing four isoforms to be determined. The spikes are speckling artefacts of the stain. **C**: Evolution uses spot volume to calculate protein expression levels. There is 7 times the quantity of Smp170410 in mature SEA compared to immature SEA and 4.4 times more in hatch fluid than in mature SEA.

2.3.2 Most Spots Were in Several Gels

In total there were 1107 different spots in the immature SEA, mature SEA, miracidial and hatch fluid preparations, most of which were present in more than one preparation (Figure 2.9). Immature SEA and mature SEA were the most alike, their shared spots accounting for 84% and 81% of their total protein content respectively. Hatch fluid contained fewer spots than the miracidial preparation (433 as opposed to 602 spots). Hatch fluid and the miracidial preparation differed significantly in that only 33% of the hatch fluid spots (equating to 21% of the total spot volume) were found in the miracidial preparation.

2.3.3 1-DE of M3-Insoluble Proteins

The number spots in a 2D gel does not equate to the number of different proteins present in it. Some proteins have several isoforms, resulting from amino acid substitutions or post-translational modifications such as phosphorylation or glycosylation. Other proteins might contain several disulphide-bonded subunits. These isoforms/subunits would appear as separate spots after 2-DE if they have different isoelectric points and/or molecular masses, and so for these proteins the number of spots that can be seen in the gel will exceed the number of proteins present in the preparation. However, there will be many other proteins whose expression levels are too low to be detected in the gel and a further set of proteins that failed to focus or were insoluble in the 2-DE buffer (see Figure 2.10). It is difficult to assess the extent to which the insoluble material differs between the preparations, especially as different quantities of protein were present in the pellets from each preparation. It is clear from Figure 2.10 however, that significant numbers of proteins are not represented in the 2-DE gels, and therefore the 1107 different spots present on the 2D gels are an underestimate of the number of proteins actually present in the egg.

2.3.4 MALDI-MSMS of 2-DE-Separated Proteins

The criteria by which spots were selected for MALDI-MSMS is explained in Section 2.1.6 (pages 64-65). However, not all of the spots that were originally detected on the gels (using Sypro Ruby stain) could be excised because the Coomassie stain that was subsequently used was less sensitive.

Original in colour

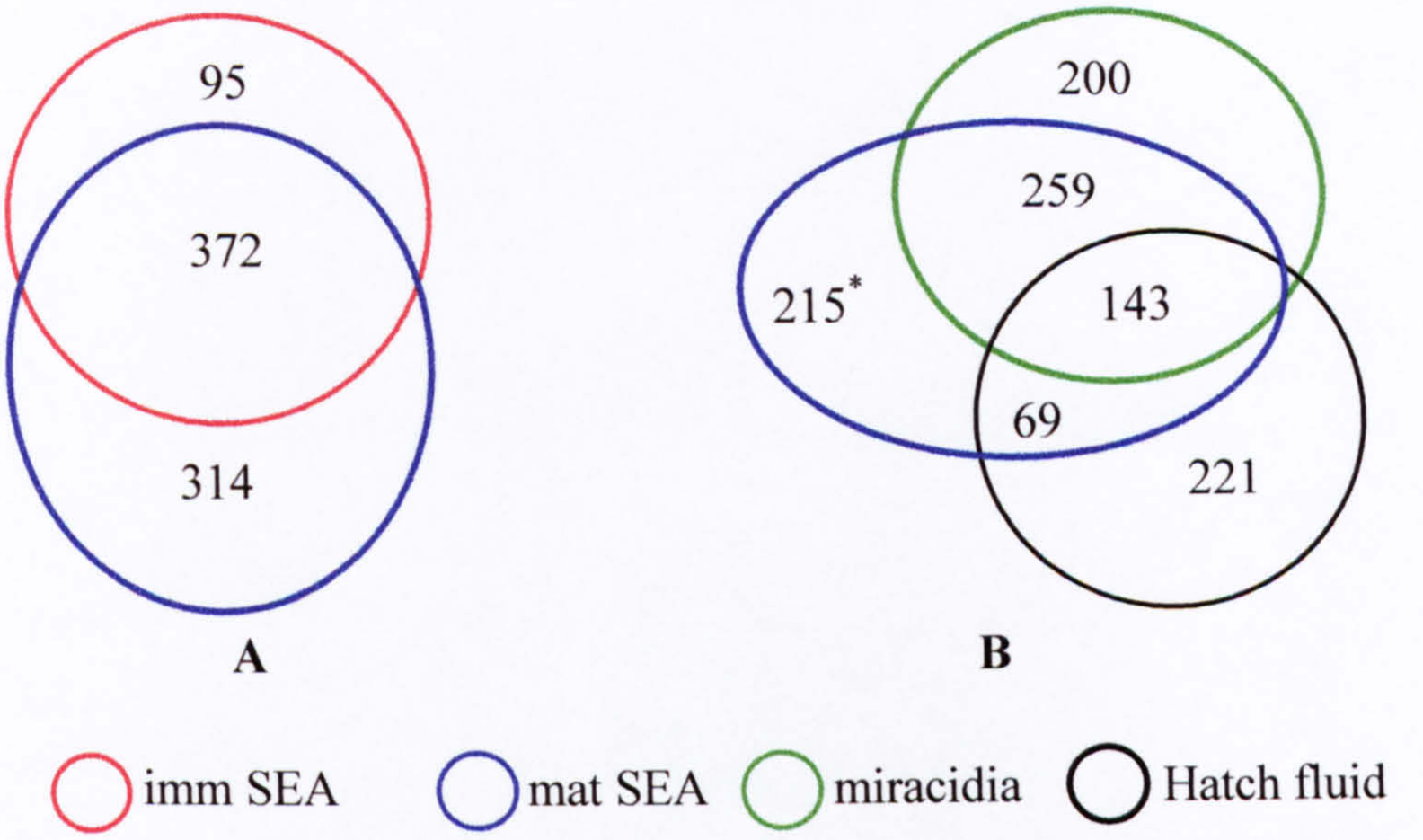

Figure 2.9. The distribution of the 1107 different spots as matched by Phoretix Evolution in the egg preparations. **A**: immature SEA contains 467 spots, 95 of which (equating to 16% of the total protein in the gel) are not present in mature SEA, and so will have been degraded during the maturation of the egg. In contrast, mature SEA has 314 spots that are not found in immature SEA, but they only represent 19% of the total protein in the gel. Thus, the differences between the immature egg and mature egg are large in terms of numbers of spots but relatively small in terms of protein quantity. **B**: the morphological components of the mature egg are very different from one another. There were 143 spots that were shared between the miracidial and hatch fluid preparations (equating to 42% of the miracidium and 21% of the hatch fluid in terms of total protein in the gel). Both the miracidial and hatch fluid preparations contain a significant number of spots that were not found in mature SEA. As the miracidium and hatch fluid are inherent parts of the egg, these spots must be present in mature SEA but were probably insufficiently abundant to have been detected in the mature SEA gel (i.e. they have been enriched for in the miracidial and hatch fluid preparations). There were a further 215 mature SEA spots (representing 10% of the mature SEA protein) that were not present in the miracidial or hatch fluid preparations. Sixty-four (representing 5% of the mature SEA protein) were also present in immature SEA, so are probably shell proteins or were derived from immature eggs that were present in the mature egg population. The remaining 151 spots that were only found in mature SEA are likely to be envelope or vesicle proteins that are insoluble in water and so were missing from hatch fluid. Spots from the female, vitellaria-enriched preparation and ESP could not be matched to the other preparations because they differed too extensively.

Original in colour

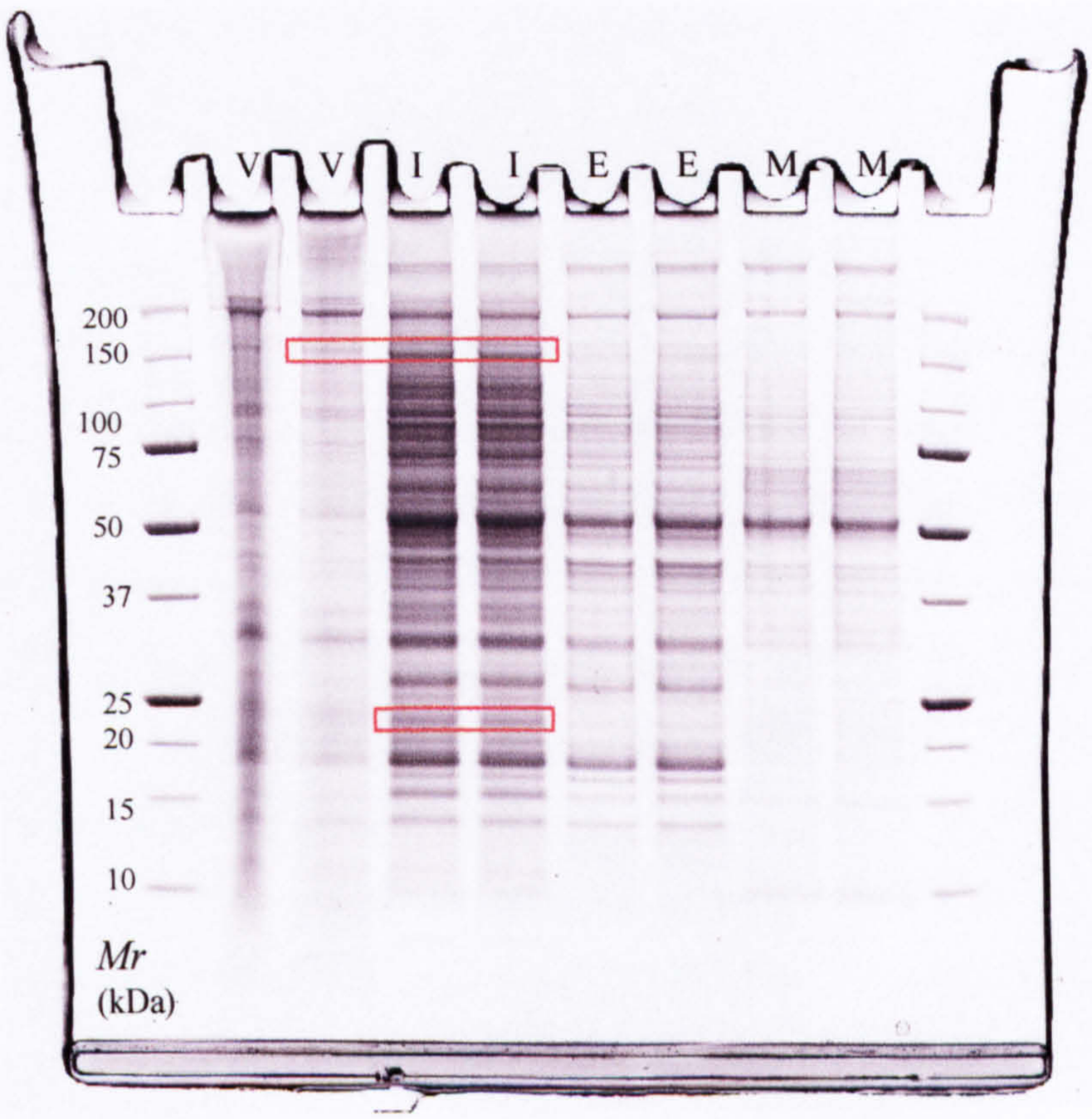

Figure 2.10 Separation of the proteins too insoluble for 2-DE. Pellets of M3-insoluble material from the vitellaria-enriched preparation (V), immature SEA (I), mature SEA (E) and miracidial preparation (M) were solubilized in SDS, separated by 1-DE and stained with Biosafe Coomassie. Most of the bands from immature SEA can also be seen in mature SEA, but there are exceptions such as the immature SEA proteins of 150kDa and 22kDa which are absent from mature SEA. The immature SEA 150kDa band is also present in the vitellaria-enriched preparation.

2.3.4.1 Protein Identification in the Female, Vitellaria-Enriched Preparation

As stated in Section 2.3.1, spot-matching using Phoretix Evolution could not be undertaken in the vitellaria-enriched preparation. Spots were therefore selected for MALDI-MSMS because they contained a large quantity of protein. Protein identities with sufficiently high ion scores to have a confidence interval > 99.9% appear in Table 2.1, along with the other gels in which the protein has been identified using MALDI-MSMS. The most abundant protein in the gel was bovine serum albumin (BSA), which was used in the preparation protocol (see Section 2.2.6). BSA was used as a lubricant during the separation of the paired worms, and although the females were washed after separation this clearly was not carried out thoroughly enough. As shown in Table 2.1, eleven of the nineteen *S. mansoni* proteins identified in the female, vitellaria-enriched preparation were also found in other egg preparations. These included ATP synthase, HSP60 and two isoforms of HSP70 that were found in immature SEA, mature SEA and the miracidial preparation but not in the hatch fluid. Ferritin was the only protein found exclusively in immature SEA and the vitellaria-enriched preparation. Proteins from the vitellaria-enriched preparation that were not found in the egg are highlighted as such in Table 2.1, but as the gel of the vitellaria-enriched preparation was not included in the Phoretix Evolution analysis it is possible that these spots were in fact present in the other gels, but were amongst the unidentified spots.

2.3.4.2 Protein Identification in the SEA, Miracidial and Hatch Fluid Preparations

Between-gel spot matching was successfully completed in the gels of immature SEA, mature SEA, the miracidial preparation and hatch fluid (Figures 2.3-2.6). The combination of Evolution and MALDI-MSMS generated identities for 90 immature SEA spots, 103 mature SEA spots, 102 miracidial spots and 58 hatch fluid spots, equating to 67 different proteins as detailed in Table 2.2. Some of the proteins (such as disulphide isomerase and Sm-p40) had different isoforms resulting from amino acid substitutions and others (such as tubulin) had multiple subunits, so in total 78 different ESTs were found. An example of two spots overlapping in the gel was found in the miracidial preparation, where Spot 323 was found to contain both actin and tropomodulin. Some proteins were present in all of the gels (such as actin, enolase, superoxide dismutase and ubiquitin) whilst others (such as lactate dehydrogenase and the host proteins) can be assigned to the miracidium or hatch fluid.

Table 2.1. Identities assigned to the gel-spots in the vitellaria-enriched preparation (Figure 2.2, page 73). Spot numbers, corresponding to those indicated in Fig. 2.2 were cut from the gel and identified by MALDI-MSMS. Only protein identities with sufficiently high ion scores to have a confidence interval >99.9% were accepted. The peptides, ions scores, confidence intervals etc. are detailed in Appendix 1.

Spot no.	Accession no[1].	Protein Identity	Other gels containing the protein[2]
50	Sm12452	14-3-3 epsilon	none
51	Sm0900	actin	all gels
52	Sm01315	aldehyde dehydrogenase	all gels
53	Sm00685	ATP synthase	imm SEA, mat SEA, miracidial
54	Sm01126	ATP synthase	none
55	gi74268269*	bovine apolipoprotein	none
56	gi30794280*	BSA	none
57	gi74267962*	BSA	none
58	Sm00296	chaperonin	none
59	Sm11433	superoxide dismutase	all
60	Sm11876	leucine aminopeptidase	none
61	Sm08285	disulphide isomerase	all
62	Sm12193	enolase	all
63	Sm04735	exportin 7	none
64	Sm12942	ferritin 1	imm SEA
65	Sm05684	fructose bisphosphate aldolase	imm SEA, mat SEA, hatch fluid
66	Sm05684	fructose bisphosphate aldolase	imm SEA, mat SEA, hatch fluid
67	Sm01537	HSP60	imm SEA, mat SEA, miracidial
68	Sm01537	HSP60	imm SEA, mat SEA, miracidial
69	Sm00325	HSP70	imm SEA, mat SEA, miracidial
70	Sm00325	HSP70	imm SEA, mat SEA, miracidial
71	Sm09042	HSP70	imm SEA, mat SEA, miracidial
72	Sm09042	HSP70	imm SEA, mat SEA, miracidial
73	Sm11575	14-3-3 epsilon	none
74	Sm12294	myosin heavy chain	none
75	Sm01066	myosin light chain	none
76	Sm04779	Sm14 fatty acid binding protein	all
77	Sm00101	Sm20.8	none
78	gi76445989*	BSA	none
79	gi74267962*	BSA	none

[1] Accession numbers are CDS unless *, which denotes NCBI.
[2] Phoretix Evolution analysis was not carried out.

Table 2.2. Identities assigned to the numbered gel spots in the immature SEA, mature SEA, miracidial and hatch fluid preparations. Spot numbers, corresponding to those indicated in Figs. 2.4-2.7 were cut from the gels, identified by MALDI-MSMS and matched between gels by Evolution software analysis.

Protein ID	Accession no[1]	Imm SEA[2]	Mat SEA[2]	Miracidia[2]	Hatch fluid[2]
aconitase	Sm07278	*258*	*97*	**358**	
actin	Sm00900	*217-219* **220**	**126-128** *129*	**322-325** *326*	
adenylate kinase	Sm06837		*158*	**359-361**	
aldehyde dehydrogenase	Sm01315	**226**	**135**	*332*	*524*
aldo keto reductase	Sm03515	*241*	**147**	*348*	*558*
alpha-N-acetylgalactosaminidase	Sm06626	*253*	**157**	357	
alpha-N-acetylgalactosaminidase	Smp179250	*286*	**196 197**	**321**	*549*
ATP synthase	Sm00685	*215 216*	**124** *125*	**320**	
calmodulin	Sm03962	*243*	**149**		
calreticulin	Sm00636	*211 212*	**119 120**	*316*	*520*
chaperonin 60kDa	Sm00497	**210**	*118*	*315*	
citrate synthase	Sm01548	*234*	**140**	*340*	
cysteine protease inhibitor	Sm01636	*235*	**141**	*341*	
dihydrolipoamide dehydrogenase	Sm00414	*209*	**115**	*312*	
disulphide isomerase	Sm00980	*221*	**130**		
disulphide isomerase	Sm08285	*261 262*	**169 170**	*373 374*	*536*
elongation factor 1 alpha	Sm01686	*237*	**143**	*343*	
enolase	Sm12193	**276** *277-279*	**184-186** *187*	**388-391**	*542 543*
ESP3-6	gi|28894857*		**101-104**		*501-503*
ESP15	Sm00193		**108**		*516*
ferritin heavy chain	Sm12942	**283**			
fructose bisphosphate aldolase	Sm05684	*248* **249**	*153*		**531-533**
GAPDH	Sm01185	*225*	**134**	*331*	
GST (26kDa)	Sm00145	*203*	**106**	*304*	**515**
GST (28kDa)	Sm02267	*238 -240*	**144** *145*	*344 345*	**526-528**
HSP10	Sm00296	*205*	*110*	**307**	
HSP60	Sm01537	*231* 232	**138** *139*	**337-339**	
HSP70	Sm00325	**206**	**111 112**	**308** *309*	
HSP70	Sm01676	*236*	**142**	**342**	
HSP70	Sm09042	**264-266** *267-270*	**172-175** *176*	**376-379** *380*	
HSP86	Sm01524	**229 230**			
HSP90	Smp069130	*287*	**194**	*399*	*548*
lactate dehydrogenase	Sm00165		**107**	*305*	
malate dehydrogenase (cytosolic)	Sm00407	*207 208*	**113 114**	**310** *311*	*518 556*
malate dehydrogenase (mitochondrial)	Sm00493		*117*	**314**	
mouse albumin	gi|29612571*				**506-511**
mouse haemoglobin alpha subunit	gi|122385*				**504**
mouse haemoglobin beta subunit	gi|31982300*				**512**
mouse hsc70	gi|1661134*				**505**
mouse regucalcin	gi 6677739*				**555**
nucleoside diphosphate kinase	Sm12959	*284*	**191**	*396*	
p25 homologue	Sm03199			**347**	
p40	Sm07196	**254-256** *257*	**159-163** *164*	*362-366* **367-371**	*534*

Table 2.2 continued

Protein ID	Accession no[1]	Imm SEA[2]	Mat SEA[2]	Miracidia[2]	Hatch fluid[2]
p40	Sm07598	*259*	**165**	*403*	*535*
paramyosin	Sm11278	*272 273*	**178** *179*	**382** *383*	
peptidyl prolyl cis trans isomerase	Sm12777	*282*	**190**	**394 395**	*545*
phosphoenolpyruvate carboxykinase	Sm00203	*204*	**109**	*306*	*517*
phosphoglycerate kinase	Sm01343	**227**	**136**	**333-335**	
plant pathogenesis family (PR1)	Smp154260	*271*	**198** *199*		**550-552**
proteasome alpha 6 subunit	Sm08991	*263*	**171**	*375*	
proteasome alpha 7 subunit	Sm02321	*244*	**146**	*346*	
Sm14 fatty acid binding protein	Sm04779	**245**	*150*	**350**	*529* **530**
Sm21.7	Sm03938	*242*	*148*	**349**	
SmE16	Smp096390	*201*	**105**	**301 302**	*513*
succinate-CoA ligase	Sm00415		**116**	*313*	
superoxide dismutase	Sm11433	*275*	**181** *182*	**385** *386*	**538**
thioredoxin	Sm11767		*183*	**387**	**539 540** *541*
thioredoxin peroxidase SmPrx3 (mitochondrial)	Sm00674	*214*	*123*	**319**	*521*
thioredoxin peroxidase SmPrx1 (cytosolic)	Sm12448	*280*	**188**		**544**
universal stress protein	Sm05431	*247*	*152*	**400**	*553*
translationally controlled tumor protein	Sm11405	*274*	**180**	*384*	*537*
triose phosphate isomerase	Sm00999	*222 223*	**131** *132*	**327 328**	*523*
tropomodulin	Sm08082		*168*	**323**	
tubulin alpha chain	Sm00654	*213*	*121 122*	**317 318**	
tubulin beta chain	Sm06624	*250-252*	**154 155** *156*	*351* **352-356**	
tubulin beta β4 chain	Sm10465		**177**	*381*	
tubulin beta chain	Smp035760	*288*	*195*	**401 402**	
ubiquitin	Sm01509	*228*	*137*	*336*	**525**
unknown function	Sm00115	*202*	**100**	*303*	*514*
unknown function	Sm01135	*224*	*133*	**329**	
unknown function	Sm05001	*246*	**151**	*351*	
unknown function	Sm14608	*233*	*98*		**546**
unknown function	Sm05341				**554**
unknown function	Sm07933	*260*	**166 167**		*522*
unknown function	Smp089370		**192**		*557*
unknown function	Smp059660	*285*	**193**	*397*	*547*
unknown function	Smp170410	*289*	*99*		**519**
valosin-containing protein	Sm12453	**281**	**189**	*392* **393**	

[1] Accession numbers are CDS unless *, which denotes NCBI.
[2] Spot numbers in bold denote identities obtained by MALDI-MSMS (the peptides, ions scores, confidence intervals etc. are detailed in Appendix 1). Only identities with sufficiently high ion scores to have a confidence interval >99.9% were accepted. Spot numbers in italics denote identities obtained utilizing Phoretix Evolution software analysis.

2.3.4.3 Protein Identification in the ESP Preparation

The fourteen ESP identities found by MALDI-MSMS are annotated on the gel in Figure 2.7 as Spots 1-14 and are listed in Table 2.3. The peptide fragmentation data are in Appendix 1.

Table 2.3. ESPs identified using MALDI-MSMS. The spot numbers correspond to those annotated on the gel of Figure 2.7.

Spot no.	Accession no[1]	Protein Identity[1]	Original ESP no.[2]
1	Sm19482	omega 1	ESP1-2
2	gi73765569*	IPSE*	not annotated
3	gi73765569*	IPSE*	ESP3
4	gi73765569*	IPSE*	ESP4
5	gi73765569*	IPSE*	not annotated
6	gi73765569*	IPSE*	ESP5
7	gi73765569*	IPSE*	ESP6
8	Smp193860/ gi82400502*/ gi8245004*	omega 1*	ESP12
9	Sm00193 / gi22094807*	ESP15	none
10	Sm11845	unknown function	ESP13
11	Sm11845	unknown function	ESP14
12	Sm12949	unknown function	ESP17
13	Sm12949	unknown function	ESP19
14	Sm00193 / gi22094807*	ESP15	ESP15

[1] Accession numbers are CDS unless*, which denotes NCBI. [2] Original ESP numbers are those assigned to the gel-spot by Ashton (2001). The peptides, ions scores, confidence intervals etc. are detailed in Appendix 1. Only identities with sufficiently high ion scores to have a confidence interval >99.9% were accepted.

As the spot pattern on the ESP gel of Figure 2.7 is visually comparable with that used by Ashton (2001) to originally number the ESPs, accession numbers can now be assigned to twelve out of the original nineteen ESPs. Some additional spots could be seen that bring the number of ESPs to at least 27. The "new" ESPs include a series of six faint spots which were basic and larger than the other ESPs plus another isoform of ESP15 (Spot 9 in Figure 2.7). The reason that these "new" ESPs can now be seen is probably because the gel in Figure 2.7 contained more protein than Ashton (2001) used (75µg as opposed to 50µg) and also because the stain used was a more sensitive one (Sypro Ruby as opposed to Coomassie Blue).

Spot 1 consisted of two isoforms, corresponding to ESP1 and ESP2, but the protein from each spot had merged in the gel too much to be separated. Searching the three fragmented peptides from Spot 1 against the NCBInr database demonstrated that ESP1-2 was Omega 1 (accession nos. ABB73002/gi824005802 and ABB73003/gi82400502). The protein sequences for these two Omega 1 annotations are identical, apart from amino acid differences at residues 26 and 136. Although a peptide covering residue 136 was fragmented, the correct sequence could not be ascertained because the discrepancy consisted of lysine (in gi82400502) and glutamine (in gi82400504), whose molecular masses are almost identical. The slightly less basic 10kDa protein ESP12 (Spot 8) was also found to be Omega 1, but as the full-length Omega 1 is a protein of 225 amino acids, ESP12 must be a truncated version of it (the single fragmented peptide consisted of the final eight amino acids). There are no SchistoCDS annotations that are sufficiently long to match the entire Omega 1 sequence, but Sm19482 covers amino acids 108-185 and Snap42294 covers amino acids 108-225. The complete length of Omega 1 is not annotated in v 4.0 of the *S. mansoni* genome either, the most complete annotation being Smp193860 (which is identical to Snap42294).

ESP3-6 was the most abundant ESP, its six isoforms (Spots 2-7) representing 83% of the total protein in the gel (Spots 2 and 5 are isoforms not described previously). The sequence YCLQLYDETYER was particularly amenable to MALDI-MSMS as it was fragmented in each of the spots 2-7 (see Appendix 1). The second leucine of this sequence (amino acid no. 34 in IPSE and no. 39 in ESP3-6) is one of the amino acid discrepancies between the GenBank entries for ESP3-6 and IPSE (see Section 2.1.3). The fragmentation spectra include the requisite y and b ions which demonstrate that the amino acid is indeed leucine (as per IPSE) rather than methionine (as per ESP3-6). Thus, IPSE is the only significant match when using the NCBInr database to search for ESP3-6 fragmentation ions. ESP3-6 is not annotated in SchistoCDS but the full IPSE nucleotide sequence is annotated in v 4.0 of the genome as Smp112110.

2.3.5 The Egg Proteome: Protein Function

The proteomes of immature SEA, mature SEA, the miracidial preparation and hatch fluid were compared in terms of protein function by assigning each identified protein to one of

eleven categories. The volume of protein in each spot was then calculated as a percentage of that in the gel. The results are shown in Tables 2.4–2.7, ranked in order of functional category expression level and then by accession number expression level. Figure 2.11 then combines all this data and presents it as four comparable pie charts. Where several spots were found to have the same accession number, their volumes were combined.

It can be seen that identities could be assigned to 52% (by volume) of immature SEA, 66% of mature SEA, 55% of the miracidial preparation and 64% of hatch fluid. HSP70 is the most abundant protein in immature SEA, its three isoforms (Sm09042, Sm00325 and Sm01676) accounting for 9.3% of the total protein. Sm09042 (the most abundant isoform) is cytosolic whilst Sm00325 and Sm01676 are mitochondrial. In mature SEA, Sm-p40 is the most abundant protein, accounting for 10.9% of the total (as opposed to 3.9% in immature SEA). The Sm-p40 found in the mature egg can be assigned to the miracidium because 15.2% of the miracidial preparation consisted of Sm-p40, compared to only 1% in hatch fluid. Chaperones were found to make up a greater percentage of mature SEA than in immature SEA (23.4% vs. 18.5%), but this could be because a smaller percent of mature SEA constituted unidentified spots. In terms of the percentage of the identified protein, chaperones make up 35% in both the mature and immature SEA preparations. Even allowing for the between-gel differences in the proportions of unidentified spots, mature SEA contains more defence proteins than immature SEA. Similar quantities of cytoskeletal proteins are present in the two preparations, although no miracidium is present in the immature egg. An additional functional category (secretory proteins) is also found in mature SEA.

The differences between the miracidial and hatch fluid preparations in the Venn diagrams of Figure 2.9 are reflected in the pie charts of Figure 2.11, so they can now be seen in terms of protein function and mapped back to the proteome of mature SEA. Almost all of the chaperones and cytoskeletal proteins of the egg are found in the miracidium whilst secretory proteins and host proteins are found in the hatch fluid. The hatch fluid also contains many more defence proteins, but fewer proteins dealing with ATP production, protein turnover and calcium-binding. Hatch fluid also contains a large proportion of the proteins of unknown function.

Table 2.4. The proteins in immature SEA, categorised in terms of their molecular function and expression levels.

Functional category (% total spot vol.)	Accession no.	Protein identity	% Total spot vol.
Unidentified (47.8%)	None	unidentified spots	47.8
Chaperone (18.5%)	Sm09042	HSP70 (cytosolic)	6.6
	Sm07196	p40	3.8
	Sm01537	HSP60	2.6
	Sm00325	HSP70 (mitochondrial)	1.8
	Sm01524	HSP86	1.6
	Sm01676	HSP70 (mitochondrial)	0.9
	Smp069130	HSP90	0.5
	Sm00296	HSP10	0.4
	Sm00497	chaperonin 60kDa	0.2
	Sm07598	p40	0.2
Cytoskeletal (10.4%)	Sm06624	tubulin beta chain	6.3
	Sm00900	actin	3.1
	Smp035760	tubulin beta chain	0.8
	Sm00654	tubulin alpha chain	0.1
ATP production (7.7%)	Sm12193	enolase	2.2
	Sm00685	ATP synthase	1.9
	Sm01343	phosphoglycerate kinase	1.0
	Sm01185	GAPDH	0.7
	Sm01548	citrate synthase	0.6
	Sm05684	fructose bisphosphate aldolase	0.5
	Sm00414	dihydrolipoamide dehydrogenase	0.4
	Sm00999	triose phosphate isomerase	0.4
	Sm07278	aconitase	0.0
Other (4.7%)	Sm00407	malate dehydrogenase (cytosolic)	1.8
	Smp179250	alpha-N-acetylgalactosaminidase	0.8
	Sm00203	phosphoenolpyruvate carboxykinase	0.6
	Sm04779	Sm14 fatty acid binding protein	0.5
	Sm11278	paramyosin	0.3
	Sm06626	alpha-N-acetylgalactosaminidase	0.3
	Sm12942	ferritin 1 heavy chain	0.2
	Sm01686	elongation factor 1 alpha	0.1
	Sm12959	nucleoside diphosphate kinase	0.1
Defence (4.0%)	Sm02267	GST (28kDa)	1.4
	Sm01315	aldehyde dehydrogenase	0.5
	Sm12448	thioredoxin peroxidase (SmPrx1)	0.5
	Sm11433	superoxide dismutase	0.4
	Sm03515	aldo keto reductase	0.3
	Sm00145	GST (26kDa)	0.2
	Sm05431	universal stress protein	0.2
	Sm00674	thioredoxin peroxidase (SmPrx3)	0.2
	Smp154260	plant pathogenesis related (PR1) family	0.2
	Sm01636	cysteine protease inhibitor	0.1

Table 2.4 continued

Protein turnover (3.1%)	Sm00980	disulphide isomerase	1.0
	Sm08285	disulphide isomerase	0.9
	Sm12453	valosin containing protein	0.5
	Sm01509	ubiquitin	0.4
	Sm08991	proteasome alpha 6 subunit	0.2
	Sm02321	proteasome alpha 7 subunit	0.0
Calcium binding (1.5%)	Sm03962	calmodulin	1.0
	Sm11405	translationally controlled tumor protein	0.3
	Sm03938	Sm21.7	0.1
	Phat12638	SmE 16	0.1
Unknown function (1.4%)	Smp170410	unknown function	0.6
	Sm01135	unknown function	0.3
	Smp059660	unknown function	0.1
	Sm05001	unknown function	0.1
	Sm00115	unknown function	0.1
	Sm14608	unknown function	0.1
	Sm07933	unknown function	0.1
Export pathway (1%)	Sm00636	calreticulin	0.5
	Sm12777	peptidyl-prolyl cis trans isomerase	0.5

Table 2.5. The proteins present in mature SEA, categorised in terms of their molecular function and relative abundance.

Functional category (% total spot vol.)	Accession no.[1]	Protein identity	% Total spot vol.
Unidentified (33.9%)	none	unidentified spots	33.9
Chaperone (23.4%)	Sm07196	p40	10.6
	Sm09042	HSP70 (cytosolic)	8.7
	Sm00325	HSP70 (mitochondrial)	1.8
	Sm01537	HSP60	1.2
	Sm01676	HSP 70 (mitochondrial)	0.4
	Sm00296	HSP10	0.3
	Sm07598	p40	0.3
	Sm00497	chaperonin 60kDa	0.1
	Smp069130	HSP90	0.0
Cytoskeletal (10.9%)	Sm06624	tubulin beta chain	5.1
	Sm00900	actin	3.0
	Sm10465	tubulin beta chain	1.6
	Smp035760	tubulin beta chain	0.9
	Sm00654	tubulin alpha chain	0.3
	Sm08082	tropomodulin	0.0
ATP production (7.9%)	Sm12193	enolase	2.1
	Sm00685	ATP synthase	1.8
	Sm01548	citrate synthase	1.1
	Sm01343	phosphoglycerate kinase	0.8
	Sm05684	fructose bisphosphate aldolase	0.6
	Sm01185	GAPDH	0.6
	Sm00999	triose phosphate isomerase	0.5
	Sm00414	dihydrolipoamide dehydrogenase	0.1
	Sm07278	aconitase	0.1
	Sm00415	succinal CoA ligase	0.1
	Sm00493	malate dehydrogenase (mitochondrial)	0.0

Table 2.5 continued

Defence (6.9%)	Sm12448	thioredoxin peroxidase (SmPrx1)	2.0
	Sm02267	GST (28kDa)	1.9
	Sm01315	aldehyde dehydrogenase	0.7
	Smp154260	plant pathogenesis related (PR1) family	0.5
	Sm00145	GST (26kDa)	0.4
	Sm03515	aldo keto reductase	0.4
	Sm11767	thioredoxin	0.3
	Sm00674	thioredoxin peroxidase (SmPrx3)	0.3
	Sm11433	superoxide dismutase	0.2
	Sm05431	universal stress protein	0.2
	Sm01636	cysteine protease inhibitor	0.1
Other (4.3%)	Smp179250	alpha-N-acetylgalactosaminidase	1.4
	Sm00407	malate dehydrogenase (cytosolic)	1.1
	Sm06626	alpha-N-acetylgalactosaminidase	0.6
	Sm04779	Sm14 fatty acid binding protein	0.3
	Sm11278	paramyosin	0.3
	Sm00203	phosphoenolpyruvate carboxykinase	0.2
	Sm12959	nucleoside diphosphate kinase	0.2
	Sm00165	lactate dehydrogenase	0.1
	Sm06837	adenylate kinase	0.0
	Sm01686	elongation factor 1 aplha	0.0
Protein turnover (3.7%)	Sm00980	disulphide isomerase	1.9
	Sm08285	disulphide isomerase	1.3
	Sm08991	proteasome alpha 6 subunit	0.2
	Sm12453	valosin containing protein	0.2
	Sm01509	ubiquitin	0.2
	Sm02321	proteasome alpha 7 subunit	0.0
Unknown function (3.5%)	Smp170410	unknown function	1.8
	Sm07933	unknown function	0.5
	Smp089370	unknown function	0.4
	Smp059660	unknown function	0.3
	Sm05001	unknown function	0.2
	Sm01135	unknown function	0.1
	Sm14608	unknown function	0.1
	Sm00115	unknown function	0.1
Secretory (2.5%)	gi|28894857*	ESP3-6	2.5
	Sm00193	ESP15	0.0
Calcium binding (2.0%)	Smp096390	SmE 16	1.2
	Sm03962	calmodulin	0.4
	Sm11405	translationally-controlled tumor protein	0.4
	Sm03938	Sm21.7	0.0
Export pathway (1.0%)	Sm00636	calreticulin	0.8
	Sm12777	peptidyl prolyl cis trans isomerase	0.2

[1]Accession numbers are from CDS unless *, which denotes NCBI.

Table 2.6. The proteins present in the miracidial preparation, categorised in terms of their molecular function and expression levels.

Functional category (% total spot volume)	Accession no.	Protein identity	% Total spot vol.
Unidentified (45%)	none	Unidentified spots	45.0
Chaperone (22.9%)	Sm07196	p40	15.1
	Sm09042	HSP70 (cytosolic)	3.9
	Sm01537	HSP60	1.7
	Sm00296	HSP10	0.8
	Sm03199	p25 homologue	0.5
	Sm00325	HSP70 (mitochondrial)	0.4
	Sm01676	HSP70 (mitochondrial)	0.3
	Sm07598	p40	0.1
	Smp069130	HSP90	0.1
	Sm00497	chaperonin 60kDa	0.1
Cytoskeletal (9.0%)	Sm00900	actin	3.5
	Sm06624	tubulin beta chain	2.5
	Sm00654	tubulin alpha chain	1.8
	Smp035760	tubulin beta chain	1.1
	Sm10465	tubulin beta chain	0.1
	Sm08082	tropomodulin	0.0
ATP production (7.7%)	Sm12193	enolase	2.9
	Sm01343	phosphoglycerate kinase	1.7
	Sm00685	ATP synthase	1.0
	Sm00999	triose phosphate isomerase	0.9
	Sm01185	GAPDH	0.5
	Sm00493	malate dehydrogenase (mitochondrial)	0.3
	Sm00414	dihydrolipoamide dehydrogenase	0.1
	Sm07278	aconitase	0.1
	Sm00415	succinate-CoA ligase	0.1
	Sm01548	citrate synthase	0.1
Other (4.5%)	Sm00407	malate dehydrogenase (cytosolic)	0.9
	Sm06837	adenylate kinase	0.9
	Sm06626	alpha-N-acetylgalactosaminidase	0.7
	Smp179250	alpha-N-acetylgalactosaminidase	0.6
	Sm04779	Sm14 fatty acid binding protein	0.5
	Sm11278	paramyosin	0.4
	Sm12959	nucleoside diphosphate kinase	0.2
	Sm00165	lactate dehydrogenase	0.2
	Sm00203	phosphoenolpyruvate carboxykinase	0.1
	Sm01686	elongation factor 1 alpha	0.0

Table 2.6 continued

Defence (3.2%)	Sm02267	GST (28kDa)	0.7
	Sm01315	aldehyde dehydrogenase	0.4
	Sm11433	superoxide dismutase	0.4
	Sm00674	thioredoxin peroxidase (SmPrx3)	0.4
	Sm05431	universal stress protein	0.4
	Sm11767	thioredoxin	0.4
	Sm01636	cysteine protease inhibitor	0.2
	Sm00145	GST (26kDa)	0.2
	Sm03515	aldo keto reductase	0.1
Calcium binding (2.9%)	Smp096390	SmE 16	1.9
	Sm03938	Sm21.7	0.5
	Sm11405	translationally controlled tumor protein	0.5
Export pathway (2.1%)	Sm12777	peptidyl prolyl cis trans isomerase	1.6
	Sm00636	calreticulin	0.5
Protein turnover (1.9%)	Sm12453	valosin containing protein	0.8
	Sm08285	disulphide isomerase	0.5
	Sm02321	proteasome alpha 7 subunit	0.3
	Sm01509	ubiquitin	0.3
	Sm08991	proteasome alpha 6 subunit	0.1
Unknown Function (0.9%)	Smp059660	unknown function	0.3
	Sm01135	unknown function	0.2
	Sm00115	unknown function	0.2
	Sm05001	unknown function	0.2

Table 2.7. The proteins present in hatch fluid, categorised in terms of their molecular function and expression levels.

Functional category (% total spot volume)	Accession no.[1]	Protein identity	% Total spot vol.
Unidentified (35.8%)	none	unidentified spots	35.8
Unknown function (19.7%)	Smp170410	unknown function	18.2
	Sm14608	unknown function	0.7
	Sm05341	unknown function	0.3
	Sm00115	unknown function	0.2
	Sm07933	unknown function	0.1
	Smp059660	unknown function	0.1
	Smp089370	unknown function	0.1
Defence (15.7%)	Sm02267	GST (28kDa)	4.4
	Sm11767	thioredoxin	4.1
	Smp154260	plant pathogenesis related (PR1) family	3.7
	Sm03515	aldo keto reductase	1.0
	Sm12448	thioredoxin peroxidase (SmPrx1)	0.7
	Sm00145	GST (26kDa)	0.6
	Sm05431	universal stress protein	0.7
	Sm11433	superoxide dismutase	0.4
	Sm01315	aldehyde dehydrogenase	0.1
	Sm00674	thioredoxin peroxidase (SmPrx3)	0.0
Secretory (11.9%)	gi|28894858*	ESP3-6	11.7
	Sm00193	ESP15	0.2
Host proteins (6.6%)	gi|29612571*	mouse albumin	4.3
	gi|31982300*	mouse haemoglobin beta subunit	1.1
	gi|1161134*	mouse hsc70	0.5
	gi|6677739*	mouse regucalcin	0.4
	gi|122385*	mouse haemoglobin alpha subunit	0.3
ATP production (4.0%)	Sm00999	triose phosphate isomerase	1.5
	Sm05684	fructose bisphosphate aldolase	1.5
	Sm12193	enolase	1.0
Other (2.8%)	Sm04779	Sm14 fatty acid binding protein	1.8
	Smp179250	alpha-N-acetylgalactosaminidase	0.5
	Sm00407	malate dehydrogenase (cytosolic)	0.3
	Sm00203	phosphoenolpyruvate carboxykinase	0.1
Export pathway (1.3%)	Sm12777	peptidyl prolyl cis trans isomerase	0.8
	Sm00636	calreticulin	0.4
Chaperone (1.1%)	Sm07196	p40	1.0
	Sm07598	p40	0.0
	Smp069130	HSP90	0.0
Protein turnover (0.9%)	Sm01509	ubiquitin	0.8
	Sm08285	disulphide isomerase	0.1
Calcium binding (0.2%)	Smp096390	SmE16	0.1
	Sm11405	translationally controlled tumor protein	0.1

[1]Accession numbers are CDS unless *, which denotes NCBI.

Original in colour

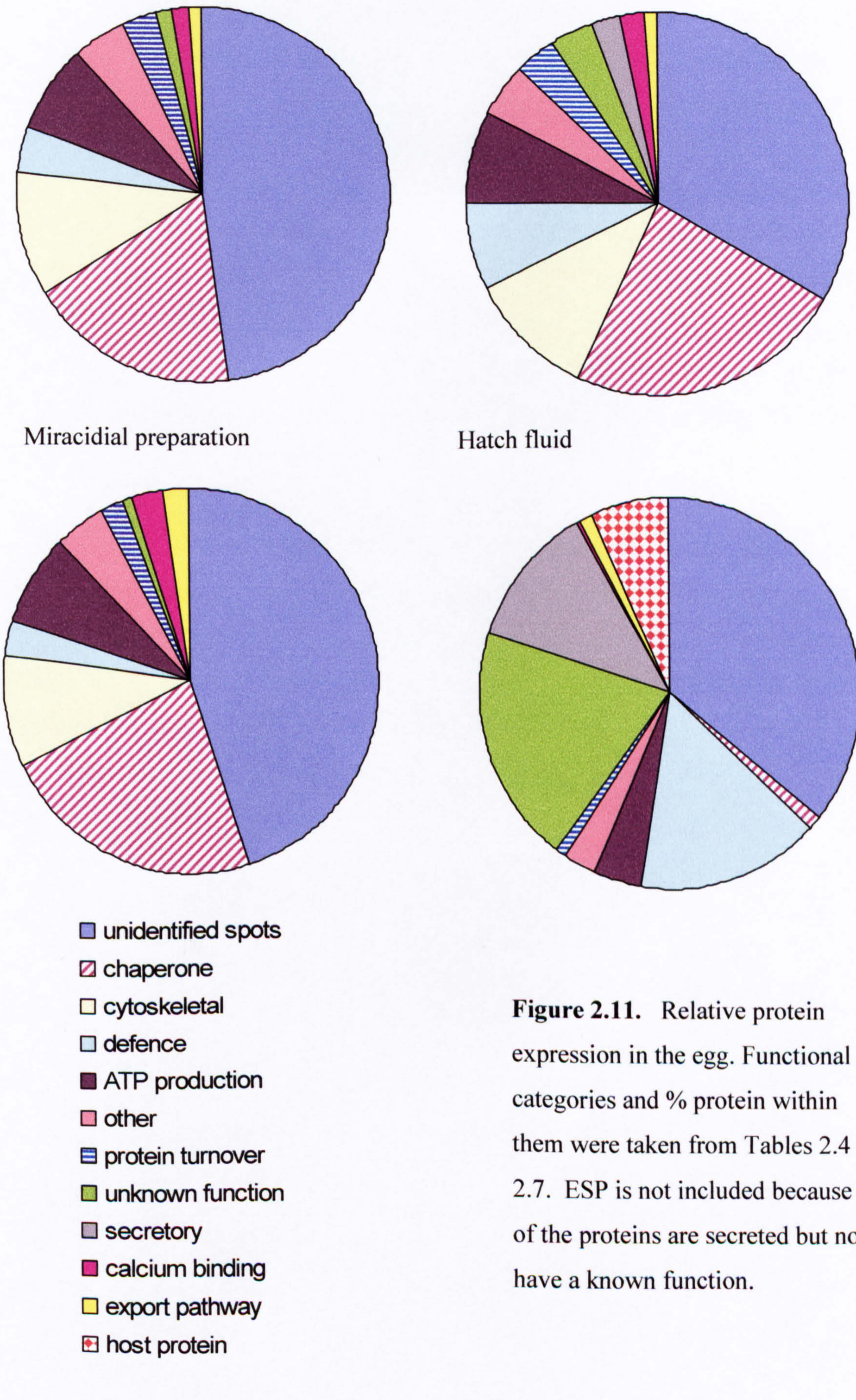

Figure 2.11. Relative protein expression in the egg. Functional categories and % protein within them were taken from Tables 2.4 – 2.7. ESP is not included because all of the proteins are secreted but none have a known function.

The most abundant protein in hatch fluid is Smp170410, which has no homology to any proteins of known function (the only significant match on the nrNCBI database being a *S. japonicum* homologue). Accounting for 18.2% of hatch fluid, Smp170410 is a 55-80kDa, very acidic protein (*pI* 3.5) with two distinct isoforms, each of which can be split into sub-isoforms (see Fig 2.8). Smp170410 is not present in either the miracidial preparation or ESP (so it will be stored between the miracidium and the envelope). It constitutes 1.8% of mature SEA and 0.6% of immature SEA, so it is present at the earliest stages of egg development but increases in abundance as the egg develops. The ten-fold difference in the abundance of Smp170410 between the hatch fluid and mature SEA preparations demonstrates the extent to which protein enrichment in the hatch fluid has occurred, and therefore that the hatch fluid makes up a relatively small proportion of the total protein in the egg.

As hatch fluid contains the greatest proportion of proteins of unknown function, a 2D-gel was stained for glycoproteins to establish the extent to which its proteome is glycosylated (Figure 2.12). The pattern of spots indicated that the two most abundant glycoproteins are the abundant protein of unknown function discussed above (Smp170410) and ESP3-6. In addition, there is a row of distinct basic spots of approx. 150kDa that are heavily glycosylated but were not sufficiently abundant to have been fragmented and identified using MALDI-MSMS.

Original in colour

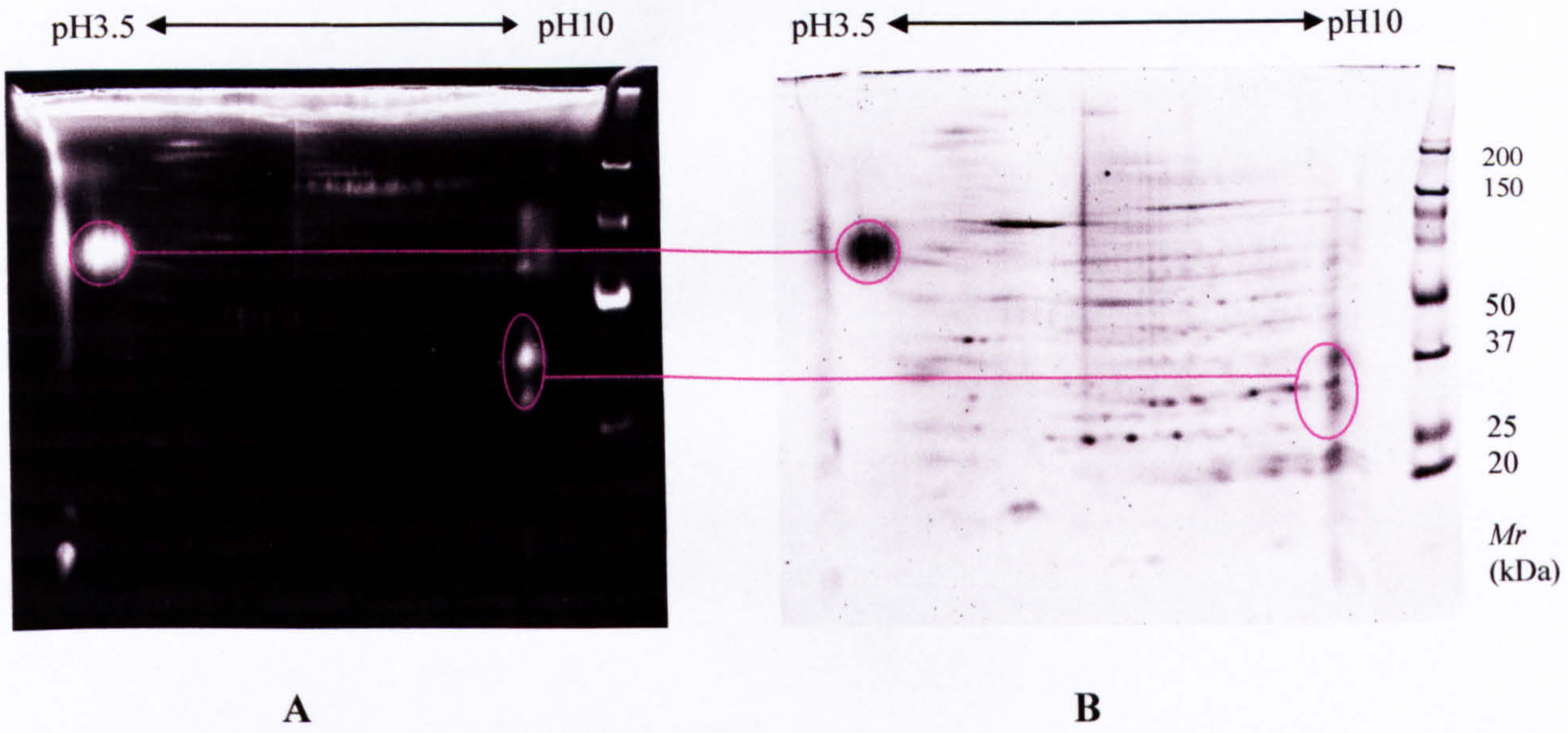

Figure 2.12 2-DE of 35µg of hatch fluid stained for protein and glycoprotein, with the identifiable glycoproteins shown in pink. (A) Pro-Q Emerald stain reveals several glycosylated hatch fluid proteins including a very acidic protein of 60-100kDa and two very basic proteins of 30-40kDa. (B) Sypro Ruby protein staining the gel allows the location of the glycoproteins to be seen relative to non-glycosylated proteins, thereby demonstrating that Smp170410 and ESP3-6 are the major glycosylated components of hatch fluid.

2.3.6 Host Albumin and "*S. mansoni* Albumin"

In order to establish whether "*S. mansoni* albumin" is of host or parasite origin, albumin from the common laboratory host *Mesocricetus auratus* (Golden Hamster) was isolated by 1-DE, trypsinised and subjected to MALDI-MS and Electrospray-MSMS. The PMF and peptide-ion data were then searched against the NCBInr database. As hamster albumin has not been sequenced, albumin from other rodents should have been the highest-scoring matches. However, as shown in Figure 2.13, hamster albumin was found to have complete homology to "*S. mansoni* albumin" (AAL08579/gi15808978). Electrospray-MSMS fragmented 38 different peptides that were matched to "*S. mansoni* albumin" with a total ion score of 1520 (the peptides and their fragmentation data are detailed in Appendix 2). The match to "*S. mansoni* albumin" was considerably better than that to the next most homologous proteins, which were albumin from *Rattus norvegicus* (11 matching peptides, total ion score 498) and the Reed Vole *Microtus fortis* (12 matching peptides, total ion score 455). Although *R. norvegicus* albumin was a better match than *M. fortis* albumin in terms of the total ion score, *M. fortis* albumin was a better match in terms of the numbers of matching peptides. The amino acid sequence of "*S. mansoni* albumin" was found to have better homology with *M. fortis* albumin (78 different residues) than with *R. norvegicus* albumin (94 different residues). The principal reason *R. norvegicus* albumin matched with a higher total ion score was because the fragmented peptide TPVSEKVTK matched it perfectly (generating an ion score of 65) whilst it matched less well to the *M. fortis* albumin sequence (generating an ion score of 35). The *M. fortis* version of the peptide had a lower ion score because glutamine is substituted in place of the lysine residue at amino acid no.6. The molecular weights of glutamine and lysine are very similar (146.15Da vs. 146.19Da) so both residues fell within the tolerance parameters of the MASCOT search, but their different molecular weights were reflected in the peptide's ion scores. Thus, the correct residue in the sequence can be identified as lysine. The "*S. mansoni* albumin" version of the peptide is the same as the *M. fortis* version (i.e. with the lower-scoring glutamine residue) and is highlighted in Figure 2.13. This glutamine residue-substituted peptide is the only peptide from *M. auratus* albumin that had more homology to albumin from another rodent than it does to "*S. mansoni* albumin".

Original in colour

A

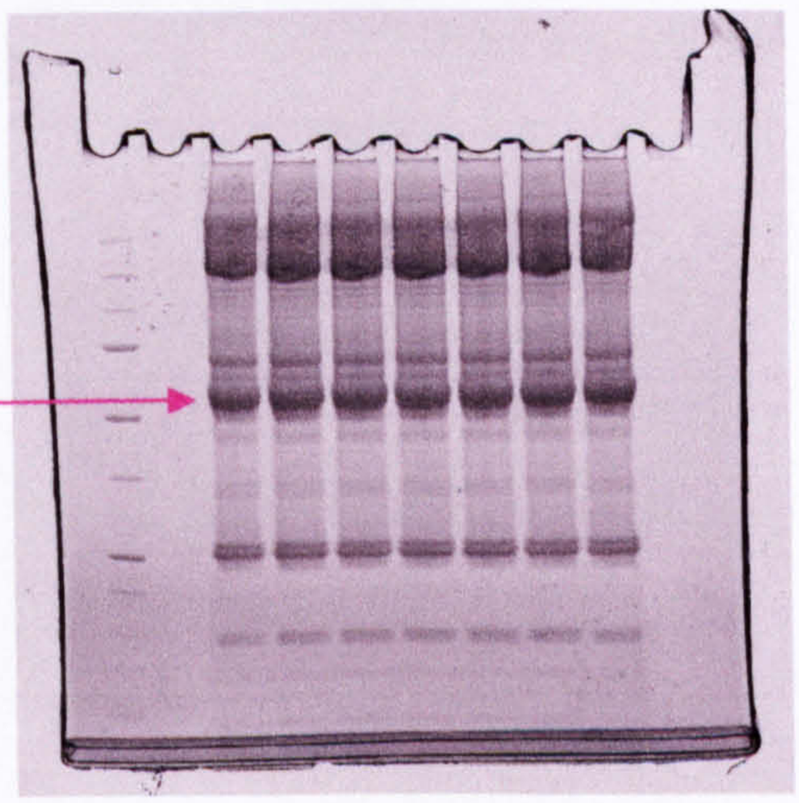

B

MKWVTFLLLLFVSDSAFSRGLFRRDAHKSEIAHRFK*DLGEQHFKGLVLIAFSQFLQKC
PYEEHVKLVNEVTDFAKTCVADESAENCDKSLHTLFGDKLCAIPTLR*DSYGELADCC
AKK*EPERNECFLKHKDDHPNLPPFVRPDAEAMCTSFQENAVTFMGHYLHEVARRH
PYFYAPELLYYAEKYSAIMTECCGEADKAACITPKLDALKEKALASSVNQRLKCSSLQ
R*FGQRAFKAWAVARMSQKFPKADFAEITKLATDLTKLTEECCHGDLLECADDRAELA
KYMCENQASISSKLQACCDKPVLK*KSHCLSEVENDDLPADLPSLAADFVEDKEVCK
NYAEAKDVFLGTFLYEYARRHPDYSVALLLRLAKKYEATLEKCCAEADPSACYGK*VLD
EFQPLVEEPKNLVKANCELFEKLGEYGFQNALIVRYTQKAPQVSTPTLVEAARNLGKVG
SKCCVLPEAQRLPCVEDYISAILNRVCVLHEKTPVSEQVTKCCTGSVVERRPCFSALP
VDETYVPKEFKAETFTFHADICSLPEKEKQMKKQAALVELVKHKPKATGPQLRTVLG
EFTAFLDKCCKAEDKEACFSEDGPK*LVASSQAALA

BLUE: secretory-signal peptide. RED: peptides identified by MSMS are in red. GREEN: peptides identified by MS are in green. BLACK: unidentified amino acids are in black. Boxed residues: amino acids that are diagnostic for "*S. mansoni* albumin" in that they are different in albumin from *Rattus norvegicu* or *Microtus fortis*. * denotes the lysine and arginine residues discussed in the text. The peptide TPVSEQVTK discussed in the text is denoted with a grey background and its glutamine residue boxed.

Figure 2.13. *Mesocricetus auratus* (Golden Hamster) albumin. ***A:*** Serum from an uninfected animal was separated by electrophoresis, the bands at 60kDa excised, pooled and subjected to Electrospray-MSMS and MALDI-MS analysis. ***B.*** The nrNCBI sequence of "*S. mansoni* albumin" (AAL08579/gi15808978), showing the homology with *M. auratus* albumin. The peptide-fragmentation data are shown in Appendix 2.

The amino acid sequence of "*S. mansoni* albumin" contains 608 amino acids (as does that from *M. fortis* and *R. norvegicus*). Eighteen residues form the signal peptide (3% of the total protein) which will be missing from the serum-derived albumin used in this experiment. Out of the remaining 590 amino acids, 386 (constituting 65% of the total protein sequence) have been fragmented and identified by Electrospray-MSMS and a further 40 amino acids (7% of the sequence) match PMFs generated by MALDI-MS. Only 155 amino acids (26% of the sequence) remained unidentified. Eighty-nine residues that are specific for "*S. mansoni*-albumin" were fragmented and identified by MSMS. These include 53 that are different in *M. fortis* albumin, 61 that differ in *R. norvegicus* albumin (including the lysine residue discussed in the previous paragraph) and 22 that are different in both. Another 10 of the "*S. mansoni*-albumin" amino acids that are missing from one or other of the rodent sequences are incorporated into peptides identified by MALDI-MS (one of which is different in both of the rodent sequences). Six of the residues (denoted by * in Figure 2.12) must be either lysine or arginine because they form cleavage points of tryptic peptides, yet they are differently annotated in the *R. norvegicus* or *M. fortis* albumin sequences.

2.4 Discussion

Overall, the 1107 different spots visible on 2D gels fall well short of the estimated 6-7000 genes expressed in each *S. mansoni* stage (Verjovski-Almeida *et al.*, 2003), but compare favourably with the 465 spots previously found in SEA (Curwen *et al.*, 2004). The number of spots are broadly comparable with the *S. japonicum* proteome study, where 1441 egg proteins were identified (Liu *et al.*, 2006). It was evident that some proteins contained peptides that were more amenable to ionisation than others, because some relatively heavily-stained gel spots failed to generate good spectra and *vice versa.* For example, in the miracidia preparation good spectra were generated for spots 359–361 (adenylate kinase) but the more heavily stained spot situated between them in the gel failed to do so.

2.4.1 Chaperones

Chaperones are the most abundant proteins in the egg, forming the largest functional category in the immature SEA, mature SEA and miracidial preparations. The hatch fluid contains very few chaperones and the egg secretions none. The two principal chaperones are HSP70 and Sm-p40. HSP70 is highly expressed throughout the egg's development, with cytosolic and mitochondrial forms making up 9.3% of immature SEA and 10.9% of mature SEA. Of the mature SEA components, HSP70 was only found in the miracidial preparation, but as it only made up 4.6% of the protein in the miracidial gel, the remaining HSP70 from mature SEA needs to be accounted for elsewhere. The most likely explanation is that the HSP70 is highly enriched in the envelope but it failed to appear amongst the hatch fluid proteins, perhaps because it is not soluble in water (Weinreb *et al.*, 2001). HSP70 undertakes a wide range of folding processes, including the folding of nascent proteins and the translocation of secretory proteins (Mayer & Bukau, 2005) so it is logical that it would be enriched for in the envelope because this is where ESP production occurs.

Unlike HSP70, Sm-p40 is more abundant in mature SEA (10.9% of the proteome) than in immature SEA (4% of the proteome). The Sm-p40 can be assigned to the miracidium because it makes up 15.2% of the miracidial soluble proteome, and so its lower level of expression in immature SEA reflects the less developed status of the miracidium in the

immature egg. These figures are consistent with an earlier report that 10% of SEA (made from a mixture of immature and mature eggs) is made up of Sm-p40 (Stadecker *et al.*, 2001).

There are three immunodominant T cell epitopes in Sm-p40, which together account for most of the T-cell response to SEA in C3H and CBA mice, both of which produce a strong granulomatous response to *S. mansoni* eggs (Finger *et al.*, 2005; Asahi & Stadecker, 2003). In contrast, T cell hybridomas derived from the smaller granuloma that develop in C57BL/6 mice do not recognise Sm-p40 (Hernandez *et al.*, 1997). Taken together, these results demonstrate that Sm-p40 is an important T cell antigen, likely to be responsible for much of the granuloma formation found in schistosomiasis. Sm-p40 is a member of the (cytoplasmic) small heat shock protein family because it contains the conserved internal α-crystallin domain, flanked by a variable N-terminal domain and a smaller C-terminal extension (Stamler *et al.*, 2005; Abouel-Nour *et al.*, 2006). Small heat shock proteins (sHSPs) play a crucial role in protecting proteins from physiological, stress-induced, irreversible aggregation without using ATP. Once suitable conditions pertain for continued cell activity protein refolding occurs, mediated by ATP-dependent chaperones such as HSP70 (Sun & MacRae, 2005). A unique group of sHSPs containing two α-crystallin domains and a truncated C-terminal extension is found in flatworms. In addition to Sm-p40 in *Schistosoma*, homologous transcripts have been found in *Taenia, Echinococcus* and *Paragonimus* (Kappe *et al.*, 2004; Merckelbach *et al.*, 2003; Benitez *et al.*, 1998; Accession no. AAK35217). The C-terminal extension is thought to be responsible for modulating oligomerization of sHSPs under non-stress conditions, disassembly of which occurs when chaperoning is required (Sun & MacRae, 2005). In *S. mansoni*, the immunodominant epitope is in this C-terminal extension region (Hernandez & Stadecker, 1999), probably because of its hydrophilic nature. Apart from the flatworm sHSPs, the only other sHSPs that don't have the C-terminal extension are the HSP12.6 proteins of *C. elegans*, (Leroux *et al.*, 1997). In the lifecycle of *C. elegans*, unfavourable growth conditions induce the development of specialised "dauer" larvae, which are adapted to survive long periods of diapause. Dauer larvae do not feed, have reduced metabolic activity, are resistant to environmental stresses such as changes in temperature, osmotic pressure and oxidative stress yet they maintain an active chemosensory system and are capable of rapid movement

(Cassada & Russell, 1975; Albert & Riddle, 1988). These environmental stresses are not dissimilar to those facing the *S. mansoni* egg as it passes through the gut wall, enters faecal matter, then water before rupturing to release the miracidium. It is therefore interesting that the α-crystallin-containing HSP20 is highly upregulated in the *C. elegans* dauer larvae (Burnell *et al.*, 2005) as is Sm-p40 in *S. mansoni* miracidia. Thus, the reason that Sm-p40 is so highly expressed in miracidia could be because it offers protection against the extreme physiological stresses that the miracidium is subjected to. Furthermore, as Sm-p40 operates in an ATP-independent manner, the protection it offers will not deplete the non-replaceable glucose reserves of the miracidium.

2.4.2 ATP Production

Schistosomes undergo metabolic changes during their life cycle in that the cercariae and miracidia use oxidative metabolism whilst the adults and intra-molluscan stages predominantly use anaerobic metabolism (Van Oordt *et al.*, 1989; Lawson & Wilson, 1980; Tielens *et al.*, 1991; Tielens *et al.*, 1992; Skelly *et al.*, 1998; Skelly *et al.*, 1993). This metabolic change makes sense in the context of the biological requirements of the parasite at each stage in its life-cycle. For the adult schistosome, glucose is a virtually unlimited resource because it is bathed in glucose-rich blood, and consequently there is no evolutionary pressure for it to continue to produce the tricarboxylic acid (TCA) cycle enzymes required for glucose-efficient, aerobic metabolism. The non-feeding miracidium on the other hand cannot replace its lost glucose yet it must be highly active as it emerges from the shell and locates, then penetrates a snail. By utilizing aerobic metabolism to generate (approximately fifteen times) more ATP per glucose molecule, the miracidium has an increased likelihood of reproducing itself.

The egg therefore represents a transition stage between anaerobic and aerobic respiration. It will need to be able to respire anaerobically whilst crossing the gut wall because the gut lumen is an anaerobic environment, but the aerobic pathway must be present as well so that it can become activated as soon as the egg hatches. Of the metabolic enzymes in immature SEA, the following are involved in aerobic respiration, so the capacity for aerobic respiration is evident early in the egg development: dihydrolipoamide dehydrogenase (which is part of the pyruvate dehydrogenase complex), citrate synthase, aconitase and ATP

synthase. Together these made up 2.9% of the protein in immature SEA, and the glycolytic enzymes made up a further 4.8%. The same set of aerobic respiration proteins were found in mature SEA plus succinate-CoA ligase and (mitochondrial) malate dehydrogenase. Overall, 3.2% of mature SEA consisted of proteins involved in aerobic respiration and another 4.6% were glycolytic proteins. Therefore, the mature egg contains more aerobic respiration proteins and fewer glycolytic enzymes than the immature egg, which is consistent with a change from anaerobic to aerobic respiration as the egg develops.

However, the picture becomes less clear when the miracidial metabolic enzymes are taken into account. Overall, aerobic respiration proteins make up only 1.7% of the soluble miracidial protein compared to the glycolytic enzymes which make up 6%. The explanation is likely to be that the glycolytic enzymes are also heavily involved in gluconeogenesis. Out of the ten glycolytic enzymes, seven are also used in the gluconeogenesis pathway and three are purely glycolytic (hexokinase, phosphofructokinase-1 and pyruvate kinase). None of the purely glycolytic enzymes were found in any of the egg preparations but two enzymes used during gluconeogenesis but not glycolysis were – namely phosphoenolpyruvate carboxykinase and cytosolic malate dehydrogenase. Gluconeogenesis occurs in the cytosol and its precursors include pyruvate, glycerol and lactate. When the precursor is pyruvate, gluconeogenesis requires it to be transported into the mitochondria where it is converted to oxaloacetate and then malate by the TCA cycle enzymes pyruvate carboxylase and malate dehydrogenase respectively. The malate is then transported back across the mitochondrial membrane into the cytosol, where it is converted back into oxaloacetate by cytosolic malate dehydrogenase. The cytosolic oxaloacetate is then converted into phosphoenolpyruvate by phosphoenolpyruvate carboxykinase and from there it proceeds along the gluconeogenesis pathway. Thus, mitochondrial malate dehydrogenase is required by the TCA and gluconeogenesis but cytosolic malate dehydrogenase is only involved in gluconeogenesis. It can be seen from Table 2.2 that mitochondrial malate dehydrogenase is present only in the miracidial and mature SEA preparations, demonstrating the relatively undeveloped state of the TCA cycle in the immature egg. Cytosolic malate dehydrogenase and phosphoenolpyruvate carboxykinase (another purely gluconeogenic enzyme) on the other hand are present in all of the egg preparations, so gluconeogenesis can be seen to be a process carried out by the egg in all its

stages of development. The proteomic study of the cercariae carried out by Curwen *et al.*, (2004) found no proteins involved in aerobic respiration, three glycolytic/gluconeogenic enzymes and no purely glycolytic ones. This indicates that the cercaria, like the miracidium, might be using its glycolytic enzymes to carry out extensive amounts of carbohydrate synthesis.

Proteins for aerobic respiration make up 3.2% of mature SEA but only 1.7% of the miracidium, so the metabolic process takes up a smaller proportion of the proteome of the miracidium compared to the mature egg. The "missing" respiratory proteins are probably contained in the envelope, which is therefore also likely to carry out aerobic respiration, although it is not part of a free-living stage of the parasite. This is supported by TEMs of the envelope that show abundant mitochondria, demonstrating the envelope's potential to carry out aerobic respiration (Ashton *et al.*, 2001; Ashton, 2007 *pers comm.).*

2.4.3 Cytoskeletal Proteins

Cytoskeletal proteins made up 9-11% of the SEA and the miracidial preparations but were completely missing from hatch fluid and the egg secretions (which is not surprising as cytoskeletal proteins are intracellular). Tubulin is the principal cytosketal protein, with three β isoforms and one α isoform identified in the gels. As microtubules are made up of α and β monomers in a 1:1 ratio it stands to reason that similar quantities of each monomer should be found. However, as only 1% of the tubulin in immature SEA, 4% in mature SEA and 33% in the miracidial preparation was of the α-type, α monomers are under-represented. Therefore cytoskeletal proteins probably constitute a larger percent of the egg proteome than is indicated. Five tubulin α isotypes and six β isotypes have been described and these differ in their amino acid sequences at the carboxyl end (Luduena *et al.*, 1992). Unfortunately, the sequences of the identified tubulins are of insufficient length to include the diagnostic C-terminus, except for Sm10465 which is probably β4 tubulin (the β4-specific sequence of EGEFXXX is present in Sm10465, except the initial glutamic acid is substituted with aspartic acid). The idea that different tubulin isoforms perform different physiological functions is not (yet) generally accepted because too little work has been published proving a correlation between isoform and function (Jensen-Smith *et al.*, 2003). However, only β1 and β4 tubulins have been found in motile cilia (Renthal *et al.*, 1993;

Roach *et al.*, 1998; Jensen-Smith *et al.*, 2003), whilst sensory cilia have been found to contain all types (Woo *et al.*, 2002). Therefore, the β4-like Sm10465 could form the motile cilia that completely cover the external surface of the miracidium or be in its flame cells. This is consistent with the absence of Sm10465 from immature SEA. The tubulin in the immature egg is more likely to be involved in cell division and intracellular transport, because processes must be occurring at high rates as the embryo rapidly develops.

The abundance of actin in immature SEA, mature SEA and the miracidial preparation (3 – 3.5% of the total protein) is consistent with Curwen *et al.*, (2004) who found it among the top 20 spots of gels of cercariae, adult worm and lung worm preparations. In the developing egg, actin is likely to be involved in morphogenesis but when fully developed the miracidia is covered by longitudinal and circular actin fibres, associated with smooth muscle and co-localised to flame cells (Bahia *et al.*, 2006).

2.4.4 Defence Proteins

Defence proteins will be required to protect the egg from toxic compounds present in serum, produced by the leukocytes of the granuloma or by the egg itself as part of its escape mechanism. As discussed in Chapter 1 (Section 1.2.4), the immature egg is immunologically inert with a less well developed granuloma around it compared with the mature egg. A smaller granuloma will produce fewer toxins which the (small) embryo, embedded amongst vitelline cells is more isolated from anyway. The immature egg does not produce ESPs and so it does not need to protect itself from any toxic properties ESP may have. So, as the immature egg is not particularly vulnerable only a relatively small proportion of its proteome needs to be comprised of defence proteins (4%). The mature egg by contrast is more vulnerable because the miracidium must be protected. Defence therefore becomes a more important issue as the egg matures, so it is not surprising that the proportion of defence proteins increases to 7% in mature SEA. Some defence proteins must be contained within the miracidium because it needs to protect itself whilst it penetrates the snail (3% of the miracidial preparation consists of defence proteins). However, the hatch fluid contained by far the largest proportion of defence proteins (16%). This is not surprising because hatch fluid bathes the miracidium whilst it is still inside the egg,

providing an insulating and protective layer which isolates it from both the host cells and the envelope where ESPs are produced.

The increase in proportion of defence proteins in hatch fluid compared to immature SEA is mostly due to increased quantities of the same proteins rather than the development of a more complex mixture of new defence proteins. However, as the identification of proteins in the experiment relied heavily on between-gel matching of spots there will be a bias towards proteins found in more than one gel. It is likely that the 314 spots which are only present in mature SEA will incorporate hatch fluid-specific, defence proteins. The only defence protein that was found in hatch fluid but not in immature SEA was thioredoxin (constituting 4.1% of the hatch fluid defence proteins). It is surprising that thioredoxin was not found in immature SEA because thioredoxin peroxidase uses thioredoxin as an electron donor and immature SEA contained two thioredoxin peroxidases. Of the thioredoxin peroxidases, SmPrx3 is mitochondrial and probably deals with self-generated oxygen radicals escaping from the mitochondrial electron-transport chain (Sayed & Williams, 2004; Chang *et al.*, 2004). It is therefore not surprising that SmPrx3 is more highly expressed in mature SEA and the miracidium compared to immature SEA, because the miracidium has switched to aerobic respiration. The expression level of SmPrx3 in hatch fluid is low, probably because hatch fluid SmPrx3 will have been derived from ruptured cells of the envelope and proteins from this source form a relatively small proportion of the total hatch fluid proteome. A second thioredoxin peroxidase (SmPrx1) which is cytosolic and resistant to over-oxidation (Sayed & Williams, 2004) is also present in the egg. SmPrx1 is the version of thioredoxin peroxidase that was reported to be excreted from the egg into the granuloma (Williams *et al.*, 2001) and discussed in Section 1.4.3, although it was not found in ESP (see Table 2.3).

Another defence protein (Smp154260), found in similar quantities in immature SEA and mature SEA but upregulated in hatch fluid has homology to the wasp venom allergen antigen 5 (Lu *et al.*, 1993), which forms part of the plant pathogenesis-related (PR1) family of proteins. These were originally described as being produced by plants in response to viral infections and are secreted by L3 hookworm larvae upon host entry (Eberle *et al.*, 2002; Asojo *et al.*, 2005; Dillon *et al.*, 2006). In *S. mansoni,* three PR-1 proteins have been

found in secretions from newly-transformed cercariae and transcripts of a fourth have been found to be up-regulated in lung stage schistosomes (Curwen *et al.*, 2006; Dillon *et al.*, 2006). The PR-1 in hatch fluid is different to all of those previously found. Nothing is known about the function of PR-1 proteins, but it is clear that they are often characterized by their resistance to protease degradation (Eberle *et al.*, 2002). The role of Smp154260 could therefore be to protect the miracidium from ESP proteases.

2.4.5 Host Proteins in the Egg

Host proteins constitute a significant proportion of the hatch fluid (6.6% of the protein volume). As none were detectible in mature SEA, host proteins are not abundant in terms of the percentage of total protein in the egg. Host proteins could be located either side of the envelope - between the envelope and the shell or between the envelope and the miracidium. The area between the envelope and the shell is much smaller in terms of volume and will also contain ESPs. It is therefore likely that a substantial proportion of the host proteins are present between the envelope and the miracidium, so it follows that there must be active transportation across the envelope. The transport of host proteins across the envelope has been previously demonstrated in only one paper, in which host L-selectin and CD3 were found between the miracidium and envelope when liver granulomata sections were probed with mAbs (El Ridi *et al.*, 1996).

It is considered unlikely that the host proteins are contaminants or artefacts derived from the outside of the shell, because any material adhering to the exterior surface of the shell would have been removed during the preparation steps, which involved a three-hour incubation in trypsin and then repeated saline washing steps. Even if any host proteins had somehow remained stuck to the shell despite the preparative regimen it is extremely unlikely that they would then be solubilized when the eggs were placed in filtered water for hatching. The possibility that the host protein identities were incorrectly generated as a result of searching conserved murine/*S. mansoni* amino acid sequences can also be rejected because three out of the five host proteins are not present in the *S. mansoni* genome (the alpha/beta haemoglobin subunits and regucalcin). The controversial existence of *S. mansoni*-albumin will be discussed later (in Section 2.4.6), but the albumin found in hatch fluid is definitely of murine origin because two of the fragmented peptides identified by

MSMS contained sequences unique to mouse albumin (DVFLGTFLYEYSR and LSQTFPNADFAEITK). The other host protein, murine HSC70 (a member of the HSP70 family) has some overall amino acid sequence homology to *S. mansoni* HSP70 (an E value of $7e^{-17}$ to Sm09042), but two of the four peptides that were fragmented (STAGDTHLGGEDFDNR and LLQDFFNGK) were in unconserved regions.

2.4.5.1 Regucalcin

Regucalcin (constituting 0.4% of hatch fluid) is a vertebrate Ca^{2+}-binding protein (Misawa & Yamaguchi, 2000). It is highly expressed in the liver where it regulates intracellular calcium homeostasis by activating calcium pump enzymes (Yamaguchi, 2005). Hepatic regucalcin is released into serum following chemically-induced liver damage in rats (Isogai *et al.*, 1994a; Isogai *et al.*, 1994b) and in humans suffering with hepatitis (Yamaguchi *et al.*, 1997). The quantity of regucalcin found in the hatch fluid suggests that it may be purified in the egg because a recent proteomic study of changes to the rat serum proteome during liver injury didn't find regucalcin amongst the proteins expressed at a detectible level (Merrick *et al.*, 2006; Merrick *pers comm.*, 2006). It is possible that the regucalcin is involved in protecting the egg from damage by superoxide, because it has been shown to increase the activity of superoxide dismutase (Fukaya & Yamaguchi, 2004), and this enzyme is present in large quantities in all of the morphological components of the egg (see Tables 2.4 – 2.7).

2.4.5.2 HSC70

HSC70 is a major cytoplasmic protein and is the most abundant a member of the HSP70-related proteins in mice, with particularly high expression in the liver, skeletal muscle and the kidney (Hunt *et al.*, 1999). HSC70 is also found in exosomes secreted by tumour cells, reticulocytes, DCs and B cells (Hegmans *et al.*, 2004; Geminard *et al.*, 2001; Thery *et al.*, 2001; Clayton *et al.*, 2005). At 40-90nm in diameter, intact exosomes are too large to enter the egg, so HSC70 must be present in reasonable concentrations in the extracellular fluid surrounding the egg, whether it be derived from burst exosomes or secreted via a different mechanism. At 70kDa, HSC70 is the largest host protein in the egg and indicates that the shell must be permeable to molecules of this size. It is unclear what benefit the egg obtains by sequestering HSC70 from the host, but as the concentration of serum HSC70 in the

hepatic granulomata of schistosome-infected mice is not known, it is possible that the quantity found in hatch fluid is consistent with passive absorption of serum proteins into the egg.

2.4.5.3 Haemoglobin

The presence of intact haemoglobin α and β chains in the egg means that erythrocyte lysis must be occurring around the egg, because erythrocytes are far too large to enter the egg intact. Once lysed, the erythrocyte will lose its haemoglobin content, the $\alpha_2\beta_2$ structure break apart and the separate chains enter through the shell. There is an inherent risk for the egg in accumulating haemoglobin because degradation of haemoglobin releases the free haem group which is toxic. Haemoglobin is digested in the gut of adult schistosomes by aspartic and cysteine proteases such as cathepsins and Sm32, which are optimally active at pH4 but completely ineffective against haemoglobin at pH6.5 (Delcroix *et al.*, 2006). Free haem released by the degradation of haemoglobin is detoxified in the adult worm by aggregating it into haemozoin (Oliveira *et al.*, 2004). In the egg, the presence of intact haemoglobin chains and the absence of haemozoin indicate that the toxic effects of haem are avoided by preventing the degradation of haemoglobin in the first place. The failure to degrade haemoglobin is likely to be a consequence of the egg having an internal pH that is inappropriate for the requisite proteases to be active. There would be no reason for the egg to produce proteases that would be incapable of activity, so it is not surprising that no Sm32 transcripts and only low levels of cathepsin B transcripts have been found in the egg (Dillon, *pers comm.*, 2006).

2.4.6 Albumin

2.4.6.1 Host Albumin in the Egg

Fatty acids are incorporated into the structure of phospholipids, which are themselves important components of cell membranes. Schistosomes can construct phospholipids from fatty acids, but they must obtain the fatty acids from the host because as they are incapable of producing them *do novo* (Brouwers *et al.*, 1997). The egg therefore requires a mechanism to obtain host fatty acids and then transport them across the membrane to the developing miracidium. Albumin is a fatty acid-binding protein with five high-affinity ligands (Simard *et al.*, 2005), and as the most abundant host protein in the egg (4.3% of the

protein in hatch fluid) its role could be to that of fatty acid importer. Albumin also has a potential role in defence because it has been shown to have anti-oxidant properties in that it can scavenge superoxide and hydrogen peroxide produced by neutrophils using an acellular mechanism (Kouoh *et al.*, 1999).

2.4.6.2 "*S. mansoni*-Albumin"

In order to establish whether the "*S. mansoni* albumin" described by Williams *et al.*, (2006) as being of parasite origin is actually of host origin, albumin from the common laboratory host *Mesocricetus auratus* (Golden Hamster) was isolated, trypsinised, analysed by MALDI-MS, Electrospray-MSMS and the peptide sequences compared to the "*S. mansoni* albumin" sequence deposited on NCBI.

Williams *et al.*, (2006) had obtained schistosomula by mechanical transformation from cercariae and adult worms by perfusing them from mice. The parasites were subjected to oxidative stress and albumin was detected by RT-PCR, but only when hydrogen peroxide was present in the culture medium. Consequently, the authors proposed that the albumin was produced by the schistosome as a sacrificial oxidant scavenger. The albumin was sequenced and was found to have the most homology with albumin from the "Red Vole *Microtus fortis*". It was then claimed that the gene had been acquired from a rodent host by lateral gene transfer and then undergone evolutionary change. (The authors presumably intended to refer to the Reed Vole *Microtus fortis*, because albumin from the Red Vole *Clethrionomys rutilus* has not yet been sequenced!)

The finding that the amino acid sequence of the proposed *S. mansoni*-albumin gene is identical to albumin from the Golden Hamster (see Figure 2.13) makes it extremely difficult to accept the gene transfer theory. Also, lateral gene transfer in schistosomes is controversial (see Section 2.1.4) and hamsters are unlikely ever to have been a natural host for schistosomes because their geographical distributions are different - hamsters, unlike *S. mansoni*, are found in southern Europe and west Asia. More specifically, the Golden Hamster is only found in the wild in Syria, where schistosomiasis is/was restricted to a few small foci of *S. haemoatobium* infections (Abdel-Azim & Gismann, 1956). Golden Hamsters are a well-used laboratory host for *S. mansoni* though, and PCR is an extremely

sensitive technique, so it is easy to see the potential for parasite samples or laboratory equipment to become contaminated with host material to generate an erroneous result. The results of the proteomic albumin experiment in this chapter are supported by data from further genomic experiments carried out by other members of this laboratory, in which no albumin gene could be detected in the *S. mansoni* genome either by *in silico* searching or Southern blotting (DeMarco *et al.*, 2007).

Nevertheless, no obvious route can be seen in which hamster albumin could have contaminated all of the experiments carried out by the Williams group. Both the Sayed *et al.*, (2006) and the Williams *et al.*, (2006) papers state that the parasites were maintained in a murine host and the schistosomula were transformed mechanically, so there was no direct physical contact between the parasite material and the host. The Sayed *et al.* study also report finding "*S. mansoni* albumin" using Electrospray-MSMS, but no fragmentation data was provided so an assessment of the quality of the data cannot be made. It is therefore possible that the albumin was derived from FCS, which was present in the culture medium. The Williams group also appear to have obtained their parasite material from an external source, so it is also feasible that they could have been provided with incorrect information with regard to the host species.

2.4.7 The Proteome of the Female, Vitellaria-Enriched Preparation

It was surprising that the preparation enriched in vitellaria bore so little resemblance to immature SEA that between-gel spot matching could not be carried out. Eight out of the nineteen different proteins from the female, vitellaria-enriched gel were not found in the egg, so there must be a significant quantity of non-vitelline material in the rear section of the female. This is despite the studies showing the vitellaria packing out this part of the worm (Spence & Silk, 1971). Two of the identified non-egg proteins (myosin light chain and Sm20.8) were among the twenty most abundant spots in cercariae and adult worms (Curwen *et al.*, 2004) and another (leucine aminopeptidase) is the enzyme that Xu & Dresden (1986) state could be a miracidial-hatching enzyme. However, the transcript found in the female, vitellaria-enriched preparation encodes a cytosolic protein, so is unlikely be a candidate for a secreted version.

The egg's vitelline cells are degraded as the embryo develops, and so proteins exclusively found in vitelline cells will be present in the gels of the female, vitellaria-enriched preparation and immature SEA, but missing from the mature SEA, miracidial and hatch fluid gels. The only protein fitting this criterion is Ferritin 1. Ferritin exists in two isoforms, of which Ferritin 2 is fairly ubiquitously present in both *S. mansoni* sexes, whilst Ferritin 1 is fifteen times more abundant in females and can be localised to the vitelline cells (Schussler *et al.*, 1995; Winnen *et al.*, 1995). Ferritin has also been found highly expressed in vitelline cells of *Clonorchis sinensis* and *Paragonimus westermani* (Tang *et al.*, 2006; Kim *et al.*, 2002). Therefore, Ferritin 1 appears to be the only protein identified from the female, vitellaria-enriched preparation which definitely forms part of the vitelline cell. The reason why so few vitelline cell proteins were found is probably due to the extensive changes that occur in vitelline cells as they develop (Erasmus, 1975) combined with the high production rate of 9,000 – 12,000 cells/day (see 1.2.1). It is therefore unlikely that the proportion of fully-mature cells found in the vitellaria at any one point in time would be particularly large, and consequently their proteins will represent a small component of the whole and not well represented in the gel.

2.4.8 The Proteome of Hatch Fluid

Hatch fluid contains the greatest proportion of proteins that have an unknown function (20.4% of its proteome). This is probably a reflection of the unstudied status of hatch fluid in schistosomes, its lack of physical structure and the scarcity of an equivalent material in other organisms. None of the hatch fluid proteins of unknown function have homology to any non-schistosome proteins either.

Smp170410 is the largest component of hatch fluid, making up 18.2% of the protein in the gel. It is more highly expressed in mature SEA than in immature SEA (1.8% compared to 0.6% - see Figure 2.8), so it is unlikely to be a vitelline cell remnant. It is possible that Smp170410 is located in the prominent vesicles that are found between the envelope and the miracidium and it therefore might be involved in the hatching process – possibly by expanding under osmotic pressure when the egg contacts fresh water.

2.4.9 The Proteome of ESP

Subjecting 75µg ESP to 2-DE demonstrated that the egg secretes more proteins than originally thought. Although 27 different spots can now be seen in the gel, 83% of the protein constituted the six ESP3-6 spots. It is therefore very likely that further ESPs will be discovered if ESP3-6 were to be separated from crude ESP and a larger quantity of non-ESP3-6 proteins separated by 2-DE. Apart from ESP1-2 (which is Omega 1) and ESP3-6 (which is IPSE), none of the ESPs had significant homology to any proteins of known function. Thioredoxin peroxidase, described by Williams *et al.*, (2001) as being secreted from the egg was not found.

ESPs 13/14 (Sm11845) and ESP 17 (Sm12949) form a series of three adjacent, acidic spots on the gel of approx. 25kDa. The amino acid sequences of Sm12949 and Sm11845 are 74% homologous and are found adjacent to each other on the same contig, although Sm11845 is shown as being transcribed from one DNA strand and Sm12949 from the other strand. As well as being secreted by the egg, ESP13-14 (Sm11845) and its associate ESP18-19 (Sm12949) have also been identified amongst the secretions from lung worms (Curwen, 2006 *pers comm.*). These proteins are clearly important to the parasite, and as they are also in the region of the zymogram where Ashton (2001) found proteolytic activity, it is possible that they may be involved in the proteolysis that is required for the egg to escape the host. No proteolytic domains were found when carrying out BLAST against the MEROPS protease database, but the Gene Ontology classification scheme (http://www.geneontology.org) predicts that Sm11845 (but not Sm12949) has a potential subtilase pro-protein convertase functional domain. This finding raises the question of whether the role of ESP13-14 might be to activate host proteases to aid the egg's passage across the gut wall. This idea is pursued further in Chapter 3.

2.4.10 Vaccine Candidates in the Egg.

Five out of the seven priority WHO vaccine candidates (Bergquist *et al.*, 2002) were relatively abundant in the egg (paramyosin, GAPDH, GST, triose phosphate isomerase and Sm14). Another vaccine candidate, IrV5 (part of the myosin heavy chain) was not found, possibly because its large size would hinder its migration through the gel. However, myosin is definitely present in the egg, because mAbs have been used to localise it to actin-rich

tubules in the flame cells (Bahia *et al.*, 2006). The presence of vaccine candidates in the egg means that they will be exposed to the host's immune system when eggs disintegrate in the liver during the normal course of infection. An adaptive immune response to the antigens would therefore be generated, and a consequential evolutionary pressure for the parasite to resist it would develop. It is therefore not surprising then that these vaccine candidates do not offer spectacular protection to the host (Pearce, 2003). Also, if vaccines were to be cross reactive to egg proteins there is a risk that the vaccine will sensitise individuals to egg proteins, causing an increased response to disintegrating eggs, thereby causing additional pathology. So, in future, vaccine candidates should consist of proteins that are not highly expressed in the egg.

Chapter 3

Functional studies of ESP

3.1 Introduction

The granuloma that forms around eggs is vital to both the host and the parasite: to the host because it forms a protective, isolating barrier around the egg and to the parasite because the leukocytes of the granuloma aid the passage of the egg through the gut wall (discussed below in Section 3.1.1). ESPs are a product of live eggs and so (unlike SEA) they represent the interface between the egg and the developing granuloma.

3.1.1 ESP and the Granuloma

The granuloma is the cellular focus that forms around the egg. In schistosomiasis, the principal cells of the granuloma are macrophages, T cells and eosinophils, the proportions of which differ depending on which tissue the granuloma develops in. For example, in CBA mice, liver granulomata mostly contain eosinophils, with smaller numbers of macrophages and T cells, but colonic granulomata contain more macrophages than eosinophils (Weinstock & Boros, 1983). These cellular differences could be attributable to local regulatory events (as the authors propose) but they could also reflect the longer developmental period of liver granulomata (that form around trapped eggs that eventually die and disintegrate) compared with those found in the intestine (where the eggs are in transit and most will be excreted whilst still alive). It is clear however that regardless of the location of the granuloma, macrophages are its principal antigen presenting cells (APCs). The roles T cells have in enabling the egg to escape from the host and in inducing the host's Th2 response to egg deposition have been discussed in Chapter 1 (Sections 1.2.5 and 1.1.4 respectively). As these responses occur whilst the egg is still alive, it is likely macrophages, presenting ESPs to the T cells of the granuloma are important early events in the process.

This chapter incorporates experiments aimed at establishing whether macrophages from naïve mice are activated by ESP and whether this activation includes the up-regulation of MHCII. In another series of experiments the hypothesis that ESP (representing the live egg) is more immunogenic than SEA (representing the disintegrating egg) is tested. Leukocytes from mice at the acute stage of infection were used in these comparative assays because

they are at the point at which the adaptive immune response to egg antigens is at its peak (Boros *et al.*, 1975; Sadler *et al.*, 2003).

3.1.2 ESP and the Escape of the Egg

As discussed in Chapter 1 (Section 1.2.3), eggs probably require proteases to cross the gut wall. It is not known whether these proteases are secreted by the egg, by the cells of the granuloma or by both. Various *in vitro* experiments have reported protease activity in egg secretions (see Chapter 1, Part 4) , the most convincing of which was a 2D casein zymogram of crude ESP (Ashton, 2001). Proteases derived from granuloma T cells have been implicated in egg-escape in an *in vivo* experiment in which mice deprived of T cells showed a drastically reduced ability to excrete eggs (Doenhoff *et al.*, 1986). Whatever their origin, the proteases are likely to be of the metalloproteases class because metalloproteases have been localised to the granulomata of infected humans and mice (Singh *et al.*, 2004; Gomez *et al.*, 1999). They have also been implicated in the degradation of extracellular matrix in cancer (Chang & Werb, 2001). There are two closely related metalloprotease families: "A Disintegrin and Metalloproteases" (ADAMs) and MMPs. The ADAM family is subdivided into two groups: "ADAMs" and "ADAMs containing a thrombospondin domain" (ADAMTs). ADAMs are membrane-bound and process/activate other transmembrane proteins, thereby influencing cell adhesion and signalling events (Mochizuki & Okada, 2007). ADAMTs are usually secreted and have been implicated in the cleavage of von Willebrand factor and the processing of collagen pro-peptides (Mochizuki & Okada, 2007; Canty & Kadler, 2005). There are seventeen secreted MMPs with different substrate specificities (von Lampe *et al.*, 2000). MMPs of potential interest in the transit of the schistosome egg are MMP-1, MMP-8 and MMP-13 (collagenases which cleave the triple helical structures in Collagen I, II, III and X) and MMP-2 and MMP-9 (gelatinases whose substrates include Collagen IV and denatured collagen of other types). All of these above-numbered MMPs are known to be secreted by macrophages, eosinophils and T cells, which as discussed above are the principal leukocytes making up the granuloma (von Lampe *et al.*, 2000; Taylor *et al.*, 2006b; Goetzl *et al.*, 1996; Lacraz *et al.*, 1994; Okada *et al.*, 1997; DiScipio *et al.*, 2006). However, if MMPs and ADAMTs are involved in egg escape they will still need to undergo further processing steps because they are secreted as inactive precursors, requiring the cleavage of an amino-terminal domain to

be activated (von Lampe *et al.*, 2000; Nagase, 1997). It is possible that ESP13-14 fulfils this role as it possibly contains a subtilase pro-protein convertase functional domain (see Chapter 2, Section 2.4.9).

Activated MMPs and ADAMTs are regulated by inhibitors such as α_2 macroglobulin and a family of secreted proteins called Tissue Inhibitors of Matrix Metalloproteinases (Gomez *et al.*, 1997). So, if the egg is to commandeer host proteases, not only has it got to induce the granuloma cells to secrete the MMPs in the first place, but it also needs to create the right environment in which the pro-proteases can be activated whilst the concentration of the inhibitory proteins is maintained at a relatively low level. Although this seems to be a tall order, there is evidence that this is what occurs because in the murine model mRNA encoding MMP-2, MMP-3 and MMP-8 is up-regulated in the colonic tissues of infected animals (Singh *et al.*, 2006).

3.1.3 Experimental Aims and Objectives

The work of this chapter aims at establishing whether leukocytes known to be present in the granuloma respond to ESP. The leukocytes were taken from naïve mice in some assays and from infected mice in others, so the results can be seen in terms of ESP-innate immune system interactions and ESP-adaptive immune system interactions. The ESP-innate immune responses represent what would occur in a new infection when egg deposition begins. Macrophages would be the initial cells that adhere to the egg to start the inflammatory focus (Co *et al.*, 2004), and the immediate egg products to which the macrophages could respond to will be ESP. The macrophages are likely to respond to the ESP by becoming activated and presenting ESP peptides on upregulated MHCII molecules. So, by measuring changes in MHCII expression and IL-6 production by naïve macrophages cultured with ESP, the antigenicity of ESP was assessed. Other experiments using the naive macrophage model involved comparing the proteolytic activity in crude ESP with that in the supernatants from macrophage-ESP cultures, to establish whether ESP contained a subtilase-like pro-protein convertase. As it was not known what class of protease to assay for, the protease assays were carried out using the QuantiCleave universal protease assay (Pierce 23267) in fluorescence resonance energy transfer (FRET) mode. Classical FRET occurs when electron energy is transferred between two different fluorophors. In the

QuantiCleave assay, FRET events occur between adjacent fluorophors, so when the (casein) substrate is cleaved a reduction in FRET occurs, which is measured as an increase in fluorescence. The ability of ESP to stimulate naïve T and B cells was also assessed by culturing splenocytes from naïve mice with ESP. In this experiment, cell proliferation was taken as a measure of activation.

After egg deposition has underway for several weeks some of the initially produced eggs will have died and disintegrated. After this point in time, all of the newly produced eggs will be in an environment where the host immune system will have seen and responded to both ESP and SEA. Although SEA is a more complex mixture than ESP and therefore containing more epitopes, it is not currently known whether ESP is more or less immunogenic. This question was addressed by stimulating mesenteric lymphocytes with both ESP and SEA and comparing their proliferative responses.

3.2 Methods

3.2.1: Preparing ESP and SEA

ESP was made as described previously (Chapter 2, Section 2.2.4), but in experiments involving the measurement of protease activity the ESP was made using Phenol Red-free RPMI-1640 (Gibco). SEA was made as described in Chapter 2, Section 2.2.3, except the eggs were not separated into mature and immature fractions before grinding and no PIC was added.

3.2.2: The Stimulation of Macrophages from Naïve Mice

Cells were elicited into the peritoneal cavity of five naïve, female C57BL/6 mice by injecting each mouse with 500µl of sterile, 3% Brewers thioglycollate medium (Sigma). Five days later the mice were killed and 10ml culture medium was injected into the abdominal cavity of each mouse. Culture medium was prepared as follows: RPMI 1640 (Gibco), plus 10% low-endotoxin FCS (Harlan), 1% 10,000µg Streptomycin sulphate/10,000 units Penicillin G sodium per ml in 0.85% saline (Invitrogen) and 1% 200nM Glutamine (Invitrogen) and 10ng/ml of rIFN-γ (Pharmingen). Peritoneal exudate cells (PEC) were dislodged from the tissue by massaging the abdomen, then extracted through a 21G needle into a 15ml falcon tube on ice and centrifuged at 350g for 5 min. The supernatant was removed, then the pellet was re-suspended in 2ml fresh culture medium and the cellular concentration of live, macrophages/monocytes was established by Trypan Blue exclusion using a haemocytometer.

The cells were plated out in 1ml aliquots at 1 x 10^6 monocytes/granulocytes per ml in a plastic 12-well plate (Nunc) and incubated for 1 hour at 37°C and 5% CO_2. The culture medium was agitated to dislodge the non-adherent cells, which were then removed in suspension leaving the plastic-adherent cells stuck as a monolayer to the base of the well. (This plastic-adherence purification method retains > 80% of monocytes/phagocytes in a cell suspension at > 95% purity (Treves *et al.*, 1980)). The purified macrophages/monocytes were immediately re-immersed in 1ml of fresh culture medium at 37°C, containing different concentrations of SEA or ESP. Polymyxin B (PMB) (Sigma) at

12.5μg/ml was added to all wells (except the appropriate controls) to eliminate endotoxin contamination. The positive control was lipopolysaccharide (LPS) at 10ng/ml.

The culture plate was then incubated for 18 hours, after which the supernatants were collected and stored at -18°C for cytokine analysis. The less-adherent macrophages were removed from the plate by rinsing them with ice-cold PBS. The more-adherent macrophages were removed by incubating them for 10 minutes with 125μl/well of 0.25% trypsin solution which contained 1mM Ethylene Diamine Tetraacetic Acid (EDTA) (Invitrogen) and then any remaining macrophages were gently dislodged with the plunger of a 1ml syringe. The macrophages were centrifuged at 350g for 5min, re-suspended in PBS containing 1% FCS and blocked with heat inactivated rabbit serum, then stained with biotin-conjugated rat anti-mouse MHCII antibody (Caltag) followed by streptavidin-conjugated to allophycocyanin (Caltag). Isotype controls were stained with the anti MHCII antibody only. MHCII expression was assessed using a flow cytometer (Dako Cyan) with optimised voltage and flow rate settings. The concentration of IL-6 in the culture supernatant was measured by sandwich ELISA using rat anti-mouse IL-6 antibody with a biotinylated detecting antibody (Pharmingen) in flat bottomed 96-well plates (Nunc).

3.2.3: The Stimulation of Splenocytes from Naïve Mice

Spleens were removed from three naïve female C57BL/6 mice that had been reared together in individually-ventilated cages (Tecniplast). Culture medium was prepared as described in 3.2.3 except IFN-γ was excluded and 0.1% 50mM β-Mercaptoethanol (Invitrogen) was added. The spleen was teased apart in culture medium using the plunger from a 1ml syringe and the splenocytes recovered by rinsing them through a stainless steel mesh (which removed the spleen tissue). The splenocytes were centrifuged at 200*g* for 7 minutes then suspended in 2ml of ACK erythrocyte-lysing buffer (150mM NH_4Cl, 10mM $KHCO_3$, 0.1mM EDTA, adjusted to pH7.2) for 2 mins. The ACK buffer was then diluted with 13ml of culture medium, the centrifugation step repeated, the buffer replaced with 2ml culture medium and the pellet re-suspended. A small aliquot of cells was stained with 0.4% Trypan Blue solution (Sigma) and a haemocytometer used to assess the concentration and viability of the cells. The splenocytes were then plated out at 2×10^5 cells/ml, in a 96-well

multi-well plate (Nunc) such that the volume in each well was 200µl. with antigen (ESP at 40µg/ml or hamster anti-mouse CD3ε chain mAb (Pharmingen) at 0.33µl/well).

The plate was incubated at 37°C and 5% CO_2 for 72 hours. 0.25µl of (methyl-^{3}H) thymidine aqueous solution, specific activity 185GBq/mmol (Amersham), was then added to each well and a second 24-hour incubation step was carried out. A cell harvester (Packard Filtermate) was used to transfer the cells onto a Unifilter GF/C 96-well plate (Perkin Elmer), which was then washed and allowed to dry overnight. Microscint-20 LSC cocktail (Packard) was added at 20µl per well before the thymidine incorporation was measured on a Top Count NXT (Packard) scintillation luminescence counter (which expresses the data as counts per min. (cpm)).

3.2.4: The Stimulation of Lymphocytes from Infected Mice

Mesenteric lymph nodes were removed from female C57BL/6 mice that had been reared together in an individually-ventilated cage (Tecniplast) after they had been infected with 180 cercariae/mouse seven weeks previously (using the protocol described in Chapter 2, Section 2.2.1). The lymphocytes were extracted and prepared for culture using the same method as Section 3.2.3 (except the ACK lysing buffer was not used and the cellular concentration was 1 x 10^6 cells/ml). The lymphocytes were stimulated with ESP or SEA at 0 - 80µg/ml, or Concanavalin-A (Con A) (Sigma) at 2.5µg/ml and then incubated, harvested and their proliferation measured as described in Section 3.2.3.

3.2.5: Protease Secretion from Naïve Macrophages stimulated with ESP

The extraction, purification and culture of naïve macrophages was carried out as described in Section 3.2.2, except three mice were used and serum-free AimV culture medium (Gibco) was used instead of the RPMI-based medium (which contained FCS). The macrophages were stimulated with different concentrations of ESP or 100ng/ml phorbitol 12-myristate 13 acetate (PMA) (Sigma). Flow cytometry (Dako Cyan) was used to establish the phenotypic profile and viability of the cells in the crude exudate from each mouse at the beginning of the experiment and for the cells from each well of the culture plate at the end of the experiment. The phenotypic profile of each sample was assessed

using the SSC/FSC plot and the % cell mortality was measured using 1% propidium iodide (PI) incorporation. Post-culture supernatants were immediately assayed for protease activity using the QuantiCleave Fluorescent Protease Assay Kit (Pierce), in which 100µl of culture supernatant and 100µl of substrate were incubated for 60 min at 26°C in white, flat-bottomed 96-well Multiwell plates (Nunc). Fluorescence was measured on a Polarstar Optima plate reader (BMG Labtech) with optimised gain adjustment and the results expressed as the change in fluorescence at the beginning and end of the incubation period (mean of duplicated wells). It was necessary to measure the protease activity of crude ESP in a separate plate (with a different gain adjustment) because the Aim V (macrophage) culture medium contained Phenol Red, whereas the RPMI-based ESP preparation did not. In order to compare the two sets of results, protease standards were made using sequencing grade porcine trypsin (Promega) that had been solubilized in the same culture medium as its accompanying test samples.

3.3: Results

3.3.1: The Stimulation of Macrophages from Naïve Mice

MHCII expression on cultured naïve macrophages was not influenced by the presence or absence of ESP (Figure 3.1). With a 1% gate, the mean percentage of $MHCII^{+}$ve cells varied between 33.9% (40µg ESP/ml) and 40.2% (20µg ESP/ml) but there were no statistically significant differences between any of the assays (standard error of the mean). It was possible to obtain increases in the percentage of $MHCII^{+}$ve cells by increasing the size of the gate, but still no statistically significant between-assay differences in expression emerged. No between-assay differences in staining intensity (calculated as the difference in mean APC units between each assay containing the MHCII antibody and its isotype control) was seen either. If the median difference rather than the mean difference in APC units was taken the results were even more homologous (due to larger error bars). When the experiment was repeated without IFN-γ in the culture medium the MHCII expression levels were lower and more homologous in all of the assays (result not shown).

Naïve macrophages secreted IL-6 when stimulated with ESP, but not when stimulated with SEA (Figure 3.2). The differences in IL-6 production in response to each concentration of ESP and its immediate doubling dilution were not statistically significant, but the difference between 40µg ESP/ml and 10µg ESP/ml was, as were the differences between any assay containing ESP and the negative control. The secretion of IL-6 was dependent upon the presence of IFN-γ in the culture medium as no IL-6 was produced when IFN-γ was absent.

3.3.2: The Stimulation of Lymphocytes from Naïve and Infected Mice

Splenocytes from naïve mice did not proliferate in response to ESP (Figure 3.3). In contrast, cells from the mesenteric lymph nodes of acutely infected mice proliferated when stimulated with either ESP or SEA (Figure 3.4). A dose-dependent increase in proliferation occurred in the ESP assay at antigen concentrations up to 40µg/ml, but the extent of cell proliferation to 80µg ESP/ml and Con A was less than that seen at 40µg ESP/ml. Dose-dependent cell proliferation also occurred in the SEA assays but to a lesser extent than that induced by ESP.

A

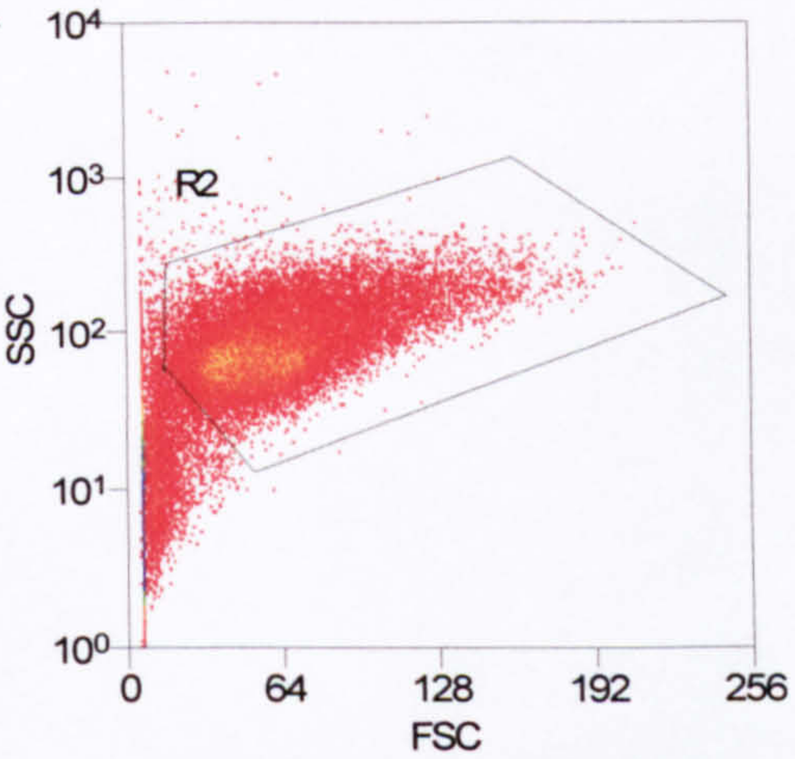

Region	Count	% Events
Total	29265	100.00
R2	21111	72.14

B

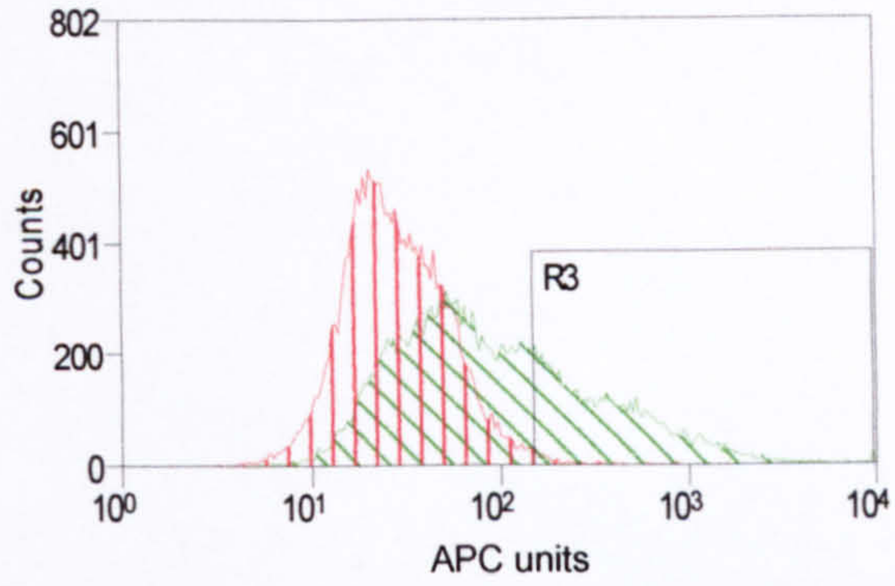

Region	Count	% Events	Mean	Median
Total	21188	100.00	35.88	26.42
R3	206	0.97	321.48	177.83
Total	21111	100.00	222.63	77.74
R3	6840	32.40	531.41	339.82

C

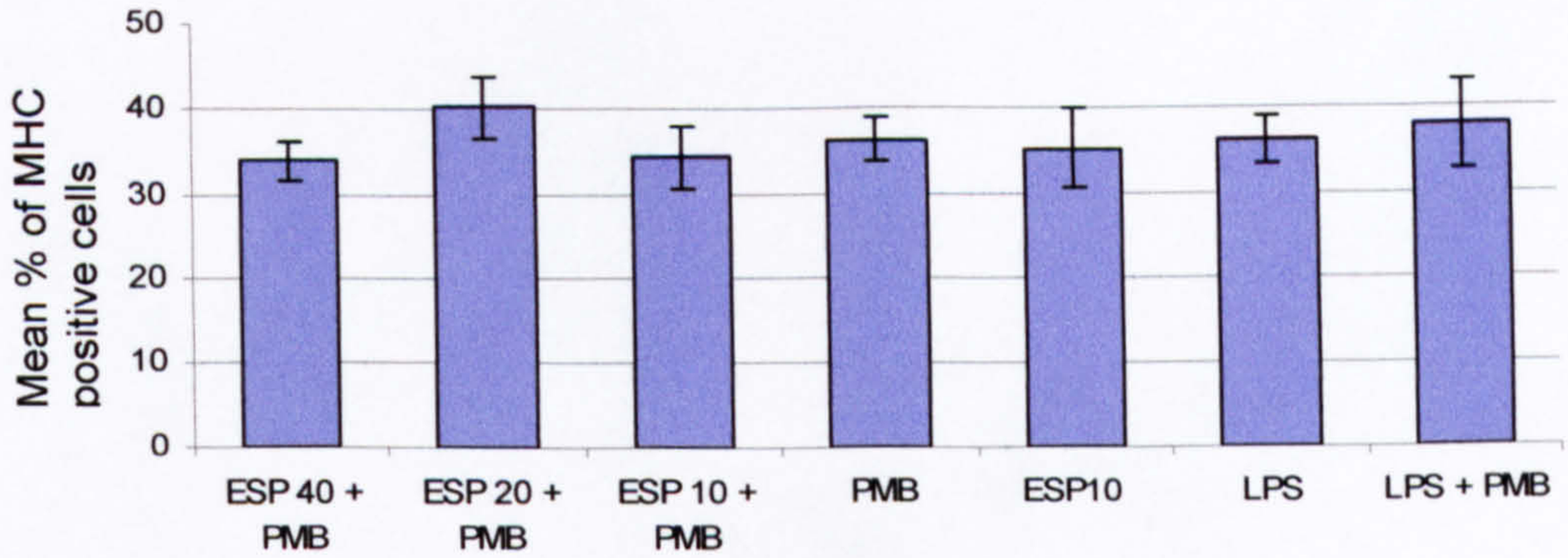

D

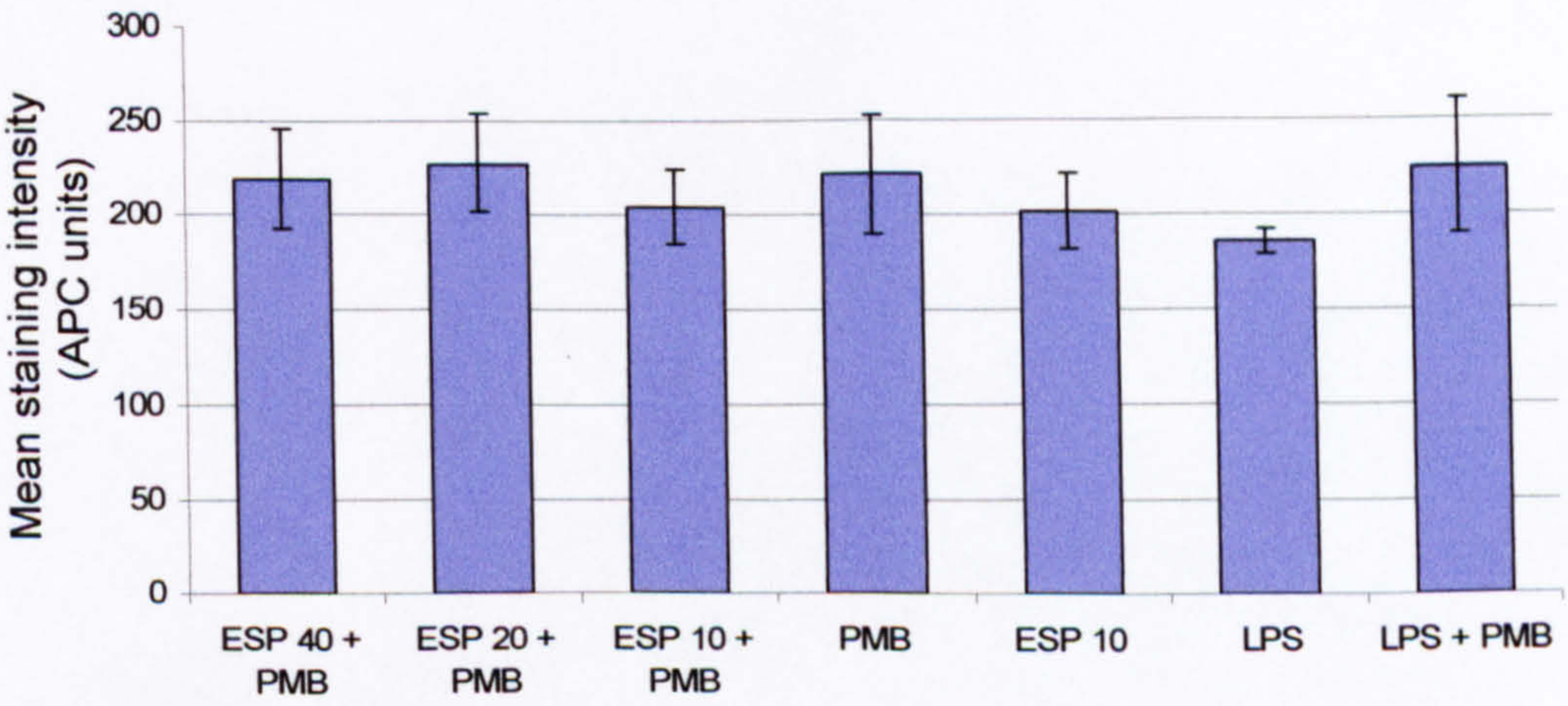

Figure 3.1 ESP does not influence MHCII expression on naïve macrophages. **A:** Typical FSC/SSC plot (Mouse 1, 10µg ESP/ml). Cells within R2 were selected for analysis. **B:** Cells within R2: macrophages positively-stained with APC-conjugated anti-mouse MHCII (green diagonal shading) compared with the isotype control (red vertical shading). Cells in R3 (1% gate) were taken to be MHCII$^+$ve **C:** Cells within R3: there is no relationship between the % of MHCII$^+$ve macrophages and the presence of ESP. **D:** The mean staining intensity on MHCII$^+$ve cells minus the mean staining intensity of isotype control cells. There is no relationship between the intensity of staining on MHCII$^+$ve macrophages and the presence of ESP. (Data in C & D are mean of five mice +/- standard error of the mean). A medium control (i.e. cells only) was not carried out.

Original in colour

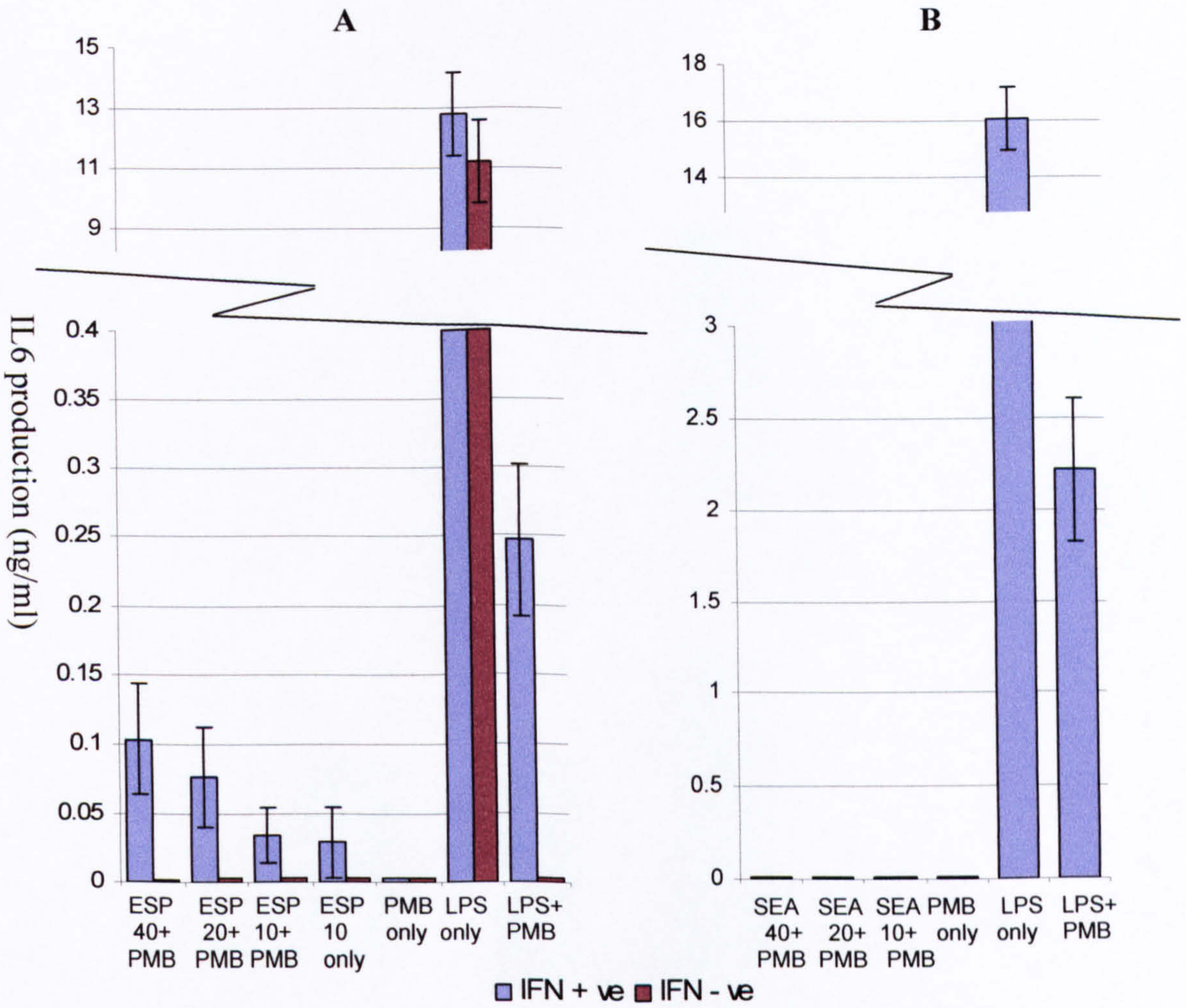

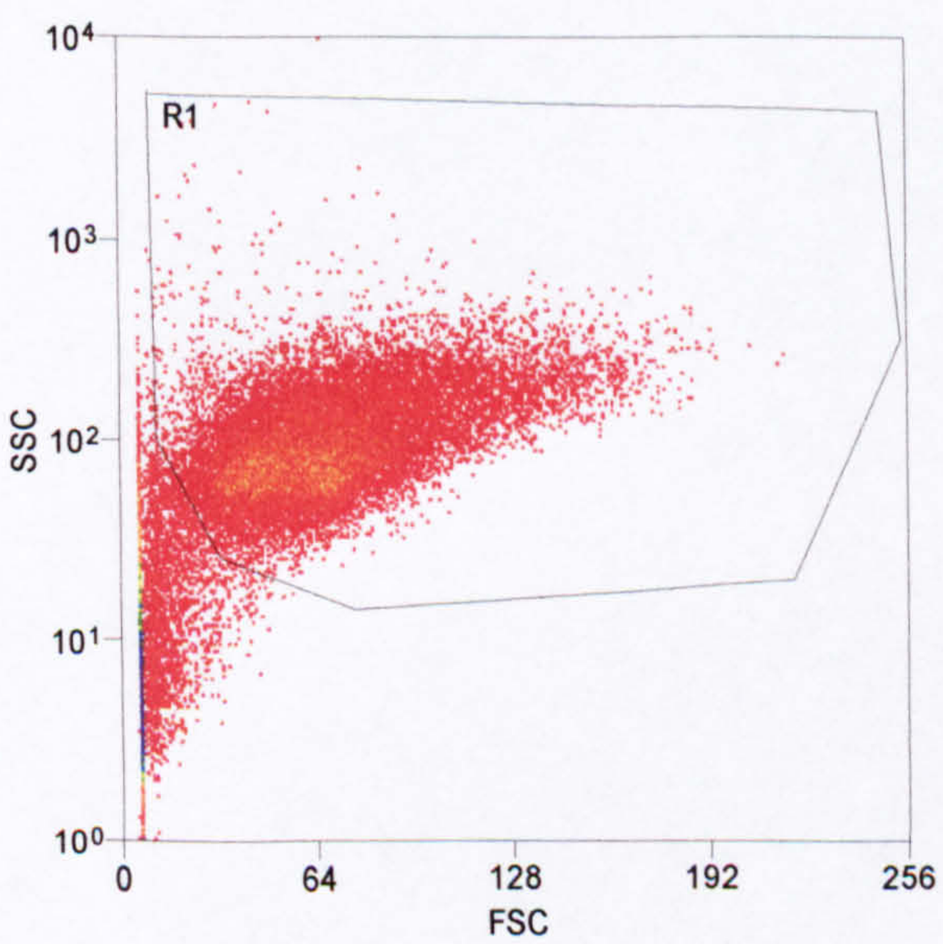

Figure 3.2 IL-6 production by naïve macrophages in response to ESP and SEA. $1x10^6$ macrophages were cultured with ESP (**A**) or SEA (**B**). IL-6 concentration in the supernatants was measured. Results are shown as the mean (+/- standard error of the mean) of replicated experiments using five mice. **C:** Cell viability was assessed using flow cytometry after culture. The plot is typical, showing the cell population consisting of macrophages. In all of the assays, 85-100% of >10,000 events were in region R1.

Original in colour

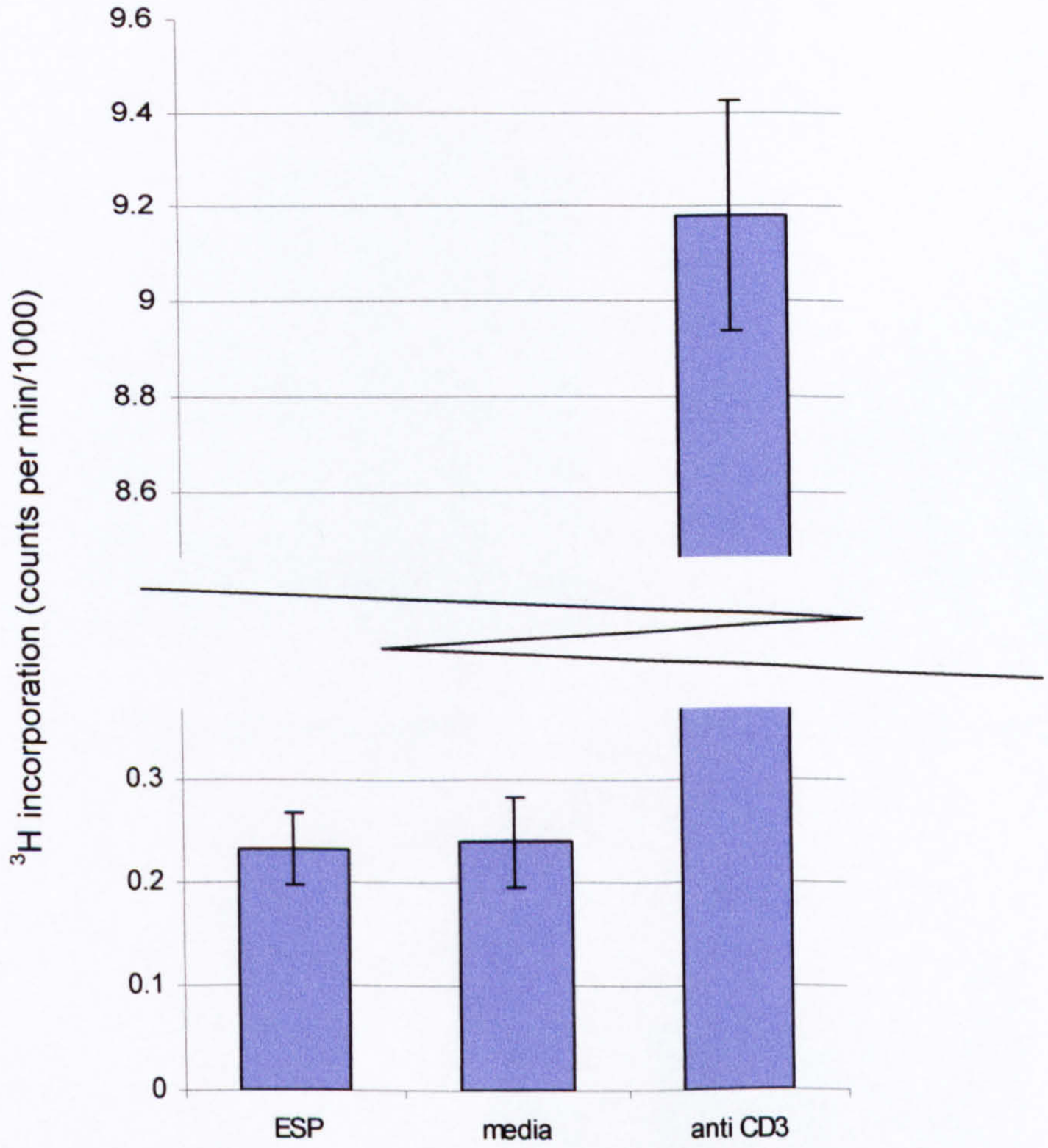

Figure 3.3 Splenocytes, taken from naïve mice do not proliferate in response to ESP. When 2 x 10^5 cells from the spleens of naïve mice were incubated with 40µg/ml ESP there was no more proliferation than was seen with media only. The proliferation index is 0.97 for the ESP assay and 39.4 in the positive control.

Original in colour

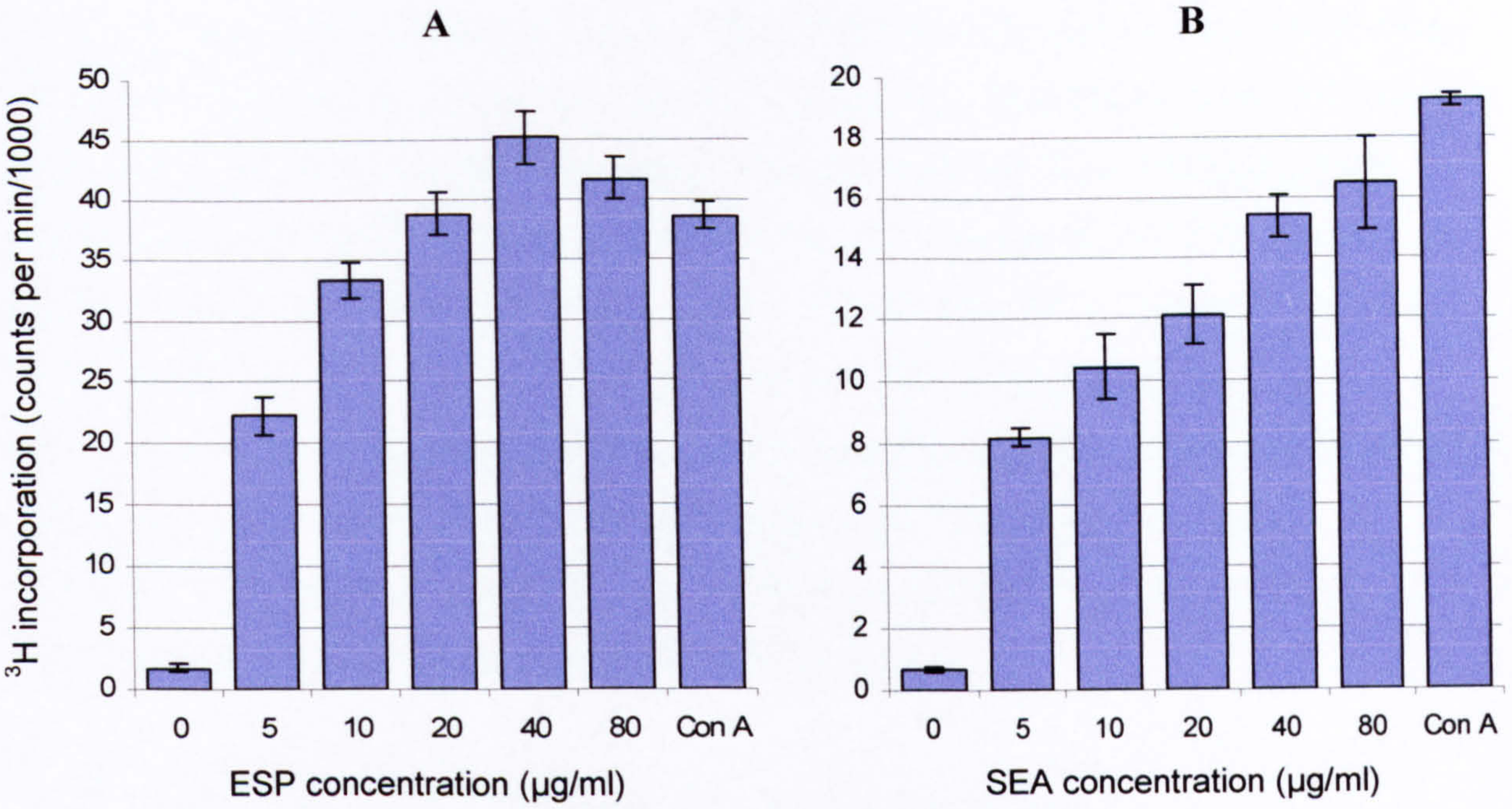

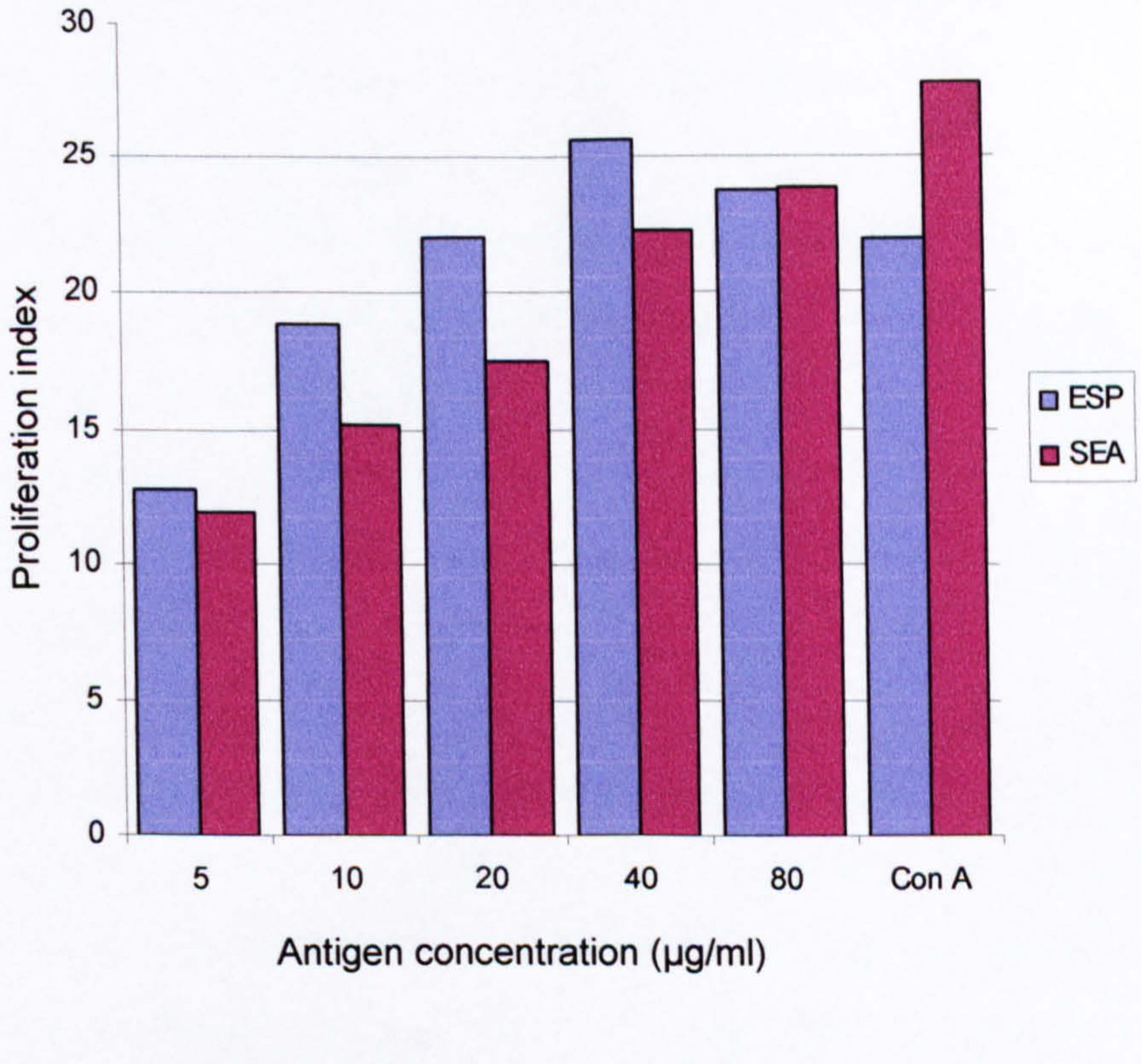

Figure 3.4 Lymphocytes taken from infected mice proliferate in response to ESP and SEA. **A:** A dose-dependent proliferative response to ESP occurred up to 40µg/ml. **B:** The response to SEA is also dose-dependent, but the amount of proliferation is lower. **C:** Comparing the proliferative index of lymphocyte responses to SEA and ESP demonstrates that ESP is more antigenic.

The reduction in the proliferation seen at 80μg ESP/ml and in the positive control of the ESP series of assays did not occur in the SEA assays. The raw data from the ESP and SEA assays are not directly comparable however, because there was more background cell proliferation in the ESP assay than in the SEA one (1758 counts/min (ESP) compared to 691 counts/min (SEA) in the negative controls). Proliferation index values (counts/min at each antigen concentration divided by the counts/min in the negative control) were therefore calculated to normalise the two sets of data (Figure 3.4C). The proliferation index values for the ESP assays were higher than those of the SEA assays at antigen concentrations ≤40μg/ml, demonstrating that ESP is more immunogenic than SEA at the acute stage of infection, certainly at lower concentrations.

3.3.3 Protease Secretion from Macrophages from Naïve Mice

Culture supernatants from naïve macrophages that had been incubated with ESP contained proteases (Figure 3.5A). The amount of protease activity (as measured by the QuantiCleave fluorescent protease assay) was dependent upon the concentration of ESP, but the level of activity was low compared with the trypsin standards (all the ESP assays had less protease activity than 1ng trypsin/ml). The culture supernatant in the negative control also contained proteases, but as the AimV media was protease-free these must have been secreted by the macrophages, indicating that some background stimulation had occurred. The same protocol was used to measure the protease activity of crude ESP (Figure 3.5B) and an inverse relationship between ESP concentration and protease activity was seen. At ≥ 40μg ESP/ml the amount of fluorescence measured at the end of the protease assay was below that seen at its start. At ≤ 20μg ESP/ml however, the amount of proteolysis in crude ESP was much higher (comparable with 16ng trypsin/ml) than that found in any of the culture supernatants of macrophages incubated with ESP (<1ng trypsin/ml). Therefore, ESP must contain proteases, but there must be some ESP-derived factor that had interacted with the fluorophor, the casein substrate or had interfered with transmittance at the wavelengths used in the assay. The latter possibility was addressed by measuring the absorbance of ESP on a Fluoromax-2 spectrofluorometer at 485nm and 520nm and then converting the data to % transmittance using the formula Absorbance. = $\log_{10}$ x 100/%Transmittance. A broadly linear relationship between ESP concentration and % transmittance was seen with the ESP absorbing a greater percentage of light at the emission wavelength (Figure 3.5C).

Original in colour

A

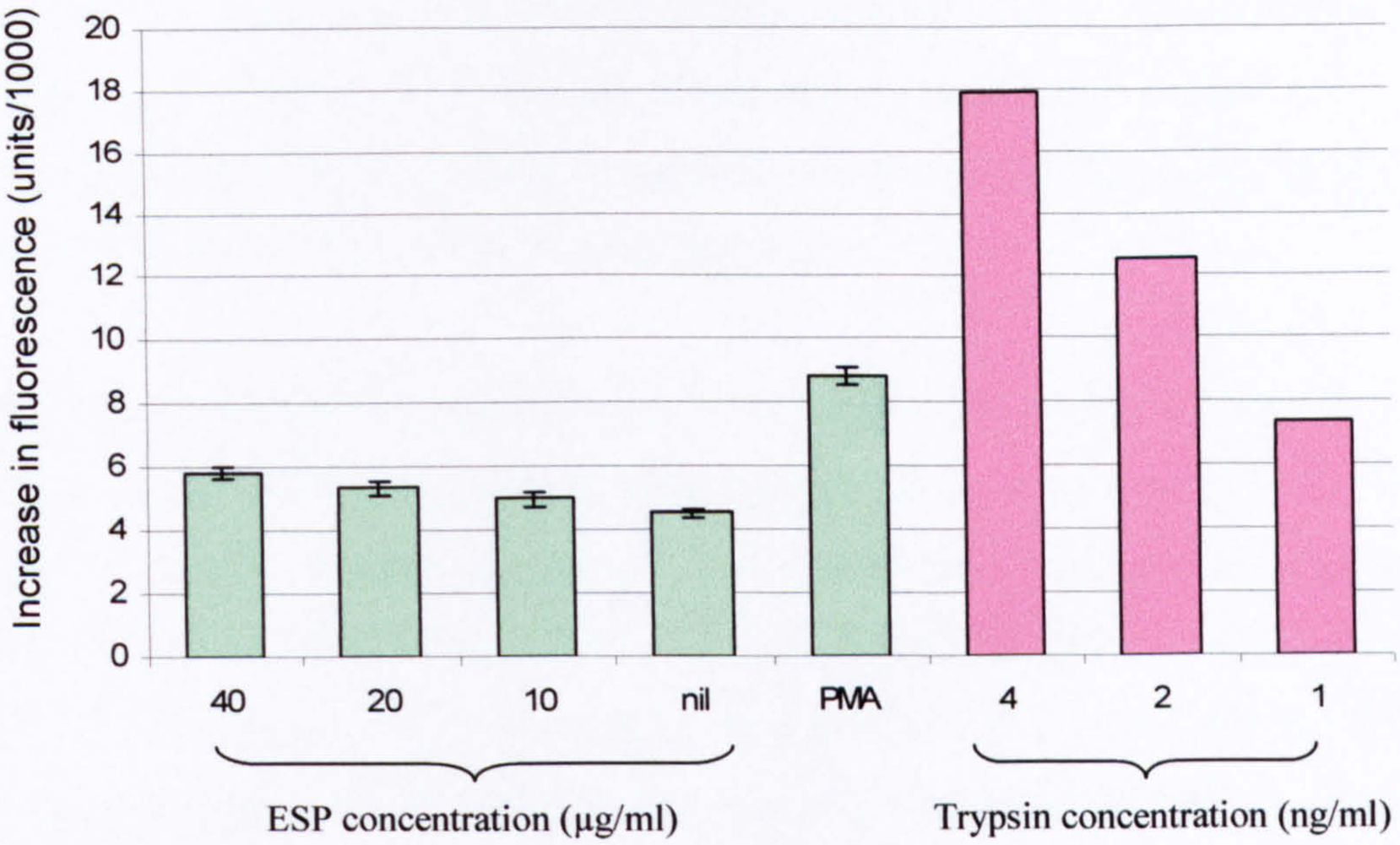

B

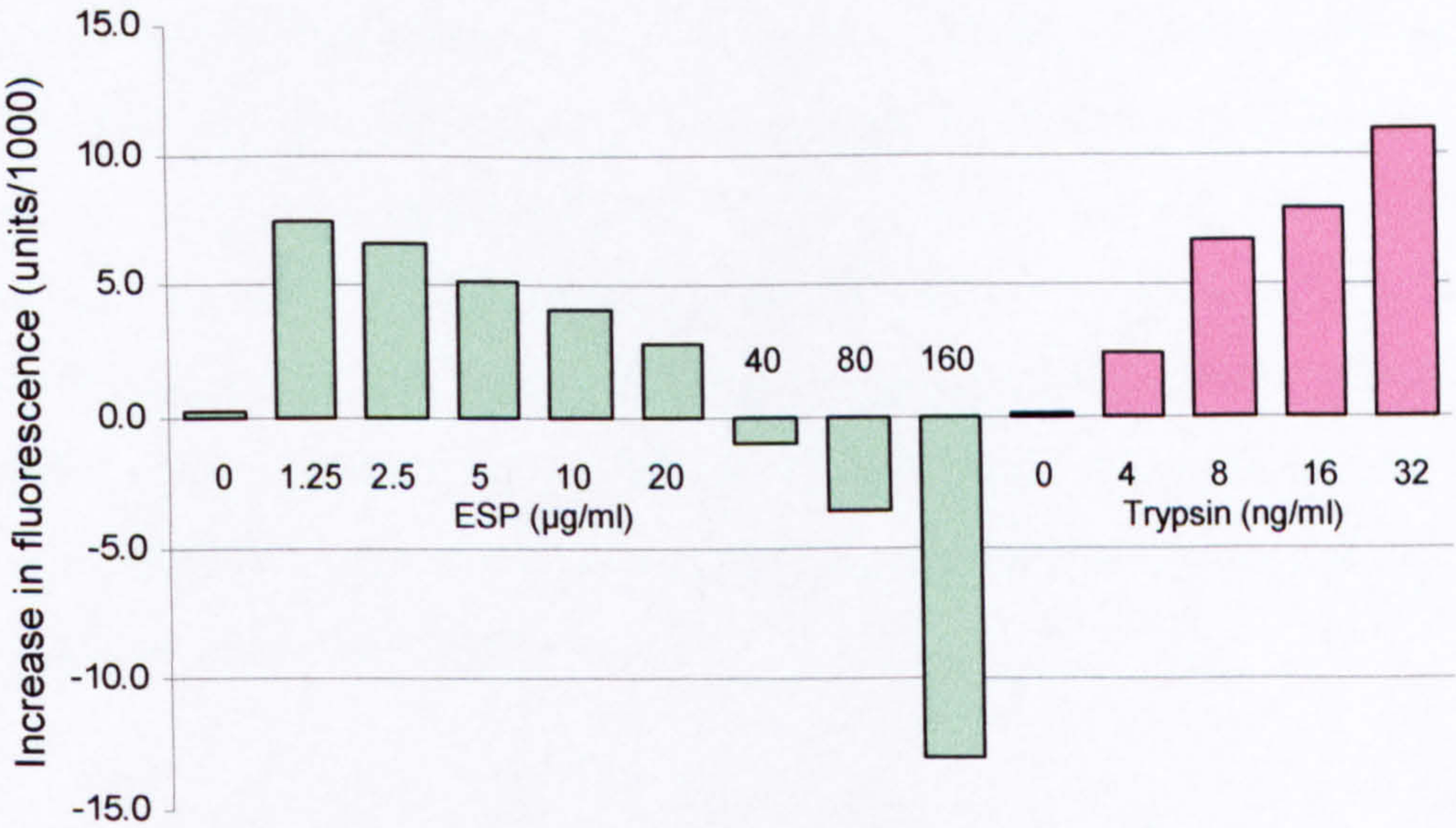

C

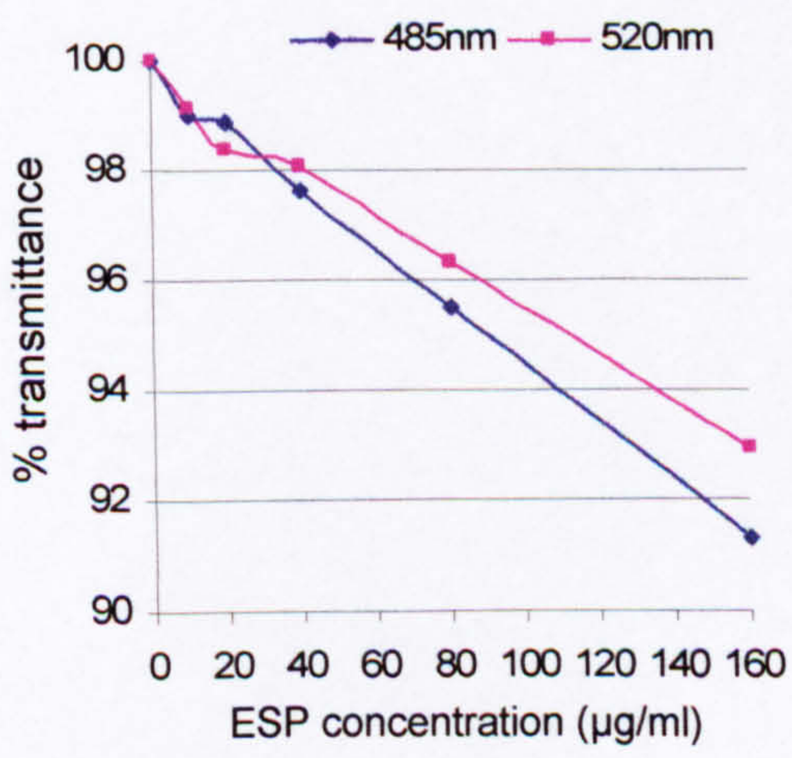

Figure 3.5 Proteases in ESP-stimulated macrophages and crude ESP. **A:** There is a dose-dependent relationship between ESP concentration and protease activity in the culture supernatants of macrophages stimulated with ESP. **B**: Protease activity in crude ESP is inversely related to protein concentration. **C:** Crude ESP does not absorb light significantly at the excitation/emission wavelengths of FITC.

However, even at 160μg ESP/ml, 93% of the light at the excitation wavelength and 91% at the emission wavelength was transmitted through the samples. Therefore, the absorbance spectrum of ESP does not substantially influence the fluorophor and can be discounted as the reason for the drop in fluorescence.

Flow cytometry was used to assess the cellular makeup of the peritoneal exudate, the effectiveness of the plastic-adherence purification procedure and the percent of apoptotic cells from each mouse at the beginning of the culture period. The results for each mouse were similar and a random example (Mouse 1) is shown as Figure 3.6. The percentage of apoptotic cells was assessed by measuring PI incorporation and it was 3.6%, 5.0% and 6.6% in the three mice. The SSC/FSC plot was used to categorise the cell-types in the crude peritoneal exudate, which was found to contain mostly monocytes, but significant numbers of macrophages and lymphocytes were also present. Selecting the plastic adherent cells successfully purified the monocytes and macrophages. At the end of the culture period the cells from each assay were again analysed by flow cytometry but now 40-50% of them were apoptotic (Figure 3.7). The extent of apoptosis was similar in all of the assays (including the negative controls) and so cannot be related to the presence or absence of ESP in the culture medium. No between-mouse differences were evident and as a similar proportion of apoptotic cells were in the serum-containing RPMI control, the serum-free medium was not responsible either.

Original in colour

A

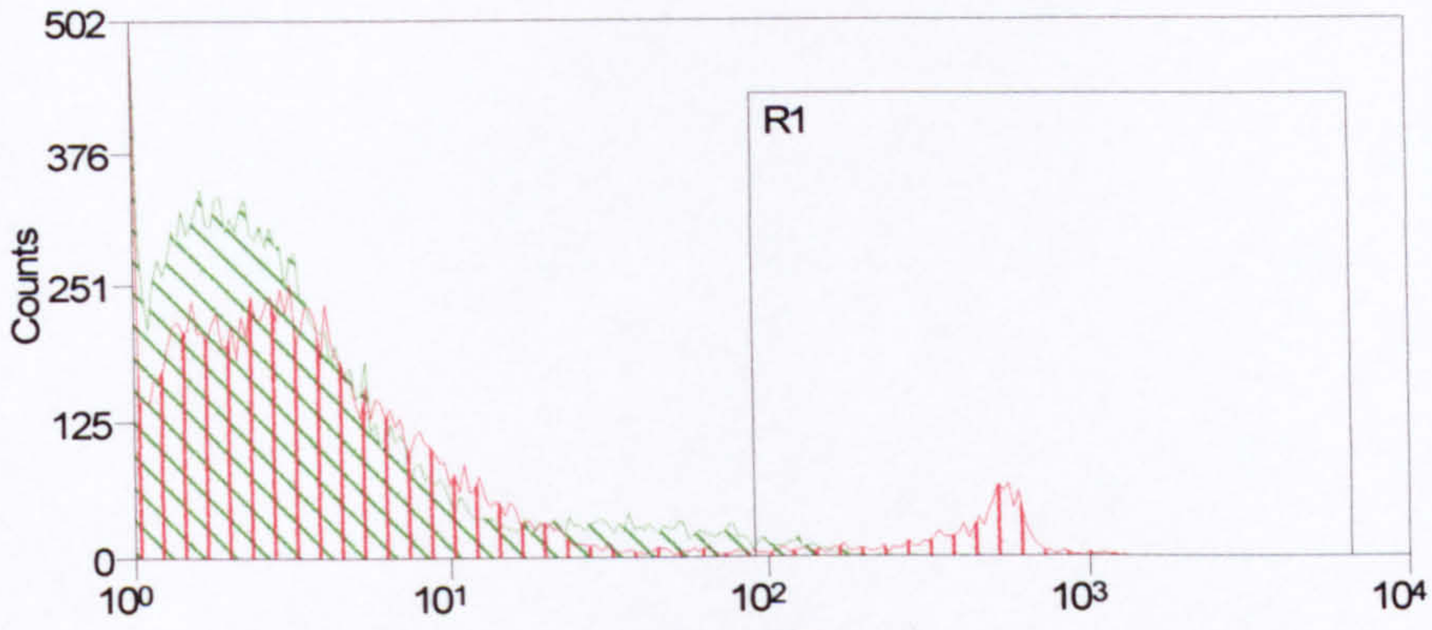

Region	Count	% Events
Total	15363	100.00
R1	1017	6.62
Total	19260	100.00
R1	201	1.04

B

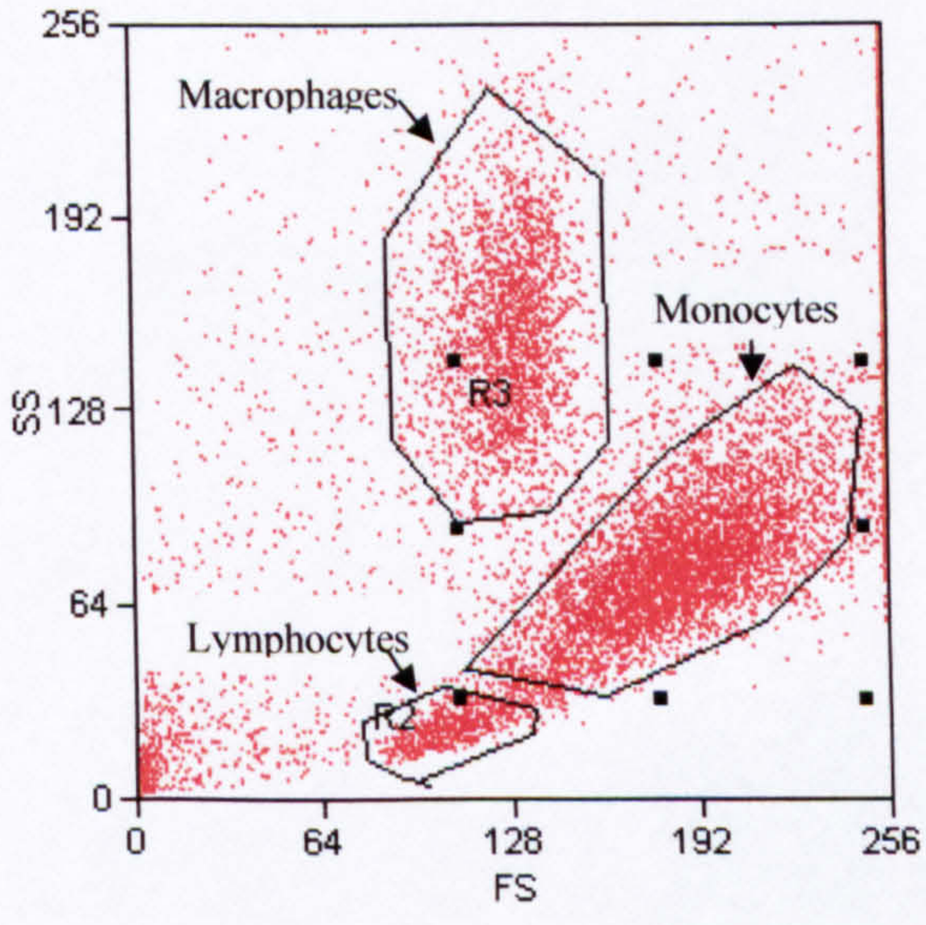

Region	Count	% Events
Total	15363	100.0
Macrophages	2550	16.6
Monocytes	5296	34.7
Lymphocytes	864	5.7

C

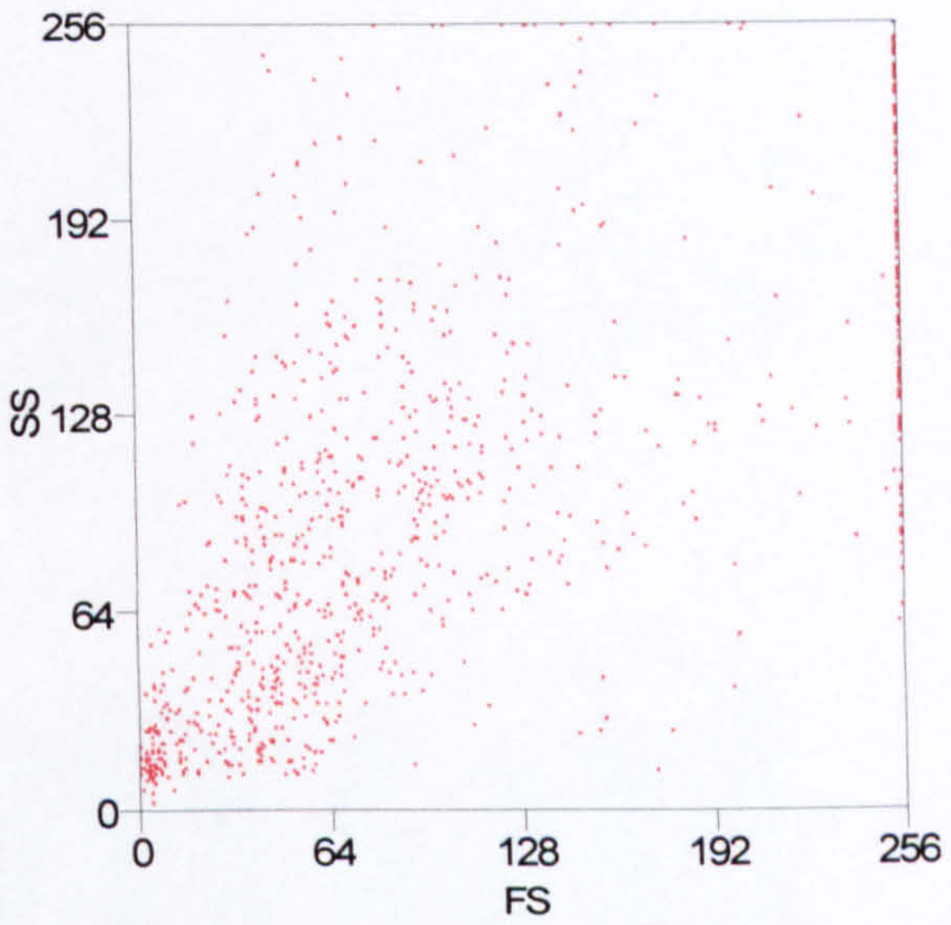

Region	Count	% Events
Total	1017	6.62

Fig 3.6 Cellular make-up and mortality of newly-extracted PECs. **A:** A typical histogram of PEC cells (from Mouse 1). PI^+ve cells (red vertical hatching) gated at 1% (R1) and control (green diagonal hatching) show that 6.6% of the cells were apoptotic. **B**: Ungated FSC/SSC plot of the PEC cells. Although no cell phenotyping was carried out, the size and granularity of the cells indicate that un-purified PECs consist of macrophages, monocytes and lymphocytes. **C:** Applying the R1 gate (i.e. PI^+ cells) to the FSC/SSC plot demonstrates that the apoptotic cells cannot be assigned to a particular cell type.

Original in colour

A

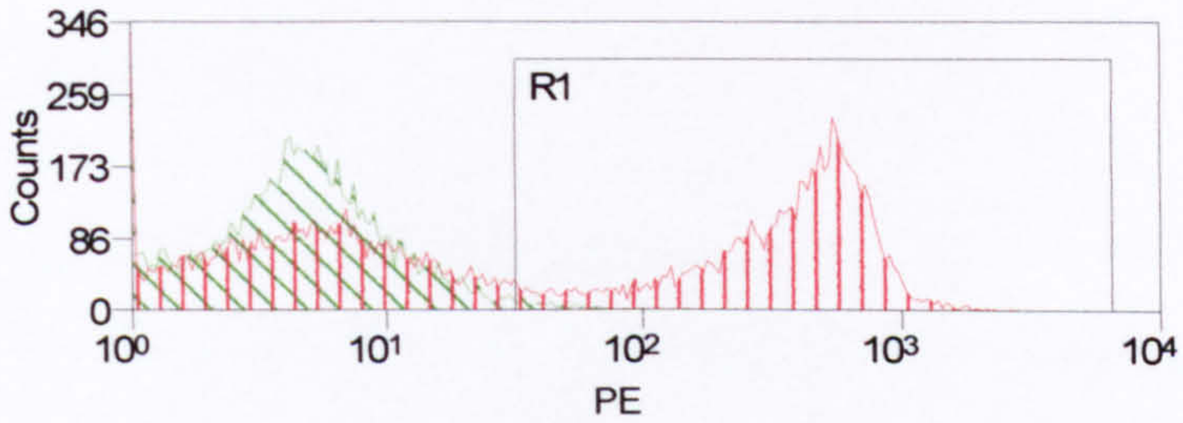

Region	Count	% Events
Total	14366	100.00
R1	7172	49.92
Total	11806	100.00
R1	121	1.02

B

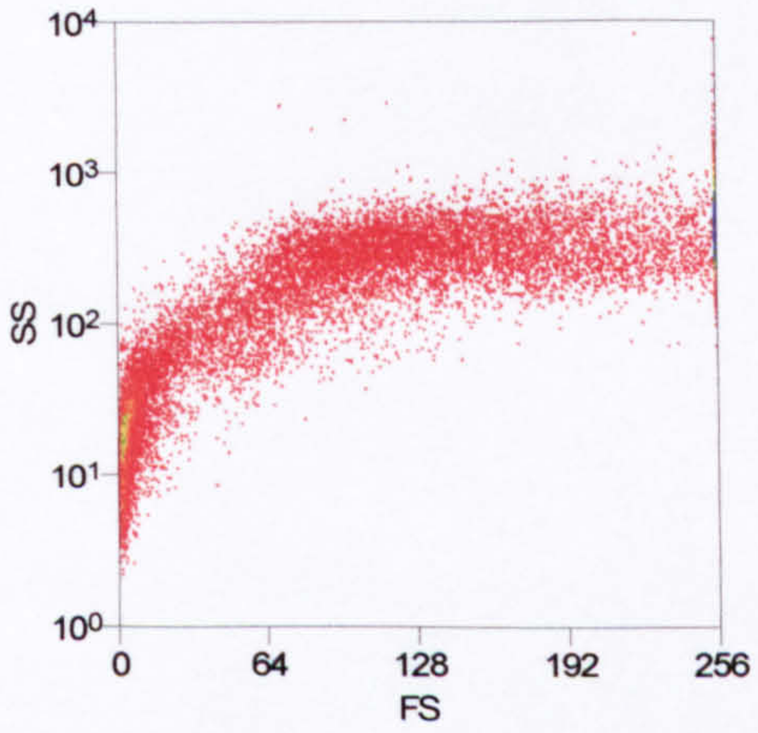

Count	% Events	Mean	Median
14366	100.00	99.48, 222.34	86.00, 191.10

C

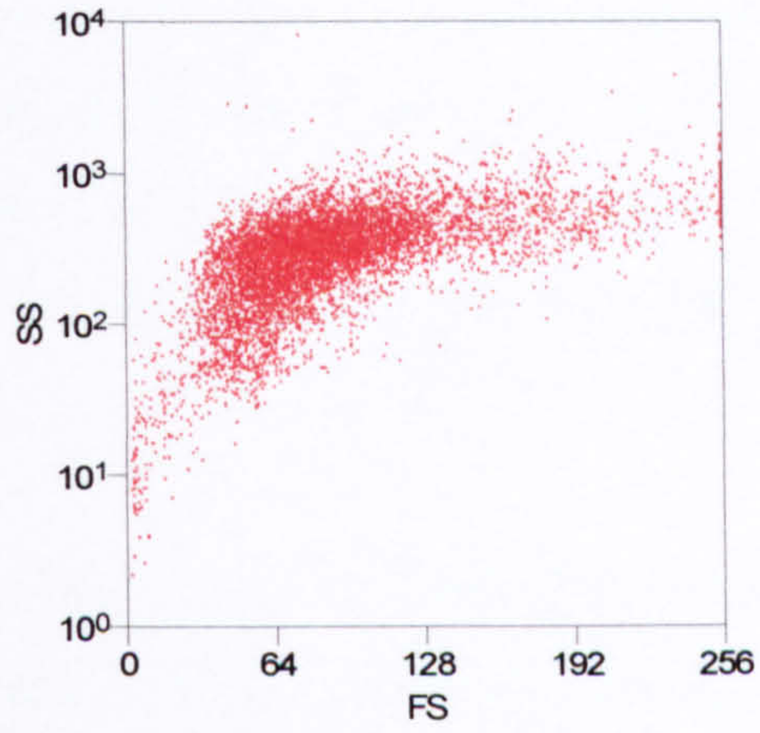

Count	% Events	Mean	Median
7172	49.92	88.07, 342.92	78.00, 305.05

D

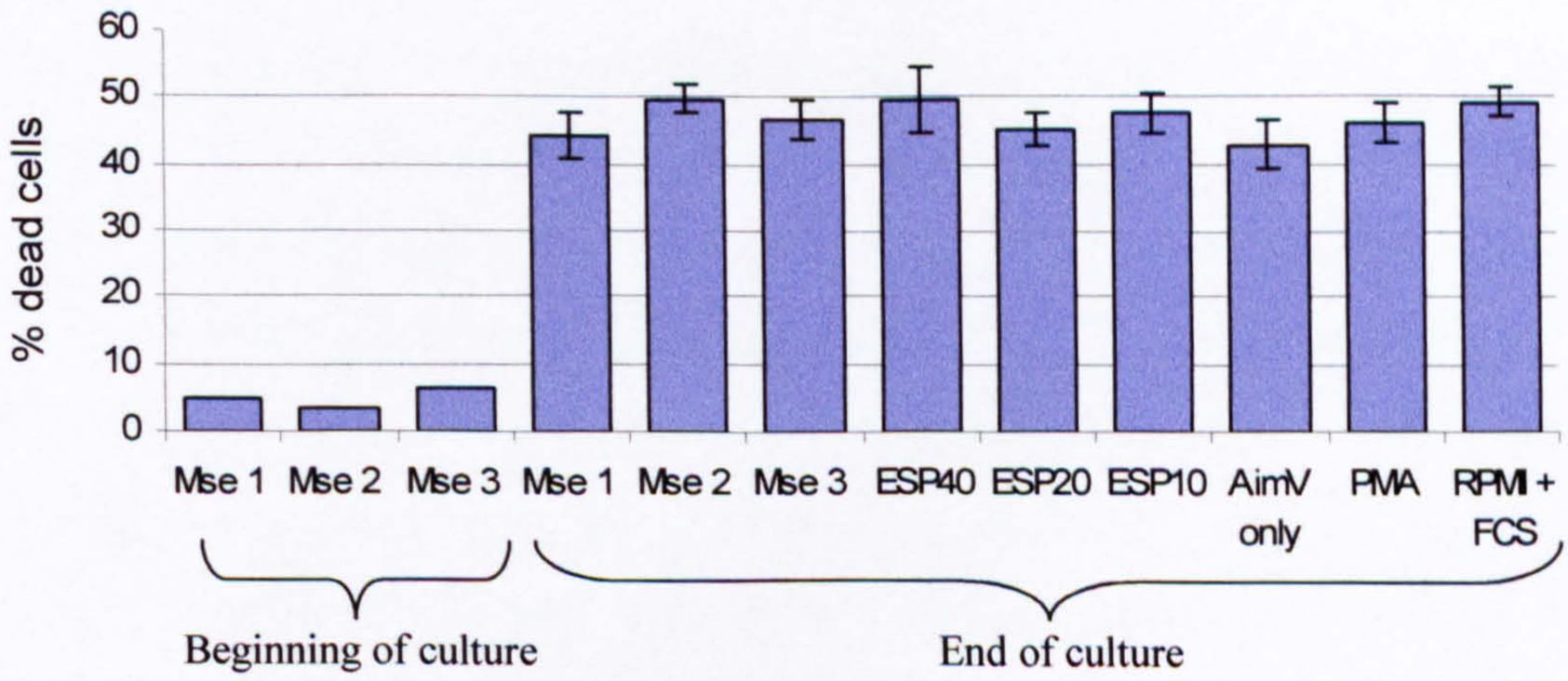

Figure 3.7 Cell mortality at the end of the culture period. **A**: A typical example (Mse 2, ESP10μg/ml) of flow cytometry histogram. PI^+ve cells (red vertical) and negative control (green diagonal) gated at 1% (R1) show 49.9% of cells are apoptotic. **B:** Ungated FSC/SSC plot shows that the plastic-adherent cells are macrophages. **C:** Fig B with R1 gate applied. The apoptotic cells consist of macrophages that are smaller but more granular than average. **D:** Cell mortality is not associated with any particular mouse, the antigen in the culture or the serum-free Aim V medium. The post-culture Mouse 1-3 data are the mean cell mortalities in all assays using cells from that mouse. Error bars are +/- standard error of the mean.

3.4 Discussion

3.4.1: ESP and the Innate Immune System

When eggs are first deposited in an infection and ESP production begins for the first time any immediate response from the host will be via its innate immune system. In order to establish whether ESP is capable of inducing innate immune responses *in vitro* experiments were carried out in which splenocytes and macrophages from naïve mice were stimulated with ESP. These cell-types were chosen because T cells have been implicated in the process of egg escape from the host and macrophages are the most abundant APCs in the granuloma (see Section 3.1.1).

A radioactive-thymidine incorporation assay demonstrated that naïve splenocytes did not proliferate in response to ESP. The splenocytes will have consisted of naïve T cells, B cells and macrophages, although the macrophage population will include cells involved in the phagocytosis of old erythrocytes and so could be considered to be "activated". The situation *in vivo* when ESP is initially produced will be slightly different however, because (as discussed in Chapter 2, Section 2.4.9) two of the ESPs (ESP13-14 and its associate ESP18-19) are also secreted by lung worms. The host may therefore have already become sensitised to these proteins before egg production commences, but as the lungs are physically remote from egg deposition sites the number of T cells reactive to these ESPs in the plasma surrounding the egg may be fairly low. There are also glycan epitopes on ESP 1-2, ESP 3-6 and ESP 12 that are cross-reactive in terms of antibody-binding with those from cercariae (Jang-Lee *et al.*, 2007; Eberl *et al.*, 2001b). However, for a cross-reactive glycan to bind to a T cell receptor, the peptide backbone in the MHC cleft will need to be cross-reactive, as well as the glycan residue itself. Also, a cross-reactive glycan would need to be attached to an amino acid pointing away from the MHC if it were to interact with the T cell receptor.

Flow cytometry was used to demonstrate that ESP did not up-regulate MHCII on naïve macrophages, either in terms of the percentage of $MHCII^{+}$ve cells or number of MHCII molecules expressed on the $MHCII^{+}$ve population of cells. These results are consistent with

a previous study (Trottein *et al.*, 2004), where transcripts encoding MHCII were not increased in DCs stimulated with live eggs. However, the Trottein *et al.* study did find up-regulated transcription of H-2M (which is involved in loading peptides onto MHCII) and the co-stimulatory molecules CD40 and ICAM-1. It is therefore possible that the macrophage-ESP incubations were not carried out for a sufficient length of time for MHCII up-regulation to become evident, or that the macrophages had already been induced to up-regulate their MHCII expression by the thioglycollate used to elicit them into the peritoneal cavity. The latter explanation would account for why MHCII expression was similar in the experimental assays and the negative control. It would also explain why the expression levels were approximately 10% higher than those found on naïve (alveolar) macrophages obtained without the use of thioglycollate (Fulton *et al.*, 2004).

The other assessment of macrophage activation (IL-6 secretion) produced a positive result in that macrophages secreted IL-6 when cultured with ESP, provided IFN-γ was present in the culture medium. The lack of measurable IL-6 in cultures without IFN-γ was also found by Trottein *et al.*, (2004) when they cultured DCs with live eggs. The quantity of IL-6 produced (0.1ng/ml at 40μg ESP/ml) is broadly consistent with the results of a study involving *Trichinella spiralis*, in which five times the number of naïve rat peritoneal macrophages were cultured with 2.5 times the quantity of parasite secretions to produce 1.2ng of IL-6 (Gruden-Movsesijan & Milosavljevic Lj, 2006). In contrast to the ESP assays, IL-6 was not produced when the macrophages were cultured with SEA, even in the presence of IFN-γ. The IL-6-negative response to SEA is consistent with an experiment in which DCs were cultured with SEA but without IFN-γ (van Liempt *et al.*, 2007). In another study culturing DCs with SEA, again without IFN-γ (MacDonald *et al.*, 2001), no IL-4, IL-10 or IL-12 was produced (IL-6 was not measured) and nor were the co-stimulatory molecules CD80, CD86, CD54, CD40 or OX-40L up-regulated (although a small amount of MHCII up-regulation was seen).

Taken together, these results show that ESP (a substitute for the live egg) induces a response from (naïve) macrophages, which are the principal APCs of the granuloma. This response is not induced by SEA (a substitute for the dead egg). However, the amount of activation is low in its extent and difficult to observe – there was no up-regulation of

MHCII and what IL-6 production did occur (the extent of which is dwarfed by the positive control) could only be induced when the macrophages have the additional stimulation of IFN-γ. The combination of lack of MHCII up-regulation but cytokine secretion suggests that ESP is probably binding to the macrophage's Pattern Recognition receptors (PRRs). PRRs are expressed on APCs and bind to conserved molecules (called pathogen-associated molecular patterns) which are commonly produced by micro-organisms but not by higher eukaryotes. The PRRs form part of the innate immune system and activate the APC upon ligation, inducing the secretion of cytokines and up-regulated expression of MHC and co-stimulatory molecules (Janeway & Medzhitov, 2002). ESP must contain a motif that is recognised by the PRR system on macrophages, but the lack of observable MHC up-regulation and the requirement for IFN-γ to induce measurable IL-6 production indicates that the interaction is fairly weak, that the PRR(s) involved have a signalling pathway that is not particularly powerful or that the end product of the PRR pathway was not MHCII or IL-6 expression.

The most studied PRRs are the family of Toll-like receptors (TLRs), which are generally associated with inducing a pro-inflammatory Th-1 response (Akira & Takeda, 2004). As egg deposition is associated with the switching of the response from Th-1 towards Th-2 it is logical that the PRRs activated by ESP are members of a different, more Th-2-inducing family. However, when DCs were cultured with live eggs it was transcripts for Th-1 cytokines that Trottein *et al.*, (2004) found up-regulated. Subsequent work from the same group, also using live eggs, found signalling occurring via TLR2, TLR3 and the TLR adapter molecule MyD88 (Aksoy *et al.*, 2005). It is possible, however, that the TLR signalling Aksoy *et al.* observed was actually a response to contamination because the ligands for TLR-2 and TLR-3 are bacterial lipopeptides and dsRNA respectively (Takeda & Akira, 2004). A more likely ESP-recognising PRR is the C-type lectin (CTL) called "dendritic-cell-specific intercellular adhesion molecule 3-grabbing nonintegrin" (DC-SIGN), which recognises SEA components with the Lexis x motif (van Die *et al.*, 2003). As Lewis x is also present in ESP3-6 (Jang-Lee *et al.*, 2007; Wuhrer *et al.*, 2006) a link between antigen and APC can be made. Although its name implies it is DC-specific, DC-SIGN has been found on macrophages from the lungs, placenta and inflammatory lesions and its expression can be induced in monocyte-derived macrophages by IL-13

(Rappocciolo *et al.*, 2006; Soilleux *et al.*, 2002), so peritoneal macrophages may also express the molecule or one of similar antigen specificity.

3.4.2: ESP and the adaptive immune system

Lymphocytes from acutely infected mice responded to both ESP and SEA by proliferating in a dose-dependent manner, with the exception of the assay at 80µg ESP/ml where the proliferation was less than that seen at 40µg ESP/ml. The lower proliferation at 80µg ESP/ml is likely to be because this quantity of ESP induced a more rapid and powerful response such that the cell proliferation had peaked and undergone a contraction phase, leaving behind dead and apoptotic cells that were too small to be retained on the cell harvesting plate. Reducing the incubation time might prevent this from occurring. The proliferation index values to the Con A positive control were not excessive compared with previous studies, the most comparable of which is a study where double the quantity of Con A was used to stimulate the same number of lymphocytes for the same period of time to induce a proliferation index of 92, measured using the same ^{3}H-thymidine-incorporation assay (Lijnen *et al.*, 1997). The high proliferative response of mesenteric lymph node cells to ESP compared to SEA demonstrated that a greater proportion of the T and/or B cells were responding to ESP than to SEA. ESP is a subset of SEA however (2.5% of mature SEA consists of ESP – see Chapter 2, Table 2.5), so an unknown proportion of the response to SEA will have been to ESP antigens. It can therefore be seen that although ESP is a small subset of SEA, lymphocytes from the mesenteric lymph nodes found it to be more antigenic than SEA. This may be because relatively few eggs had disintegrated in the gut wall so fewer lymphocytes were present to recognise SEA components, or it could be that SEA contains factors capable of down-modulating the immune response. If the latter were to be the case, it is possible that the down-modulation seen at chronic infection is induced by the build-up disintegrating eggs in the liver which release SEA.

3.4.3: Proteases and ESP

The egg must pass through the tissues of the gut wall to escape from the host. The proteases involved in degrading the tissue to achieve this could either be secreted by the egg itself, by the cells of the granuloma or by a combination of both. It was established by Ashton (2001) that ESP contains two proteases, and the egg proteome study of Chapter 2 has shown that

ESP 13-14 has a subtilase pro-protein convertase functional domain (Section 2.4.9).

Experiments were therefore carried out with the aim of establishing whether ESP induces macrophages to secrete proteases or pro-proteases that could be activated by ESP13-14. Two completely different patterns emerged: the culture supernatants of macrophages incubated with ESP showed protease activity that was ESP-dose-dependent (but with very low activity compared to the trypsin standards) but the protease activity of crude ESP was inversely ESP-dose-dependent. The unexpected result in the crude ESP assays cannot be attributed to the absorbance spectrum of ESP because even at 160µg ESP/ml less than 10% of light at the excitation and emission wavelengths of the fluorophor is absorbed. The most likely explanation is that an ESP binds to the fluorophor and absorbs energy from it by FRET, a phenomenon expressed as a dose-dependent reduction in fluorescence. The binding must be to the fluorophor itself rather than to the casein substrate because at concentrations above 40µg ESP/ml, the amount of fluorescence is less than that seen in the negative control (when no proteolysis can be happening). The most likely fluorophor-binding candidate is ESP3-6, because this ESP is capable of binding to eosinophils (Schramm *et al.*, 2003; Smith *et al.*, 2005), chemokines (Smith *et al.*, 2005) and to other ESPs (see the following Addendum). The reason why ESP3-6 has such universal binding characteristics may be because of its high *pI*, which means it would have a positive charge in solutions of pH < 9. It is clear however that ESP does have proteolytic activity because at concentrations below 20µg/ml there is an increase in fluorescence compared with the negative control. The concentration of proteases was higher in crude ESP than that found in the culture supernatants of macrophages incubated with ESP, because even at 1.25µg ESP/ml, crude ESP had more proteolytic activity than any of the macrophage assays. The low amount of protease activity from the macrophage assays might have been influenced by the extent of cell death that occurred during the course of the incubation (40-50% of the macrophages were apoptotic or necrotic after the incubation, regardless of the antigen used or mouse from which they had been derived). It is not known whether the proteases in the macrophage supernatants were from residual ESPs or whether they had been secreted by the macrophages themselves. It would be necessary to submit the supernatants to MSMS in order to establish whether the proteases therein were of murine-macrophage or schistosome origin.

The experiments conducted in this chapter demonstrate that ESP does not induce naïve macrophages to secrete significant quantities of proteases. It is possible that at the acute or chronic stage of infection macrophages would be maturing in a more stimulatory environment and this would induce them to be more reactive in terms of protease secretion. However, it is also possible that in fact $CD4^+$ cells secrete the proteases that enable eggs to cross the gut wall. This would be consistent with the work of Doenhoff *et al.*, (described in Chapter 1, Section 1.2.5) in which mice lacking T cells had impaired ability to excrete *S. mansoni* eggs.

Addendum to Chapter 3: Purification of ESP components using HPLC

3.5: Introduction

Crude ESP comprises 27 spots in a 2D gel, with the proteins having little homology to any other proteins of known function (Chapter 2, Section 2.3.4.3). Although the functional assays described in Chapter 3 went some way towards assigning functional characteristics to ESP as a whole, a method of fractionating ESP into its components was anticipated to be required if specific properties were to be attributed to individual ESPs. It was anticipated that by repeating the functional assays with individual ESPs rather than with the crude protein mixture a picture might emerge as to which ESPs were responsible for particular functional properties. It was with this aim in mind that the work of this Addendum was carried out. HPLC was the obvious method by which to carry out the fractionation because it can do so without altering the functional properties of the proteins.

The work of this Addendum is the first attempt at fractionating crude ESP, but Schramm *et al.*, (2003) had used HPLC to enrich for IPSE (aka ESP3-6), but with SEA as the source material. The paper describes using a cation exchange column to obtain an IPSE-enriched SEA fraction and then using lectin affinity chromatography to remove the IPSE from the other SEA components. The lectin that was used had been derived from *Aleuria aurantia* (Orange Peel Fungus) and is commercially available already bound to agarose beads. The authors abbreviated "agarose-bound *Aleuria aurantia* lectin" to "AAA".

The protocol that was devised to purify ESP components is complex and involves up to five dimensions. The dimensions are described in their order (AAA-affinity → AAA-affinity → anion exchange → cation exchange → size exclusion) and a flow chart is provided, showing which ESPs were purified during each dimension (Figure 3.8, page 146). There is also a Table that lists each ESP and details the protocol that can be used to purify it (Table 3.1, page 158). The success of each dimension and the logic used to decide on the following dimension are explained in the Results section.

3.6: Methods

All HPLC was conducted on an AKTA10 purifier system (Pharmacia) at room temperature.

3.6.1: Dimensions 1 and 2: Lectin-Affinity Chromatography

An empty 1.25ml HIS Select column (Sigma) was filled with AAA (Vector Laboratories).

Dimension 1: 1mg crude ESP (approx. 800µl) was applied to the column at 0.2ml/min in PBS, pH7.2, then equilibrated with 2 column-volumes (cv) PBS and eluted over 10cv with a 0-100% continuous gradient of 100mM L-fucose (Sigma) in PBS. Fractions were collected in 0.5ml aliquots. 100µl of the protein-containing eluate (pooled fractions) and effluent were dialysed into 20mM Tris HCl pH7.2 using Slide-A-Lyzer mini dialysis units (Pierce), concentrated to 35µl with an Amicon Ultrafree centrifugal concentrator (Millipore), reduced and subjected to 2-DE using a 7cm, pH 3 – 10 IEF strip (Bio-Rad) and 7cm NuPAGE 4-12% Bis-Tris gel (Invitrogen) as described in Chapter 2 (Section 2.2.9.2). The gels were stained with Sypro Ruby (Bio-Rad), then Biosafe Coomassie (Bio-Rad), the visible spots excised and subjected to MALDI-MSMS, using the protocols described in Chapter 2 (Sections 2.2.10 and 2.2.11).

Dimension 2: the remaining effluent (3ml) was then re-applied to the column in PBS, equilibrated with 7cv and eluted with a single step-gradient of 50mM L-fucose in PBS. 200µl of effluent was separated by 2-DE and analysed by MALDI-MSMS (as described above). 40µl of eluate was concentrated, separated by 1-DE in a NuPAGE 4-12% Bis Tris gel (Invitrogen) using the protocol described in Chapter 2, Section 2.2.8.2 (except no reducing agent was added). The gel was then stained with Sypro Ruby.

3.6.2: Dimension 3: Anion Exchange Chromatography

The fractions containing the effluent from Dimension 2 were pooled (4ml) then applied to a Mono Q HR 5/5 (1ml) column (Pharmacia) with 8ml of 20mM Tris HCl pH7.5 at 0.75ml/min. The column was equilibrated with 5cv, the effluent collected and the bound proteins eluted with a 0-100% gradient over 20cv with 20mM Tris plus 1M NaCl, adjusted to pH 7.5 with 5M HCl. The eluate was collected in 0.5ml fractions and pooled according

to the chromatogram peaks. 60µl of each aliquot was concentrated to 20µl using Amicon Ultrafree centrifugal concentrators and separated by 1-DE without reducing agent in a NuPAGE 10% Bis Tris gel (Invitrogen) using the same protocol as before. The gel was stained with Sypro Ruby and then with Silver (the MS-compatible protocol described in the PlusOne Silver Staining Kit (Amersham)). Both methods of staining were used because it was found that some protein bands were more sensitive to Sypro Ruby whilst others were more amenable to silver staining. The bands were excised, de-stained and subjected to MALDI-MSMS (as described in Chapter 2, Sections 2.2.10 and 2.2.11).

3.6.3: Dimension 4: Cation Exchange Chromatography

The fractions containing the effluent from the anion exchange column (Dimension 3) were pooled and subjected to three regimens of buffer exchange with 20mM sodium phosphate (8% Na_2HPO_4, 92% NaH_2PO_4) plus 25mM NaCl and adjusted to pH 5.8 (5M NaOH) using a 6ml, 5kDa-cutoff Vivaspin centrifugal concentrator (Sartorius). The protein (6ml) was then applied to a Mono S HR 5/5 (1ml) column at 0.8ml/min with 12ml of 20mM sodium phosphate buffer plus 25mM NaCl pH5.8 and the effluent collected. After equilibration (5cv), proteins were eluted with a 0-100% gradient of 20mM sodium phosphate buffer plus 800mM NaCl pH5.8, over 20cv. The eluate was collected in 0.5ml fractions, pooled according to the chromatogram peaks, concentrated then subjected to 1-DE followed by MALDI-MSMS using the same protocol described in Section 3.6.2 (except a 4-12% Bis Tris gel was used).

3.6.4: Dimension 5: Size-Exclusion Chromatography

Fractions from the cation exchange column containing more than one protein were applied to a Superdex HiLoad 75 HR 16x60 size-exclusion column (Pharmacia) at 0.2ml/min in 100mM NaCl plus 25mM Tris, pH 7.2. The size-exclusion fractions were collected in 1ml aliquots, pooled according to the chromatogram peaks concentrated to approx. 25µl initially with a 20ml Vivaspin polyethersulphone centrifuge concentrator (Sartorius) and then with a 400µl Amicon Ultrafree centrifugal concentrator (Millipore). The concentrate was separated by 1-DE, stained with Sypro Ruby and silver and the bands analysed by MALDI-MSMS as described above.

3.7: Results

Several attempts were made to devise an effective protocol for purifying ESP components by HPLC, the most effective of which is illustrated in Figure 3.8. It was found to be absolutely imperative that ESP3-6 was removed from crude ESP in the first step. A failure to do so resulted in ESP3-6 appearing in all of the protein-containing fractions, regardless of whether ion exchange or size-exclusion steps were used. For example, the ubiquitous presence of ESP3-6 in almost all fractions after crude ESP was applied to a size-exclusion column is shown in Figure 3.9.

3.7.1: Dimensions 1 & 2: Lectin-Affinity Chromatography

Crude ESP was applied to the AAA column in Dimension 1 to remove (and hopefully purify) the ESP3-6. When the column-bound material was eluted with a linear gradient of L-fucose, subjected to 2-DE and then MALDI-MSMS it was seen that ESP3-6 had been purified in the eluate, along with some of the ESP1-2 and ESP12 (Figure 3.10). The effluent contained most of the ESP1-2 and ESP12 along with all the other ESPs. A shoulder can be seen on the chromatogram (illustrated by a black arrow in Figure 3.10A) indicating that the minority components (ESP1-2 and/or ESP12) bound to the column at a lower affinity than ESP3-6 did. As ESP3-6 makes up >80% of crude ESP in terms of protein quantity (see Chapter 2, Section 2.3.4.3) the eluate will contain more protein than the effluent, but this wasn't reflected in the 280nm trace. This is probably because light at 280nm is principally absorbed by tryptophan, of which there are only two residues in ESP3-6. When the effluent (containing all the ESPs except ESP3-6) was re-applied to the AAA column all of the remaining ESP1-2 became purified in the eluate and none was in the effluent (Figure 3.11). ESP12 (a small quantity of which was in eluate in the first chromatography run) was untraceable in the eluate of the second run: no proteins of 10kDa could be seen following 1-DE (Figure 3.11C).

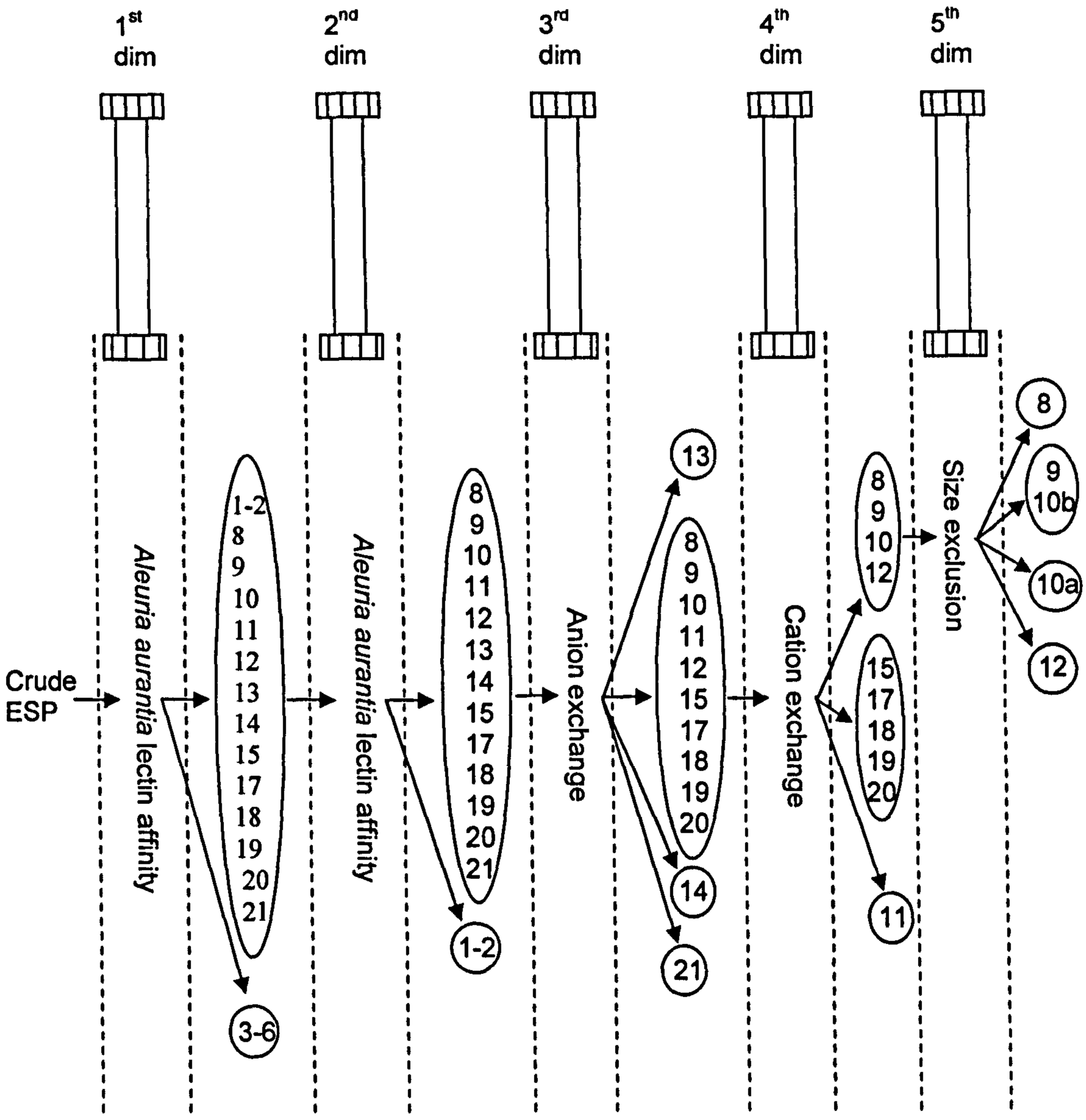

Figure 3.8 Diagrammatic illustration of the purification protocol that was devised to fractionate crude ESP, using up to five dimensions of HPLC. The circled ESPs have been purified whilst those that remain inside an ellipse have not.

Original in colour

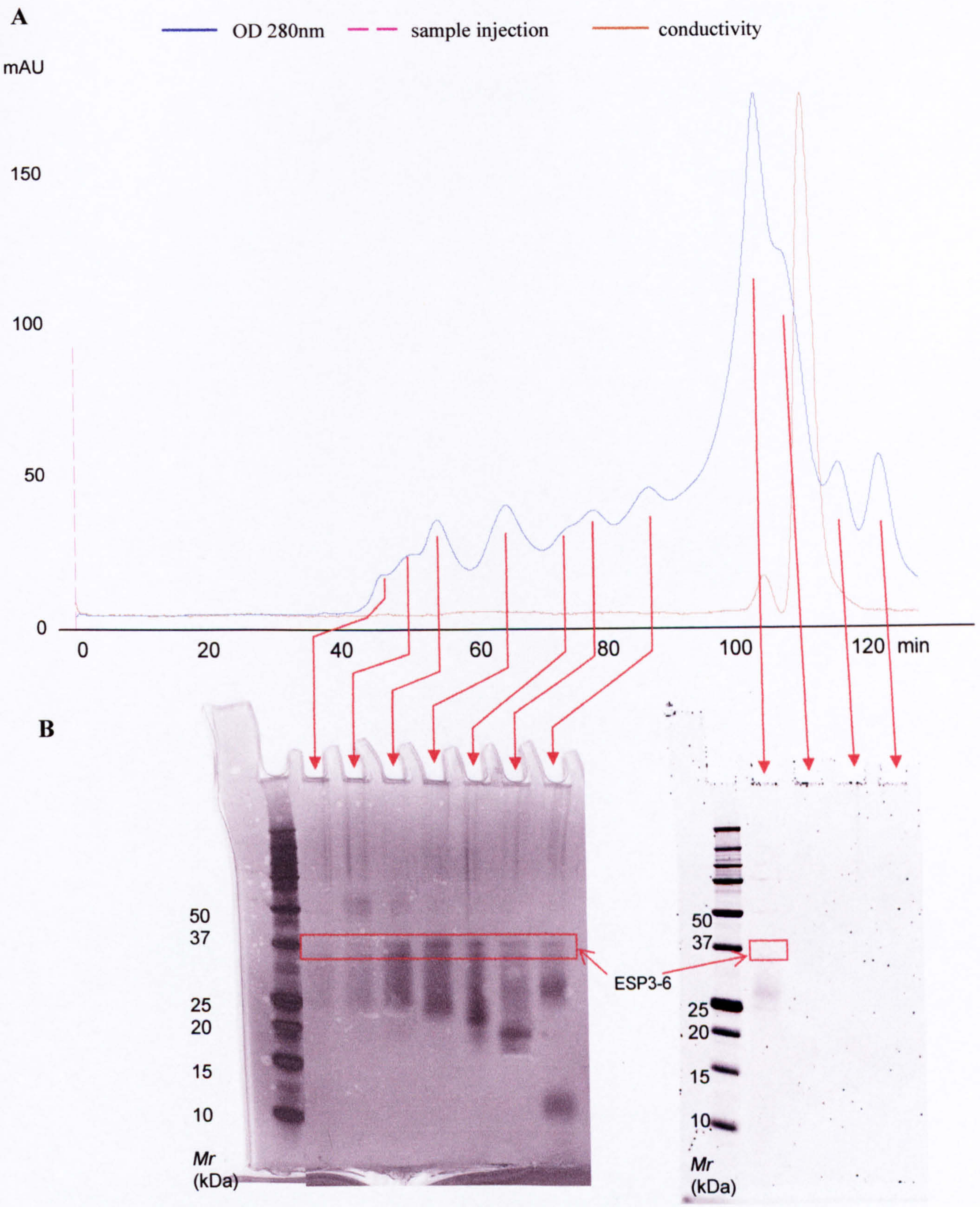

Figure 3.9 Separating crude ESP using size-exclusion chromatography **A:** When applied to a Superdex column, crude ESP separates into seven peaks. The peaks at 45-55 mins and 95-110 mins have distinct shoulders, indicating more than one protein is present. **B**: 1-DE (no reducing agent) was used to visualise the protein content of the chromatogram peaks as indicated. ESP3-6 was present in all of the fractions. The left hand gel was stained with silver and the right hand gel with Sypro Ruby. Although the OD280nm trace indicated peaks at 115 and 120 mins, no protein was detectible on the gel.

Original in colour

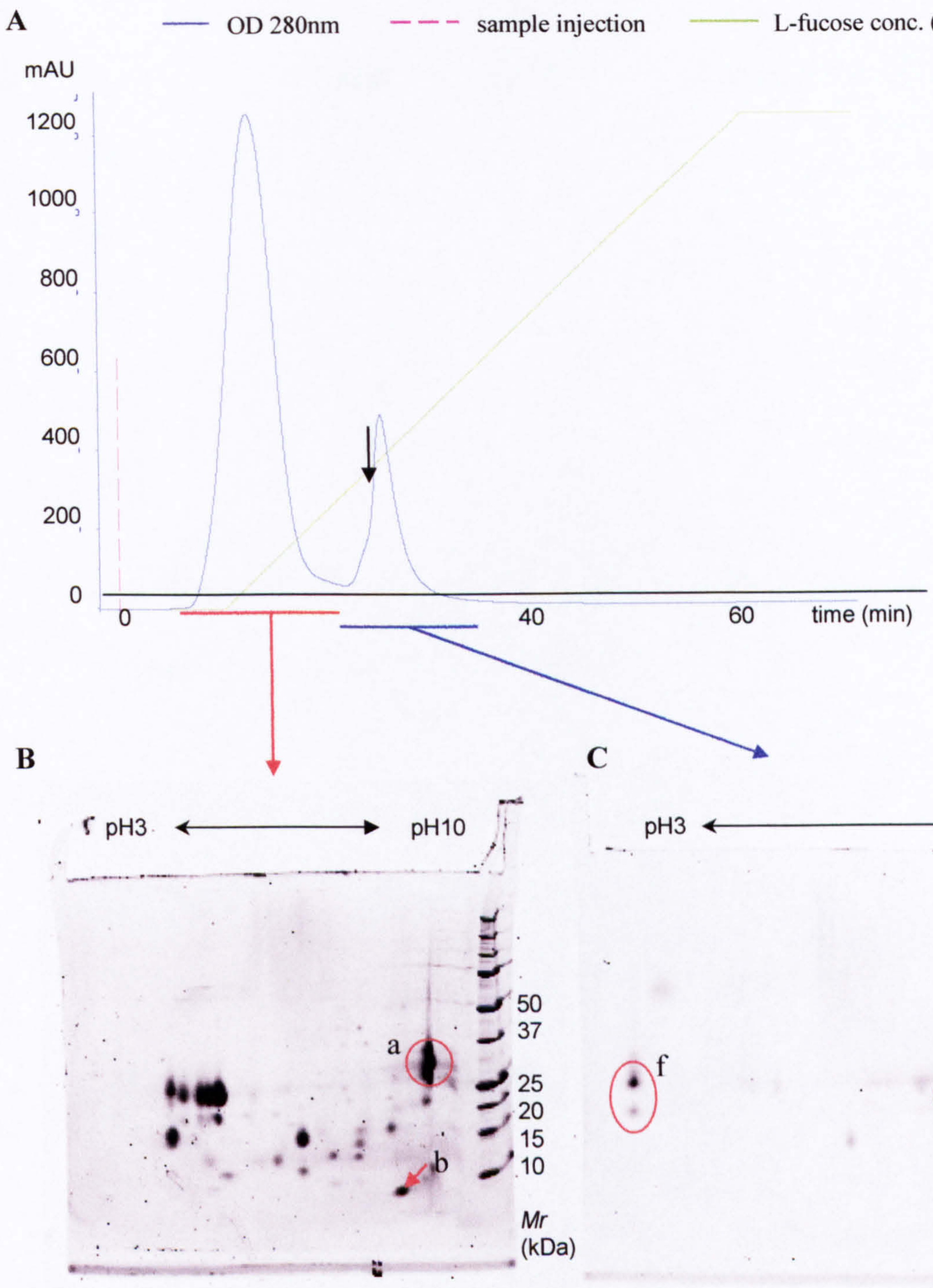

Figure 3.10 Separation of Crude ESP. **A:** *Aleuria aurantia* lectin affinity chromatogram. 1mg crude ESP was applied to an AAA column in PBS and eluted with 0-100% gradient of 100mM L-fucose. The indicated fractions were pooled, subjected to 2-DE and the resulting spots analysed by MALDI-MSMS. The black arrow denotes the shoulder as discussed in the text. **B**: All the ESPs except ESP3-6 were present in the effluent, including ESP1-2 (a) and ESP12 (b). **C:** The eluate contained ESP3-6 (c), but also ESP1-2 (d) and ESP12 (e). Some of the ESP3-6 failed absorb into the IEF strip so it did not focus (f).

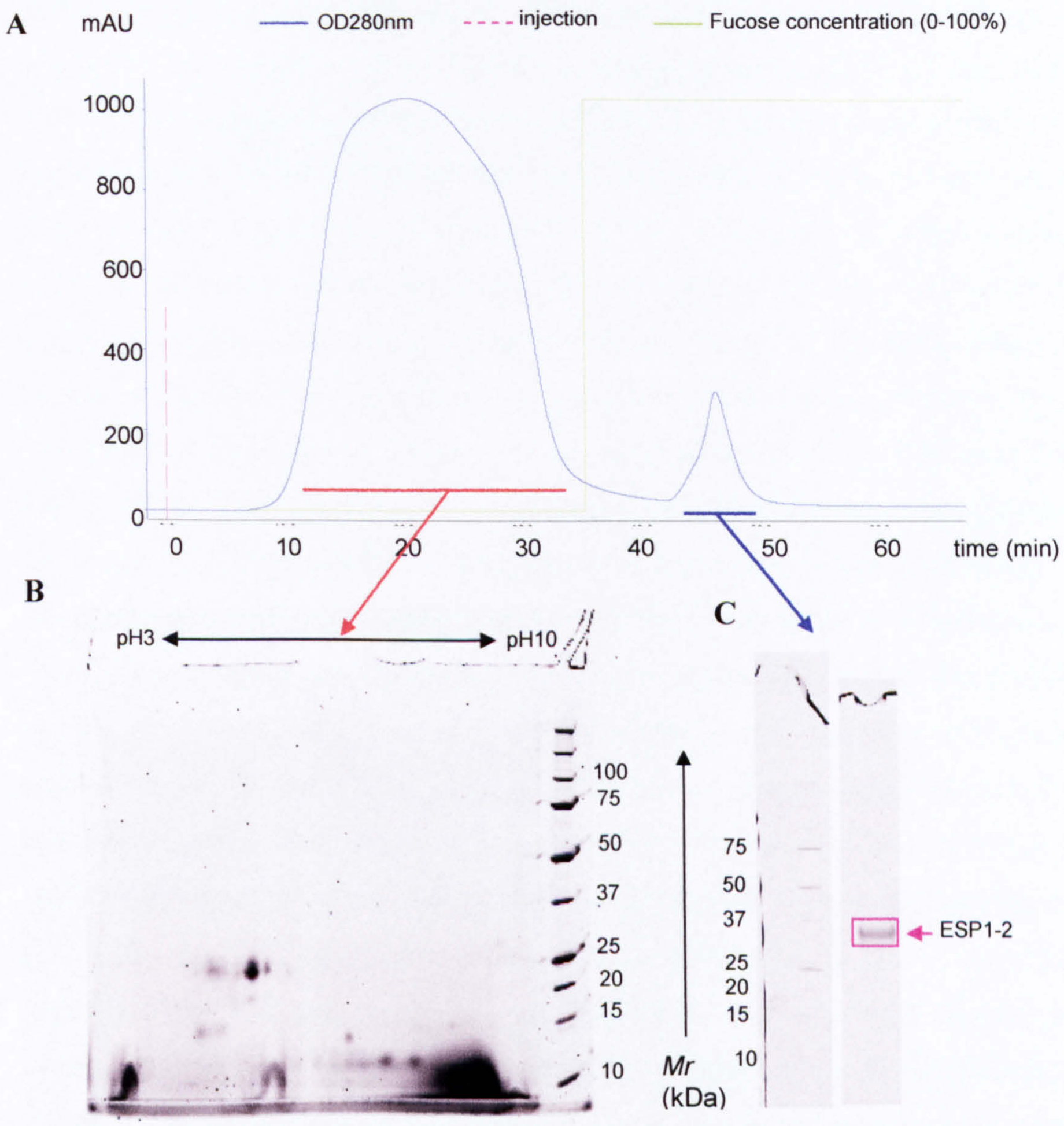

Figure 3.11 Separation of effluent from Figure 3.10 using AAA affinity chromatography. **A:** Crude ESP minus ESP3-6 (i.e. the protein in Figure 3.10B) was applied to the column and eluted with 50mM L-fucose. The indicated fractions were subjected to electrophoresis. (**B**): 2-DE of the effluent shows that ESP1-2 has now been removed. The protein mixture now consists of crude ESP minus ESP1-2 and ESP3-6. (**C**): The ESP 1-2 has been purified in the eluate.

3.7.2: Dimension 3: Anion Exchange Chromatography at pH7.0

2-DE of the effluent from the second regimen of AAA chromatography (Figure 3.11B) showed that the protein mixture could be broadly grouped into acidic proteins of *pI*<5 (ESPs 13-21) and basic proteins of *pI*>8 (ESPs 8-12). Anion exchange at pH7.5 was therefore undertaken to separate the basic proteins as effluent and then purify the individual acidic proteins in eluate fractions (Figure 3.12). The OD280nm trace indicated that the eluate and effluent contained similar quantities of protein. The linear NaCl gradient eluted the bound proteins as four distinct peaks, the first of which (i.e. the least acidic) contained multiple components. The third peak had a distinct shoulder so it contained at least two components. When the eluate fractions were separated by 1-DE, only the content of the first peak could be visualised after staining (although the OD280nm trace indicated that there were broadly similar quantities of protein in each peak), but the bands contained insufficient protein to be identified by MS or MSMS. The fractionated ESPs were therefore identified by matching the chromatogram peaks (representing proteins eluted in order of charge) with the spots on the 2D gel. It could thereby be seen that the first eluate peak (eluted between 20 and 25 mins) was probably a series of 20kDa proteins too low in abundance to stain in the 2D gel, followed by ESP13. The second peak (eluted at 30 mins.) probably represented ESP14, which was the most intensely-stained gel-spot that bound to the column so should have generated the most prominent peak in the chromatogram. The shoulder of the third peak probably represented ESPs 17 and 20, and the peak's apex ESPs 15,18 and 19 (all of which have the same *pI*). The final peak, eluted after 40 mins was probably ESP21 (the most acidic ESP). Thus, the anion exchange step can be seen to have completely purified ESP13, ESP14 and ESP21. The acidic ESPs 15, 17, 18, 19 and 20 remain un-separated (there is no ESP16) and the effluent will contain the basic ESPs 8-12.

3.7.3 Dimension 4: Cation Exchange Chromatography at pH5.8

The effluent from the anion exchange step (containing ESPs 8-12, whose *pI*>7.5) was applied to the cation exchange column at pH5.8 (Figure 3.13). All of the material should have bound to the column, so it was surprising to find effluent containing proteins that resolved themselves into bands at 10, 20 and 25kDa after 1-DE. However, the quantity of protein in the effluent of the anion exchange was relatively small compared to that seen in the effluent of the cation exchange step (50mAU as opposed to 120mAU).

Original in colour

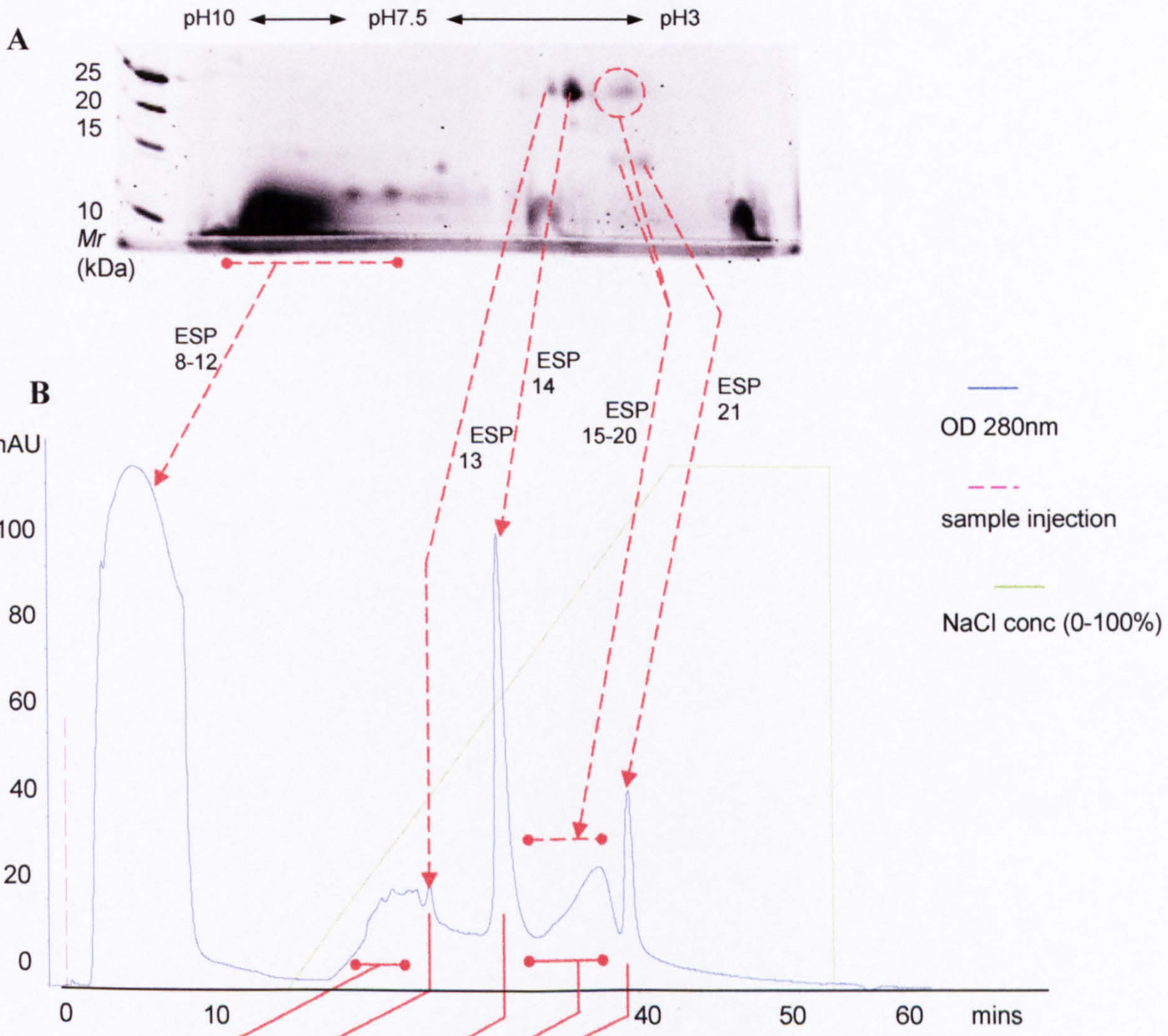

Figure 3.12 Anion exchange at pH7.5 of the effluent from Figure 3.11. **A**: Horizontally-flipped reproduction of Figure 3.11B, showing the protein mixture that was applied to the column. **B:** Proteins were eluted from the column in four peaks. **C:** 1-DE of the eluate (stained with silver) shows purification of two ESP components, which could not be identified by MALDI-MS or MSMS. Solid arrows denote chromatogram fractions applied to the gel and dashed arrows denote the likely origin of the purified components. An unknown ESP (lane 3) and ESP13 have probably been purified.

Original in colour

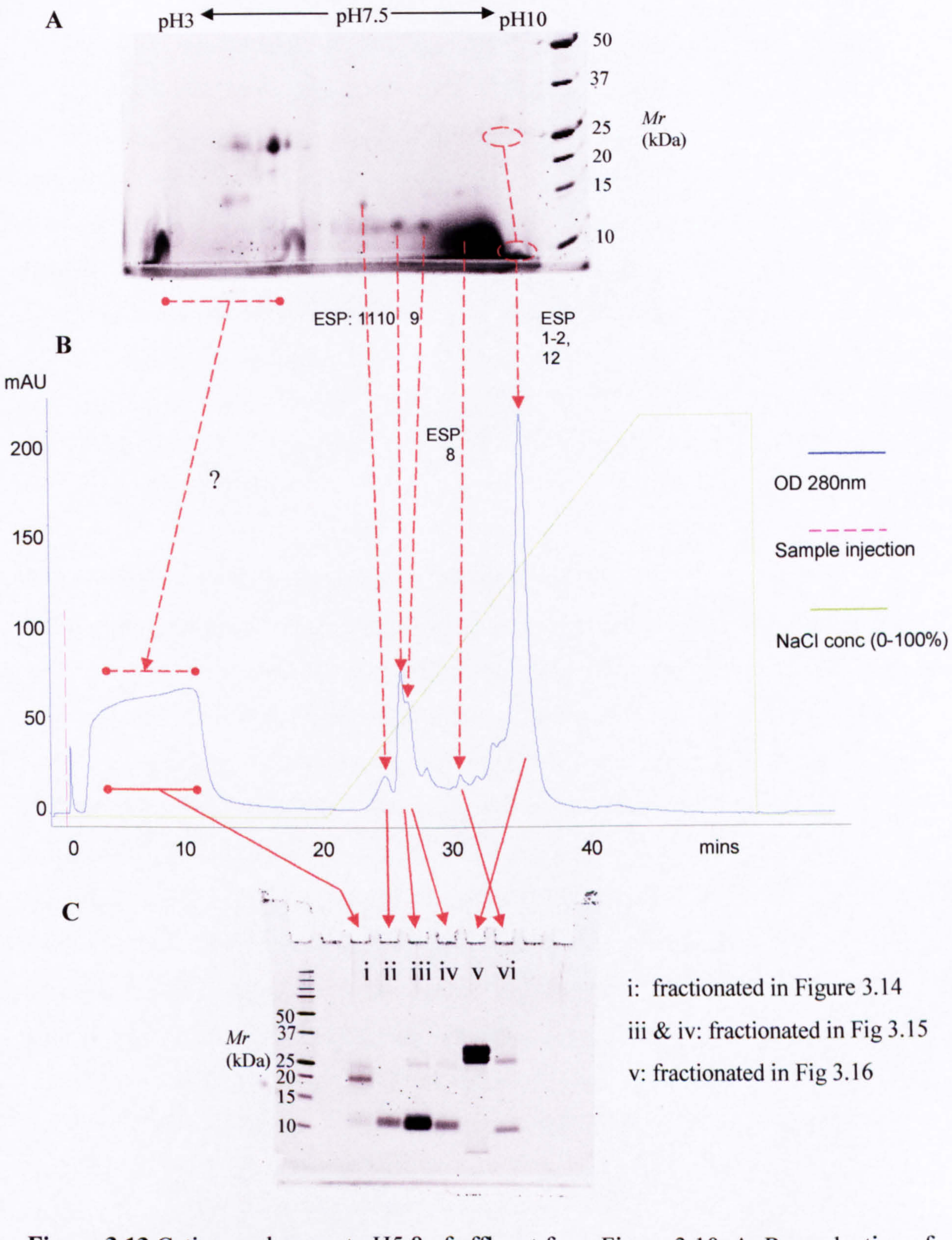

Figure 3.13 Cation exchange at pH5.8 of effluent from Figure 3.10. **A**: Reproduction of Figure 3.10B. The protein mixture applied to the column should consist of the proteins of *pI* >7.5 (i.e. ESPs 8-12). **B:** Proteins were eluted into fractions with increasing NaCl concentration. **C:** 1-DE (Sypro Ruby stain) shows the likely purification of ESP11 but no identities could be confirmed by MS or MSMS. Solid arrows denote the fractions applied to the gel and dashed arrows denote their probable origin.

Unfortunately, the gel-bands contained insufficient protein to be identified by MS or MSMS, so identification of the purified ESPs had to be carried out as in the anion exchange step (by matching chromatogram peaks to 2D gel-spots). ESP11 had probably been purified successfully and could be seen as the first protein to be eluted in Figure 3.13C (lane ii). ESPs 9 and 10 probably eluted together in the second peak, 26 mins into the run (lanes iii and iv), the right shoulder of which probably consisted of ESP 9 (lane iv). However, another protein of approx. 25kDa was also present in both fractions. The most intense peak (200mAU) contained the most basic ESPs, including the 5kDa ESP12. This fraction also contained more heavily-staining proteins of 25 and 30kDa, the latter of which was probably ESP1-2, which had been insufficiently abundant to have been visible in the 2D gel in Figure 3.11B.

3.7.4: Dimension 5: Size Exclusion Chromatography

The cation exchange fractions containing more than one protein can be seen in Figure 3.13C, lanes i, iii, iv, v and vi. The differences in molecular mass between these ESPs make them potentially amenable to purification using size exclusion chromatography. The fractions from lanes iii and iv, each containing ESPs 9 and 10 plus the unknown 25kD protein were pooled, and so four size exclusion runs were carried out. The size exclusion run containing ESP8 plus the 25kda fraction (Figure 3.13C, lane vi) failed because the combination of the small quantity of protein that was applied to the column and the diluting nature of the technique resulted in only one peak appearing in the chromatogram (which emerged from the column at a point consistent with (the 10kDa) ESP8 rather than the 25kDa component. However, when the fractions from this peak were concentrated and applied to a 1D gel there was insufficient protein to stain. The remaining size exclusion runs are shown as Figure 3.14 (the unexpected effluent from the cation exchange separation), Fig. 3.15 (ESP9, ESP10 plus the unknown 25kDa protein) and Figure 3.16 (ESP12, plus ESP1-2 plus the unknown 27kDa protein).

The effluent from the cation exchange column (Figure 3.14) resolved into three peaks. The largest peak (30mAU) emerged from the column after 350 mins and contained a single protein of approx. 18kDa. This was subsequently identified as Sm11845 by MSMS (i.e. an ESP13-14 homologue).

The second peak contained three proteins of 20, 10 and 8kDa, the latter two which were identified by MSMS as thioredoxin and ubiquitin respectively. The resolution of the column was sufficient to separate proteins of 8-10kDa from proteins of 20kDa, so the most likely explanation as to why the proteins appeared together was either that they formed a complex or that they bound to the column medium in some way. The time-point at which the peak occurred in the chromatogram (420 mins) is consistent with the proteins of approx. 25kDa in Figure 3.15, but as the 18kDa protein was eluted at 370 mins in Fig. 3.14 the two chromatograms are not comparable in terms of elution times vs. protein size.

Applying the pooled fractions from lanes iii and iv of Figure 3.13C (i.e. ESP9, ESP10 and the unknown 25kDa protein) to the size exclusion column produced a chromatogram with three peaks, the last two of which failed to completely resolve (Figure 3.15). Unfortunately, none of the peaks contained sufficient protein to stain after 1-DE, but the peak at 420mins was probably the 25kDa component and the second peak at 500-550 mins was probably ESP9 and ESP10. ESP10 consists of two isoforms with slightly different molecular mass but not charge (ESP10b has the same mass as ESP9 and ESP10a is slightly larger). It is therefore likely that ESP9 cannot be separated from ESP10, although the second peak in the chromatogram was probably enriched in ESP10a.

The largest and most basic peak in the cation exchange chromatogram (Figure 3.13C, lane v) contained proteins of 5kDa (ESP12), 25kDa (an unknown protein) and 30kDa (probably ESP1-2). When applied to the gel filtration column a relatively large quantity of protein was recovered at 350mins and a smaller quantity at 520mins (Figure 3.16). 1-DE demonstrated that the first peak contained the 25 and 30kDa components, plus a further 60kDa protein. The second peak contained insufficient protein to stain, but it most likely to be the 5kDa ESP12. MSMS was used to identify the 25kDa protein as Sm00193 (an ESP15 homologue) and the 30kda protein as ESP1-2.

Original in colour

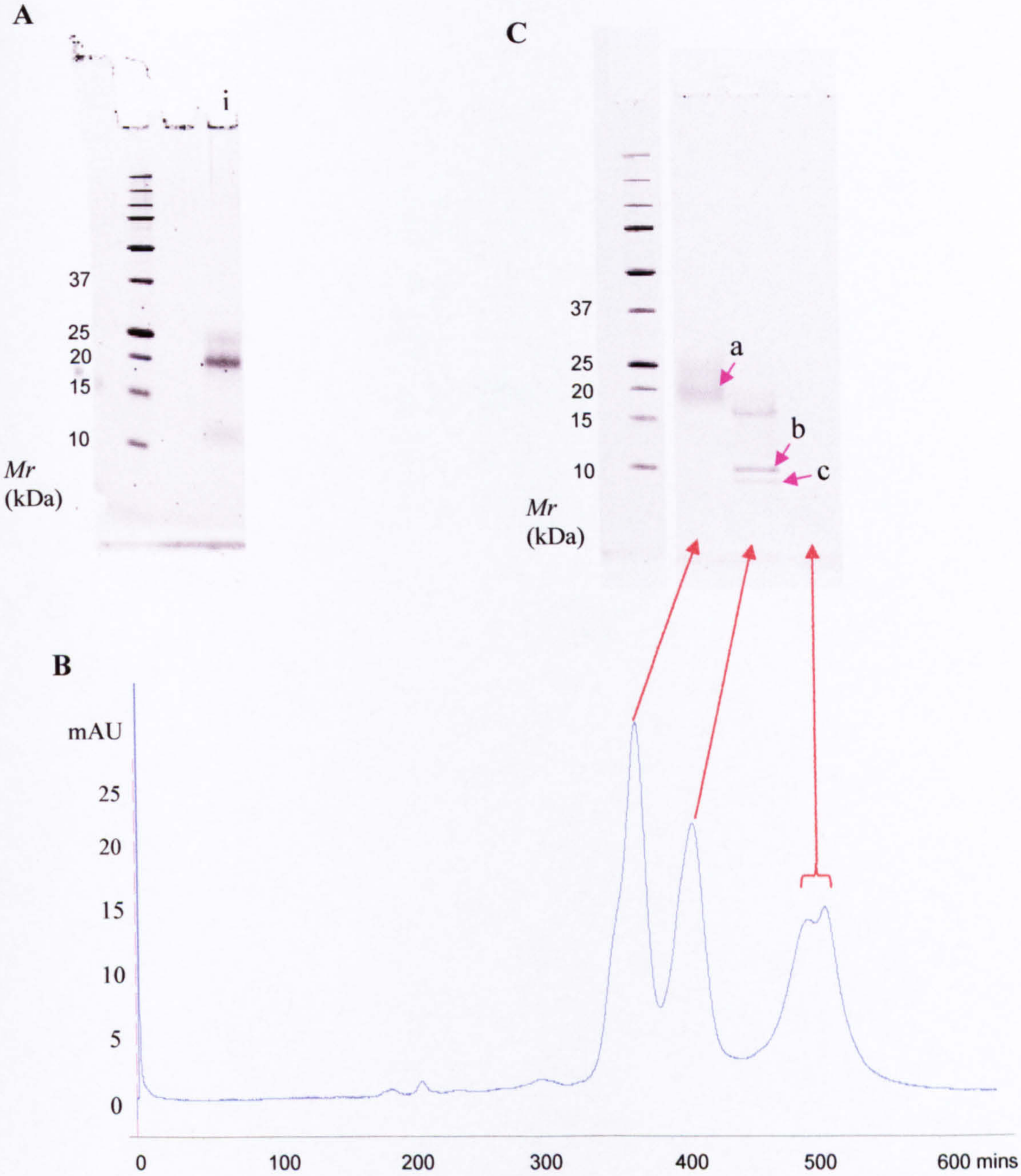

Figure 3.14 Size exclusion chromatography of Fraction i from Figure 3.13C. **A:** Reproduction of Fig 3.5C lane i, showing the proteins of approx. 12, 20 and 25kDa applied to the column. **B:** The three bands of A separate into three peaks when applied to the column. **C:** 1-DE of each of the three peaks from B shows that complete fractionation has not been achieved. When the bands are analysed by MALDI-MSMS the proteins are identified as ESP13-14 (a), ubiquitin (b) and thioredoxin (c). The chromatogram peak at 500 mins contained insufficient protein to stain

Original in colour

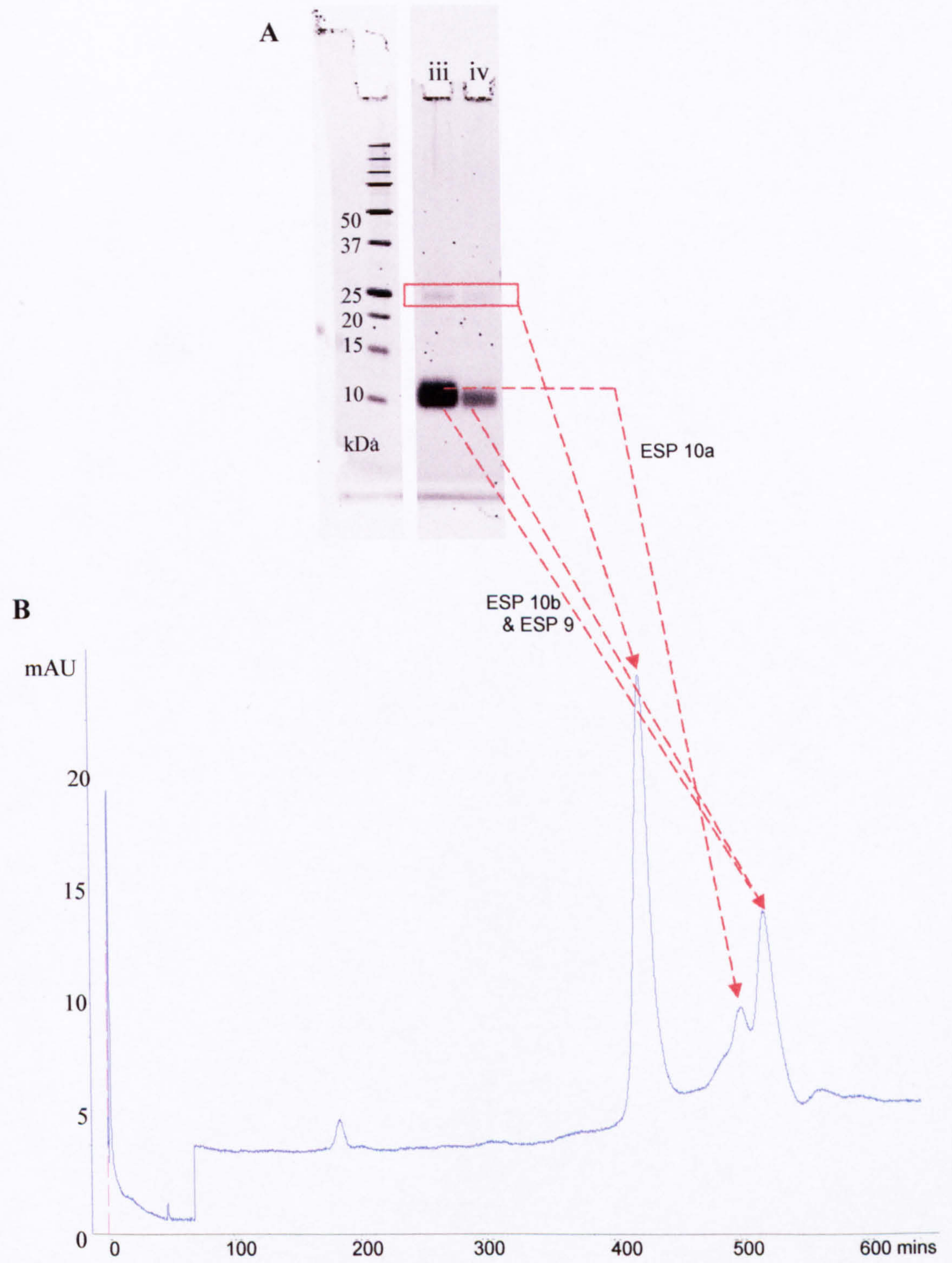

Figure 3.15 Size exclusion chromatography of fractions iii & iv from Figure 3.13C. **A:** Reproduction of Figure 3.13C lanes iii and iv, showing proteins of 10-12 and 25kDa that were applied to the column. **B:** The proteins of A separated into three peaks but insufficient protein was recovered to be visualized by 1-DE. Likely sources for the chromatogram peaks are shown by dashed arrows.

Original in colour

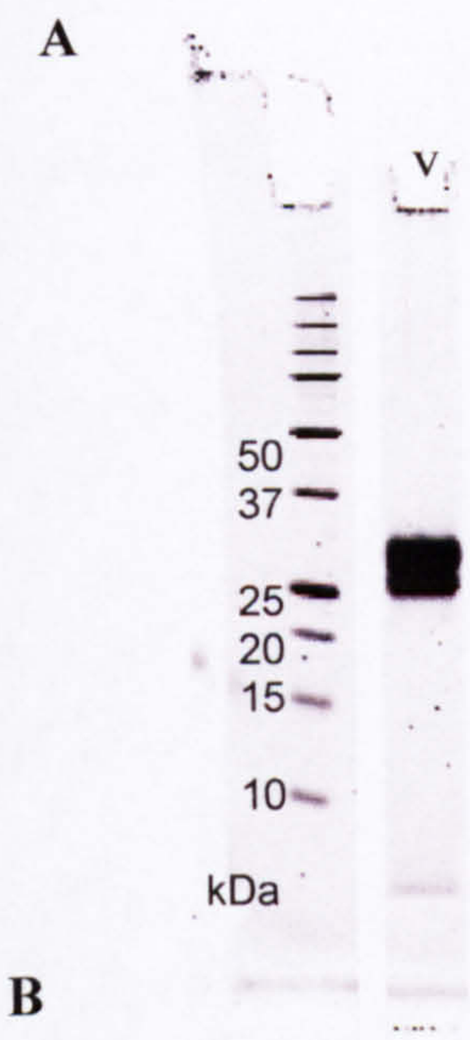

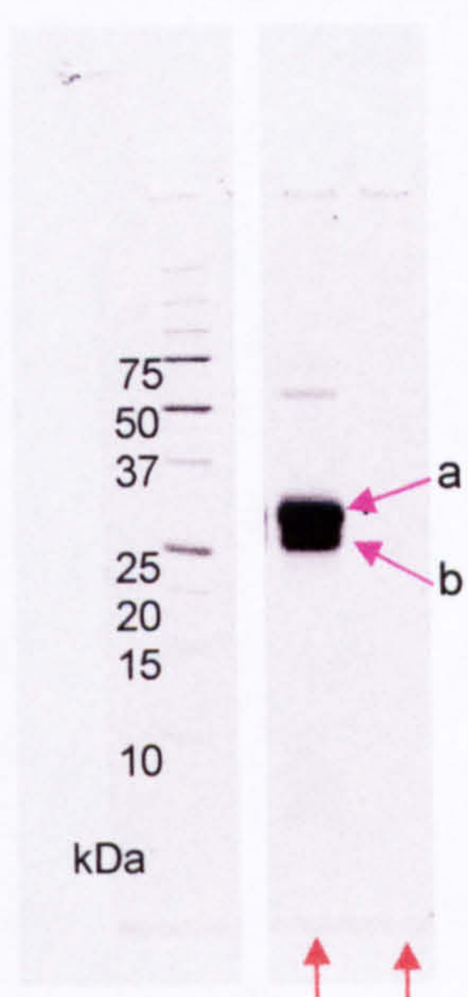

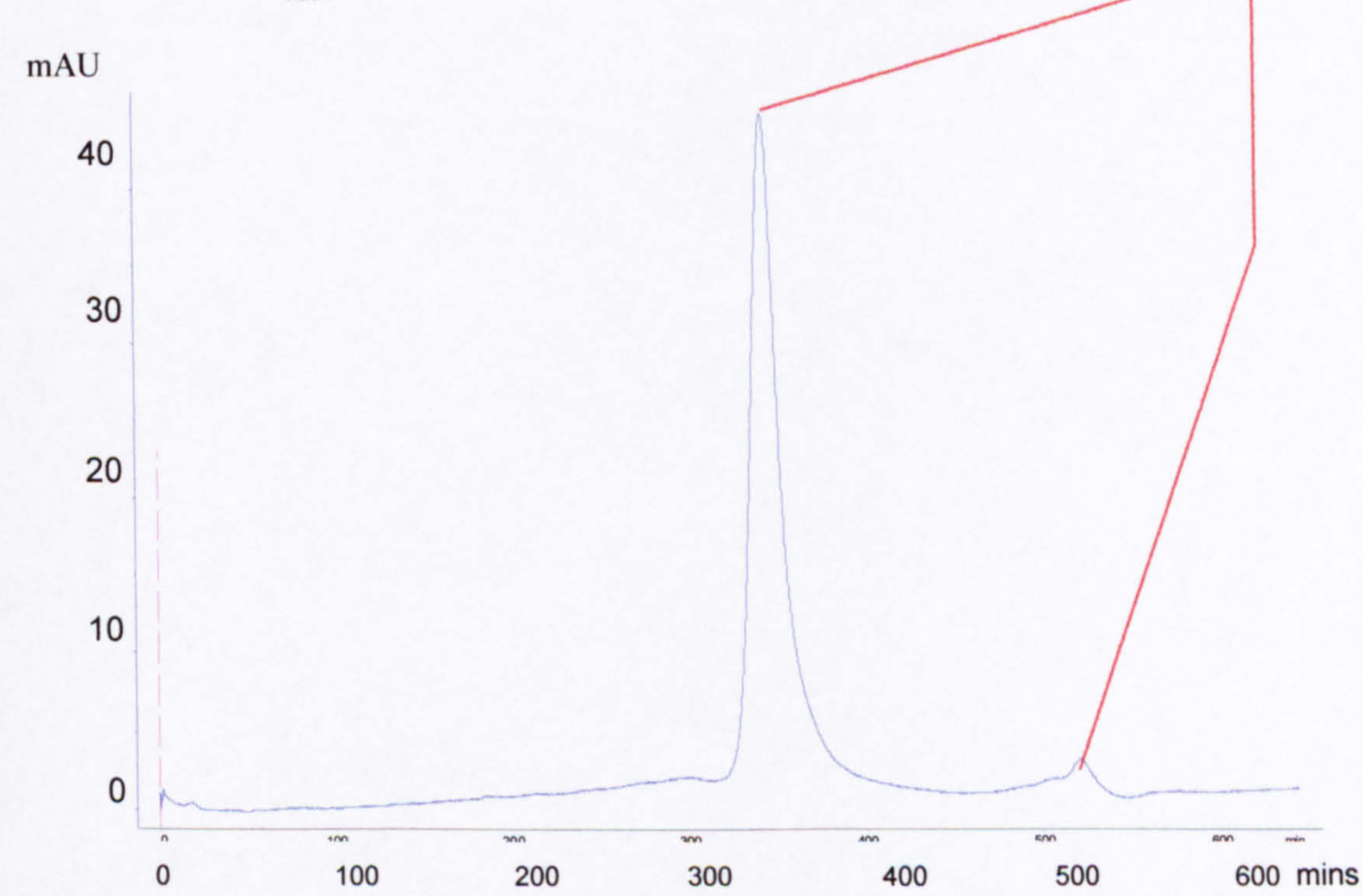

Figure 3.16 Size exclusion chromatography of Fraction v from Figure 3.13C. **A:** Reproduction of Figure 3.13C, lane v, showing that proteins of approx. 30, 28 and 5 kDa were applied to the column. **B:** The three bands from A separate into two peaks, the largest of which has a shoulder suggesting it contains two components. **C:** 1-DE of the two peaks shows that the largest peak contains the 30kDa and 28kDa components and a further 60kDa protein has also been purified. The small peak contained insufficient protein to stain in 1-DE but is presumably the 5kDa protein. The proteins were identified by MALDI-MSMS as ESP1-2 (a) and ESP11/15 (b).

Table 3.1 A summary of the protocol devised to purify individual ESPs using HPLC.

ESP no	Purifiable?	1st Dim. AAA	2nd Dim. AAA	3rd Dim. Anion exchange	4th Dim. Cation exchange	5th Dim. Size exclusion	Notes
1-2	yes	effluent and eluate	eluate				1
3-6	yes	effluent					2
8	no	effluent	effluent	effluent	eluate	?	3
9	no	effluent	effluent	effluent	eluate	Can't separate from ESP10b	
10	partially	effluent	effluent	effluent	eluate	ESP10a purified	
11	yes	effluent	effluent	effluent	eluate		
13	yes	effluent	effluent	eluate			
12	yes	effluent and eluate	effluent	effluent	eluate	purified	
13	yes	effluent	effluent	eluate			
14	yes	effluent	effluent	eluate			
15	no	effluent	effluent	eluate			4
17	no	effluent	effluent	eluate			5
18	no	effluent	effluent	eluate			5
19	no	effluent	effluent	eluate			5
20	no	effluent	effluent	eluate			5
21	yes	effluent	effluent	eluate			
22	no	unknown	unknown	unknown	unknown	unknown	6

Notes

1. Increasing the ionic strength of the buffer in Dimension 1 should retain all the ESP1-2 in effluent.
2. The ionic strength of the buffer should be reduced for Dimension 2 to allow binding to the column.
3. ESP8 is can probably be purified during size exclusion dimension.
4. ESP15 likely to be purified by applying eluate from anion exchange to size exclusion column.
5. Improvement of resolution should be possible by reducing the pH of the buffers and the rate of increase of the elution buffer concentration after 30 mins.
6. ESP22 was not found. It should be capable of purification by applying the ESP13 fraction to the size exclusion column.

Original in colour

A

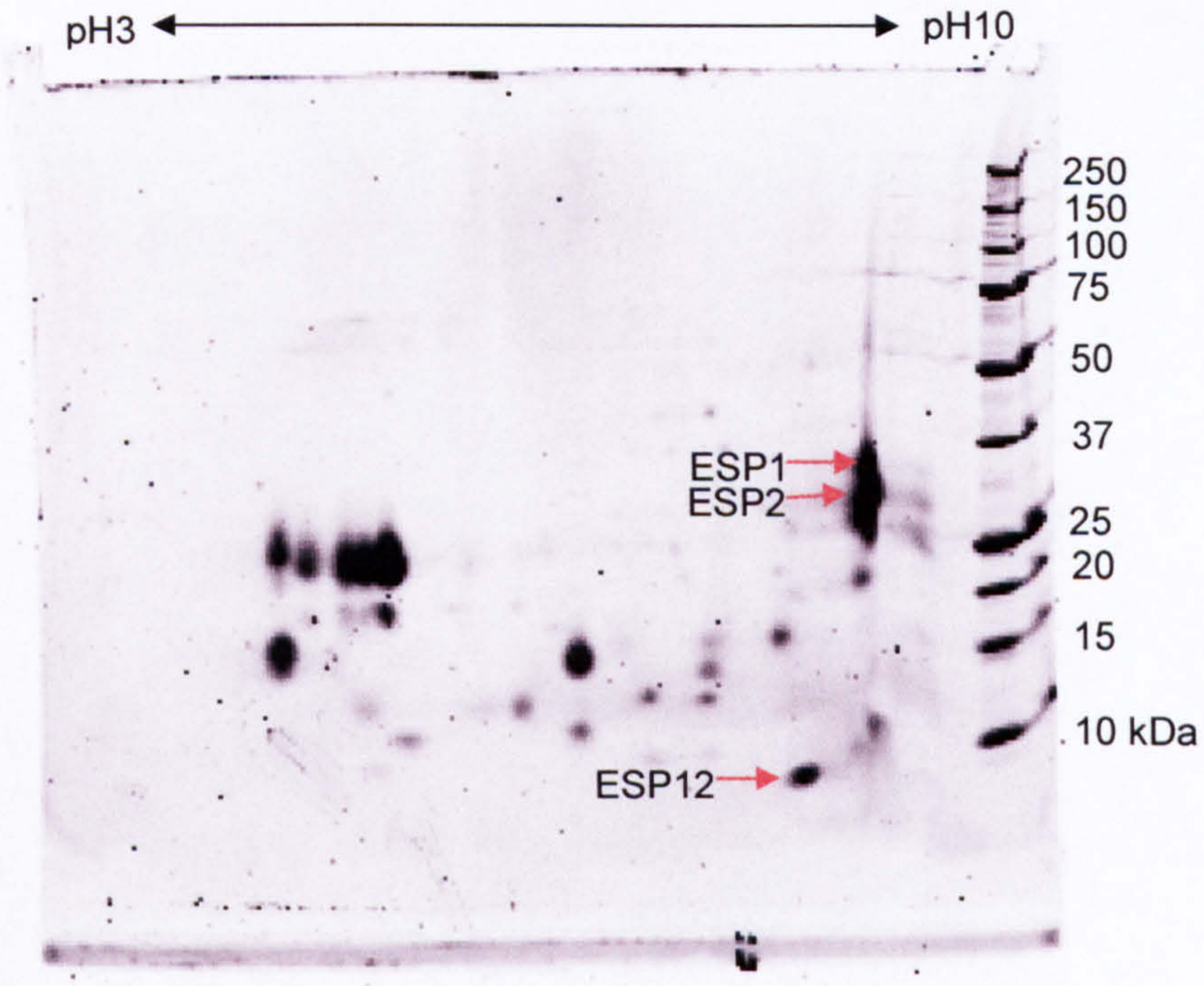

B

```
Sm19482     LVYQMFSTLSTFRRHEFEKHGLCAVEDPQVFNQYGYFKFGIKLMQKLNLLKTLMKYKISP
Smp193860   ----MFSTLSTFRKHEFEKHGLCAVEDPQVFNQYGYFKFGIQLMQKLNLLKTLMKYRISP
             *********:*******************************:***************:***

Sm19482     HDSRQYDTINLMNVLERESGYNGSANCIRKP----------------------------
Smp193860   HDSRQYDTINLMNVLEREFGYNGSANCIRKPGRRGMYHLEEVHVCLNRKHEFMNCPFLGN
            ******************* ************

Sm19482     ----------
Smp193860   CPKKFIFPPFQ
```

Figure 3.17 The related ESP1-2 and ESP12 genes. **A**: Sm19482 (ESP1-2) and Smp_193860 (ESP12) encode proteins of a similar *pI* but different molecular weights. **B:** ClustalW alignment of Sm19482 and Smp_193860 demonstrate that they are 95% homologous at the amino acid level (BLAST expect score of 2.9e-43).

Original in colour

A

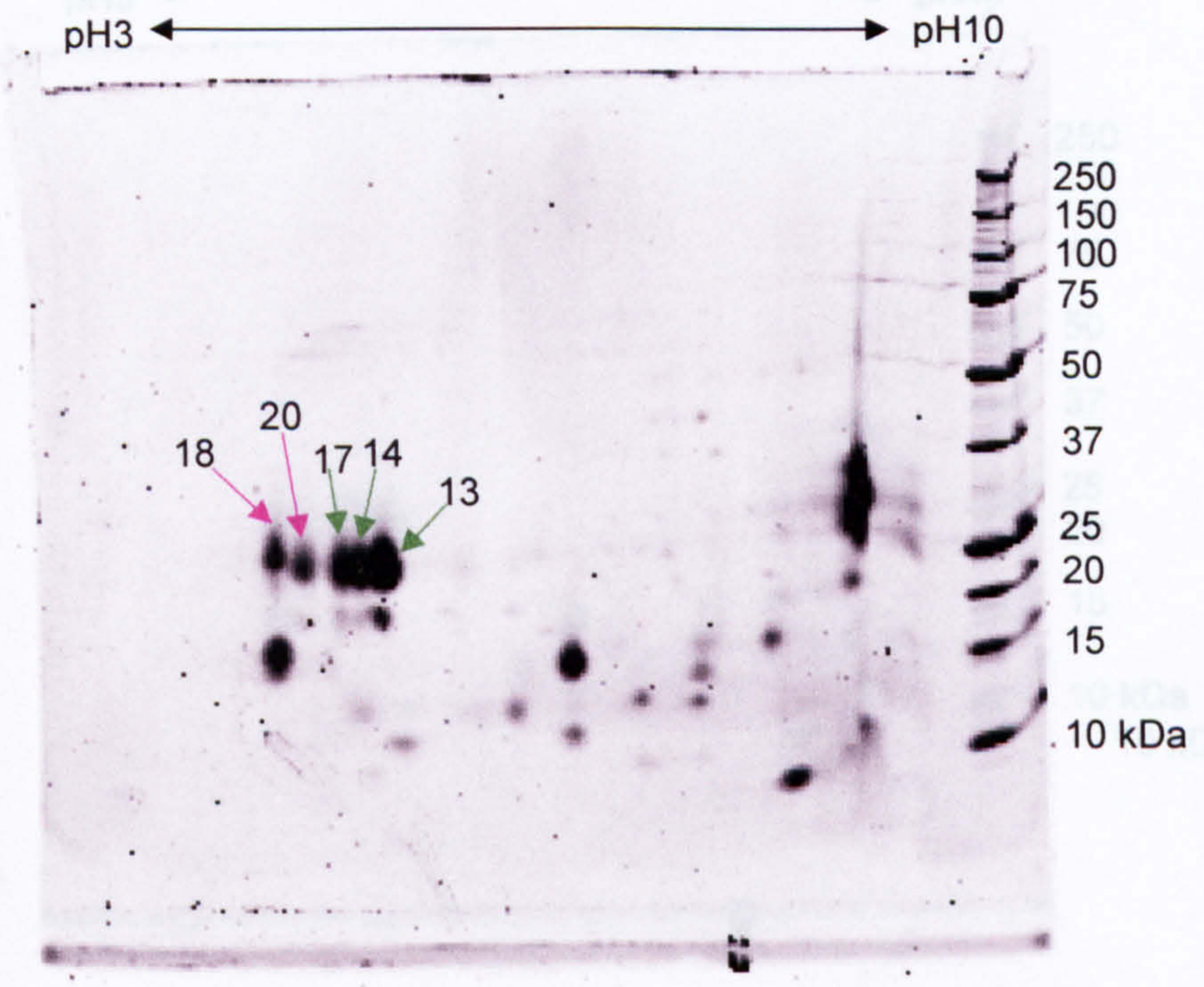

B

```
Sm11845    SGVRTTTHRLVKMLFVALILIISLHSFDCVFTAQETRDAERECKKHCEGNNEYVTRYCGG
Sm12949    ----STTHRLVKMLFVALILIISLHSFDCVFTARET---QQECVRHCGGHNEYVTRYCGG
               :**********************************:**   ::** :** *:**********

Sm11845    LCSSNTGPQTFYCYLGCSHNASTQDDFDKCLPKCNDRVQLTEENCRNDCGRVTSHHELCG
Sm12949    LCSGSTGPQTFYCYLGCSHNASNQNDFDKCLPKCNGSPQLTESSCQNDCGRVTTHPELCG
           ***..******************.*:**********.  ****..*:*******:* ****

Sm11845    DVCGGNHGGSFPLCLYNCDQEHPREYERGYDKCKEKCYAMEGR
Sm12949    IVCGGNDGGSFPICLYNCDQGNG---SGNFDECKTKCYEMAGR
            *****.*****:******* :    . .:*:** *** * **
```

Figure 3.18 The related Sm11845 and Sm12949 genes. **A**: Sm11834 (ESPs 13,14 & 17 arrowed in green) and Sm12949 (ESPs18 & 20 arrowed in pink) form a series of spots of similar size but slightly different *pI* following 2-DE. **B:** ClustalW alignment of Sm11845 and Sm12949. The two genes are 74% homologous at the amino acid level (BLAST Expect score of 1.4e-66). The genes are located adjacent to each other on the contig, but are transcribed in opposite directions.

Original in colour

A

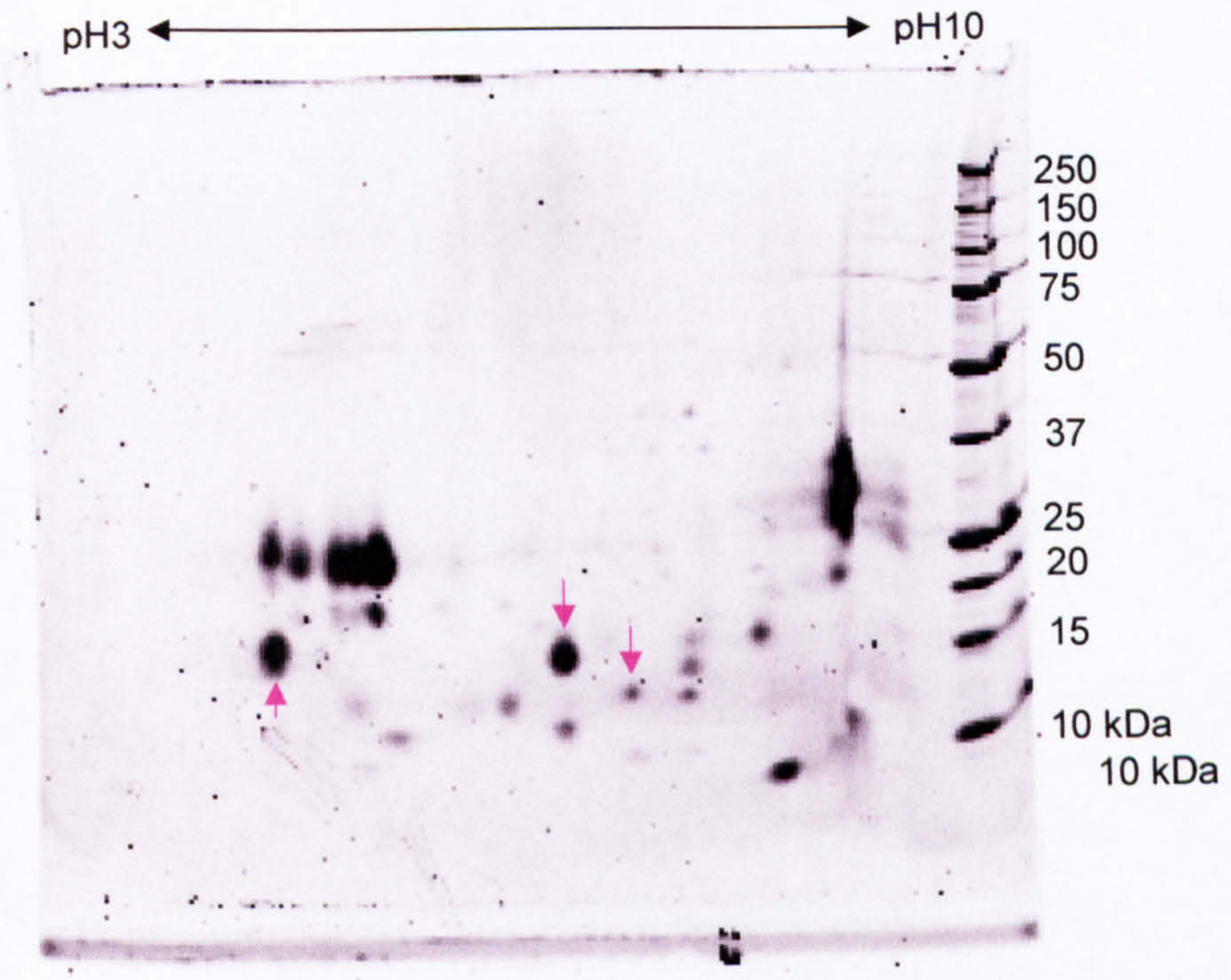

B

```
Sm00193          HATRQFRCASEDGKKGSLCCEKDGCPIPS-TPDLLLGNYQRHQRMKNYLEEVCKYYI
Smp180310        ----TVCCESEDGKAGSLCCEKNGCSVPSGTHDLLSENYRRHQRMKNYLKEVCKYFK
                      . * ***** *******:**.:** * ***  **:**********:*****:
```

Figure 3.19 The ESP15 proteins. **A**: 2-DE of ESP3-6-deprived ESP with ESP15 isoforms arrowed in pink. **B:** In addition to the ESP15 variant found in A (Sm00193) the *S. mansoni* genome also contains a putative gene with significant homology to it. Although Smp_180310 was not identified by MSMS, it has 75% homology to Sm00193 at the amino acid level (BLAST expect score of 1.3e-17).

3.8: Discussion

The purification of individual ESP components proved to be a lengthy and difficult exercise which was only partially successful. Various combinations of ion exchange and gel filtration protocols were initially attempted but they consistently failed because protein complexes formed that were too robust to be disassociated. Specifically, ESP3-6 appeared in almost all protein-containing fractions when crude ESP was applied to a cation exchange, anion exchange or size-exclusion column. However, by removing ESP3-6 using the AAA lectin affinity column in the first step an HPLC regimen was devised that can be used in the future to isolate specific ESPs (see Table 3.1). The limiting factor in developing the protocol was the low quantity of crude ESP which was available because many of the less abundant ESPs were lost entirely.

The first two separation steps using the AAA column purified ESPs1-2, 3-6 and ESP12, so these proteins must be glycosylated. ESP12 had already been shown to be a (smaller) isoform of ESP1-2 in Chapter 2 (Section 2.3.4.3), but the binding of ESP12 to the AAA column demonstrates that the larger size of ESP1-2 cannot be attributed to glycosylation alone. ESP3-6 has more affinity to AAA than ESP1-2 (because no ESP1-2 was present in the eluate in the first AAA regimen when the column was overloaded), so either ESP3-6 is more heavily glycosylated than ESP1-2 or its glycans have more affinity to *A. aurantia* lectin.

Thioredoxin was purified in the size exclusion regimen but it has previously been demonstrated by Western Blotting to be found in *S. mansoni* egg culture supernatant (Alger *et al.*, 2002). The authors proposed that the thioredoxin protects the egg by detoxifying the hydrogen peroxide produced by the cells of the granuloma. However, it is likely that the thioredoxin present amongst the actively-secreted ESPs is actually derived from damaged eggs. Thioredoxin is a small (approx 12kDa) and it makes up over 4% of hatch fluid protein (see Chapter 2, Section 2.4.4), so it is easy to see how a small tear in the envelope would result in its escaping to the external environment. If the thioredoxin does have a protective role then it is more likely to be effective when it is concentrated between the envelope and the miracidium, rather than dissipated into the granuloma. Also, when in the egg the

the miracidium, rather than dissipated into the granuloma. Also, when in the egg the thioredoxin is in close proximity to thioredoxin peroxidase, which is also present in hatch fluid and is used to maintain thioredoxin in its reduced state. It is, however, possible that thioredoxin is indeed an actively-secreted ESP but its role is not that of an oxidant scavenger. Secreted thioredoxin has been described as a chemoattractant for leukocytes (Bertini *et al.*, 1999) and when secreted by DCs it contributes to T-cell activation (Angelini *et al.*, 2002). The problem with these studies was that the receptors and mechanisms by which extracellular thioredoxin operates was unknown. However, it has recently it has been reported that extracellular thioredoxin interacts with the TNF receptor CD30 on lymphoid cell lines (Schwertassek *et al.*, 2007). CD30 is expressed on activated T cells in response to IL-4 and when ligated it induces cell proliferation and cytokine production (Watts, 2005). CD30 has also been implicated in the promotion of Th2 responses in humans (Duckett & Thompson, 1997). It is therefore possible that egg-secreted thioredoxin is involved in the process of granuloma formation, T cell activation and the maintenance of the Th2 bias in the immune response that is a characteristic of egg deposition.

Ubiquitin was identified in the same HPLC fraction which contained thioredoxin. The UPP in the *S. mansoni* egg is the subject of the next chapter and so this finding will be covered at that point.

Another important result of the ESP purification regimen has been the insight into gene families which it has provided. Specifically, ESP12 and ESP1-2 are closely related (see Figure 3.17). It has also been proven that ESPs 13,14 and 17 are all variants of Sm11845, which itself has 74% homology to ESPs 18 and 20 (see Figure 3.18). ESP15 also has different secreted variants (see Figure 3.19).

Chapter 4

The Ubiquitin-Proteasome Pathway in the *S. mansoni Egg*

4.1 Introduction

There are three mechanisms of protein turnover in eukaryotic cells: apoptosis, autophagy and the ubiquitin-proteasome pathway (UPP). Apoptosis (the regulated self-destruction of cell) and autophagy (where a cell degrades and reuses its cytoplasmic proteins) have been described in some detail in Chapter 1 (Section 1.6.1 and 1.6.2). The UPP, which is responsible for the controlled intracellular degradation of targeted proteins is the subject of this chapter and so has not been described in detail until this point. The UPP uses a ubiquitinylation enzyme cascade which attaches multiple copies of ubiquitin to a protein requiring degradation. The degradation is then carried out by the proteasome which is located in the cytosol or nucleus. The UPP is responsible for many cellular functions, such as protein quality control and regulating the cell cycle and transcription. The UPP is also vital for growth and development because in various parasite models (*Entamoeba invadens, E. histolytica, Leishmania mexicana, Trypanasoma cruzi, T. brucei, Plasmodium berghei, Toxoplasma gondii* and *Schistosoma mansoni*), blocking the UPP results in the cessation of growth (Makioka *et al.*, 2002; Robertson, 1999; de Diego *et al.*, 2001; Nkemngu *et al.*, 2002; Gantt *et al.*, 1998; Shaw *et al.*, 2000; Guerra-Sa *et al.*, 2005).

4.1.1 The Proteasome

Proteasomes are abundant, non-specific proteolytic machines that are present in eukaryotic cells where they make up about 1% of the cellular protein (Tanahashi *et al.*, 2000). Proteasomes are comprised of α and β subunits that assemble as seven-member rings. Four of these rings stack together to form a cylinder in the conformation α_{1-7}, β_{1-7}, β_{1-7}, α_{1-7} to produce a barrel-like particle of approximately 750kDa (Hegerl *et al.*, 1991; Kopp *et al.*, 1993; Zwickl *et al.*, 1992). This four-ringed structure, called the 20S proteasome is named after its sedimentation coefficient (Tanahashi *et al.*, 2000). The six proteolytic subunits are located at the β_1, β_2 and β_5 positions with their active sites pointing towards the interior of the proteasome, so proteolysis is confined to an internal chamber and the uncontrolled degradation of proteins is avoided (Baumeister *et al.*, 1998). The chamber is accessed through the hole in the centre of each of the outer α-subunit rings. As the entrance holes are only 2nm in diameter, only unfolded proteins can pass through them to enter the proteolytic chamber. The entry holes are also gated by projecting N-terminal extensions on the α

subunits (Groll *et al.*, 1997). The three proteolytic subunits have different substrate specificities: caspase-like (β_1), trypsin-like (β_2) and chymotrypsin-like (β_5), which together degrade most proteins to peptides of 3-22 amino acids in length, depending on their amino acid sequence (Orlowski & Wilk, 2000). These post-proteasomal peptides are then further degraded into their constituent amino acids by conserved families of endopeptidases, aminopeptidases and carboxypeptidases (Chandu & Nandi, 2004).

The 20S proteasome is only capable of degrading unfolded proteins, so if it was to act alone its proteolysis would be restricted to proteins such as β-casein, phosphorylated casein and α- and β-crystallin (Orlowski & Wilk, 2000). The 20S core therefore associates with a 900kDa multi-subunit molecule called the 19S regulatory complex (also known as PA700), which caps one or both ends of the 20S proteasome. The 19S regulatory complex recognises the proteins requiring proteasomal destruction, unwinds them and feeds them into the 20S proteasome. The recognition signal which tags a protein for destruction is the covalent attachment of a string of ubiquitin molecules.

Each 19S regulatory complex contains at least 17 subunits with diverse functions. The subunits include a ubiquitin ligase, a de-ubiquitinylation enzyme and several ATPases that unfold the target protein and interact with the N-terminal extensions of the 20S α-subunits to open the entrance to the proteasome core (Pickart & Cohen, 2004). So, the active proteasome consists of the 20S proteasome core plus its two 19S regulatory complexes. This mega-complex is called the 26S proteasome. Both the 20S proteasome core and the 19S regulatory subunits also undergo post-translational modifications, including phosphorylation, N-acetylation and O-GlcNAc glycosylation (Mason *et al.*, 1998; Rivett *et al.*, 2001; Kimura *et al.*, 2000; Sumegi *et al.*, 2003; Zhang *et al.*, 2003). It is not known how the post-translational modifications operate to influence proteasomal activity, but they are likely to have various regulatory roles.

Proteasomal degradation of proteins is important in numerous processes in the cell. In addition to recycling damaged or mistranslated proteins, the proteasome regulates the cell cycle by degrading cyclins (Clurman *et al.*, 1996), controls apoptosis by degrading pro- and anti-apoptotic molecules (Friedman & Xue, 2004) and influences transcription by

degrading transcription factors, transcription factor inhibitors and RNA polymerases (Muratani & Tansey, 2003).

4.1.2 Ubiquitin

Ubiquitin is an 8.5kDa protein of 76 amino acids, best known for its role in tagging misfolded proteins for proteasomal degradation. The process of conjugating ubiquitin to its target protein (illustrated in Figure 4.1 overleaf) is a multi-step process involving three enzymes. Firstly, a ubiquitin molecule is activated by an enzyme called E1, which uses ATP to catalyse the formation of an intermediate thioester bond between the C-terminus of ubiquitin and a cysteine on E1. The ubiquitin-E1 complex then binds to a ubiquitin-conjugating enzyme called E2. The E1-bound C-terminus of ubiquitin is transferred to a cysteine in E2, forming a second intermediate thioester bond, but this time between ubiquitin and E2. E1 then disassociates from E2 and can be reused. A ubiquitin-substrate ligase called E3 then promotes the transfer of the ubiquitin from the E2-ubiquitin conjugate to the target protein. The ubiquitin-substrate bond is usually between the amino group of a lysine side chain on the target protein and the C-terminus of ubiquitin, but sometimes the ubiquitin is conjugated to the NH_2-terminal amino group of the substrate (Glickman & Ciechanover, 2002). E3s contain binding sites for two substrates: the target protein and the E2-ubiquitin conjugate. In the commonest, RING (really interesting new gene)-finger domain family of E3s, the ubiquitin is brought into close proximity to the target protein's lysine and the ubiquitin is transferred directly from E2 to the target protein (Ozkan *et al.*, 2005). In the HECT (homologous to the E6-AP COOH terminus)-domain E3s, the ubiquitin is not transferred to its target directly, but via a third thiol ester intermediate bond to a cysteine residue on E3 (Glickman & Ciechanover, 2002).

If the target protein is released from E3 with a single ubiquitin attached to it the process is called mono-ubiquitination. However, repeated cycles of ubiquitin-conjugation often occur whilst the target protein remains bound to E3. Several ubiquitin molecules can become attached to different lysines on the target protein (a process called multi-ubiquitination) or chains of ubiquitins can be generated when the C-terminus of another ubiquitin is attached to a lysine residue of the previously-conjugated ubiquitin (a process called poly-ubiquitination).

Original in colour

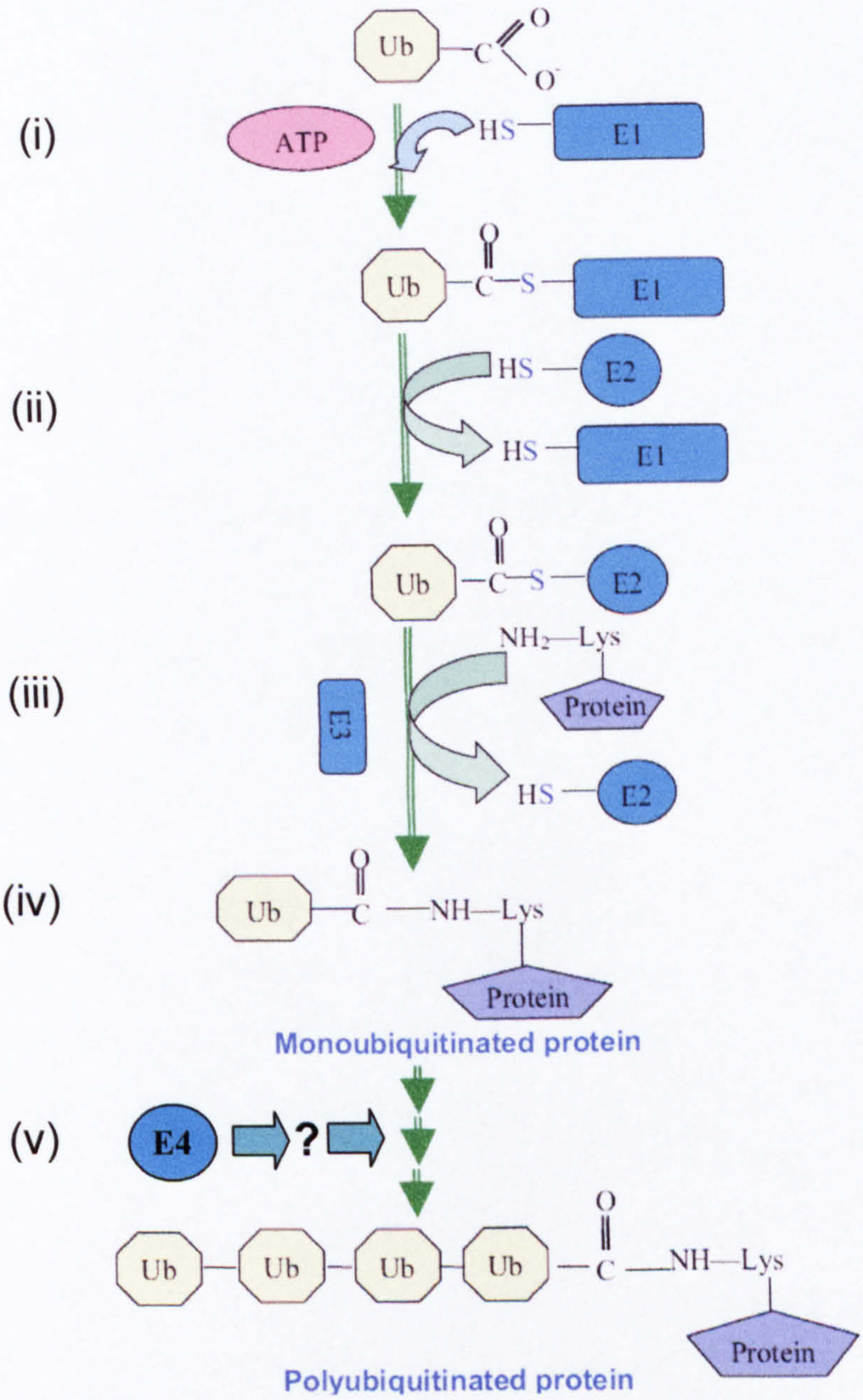

Figure 4.1 Ubiquitinylation of a substrate protein. Ubiquitin is activated by E1 in a reaction requiring ATP, forming a ubiquitin-E1 complex (i). The ubiquitin is transferred to a member of the E2 family (ii). The ubiquitin is then transferred from E2 to the substrate protein via a substrate-specific E3 ubiquitin-ligase (iii). The substrate is now mono-ubiquitinylated (iv). Possibly involving E4, repeated ubiquitinylation produces a poly-ubiquitinylated protein (v).

Although the ubiquitination of a protein is a progressive reaction that only requires E1, E2 and E3, the presence of an additional ubiquitin-conjugation protein called E4 has been described. E4 is thought to make the production of poly-ubiquitin chains more efficient by aiding the binding of one ubiquitin to another whilst the target protein remains bound to E3 (Kuhlbrodt *et al.*, 2005; Koegl *et al.*, 1999). E4 ubiquitin ligases have been found in yeasts, mammals, *Dictyostelium discoideum* and *C. elegans* (Hoppe, 2005). There is also a gene encoding a putative E4 enzyme in the *S. mansoni* genome (Smp138830).

Ubiquitin has seven lysine residues, all of which are potential conjugation sites, but most poly-ubiquitin chains are linked via lysine 48 or lysine 63 (Peng *et al.*, 2003). A chain of four or more ubiquitins (where the C-terminus of each ubiquitin is linked to lysine 48 of the preceding ubiquitin) is the destruction signal recognised by the 26S proteasome (Thrower *et al.*, 2000). By contrast, attaching a lysine-63-linked poly-ubiquitin chain to a substrate protein is associated with non-proteolytic mono- and multi-ubiquitination functions such as endocytosis, signal transduction, transcriptional regulation, ribosome function and DNA-repair pathways (Hicke, 2001).

Although poly-ubiquitination for proteasomal destruction is ubiquitin's most well-known role, it is becoming increasingly recognised that the mono- and multi-ubiquitination of proteins is commonplace, so ubiquitin can be described as a multi-functional protein. Ubiquitin's central structure, the "ubiquitin superfold" has also been found incorporated into much larger proteins (collectively called "ubiquitons"). Ubiquitons are less-well studied, but they include kinases and kinase-interacting proteins, so ubiquitons are likely to be involved in signal transduction (Nassar *et al.*, 1995; Cavanaugh, 2004; Hirano *et al.*, 2004). Ubiquitons have also been identified as transport proteins that bind to poly-ubiquitinylated proteins and transport them to the 26S proteasome for destruction (Hofmann & Bucher, 1996; Bertolaet *et al.*, 2001; Wilkinson *et al.*, 2001).

The process by which the target proteins are selected for ubiquitinylation in the first place involves molecular chaperones, but operates differently depending on whether the targets are cytosolic or in the secretory pathway. Overall, it has been estimated that 30% of new proteins are misfolded during their biogenesis, to be degraded by the UPP (Schubert *et al.*,

2000). For cytosolic proteins the chaperones are HSPs, principally HSP70 and HSP90. Inhibiting the UPP induces the up-regulation of HSPs (including HSP70), and HSP70 and HSP90 are required for proteasomal degradation of some substrates (Lee & Goldberg, 1998; Bercovich *et al.*, 1997; Doong *et al.*, 2003). A link between HSPs and the UPP has been demonstrated in that the co-chaperone CHIP (C-terminus of HSP70-interacting protein), which interacts with HSP70 and HSP90, is also a functional E3 ubiquitin ligase, which as discussed below is involved in attaching ubiquitin moieties to substrate proteins (McClellan & Frydman, 2001; Cyr *et al.*, 2002). By ubiquitinylating misfolded proteins that associate with HSPs, CHIP transfers them to the UPP (Connell *et al.*, 2001).

In the secretory pathway, folding efficiency is regulated in the lumen of the endoplasmic reticulum (ER). Misfolded proteins are recognised, unfolded and retro-translocated to the cytosol for ubiquitinylation and proteasomal destruction in a process known as "endoplasmic reticulum-associated degradation" or "ERAD". ERAD of glycoproteins is initiated when misfolded proteins are recognised by a combination of ER mannosidase I and a mannose-specific lectin called EDEM, or by BiP when the misfolded proteins are not glycosylated (Romisch, 2005; Molinari & Sitia, 2005). After recognition, the misfolded proteins are unfolded by members of the protein disulphide isomerase family (whether or not they contain disulphide bonds) and are then exported across the ER-membrane (Gillece *et al.*, 1999; Wang & Chang, 2003). It has been known for a long time that the unfolded proteins are retro-translocated from the ER through *sec61* (Wiertz *et al.*, 1996; Pilon *et al.*, 1997) but more recently another family of proteins called "derlins" have been described that can also form an export channel (Lilley & Ploegh, 2004; Ye *et al.*, 2004). The energy required for retro-translocation is provided by Cdc48p (p97 in mammals), which is a member of the AAA-ATPase family of chaperones (Romisch, 2005). The process of ubiquitinylation takes place in the cytosol, with the initial ubiquitin moiety being attached to the substrate whilst it is still associated with the ER membrane-pore (Shamu *et al.*, 2001; Jarosch *et al.*, 2002; Flierman *et al.*, 2003).

4.1.3 The Schistosome Proteasome

The UPP in schistosomes has not been intensively studied until recently. The earliest paper describes the cloning and sequencing of the *S. mansoni* 20S α5-subunit as part of a study

that identified antigenic proteins present in the supernatants of lung-stage worms cultured *in vitro* (Harrop *et al.*, 1999). A ubiquitin-binding subunit of the *S. mansoni* 19S regulatory complex has also been cloned and sequenced (Harrop *et al.*, 1999; Nabhan *et al.*, 2001). Guerra-Sa *et al.*, (2005) demonstrated that functional proteasomes are required for cercariae to successfully transform into lung-worms and also that 20S proteasomes in cercariae were less active than those of adults. Then, leading on from the Guerra-Sa *et al.* study, the 20S proteasome in *S. mansoni* was fully characterised (Castro-Borges *et al.*, 2007). In the Castro-Borges *et al.* paper, 20S proteasomes were purified from adult worms using a sequence of HPLC steps and then separated into their subunits using 2-DE. The subunits were identified using MALDI-MSMS. The fourteen 20S α- and β-subunits appeared as fifty-eight spots on the 2D gel (reproduced overleaf as Figure 4.2). A search of the *S. mansoni* genome assembly revealed that each 20S subunit was only encoded by a single gene, so the multiple spots of each subunit represented different post-translational modifications. Each subunit's spot-pattern was one where a single large, intensely-staining spot was in close proximity to several smaller spots that differed slightly in charge but not mass, suggesting that the post-translational modifications consisted of different degrees of phosphorylation. When 2D Western Blots of *S. mansoni* adult and cercarial preparations were probed with an antibody that recognises *S. mansoni* α3 and α6 subunits, Castro-Borges *et al.*,(2007) were able to show that the spot patterns were different, thereby demonstrating that life-cycle stage-specific differences in expression occurred.

4.1.4 Protein Turnover in the Developing Schistosome Egg

When released by the female schistosome, the immature egg consists of a fertilised ovum plus about thirty nutritive vitelline cells. As the egg matures, the vitelline cells decrease in volume as their contents are degraded and exported as raw materials for the developing ovum (see Chapter 1, Sections 1.2.1 and 1.2.2 for a detailed description of the egg-development process). As a large proportion of this traffic must consist of amino acids, it follows that a mechanism of regulated protein degradation must be of huge importance in the developing egg. Despite this, no work has been done to study the mechanisms by which the protein degradation might be occurring. What little is known about protein turnover in the development of invertebrate eggs results from studies that have used insect models and have focussed on gaining a better understanding of apoptosis and (occasionally) autophagy

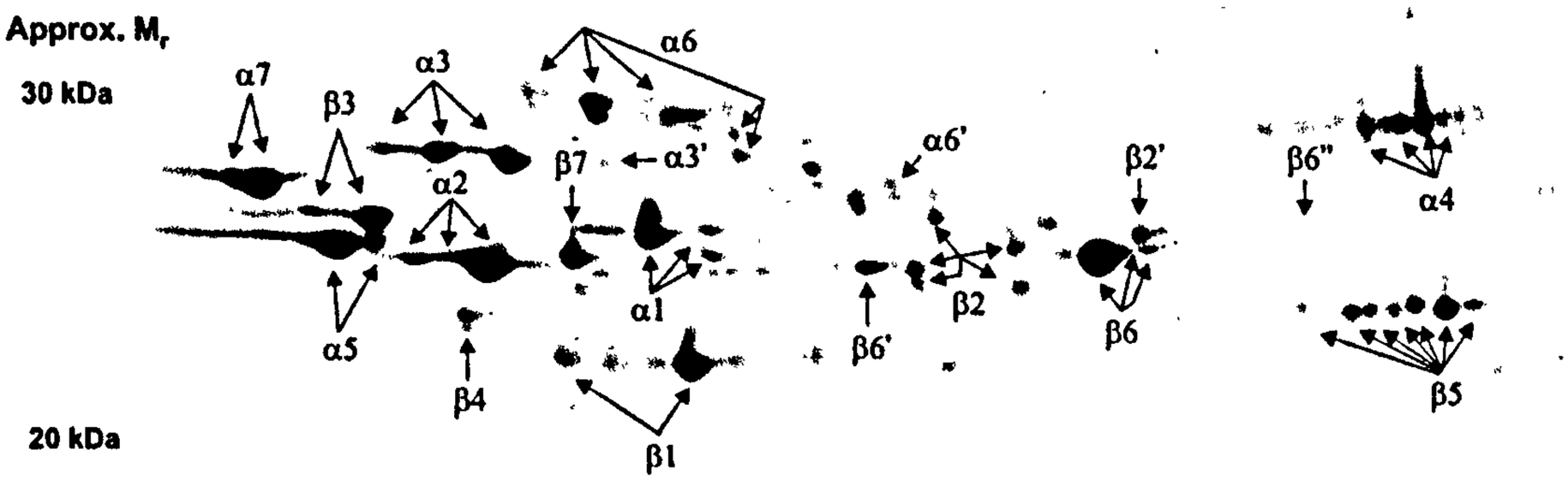

Figure 4.2 The 20S proteasome subunits in *S. mansoni* adults. 100μg of 20S proteasomes purified from adult worms, separated by 2-DE and stained with Sypro Ruby. The spots were excised from the gel, digested with trypsin and identified using MALDI-MSMS. The image is taken from Castro-Borges *et al.*, (2007), who also demonstrate that the mAb used in this thesis (which recognises the human 20S subunits α1, 2, 3, 5, 6 and 7) only binds to the 20S α3 and α6 subunits in *S. mansoni.*

(Baum *et al.*, 2005; McCall, 2004; Mpakou *et al.*, 2006). As such, these studies do not even address the question as to whether the UPP is involved in oocyte development.

In insects, eggs develop in an egg chamber, made up of the ovum and some nutritive nurse cells which is surrounded by a layer of somatic epithelial cells called "follicle cells". The egg chamber moves through the ovariole as it develops, from previtellogenesis, through vitellogenesis (yolk uptake) and choriogenesis (eggshell formation). The nurse cells play a similar nutritive role as vitelline cells in the schistosome egg and degenerate as the oocyte develops (Mahajan-Miklos & Cooley, 1994). The most detailed studies, involving *Drosophila,* show that cytoplasm is transferred from the nurse cells to the developing oocyte, after which DNA fragmentation begins in the nurse cells, they undergo apoptosis and their remnants are phagocytosed by the somatic follicle cells (Foley & Cooley, 1998; Nezis *et al.*, 2000). Although these studies demonstrate that apoptosis is utilized in the final *coup de gras* of the nurse cells, they fall short of establishing the extent to which the UPP is involved in the earlier proteolytic degradation of the nurse cell's contents. Thus, the UPP could be a central part of the process by which nurse cell intracellular proteins are degraded. There is of course a fundamental difference between the situation in the schistosome egg and that in the insect egg in that the vitelline cells of the schistosome egg are not surrounded by follicular cells with a phagocytic capability. As neither the developing miracidium nor the envelope have been demonstrated to undertake phagocytosis, it is unlikely that apoptosis has evolved to become the principal mechanism by which vitelline cells degrade.

4.1.5 Experimental Aims and Objectives

The work in this chapter follows on from the Guerra-Sa *et al.*, (2005) and Castro-Borges *et al.*, (2007) papers and also links to the previous work in this thesis by studying the UPP in the *S. mansoni* egg. The extent to which 20S α-subunit expression changes as the egg develops is assessed by comparing 2D Western Blots of the female vitellaria-enriched preparation (representing the egg's vitelline cells), immature SEA (representing eggs at an intermediate stage of development) and mature SEA. *In vitro* assays using a fluorogenic substrate are then used to establish whether α-subunit expression changes seen by blotting can be linked to the proteolytic activity of the proteasome. Western Blotting is also used to

compare the expression patterns of the 20S α-subunits of the mature egg's components (ESP, miracidium and hatch fluid) to gain insights into how the UPP might be used by the egg to pass through the gut wall to emerge into the gut lumen. The pattern of ubiquitinylated proteins in each of the egg preparations is also visualised using blots and linked where possible to the information obtained with regard to proteasomal expression and activity.

4.2 Methods

The methods that were used to obtain the biological material have already been described in the following sections of Chapter 2: obtaining *S. mansoni* eggs (Section 2.2.1), making soluble protein preparations (Sections 2.2.2 – 2.2.6) and determining protein concentrations (Section 2.2.7).

4.2.1 Detecting Proteasome α-Subunits and Ubiquitinylated Proteins by Western Blotting

35µg of female vitellaria-enriched preparation, immature SEA, mature SEA, miracidial preparation and hatch fluid were separated by 2-DE as described in Chapter 2, Section 2.2.9.2. Immediately following the PAGE, each gel was removed from its plastic case, separated from its IEF strip and placed on 8.3cm x 7.3cm Invitrolon 0.2µm polyvinylidenefluoride (PVDF) membrane (Invitrogen) that had been equilibrated in NuPAGE Transfer Buffer (Invitrogen). The gel/membrane was sandwiched firstly between the membrane's filter papers and then between fibre pads before being installed into an XCell II Blot Module (Invitrogen). The blot module was filled with transfer buffer and the proteins transferred from the gel to the membrane by applying a constant current of 30V for 75 mins. Successful protein-transfer was confirmed by staining the membrane with Sypro Ruby protein blot stain (Invitrogen) as per the manufacturer's instructions and imaging it using a Versa Doc (Bio-Rad). The blot was washed, incubated overnight in blocking solution (100mM NaCl/50mM Tris HCl pH7.5 plus 5% milk powder and 0.05% Tween 20) and then probed with mouse anti-human 20S proteasome IgG, specific for human subunits α1, 2, 3, 5, 6 and 7 (Biomol PW8195), but which only recognises α3 and α6 subunits in *S. mansoni* (Castro-Borges *et al.*, 2007). The antibody was diluted 1:4000 in blocking solution. Probing was carried out over 3 hours on a rocking agitator set at a slow speed, after which the unbound antibody was removed by washing the blot three times in 200ml of 10mM Tris pH7.5. The blot was then incubated for 90 mins in goat anti-mouse IgG peroxidase conjugate (Sigma A8924) that had been diluted 1:4000 in blocking solution. The image was visualised using the "Enhanced Chemiluminescent" ECL Plus Western Blotting Detection System with Hyperfilm ECL paper (both Amersham) processed in an Compact X4 automatic film processor (Xograph). Each blot was then washed three times in

300ml ddH_2O, incubated for 20 mins in Restore Western Blot Stripping Buffer (Pierce), washed again (three times in 10mM Tris HCl pH7.5) and blocked overnight with blocking solution. The blots were then probed for a second time using the same protocol used for the proteasome immunodetection, but with a 1:1000 dilution of rabbit anti-ubiquitin IgG (Sigma U5379), which recognises mono-, multi- and poly-ubiquitinylated proteins. The detection antibody was goat anti-rabbit IgG alkaline phosphatase conjugate, diluted 1:500 in blocking solution. The image was detected using the chromogenic substrate 5-Bromo-4-Chloro-3-Indolyl phosphate/Nitro Blue Tetrazolium (Sigma).

4.2.2 Probing ESP for Poly-Ubiquitin

15µg of ESP, mature SEA and cercarial secreted protein (a gift from Dr. Rachel Curwen) were reduced and then separated by 1-DE as described in Chapter 2, Section 2.2.8.2. The proteins were then blotted onto a PVDF membrane, stained with Sypro Ruby, blocked and probed for poly-ubiquitin using the protocol described in Section 4.2.1. Probing was carried out using a 1:4000 dilution of mouse anti-poly-ubiquitin IgM (Biomol PW8805) which was detected by a 1:10000 dilution of goat anti-mouse IgM peroxidase conjugate (Sigma A8786). The poly-ubiquitin image was visualised using the ECL procedure, after which the blot was stripped and re-probed for all forms of ubiquitin as described in Section 4.2.1.

4.2.3 Measuring Proteasomal Activity in Immature and Mature SEA

Approximately 3 million eggs were extracted from the livers of seven-week infected mice then separated into mature and immature fractions as described in Chapter 2, Sections 2.2.1 and 2.2.2. The immature and mature egg fractions was then ground for three minutes in 200µl of 40mM Tris HCl pH7.5 plus 5% glycerol and 1mM DTT using a polypropylene pestle (Sigma) attached to Kontes motor (Fisher). The grinding took place on ice, in three cycles consisting of a minute's grinding followed by a minute's rest. Protein concentrations were assayed using the Coomassie Plus Protein Assay (Pierce) and then adjusted to 350µg/ml with the same 40mM Tris/glycerol/DTT buffer used to make the SEA. Chymotrypsin-like activity was measured by incubating 75µg of immature and mature SEA at 37°C for 1 hour in a 96-well microtitre plate (Nunc), with 25µM of the fluorogenic substrate *N*-Succinyl-Leu-Leu-Val-Tyr-7-amino-4-methylcoumarin (Biomol P802) plus 5mM $MgCl_2$ (making a total volume of 240µl per well). In order to distinguish between 20S

proteasomal activity and non-proteasomal chymotypsin-like activity, the assay was carried out in the presence and absence of 0.02% SDS (see the following paragraph for the rationale). After incubation, the reactions were stopped with 240µl/well of 1% SDS and the fluorescence measured on a Polarstar Optima plate reader (BMG Labtech) set at 320nm excitation and 460nm emission wavelengths. The fluorescence of the blank was deducted from the fluorescence of each assay and the results expressed as means (+/- standard error of the mean) of duplicated assays.

The SDS is important in this assay because it enables the non-proteasomal, chymotryptic enzymes to be controlled for. In the SDS $^{-}$ve assays, no proteasomal degradation of the substrate occurs because the substrate is not ubiquitinylated and the 20S proteasomes are capped by the 19S regulatory subunits. So, all the substrate degradation is caused by non-proteasomal chymotryptic proteases. In the SDS^{+}ve assays however, proteasomal degradation of the substrate does occur. Although it is not known how the SDS operates, it is likely that it causes the 19S regulatory subunits to disassociate from the 20S proteasome core, enabling the 20S proteasomes to degrade the substrate; and as the concentration of SDS is low, the 20S proteasomes remain intact and functional (Tanaka *et al.*, 1989; Stein *et al.*, 1996). So, the fluorescence in the SDS $^{-}$ve assays represents the activity of the non-proteasomal chymotryptic proteases only, and the fluorescence in the SDS $^{+}$ve assays represents the activity of all the chymotryptic-like enzymes, including the 20S proteasome. Therefore, it is the difference between the fluorescence in the SDS $^{-}$ve assays and that in the SDS $^{+}$ve assays which represents the activity of the 20S proteasome.

4.3 Results

4.3.1 Western Blots of Proteasomal α-Subunits in the Developing Egg

Proteasomal 20S α-subunits were found in all of the egg preparations except ESP, but the spot-pattern on each blot was different. The ECL image of the female vitellaria-enriched preparation blot (representing the vitelline cells) contained seven spots, comprising five 20S proteasome α6 and two α3 isoforms, two of the former being much fainter spots. This spot pattern was distinctive, so shared spots could be matched exactly when the ECL images from the immature and mature SEA blots were superimposed onto that of the female vitellaria-enriched preparation. This spot-matching exercise enabled changes in expression of the individual isoforms to be linked to egg maturation (Figure 4.3). In the immature SEA blot all the spots had diminished in both size and intensity except that of the most acidic α3 isoform, which was now the largest spot by far. The more acidic of the two small, faint α6 isoform spots in the female vitellaria-enriched preparation had disappeared in the immature SEA blot. Spots continued to diminish in number between the immature and mature SEA blot images such that only a single α3 isoform and a single α6 isoform were visible in the latter. Although the α6 spot had diminished in size, the α3 spot had not and remained the same size as it was in the female vitellaria-enriched preparation blot.

4.3.2 *In Vitro* Assessment of the Proteasomal Activity in Immature and Mature SEA

As the immature SEA blot contained more proteasomal α-subunit isoforms than the mature SEA blot, an assay was carried out in which the levels of chymotrypsin-like activity in immature and mature SEA were compared, using a fluorogenic substrate in the presence and absence of 0.02% SDS. As shown in Figure 4.3D, the amount of fluorescence in the SDS $^{-}$ve assays was 6% higher in mature SEA compared to immature SEA (36013 vs. 33998 fluorescence units), demonstrating that non-proteasomal chymotryptic proteases are slightly enriched for in mature SEA. In the SDS $^{+}$ve assays the fluorescence increased by 12.5% in mature SEA (from 36,013 to 40,535 units), which is only a fifth of the 66% increase (from 33998 to 56446 units) that SDS induced in the immature SEA assays. It can therefore be seen that immature SEA has five times more 20S proteasomal activity than mature SEA.

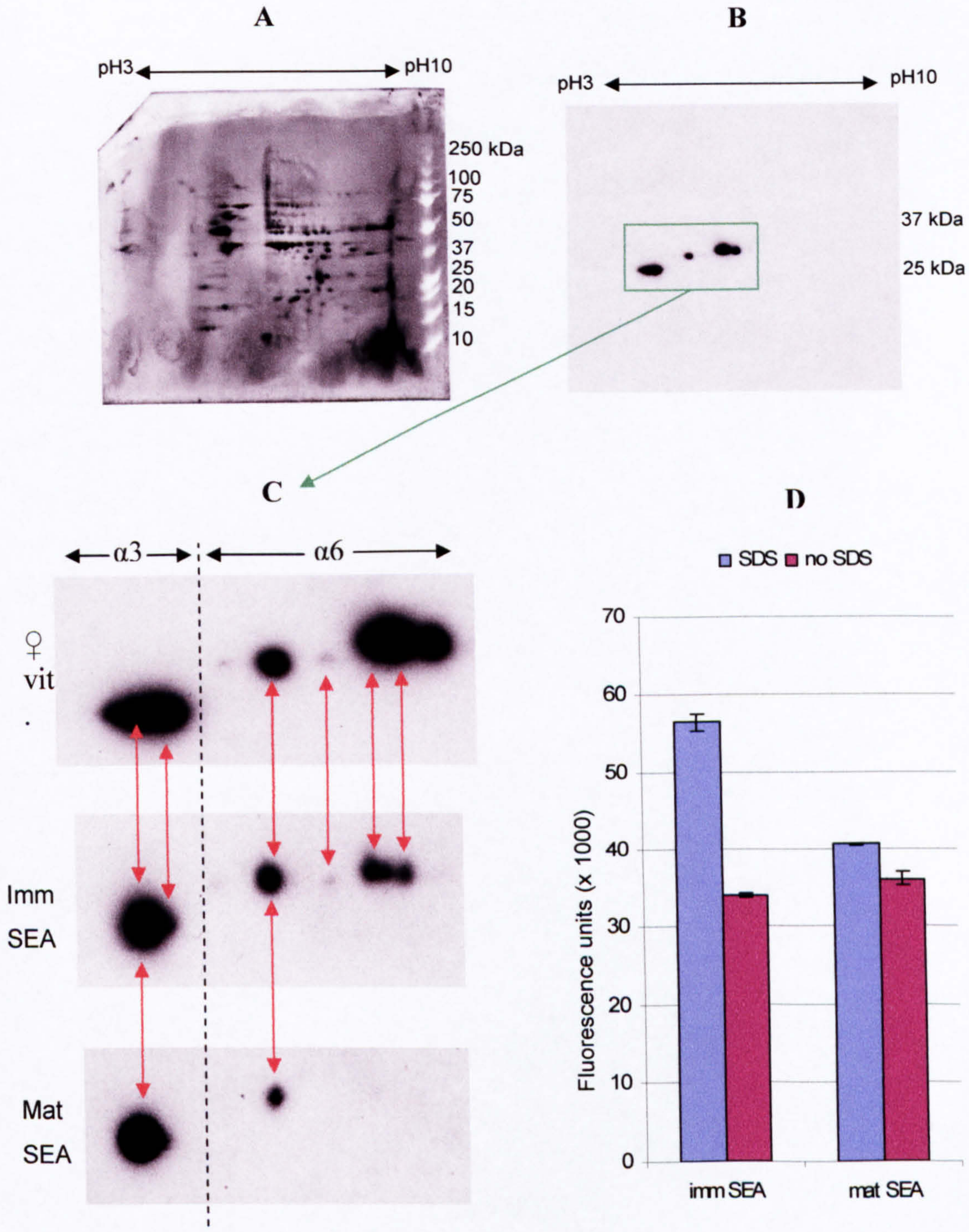

Figure 4.3. The 20S proteasome in the developing egg. **A:** Blot of 35µg of female, vitellaria-enriched preparation, stained with Sypro Ruby protein stain. **B** ECM of the blot from A, probed with an antibody that recognises α3 and α6 subunits of the 20S proteasome. **C:** Enlarged section of the blot from B, compared with similar blots of immature and mature SEA. Matching subunits are linked by red arrows. The α3 and α6 group of isoforms could be distinguished because of their different molecular weights and *pI*. **D:** Chymotrypsin-like activity in immature SEA compared with that in mature SEA. Regulatory subunits prevent proteasomal-degradation of the substrate in the SDS $^{-}$ve assays, but these are thought to disassociate in the SDS $^{+}$ve assays, enabling 20S proteasomal degradation of the substrate to occur. Therefore, the 20S proteasomal activity is represented by the difference between the fluorescence in the SDS $^{+}$ve and SDS $^{-}$ve assays.

4.3.3 Western Blots of Proteasomal α-Subunits in Hatch Fluid and the Miracidium

Hatch fluid and the miracidium are components of the fully-developed egg. By comparing the spot-patterns on the hatch fluid and miracidial blots with each other and with the mature SEA blot it was possible to see which preparation was enriched with 20S α3 and α6 subunit isoforms (Figure 4.4). The hatch fluid's spot-pattern was completely different to that of any of the other blots, with three horizontal rows of spots containing sixteen spots, ten of which (including the largest 50kDa spots) were not present in any of the other preparations. An identical spot pattern occurred when the 2D hatch fluid blot was repeated, but in an earlier 1D hatch fluid blot the antibody only recognised bands at 25kDa and 30kDa (results not shown). The miracidial blot contained six visible spots, all of which could be matched to hatch fluid spots and three of which could be matched to the spots on the mature SEA blot. Five out of the six miracidial spots also matched to spots on the female vitellaria-enriched preparation blot.

4.3.4 Western Blots of Ubiquitinylated Proteins

As there was a considerable variation in the expression of proteasome α-subunits between the various egg preparations, the blots were stripped and re-probed with an anti-ubiquitin mAb that recognises mono-, multi- and poly-ubiquitinylation (Figure 4.5). The ubiquitin blots demonstrated that ubiquitinylated proteins were abundant in all of the preparations, with many spot patterns being distinctive and present in more than one preparation. For example, the 15kDa slightly acidic proteins (annotated as "A" in Figure 4.5) were in all of the preparations except ESP, and the series of spots "B" were present in all of the blots except that of the miracidial preparation. The very acidic protein of 50-100kDa "C" was the most heavily staining protein on the blots and was highly ubiquitinylated in both the immature and the mature egg, where it can be assigned to ESP and hatch fluid, but not the miracidium. It also appeared in the female, vitellaria-enriched preparation but it was not heavily ubiquitinylated. The location, size, shape and pattern of expression of the spot was similar to that of Smp170410, the most abundant hatch fluid protein (of unknown function) described in Chapter 2 (Section 2.4.8) and annotated as Spot 519 in the 2D hatch fluid gel (Figure 2.6, page 77).

Original in colour

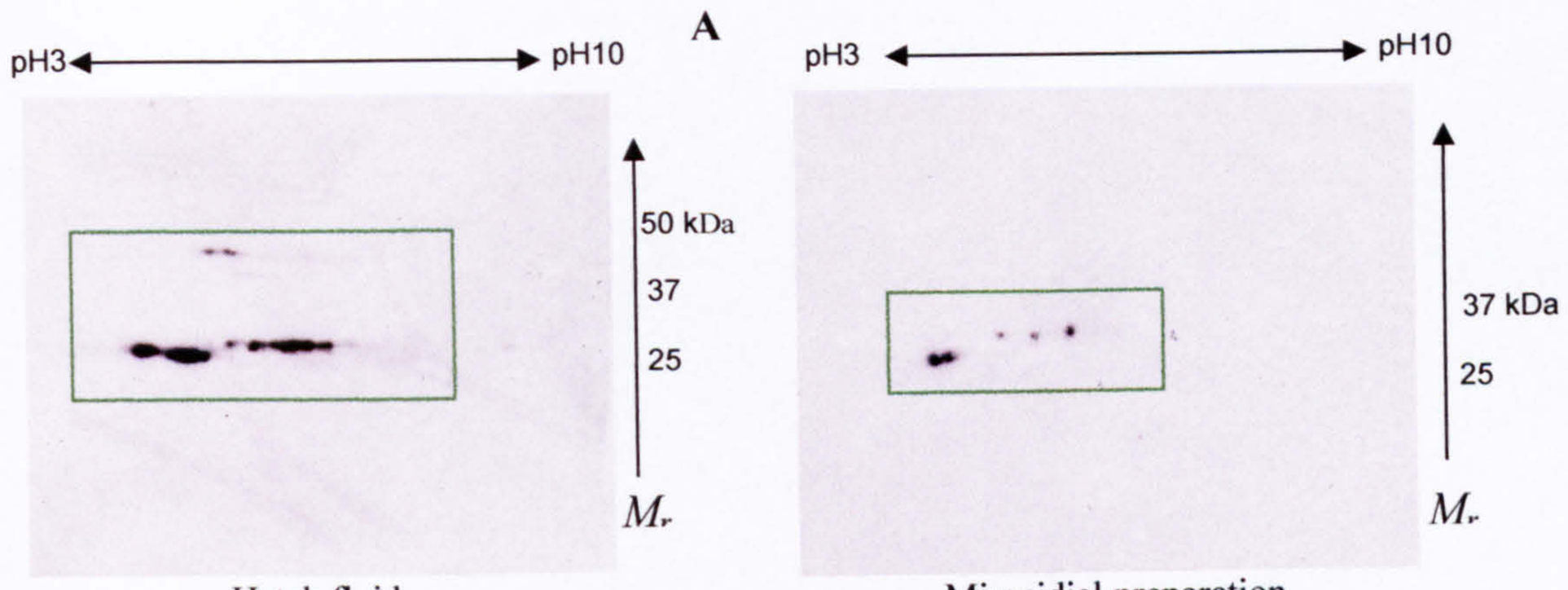

Figure 4.4. Proteasome 20S α-subunit isoform expression in the mature egg. **A:** Blots of the hatch fluid and miracidial preparations were probed with anti 20S proteasome α3 and α6-subunit mAb and imaged using ECL reagents. The areas inside the green boxes are enlarged in B. **B:** The proteasome α-subunit-containing sections of A with shared subunit isoforms shown in pink arrows. For comparison, the mature SEA blot from Figure 4.3C is also shown. **C:** A similar comparison, but between the miracidial and female, vitellaria-enriched blots.

Original in colour

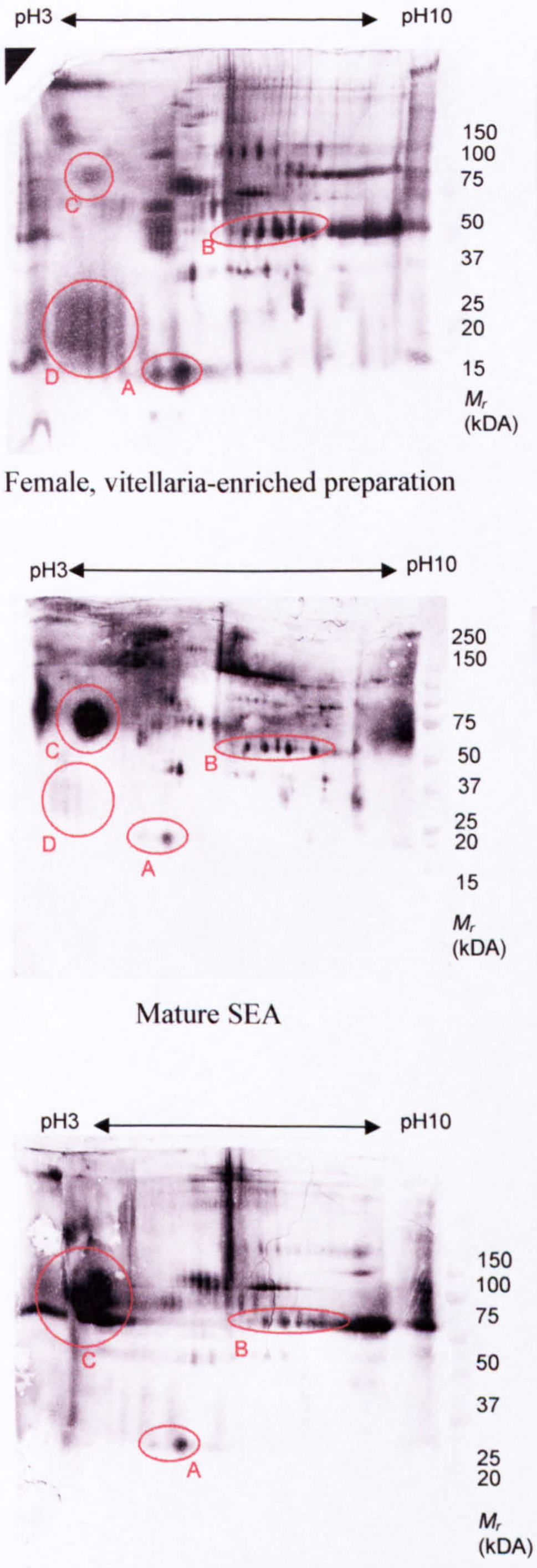

Female, vitellaria-enriched preparation

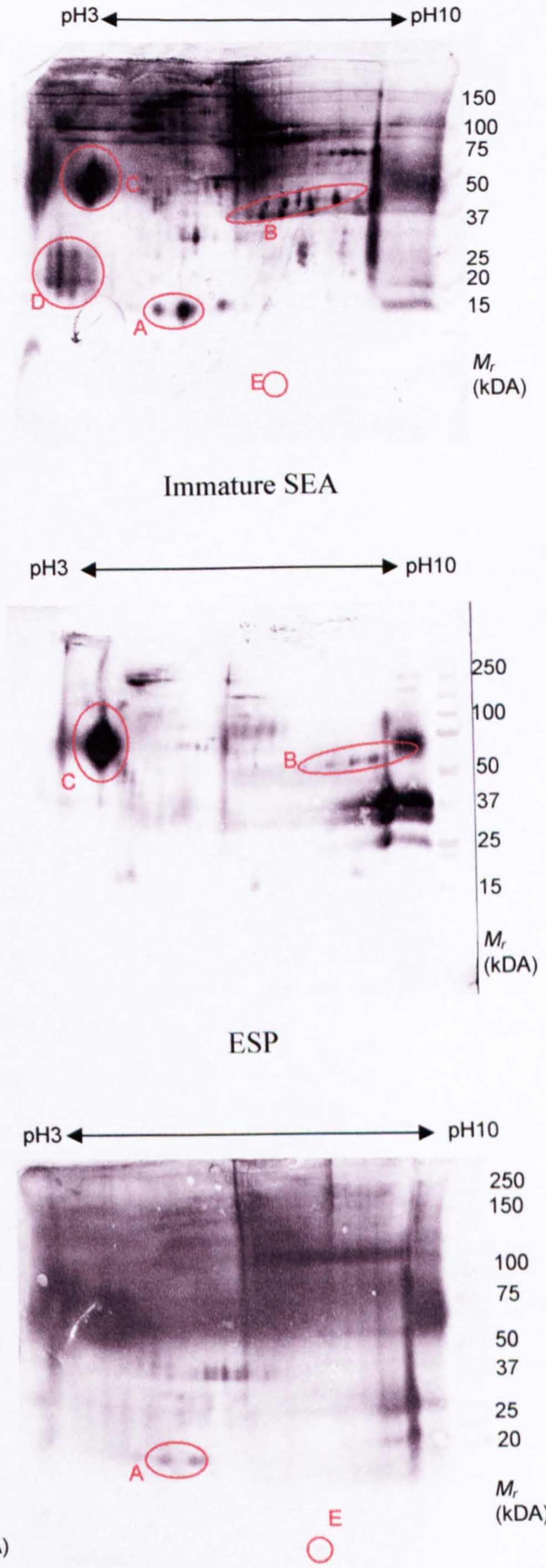

Immature SEA

Mature SEA

ESP

Hatch fluid

Miracidial preparation

Figure 4.5 Ubiquitinylated proteins in the egg. 2D blots of 35µg of protein from each egg preparation were probed with an anti-ubiquitin mAb that recognises mono-, multi- and poly-ubiquitinylated proteins. The blots were imaged using alkaline phosphatase reagents. The spots annotated A-F are discussed in the text.

Some ubiquitinylated proteins were very abundant in the female, vitellaria-enriched preparation and immature SEA but declined in abundance as the egg matured (e.g. the spots annotated as "D" in Fig. 4.5). Free ubiquitin (i.e. unbound ubiquitin) could be seen in the blots of immature SEA and the miracidial preparation ("E" in Fig. 4.5).

4.3.5 Ubiquitinylation of ESP

It was surprising to find large numbers of ubiquitinylated proteins in ESP because the UPP operates in the cytosol. In order to rule out leakage from dead eggs as the source of the ubiquitinylated proteins in ESP a comparison was made between ubiquitin blots of ESP and mature SEA (Figure 4.6A). As the banding patterns in the mature SEA and ESP blots differed, the ubiquitinylated proteins in ESP cannot be sourced to ruptured eggs in culture. When a 2D blot of ESP was probed with the same anti-ubiquitin mAb used in Section 4.3.4 (i.e. one that recognises all forms of ubiquitinylation) and then compared to a 2D protein gel it could be seen that many of the previously described ESPs were ubiquitinylated (Figure 4.6B). There were differences in the relative staining intensities of spots on the gel compared with those on the blot so there was no obvious relationship between the levels of protein expression and ubiquitinylation. For example, the most heavily ubiquitinylated spot in ESP was the very acidic protein of 50-100kDa (probably Smp170410), which was only just detectible in the protein gel, whereas ESP13 stained heavily in the protein gel but was difficult to detect in the blot. Another series of spots of *pI* 4-5 and of approx 250kDa were also heavily ubiquitinylated but failed to stain visibly for protein.

As the anti-ubiquitin antibody used in the previous experiments cannot distinguish between mono-, multi- and poly-ubiquitinylated proteins, 10µg of ESP was separated by 1-DE (with mature SEA and cercarial secreted protein for comparison), blotted, probed with anti-poly-ubiquitin IgM, stripped and then re-blotted with the anti ubiquitin IgG used previously (Figure 4.6C). The anti-poly-ubiquitin IgM only binds to poly-ubiquitinylated proteins and does not recognise either mono- or multi-ubiquitinylated proteins. Consequently, the nature of the ubiquitinylation was established by using the antibodies in concert. Apart from faint bands at approx. 22kDa in ESP and 15kDa in the cercarial secretion preparation (boxed in pink in Fig. 4.6B), no proteins in the secretory preparations were poly-ubiquitinylated.

Original in colour

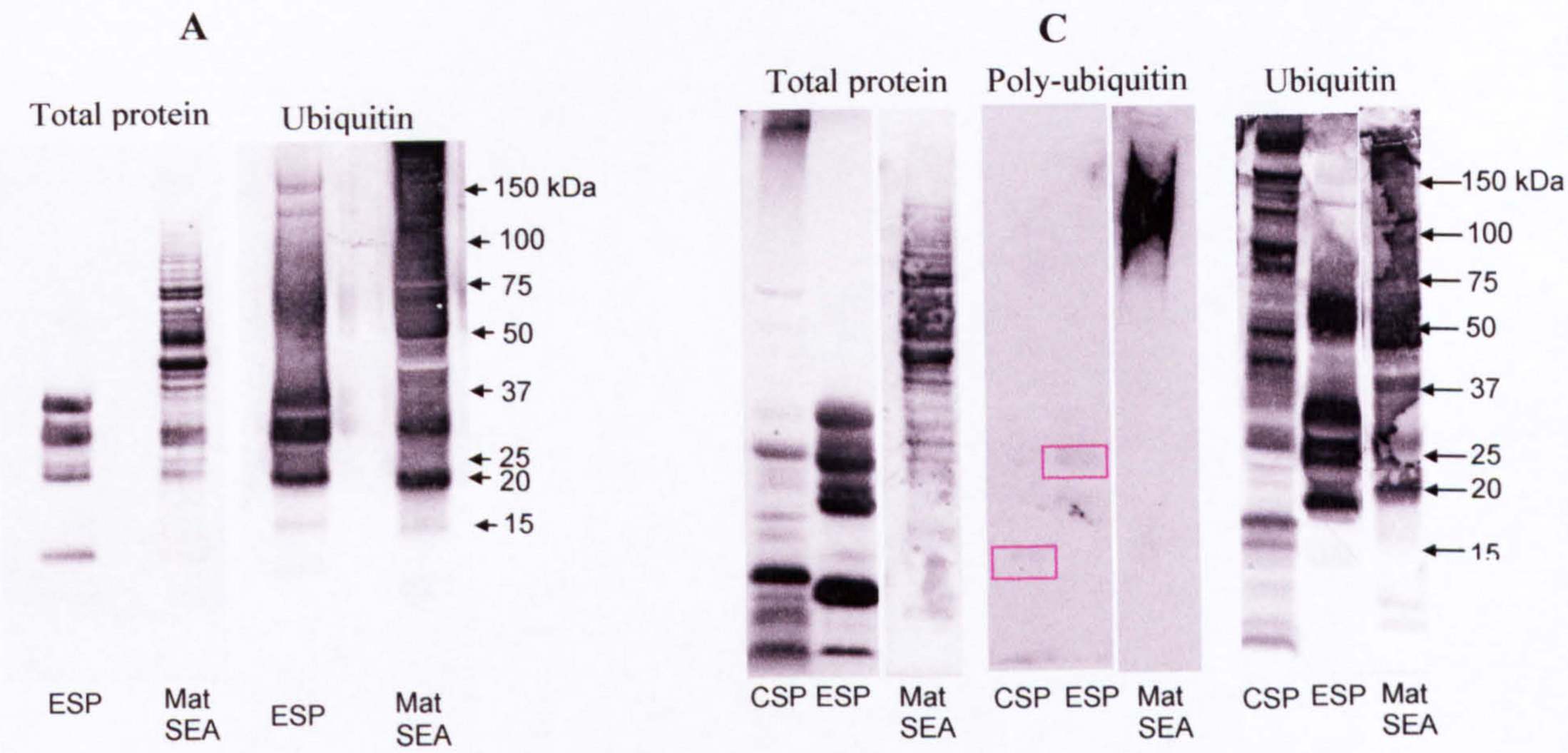

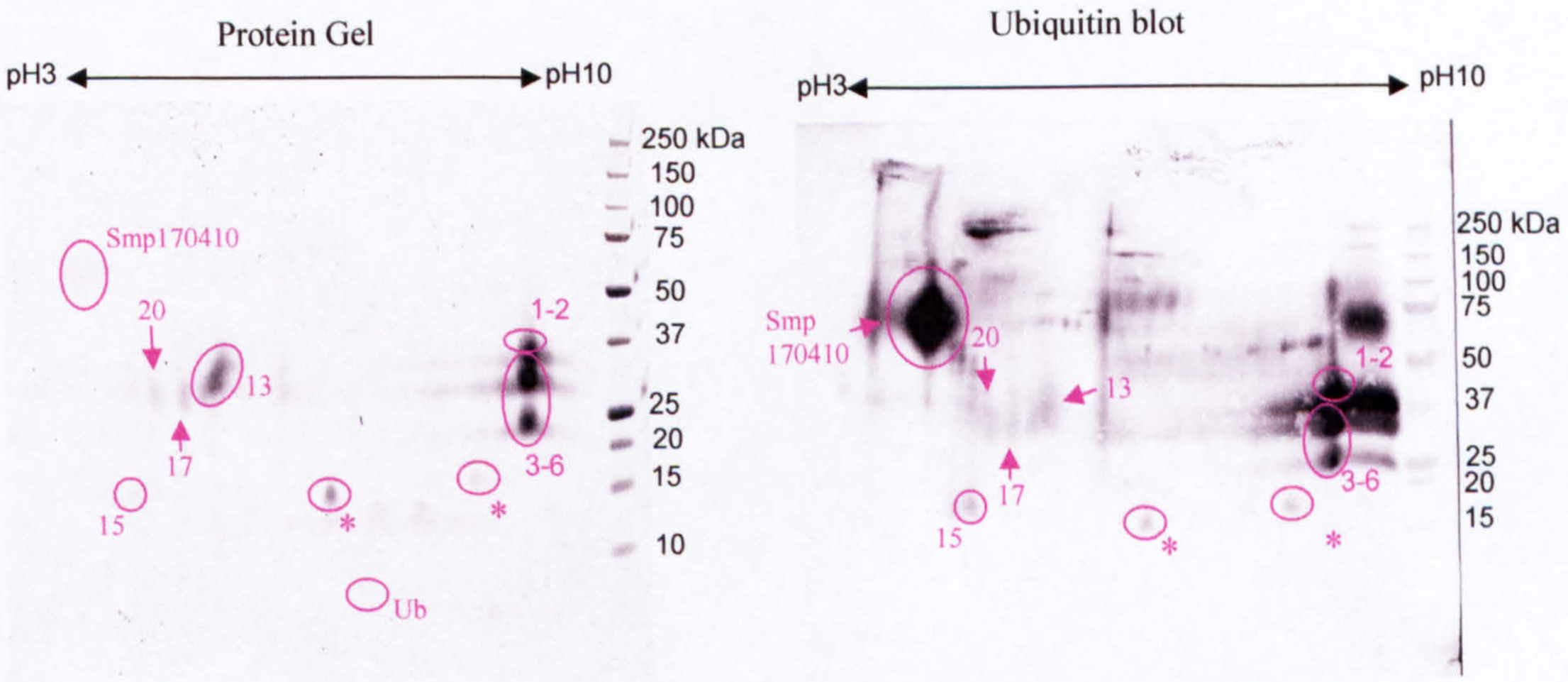

Figure 4.6 Ubiquitinylation of ESP. **A:** ESP has a different ubiquitinylation pattern compared with mature SEA. **B:** Ubiquitinylated proteins in ESP include Smp170410, ESP1-2, ESP3-6, ESP13, ESP15, ESP17, ESP20 (annotated in pink) plus two of the new ESPs described in Chapter 2 (annotated as *). Unbound ubiquitin is annotated as Ub
C: Cercarial secreted proteins (CSP), ESP and mature SEA blotted for poly-ubiquitinylated proteins only. Proteins at 22kDa in ESP, 10kDa (CSP) and a smear of mature SEA proteins at >75kDa were poly-ubiquitinylated.

The mature SEA blot reacted positively to the poly-ubiquitin antibody, producing a smear of proteins of >75kDa. It was not possible to assign identities to the poly-ubiquitinylated proteins because it is not known how many ubiquitins were attached to each substrate, and therefore the substrate's molecular weight cannot be established. The band at 15kDa in the cercarial secretion preparation has a molecular weight consistent with ubiquitin dimers that were not attached to substrate proteins. The smear at >75kDa in the mature SEA blot demonstrates that it contains numerous poly-ubiquitinylated proteins. As the molecular weight of ubiquitin is 8.5kDa, a poly-ubiquitin chain of four ubiquitins adds 35kDa to the substrate's molecular weight. As the smear of proteins started at 75kDa, it can be estimated that most of the poly-ubiquitinylated substrates were >40kDa in size, which is consistent with the banding pattern in the protein stain. After the blot had been probed for poly-ubiquitinylated proteins the membrane was stripped, re-probed with the anti-mono-, multi- and poly-ubiquitin IgG used in the previous experiments, and the same spot pattern seen previously in Fig 4.6A re-emerged. Therefore, the negative result from the poly-ubiquitin blot of ESP cannot be attributed to poor protein transfer from the gel to the membrane. A 2D gel of 35µg ESP was subsequently blotted and probed with the anti-poly-ubiquitin antibody but on this occasion there was no reactivity at all (result not shown). It is therefore probable that the 22kDa band seen in the poly-ubiquitin blot of ESP in Figure 4.6C could be an artefact.

An attempt was made to assess the extent of ubiquitination in ESP using LC-MALDI-MS and MSMS. 7.5µg of crude ESP was digested with trypsin, desalted, separated with a monolith reverse phase column and eluted onto a MALDI plate over 180 spots, each of which was firstly analysed by MALDI-MS. The MS spectra from all of the spots were then manually searched for peaks that had m/z ratios (with a tolerance of +/- 0.2Da) that corresponded with those expected from a tryptic digest of ubiquitin (as calculated by the ProteinProspector v. 4.0.8 program). Then, by comparing the strength of the signals generated from ubiquitin peptides with the strength of signals from ESP peptides an estimation of the relative abundance of ubiquitin compared with each ESP was made. Although a tryptic digest of ubiquitin could theoretically generate 29 peptides of > 800Da in mass (allowing for ≤2 missed cleavages) only one peptide was found. The peptide had a MS peak of 1787.9 Da, equating to the sequence TITLEVEPSDTIENVK (which

ProteinProspector calculates to have a mass of 1787.93Da). This peptide appeared in a total of 17 spots, the most intense signal of which was in Spot 140, generating a signal-to-noise ratio of 16.2 (Figure 4.7A). The peak at 1787.9Da could be seen in the MS spectrum of Spot 140 (Figure 4.7B), with a slightly more intense peak 1Da larger and a third, less intense peak which was 2Da larger. The sum of all three peaks represents the signal from the ubiquitin peptide, with the different masses representing peptides containing zero, one or two C^{14} atoms respectively. An attempt was made to subject the peptide to MSMS but it was too low in abundance to fragment sufficiently well. By way of comparison, a tryptic peptide of 1276.6Da from ESP3-6 was much more abundant. It was eluted over 43 spots (so was more dilute compared with the ubiquitin peptide) yet it achieved a maximum signal-to-noise ratio of 960, which was more than sixty times higher than the ubiquitin peak (Figure 4.8A). This more intense signal means that the MS spectrum from the most intense spot (Spot 120) was much clearer than that seen in the ubiquitin peptide with no background noise evident (Figure 4.8B). The much greater abundance of the ESP3-6 peptide is also demonstrated because there are discernable variants of the peptide containing up to four C^{14} atoms.

Original in colour

A

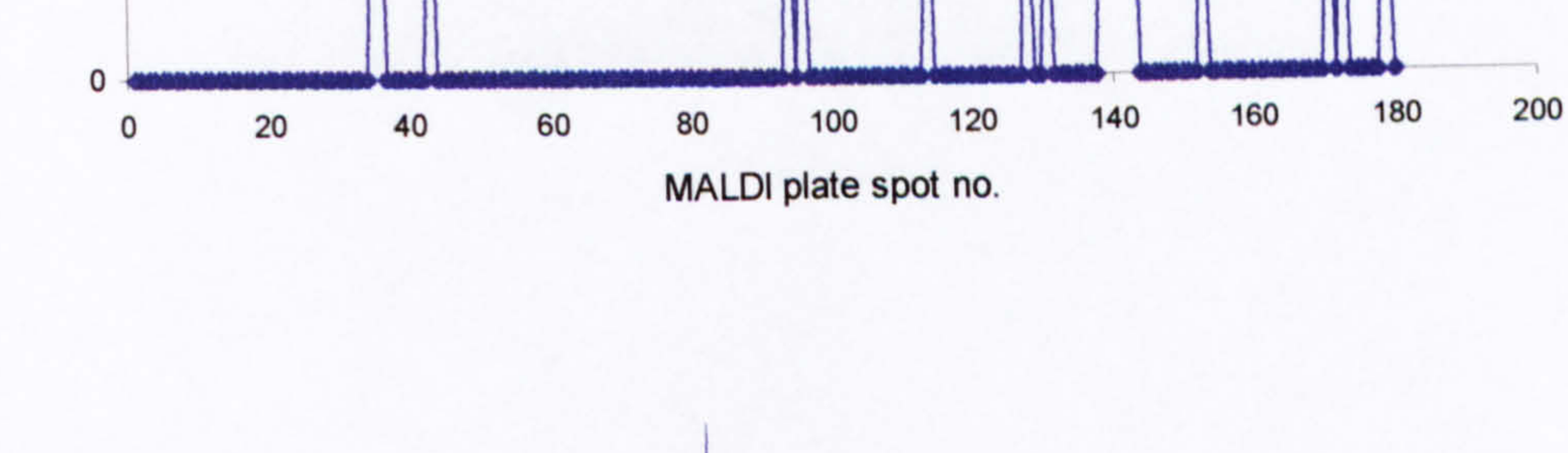

B

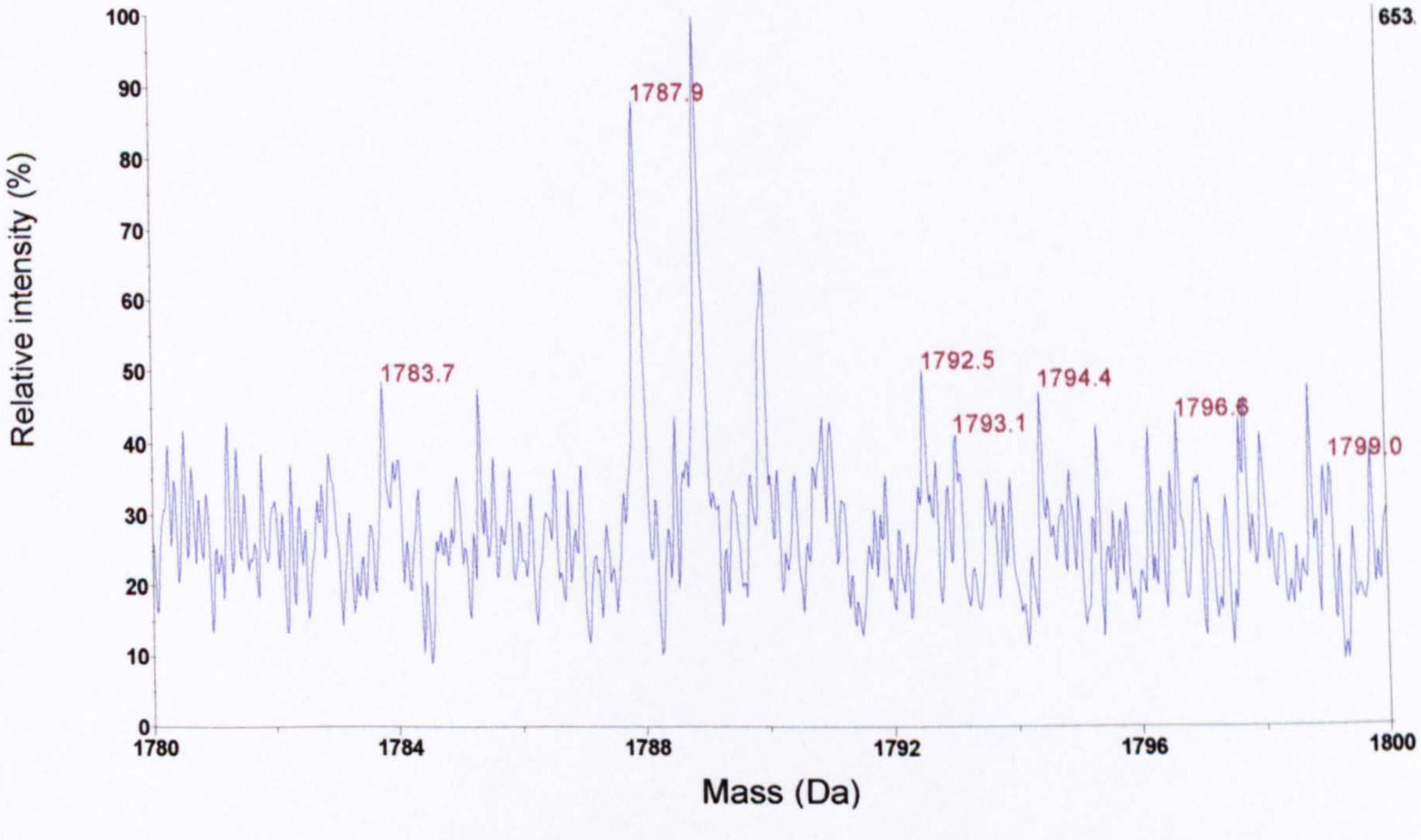

Figure 4.7 Identification of a ubiquitin peptide in ESP by LC-MALDI-MS. **A:** The elution pattern of ubiquitin peptides of 1787.9Da. The strongest signal was found in Spot 140 on the MALDI plate, generating a signal-to-noise ratio of 16.2. **B:** The 1780-1800Da region of the MS spectrum of Spot 140 showed the 1787.9Da ubiquitin peptide plus its other isoforms that were either 1 or 2Da larger, depending upon whether they contained one or two C^{14} atoms. The small quantity of protein means that the signal/noise ratio is low.

A

Original in colour

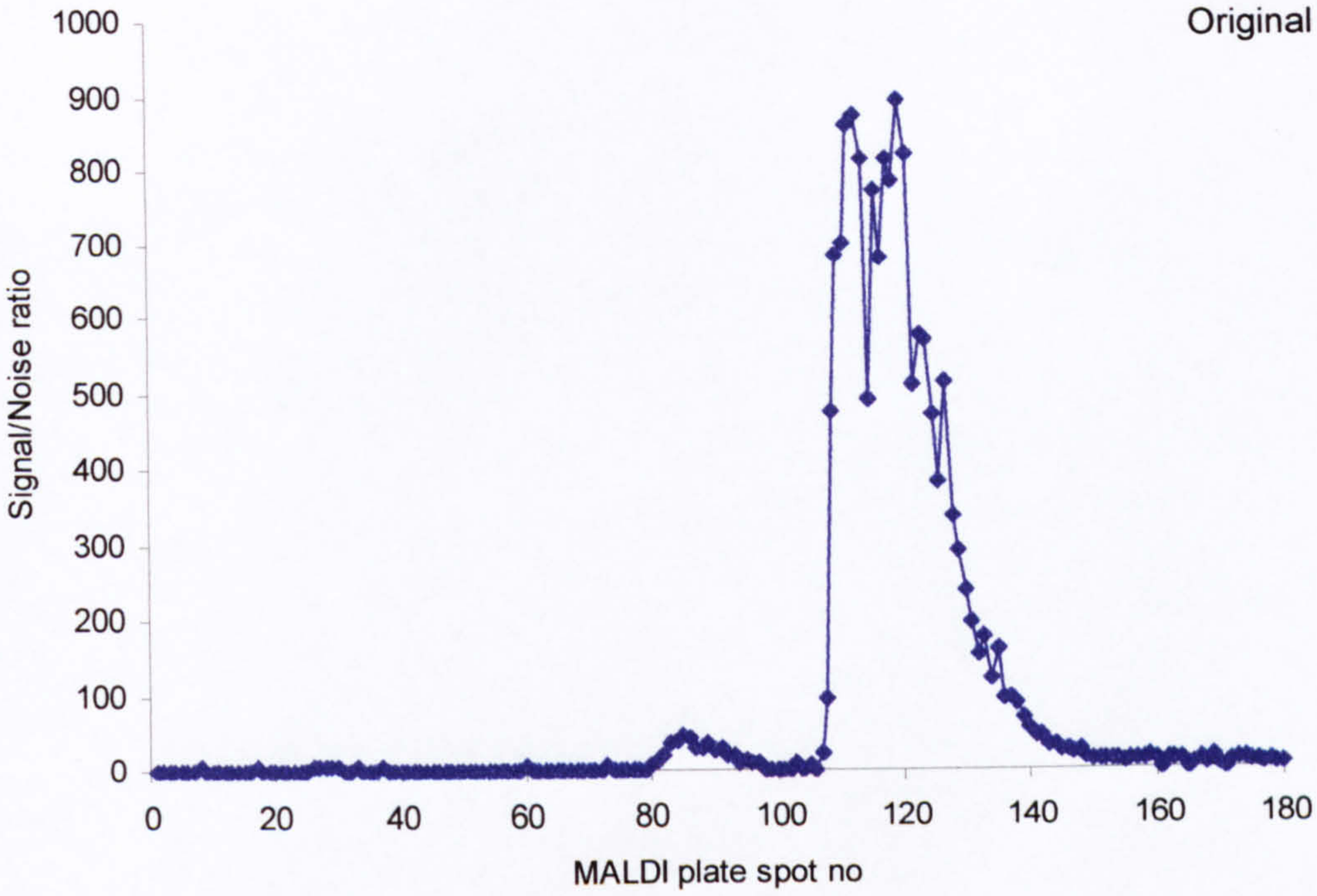

B

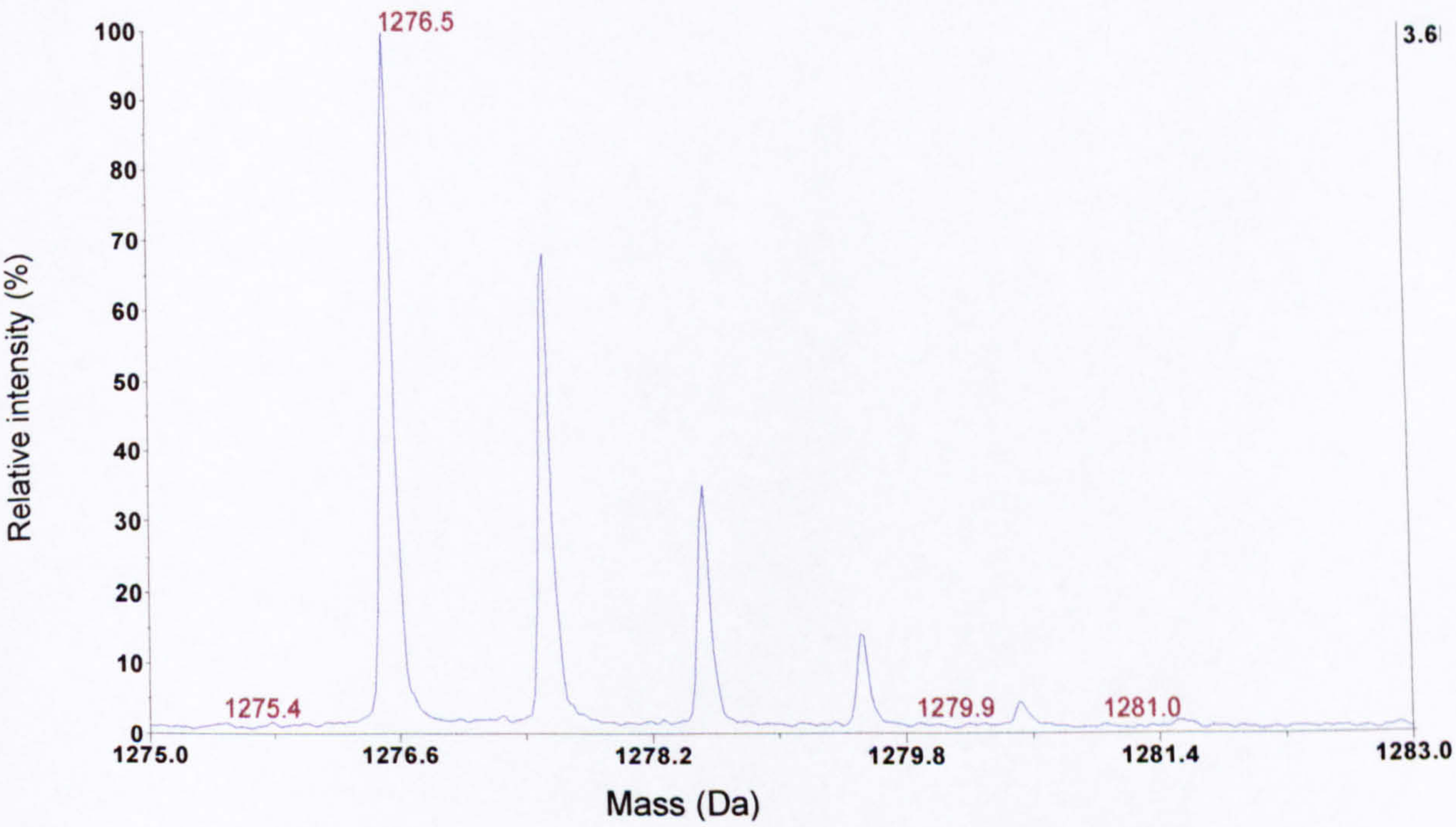

Figure 4.8 Identification of an ESP3-6 peptide by LC-MALDI-MS. **A:** ESP3-6 peptides of 1276.6Da were eluted onto the MALDI plate between Spot 107 and Spot 150. The maximum signal-to-noise ratio was 960. **B:** The 1275-1283Da region of the MS spectrum for Spot 120 shows no background noise, a reflection of the strong signal. Isoforms of the peptide containing up to four C^{14} atoms can be seen.

4.4 Discussion

4.4.1 The Ubiquitin-Proteasome Pathway and the Developing Egg

Western blots have shown that the 20S proteasome is more highly expressed in the immature egg than in the fully-developed egg. The results from the fluorogenic substrate assays reinforces the blotting evidence in that 20S proteasomal chymotryptic-like activity was higher in immature SEA than in mature SEA. The decline in the activity of the UPP as the egg matures is consistent with two scenarios. There could be a reduction in the extent to which the embryo is damaged by the host's immune system, or the vitelline cells of the immature egg could utilize the UPP more actively than the cells of the miracidium and envelope of the mature egg.

Granulomata do not form around immature eggs (Boros *et al.*, 1975), so the immature egg will be surrounded by fewer host cells than the mature egg. It therefore follows that the immature egg will be in an environment that has lower concentrations of toxic compounds than the mature egg. Also, as the embryo is small in the immature egg, the thick, protective layer of vitelline cells would buffer it from any external toxic compounds which enter the shell. Thus, the embryo of the immature egg is at less risk of being damaged by the products of host cells than the miracidium and envelope of the mature egg. Consequently, the more active UPP in the immature egg can be attributed to some factor(s) relating to the purpose of the vitelline cells. As the vitelline cells provide an auto-degrading reservoir of nutrients for the developing ovum (Smyth & Halton, 1983), it is hypothesised that that the relatively high activity of the UPP in the immature egg is due to the degradation of the contents of the vitelline cells.

It makes sense in that the UPP would be used for vitelline cell degradation because the process is highly regulated. The regulation can occur at the stage of substrate ubiquitinylation or at the proteasome itself. At the ubiquitinylation stage, the substrate specificities of the E3 ubiquitin ligases determine which proteins become ubiquitinylated, and then the rate of their ubiquitinylation will also depend upon the availability of free ubiquitin. At the proteasome level, regulation can occur via a family of proteins called

"proteasome interacting proteins" that associate with the 19S regulatory complex (Verma *et al.*, 2000). These proteins include de-ubiquitinylation enzymes such as Ubp6, which can progressively remove ubiquitin moieties from substrate proteins to delay their proteasomal degradation (Hanna *et al.*, 2006). Also, as proteasomal degradation is highly ATP-dependent (Benaroudj *et al.*, 2003), intracellular ATP concentration will also regulate proteasomal function. Thus, by using the UPP, the contents of the vitelline cells would degrade slowly, forming an amino acid-concentration gradient between the vitelline cells and the developing miracidium, capable of delivering the amino acids that the miracidium requires for its growth.

The other potential mechanisms by which vitelline cells degrade could be apoptosis and/or autophagy. There is little evidence that apoptosis is particularly active in schistosomes. The *S. mansoni* transcriptome was found to contain some but not all of the components of the apoptotic pathway (Verjovski-Almeida *et al.*, 2003). Also, the apoptotic pathway is relatively uncontrollable once it has begun, with the process of caspase activation taking minutes to complete and then, once a cell has undergone a commitment to undergo apoptosis the process is complete within several hours (Tyas *et al.*, 2000). So, even if the apoptotic pathway was utilised in the egg, it is difficult to reconcile such a rapid and uncontrollable mechanism of protein degradation with the slow and steady release of amino acid that the developing miracidium would require.

Autophagy is more likely than apoptosis to be involved in vitelline cell degradation because almost all of the autophagic components have been found in the transcriptome and studies have found autophagy occurring in adult schistosomes (Verjovski-Almeida *et al.*, 2003; Al-Adhami *et al.*, 2003; Bogitsh, 1975). Autophagy is known to function as a mechanism to eliminate unwanted cells during developmental cell death in various taxa, including the ovarian nurse cells in *Bombyx mori* and *Ceratitis capitata* (Levine & Klionsky, 2004; Mpakou *et al.*, 2006; Velentzas *et al.*, 2007). It is therefore quite likely that both autophagy and the UPP are involved in the degradation of vitelline cells, perhaps with the UPP at the earlier stages and autophagy operating at a later time point. The egg does not contain any phagocytic cells, so after their degradation, any remnants of vitelline cells will probably

remain inside the egg. It is possible that these vitelline cell remnants go on to form the vesicles of the fully mature egg.

The relative expression levels of ubiquitin in immature and mature SEA also supports the hypothesis that the UPP is more active in the immature egg. Unbound ubiquitin was found in both the immature and mature SEA gels, where it constituted 0.4% of the former but only 0.2% of the latter (see Chapter 2, Tables 2.4 and 2.5). The larger pool of free ubiquitin in immature SEA is indicative of fast protein turnover whilst the smaller pool in mature SEA suggests a build up of ubiquitinylated proteins awaiting degradation because the UPP is operating more slowly.

Although more proteasome α3 and α6 subunit isoforms were expressed in the immature egg than in the mature egg, the greatest expression was seen in the blots of the female, vitellaria-enriched preparation. The female, vitellaria-enriched preparation contains vitelline cells in various stages of development as well as the vitelline follicles, which actually produce the vitelline cells. It is therefore impossible to proportion the proteasome subunit isoforms seen in the blot between the vitelline cells and the vitelline follicles. However, the vitellaria must be very active in terms of protein production because it produces 9,000 – 12,000 vitelline cells per day (discussed in Chapter 1, Section 1.2.1). Such a high rate of protein production is inevitably going to mean that large numbers of misfolded proteins are constantly going to be produced and these will quickly need to be degraded. The UPP is inevitably going to be highly active in this process so consequently, it is not surprising that the female, vitellaria-enriched preparation contains more proteasome α-subunit isoforms than either the immature egg or the mature egg. It can also be argued that the female, vitellaria-enriched preparation is more enriched in vitelline cells than immature SEA, and as the vitelline cells themselves are enriched in proteasomes, the blot of the female, vitellaria-enriched preparation will have more visible proteasome subunit isoforms for this reason alone.

4.4.2 The Ubiquitin-Proteasome Pathway in Hatch Fluid and the Miracidium

The mature egg can be sub-divided into the miracidium, the hatch fluid and ESP, all of which have different proteasomal and ubiquitin blots. The spot pattern on the 20S

proteasome α-subunit isoform blot of the miracidial preparation was a sub-set of that of hatch fluid. This could partially due to the methods adopted to make each preparation. Hatch fluid only contains water-soluble proteins (including the proteasome) whilst the miracidial preparation was made using a buffer containing urea, thiourea and CHAPS, which will also have solubilized some hydrophobic proteins. So, as the two blots contained the same quantity of crude protein, the proteasome will be more enriched in the hatch fluid preparation. However, the difference between the blots was too dramatic to be solely due to the more complex nature of the miracidial preparation (hatch fluid contained 433 spots in the 2D gels of Chapter 2 whilst the miracidial preparation contained 602 spots). It is more likely that hatch fluid contained more 20S α-subunit isoforms because the UPP is highly active in the envelope, the intracellular content of which forms part of hatch fluid. The envelope is responsible for producing the ESPs, so it has a high rate of protein production, and will consequently need to have an active UPP in order to degrade those that become misfolded. By contrast, the miracidium is short-lived and does not secrete proteins whilst it is in the egg. The miracidium's principal requirement is to find and penetrate an intermediate host, and as it does so without feeding it will need to conserve ATP. It has been calculated that 300-400 ATP molecules are used during the degradation of one substrate protein through the UPP (Benaroudj *et al.*, 2003), so for the miracidium it could be that operating the UPP is just too expensive in terms of ATP expenditure. Instead, the miracidium might utilize its high levels of the non-ATP-requiring chaperone p40 to store its misfolded proteins. It is likely that any misfolded proteins associating with p40 are effectively removed from the UPP because p40 does not contain the tetratricopeptide repeat motifs that are found in HSP70 and HSP90. The tetratricopeptide repeats are important because they interact with the E3 ubiquitin ligase CHIP and thereby form the bridge between chaperones and the UPP. (The link between chaperones and the UPP and the involvement of CHIP has been described in Section 4.1.2). CHIP is present in the *S. mansoni* transcriptome (Sm03288).

4.4.3 Ubiquitin in ESP

It was surprising that the blot of ESP contained more than 100 ubiquitinylated proteins and unbound ubiquitin, firstly because the UPP is intracellular and secondly because only twenty-seven spots are visible in protein gels of ESP (see Chapter 2, Figure 2.7). The ESP

blots that were probed for poly-ubiquitin and 20S proteasomal α3 and α6 subunit isoforms were both negative (except for the faint 23kDa band in the poly-ubiquitin blot), which demonstrates that ESPs are either mono- or multi-ubiquitinylated. It is not clear how ubiquitinylated proteins could be secreted because proteins must be retro-translocated from the ER (i.e. removed from the secretory pathway) prior to their ubiquitinylation. It is possible that a failure of E2 and/or E3 to complete the poly-ubiquitinylation process might lead to the inability of mono-ubiquitinylated proteins to disassociate from *sec61* and their consequential return into the secretory pathway. This theory is supported by a study in which it was demonstrated that poly-ubiquitinylation was required if a misfolded protein emerging from *sec61* was not to be returned back into the ER lumen (Shamu *et al.*, 2001).

There is other evidence which demonstrates that ubiquitin is not exclusively intracellular. A proteomic study of the content of secretory vesicles found ubiquitin, but it was impossible to establish whether the ubiquitin was unbound or had been conjugated to substrate proteins (Wegrzyn *et al.*, 2007). The plasma of patients suffering from diabetes, alcoholism and schistosomiasis mansoni contains unbound ubiquitin (Akarsu *et al.*, 2001; Takagi *et al.*, 1999; Asseman *et al.*, 1994) but none of these studies could demonstrate that the ubiquitin had not leaked from ruptured cells. Ubiquitinylated membrane proteins have been found on the external surface of sperm and are used as a measure of sperm quality (Muratori *et al.*, 2005). So, the mono-ubiquitinylated ESPs could be misfolded ESPs that failed to become poly-ubiquitinylated and proteasomally degraded and so they became secreted instead. However, if this were to be the case, then the relative abundances of the proteins on the ubiquitin blot should be similar to that seen in the protein gel. This was not the case however - the spot patterns on the ESP blot and gel were different.

It is therefore most likely that the mono- or multi-ubiquitinylated proteins seen in the ESP blot were intracellular proteins, derived from ruptured cells leaking into the culture media. It is unlikely that the leakage was from dead eggs that had ruptured and disintegrated because the pattern of mono-ubiquitinylation in ESP differed from that of mature SEA (see Figure 4.6A) and also because 97% of eggs remained viable after the culture period (see Chapter 2, section 2.2.4). It is more likely that the envelope had become damaged whilst the eggs were being prepared for culture, resulting in leakage across the envelope's

membrane on the side facing the eggshell as opposed to that facing the miracidium. Such damage could have been caused when the liver tissue was undergoing tryptic digestion to retrieve eggs because the porcine trypsin that was used has a molecular weight of 23.8kDa, which is sufficiently small to pass through the eggshell and attack any membrane proteins in the envelope. The similarity between the ubiquitin blots of ESP and hatch fluid add weight to this possibility because the water soluble intracellular envelope proteins form part of hatch fluid.

It is logical that intracellular ubiquitinylated proteins, ultimately destined for proteasomal degradation would include mono-ubiquitinylated proteins awaiting poly-ubiquitinylation and poly-ubiquitinylated proteins awaiting proteasomal destruction, both of which could leak into the ESP cultures. However, the blots demonstrated a dearth of poly-ubiquitinylated proteins compared to those that had been mono-ubiquitinylated. No work has been done to establish the timing of the various ubiquitinylation events in the UPP, but it is likely that the process of generating a poly-ubiquitin chain is lengthy compared with the time it takes between poly-ubiquitinylation and the removal of the ubiquitin moieties by the 19S regulatory subunit. The 26S proteasome is very abundant (Tanahashi *et al.*, 2000) so the transit time to the proteasome will consequently be short, particularly for protein substrates removed from the secretory pathway, where the 26S proteasomes are in very close proximity to the ER membrane (Romisch, 2005). Consequently, it is not surprising that poly-ubiquitinylated proteins were scarce in the blots compared with mono-ubiquitinylated proteins. The partial loss of the membrane's integrity need not be fatal for the miracidium because the eggs were cultured in a non-hostile environment where neither the hatch fluid's defence role nor its ESPs are obviously required for miracidial survival. The finding that the envelope becomes damaged during the extraction of eggs from liver tissue leading to envelope-leakage into egg cultures is important. It explains why intracellular proteins such as thioredoxin peroxidase, histones, HSP70 and p40 have all been found in egg cultures (Williams *et al.*, 2001; Cass *et al.*, 2007). These proteins were all identified using Western blots or non-gel-based MSMS, which are more sensitive, but less quantifiable techniques than the gel-based proteomics that was used in Chapter 2.

Chapter 5

Concluding Discussion

This chapter summarises the rationale behind this thesis and places it in the context of preceding work. The most important results and the limitations of the work are highlighted and attention is drawn to potential future avenues of research.

The aims of the study were to characterise the proteome of *S. mansoni* egg and then to establish whether any of the egg's proteins could be assigned specific biological activities. The schistosome egg is important for two principal reasons: it forms the focus of the host's immune response (which in turn causes the pathology in schistosomiasis) and it is the means by which the parasite transmits itself between hosts. Egg proteins involved in these functions were therefore of particular interest.

When it is released from the female worm the *S. mansoni* egg is completely undeveloped. It comprises of a fertilised ovum surrounded by thirty-forty vitelline cells, encapsulated in a cross-linked protein shell. The ovum and vitelline cells are produced by different organs spatially separated from each other. The vitelline cells are produced by a large organ called the vitellaria, which occupies the posterior two-thirds of the worm. The oocyte is produced by the ovary which is situated above the vitellaria. Both the ovary and vitellaria are linked via ducts, with the oviduct incorporating a dilated region where sperm are stored. The egg is packaged together at a point just downstream of where the oviduct (discharging the oocyte and sperm) and the vitelline duct (discharging mature vitelline cells) meet. The shell is also formed from precursors in the vitelline cells at this point. The newly-packaged egg then passes along the uterus and is deposited by the worm against the epithelium of the mesenteric veins. At this point, no observable intra-egg structures can be seen under compound microscopy. Then, as the egg starts to develop, the vitelline cells collapse as their contents are degraded. The mechanism by which the degradation occurs has never been studied, but it is unlikely to be apoptotic because this pathway is rapid and uncontrollable once underway and there is little evidence from the *S. mansoni* transcriptome that apoptosis is used by schistosomes. The degradation is therefore probably dependent upon autophagy or the UPP. Concurrent with the degradation of the vitelline cells the oocyte starts to develop into a miracidium. An envelope forms between the developing miracidium and the shell, which thickens, acquiring structures associated with protein production such as rough endoplasmic reticulum. The envelope then starts to

secrete a protein mixture called "ESP", which emerges through the eggshell. A viscous liquid containing vesicles forms in the area between the miracidium and the envelope. If the egg is still located at its site of deposition in the mesenteric veins it crosses the blood vessel wall, the mesenteric tissues and the gut wall to emerge in the lumen of the gut, from where it is excreted from the host. If the egg encounters fresh water the vesicles swell, the shell ruptures and the miracidium swims away in search of a snail intermediate host, tearing through the envelope if it remains structurally intact. Fresh water floods into the shell causing the vesicles to burst and many of the cells of the envelope to lyse. So, at hatching the egg releases not only the miracidium but also a milieu of other water-soluble proteins called "hatch fluid". Hatch fluid is therefore derived from the envelope, those egg secretions that had been produced by the envelope but had not yet emerged from the shell, the liquid that surrounded the miracidium and the vesicles. Unlike the undifferentiated immature egg, the mature egg can therefore be seen as consisting of the miracidium, the hatch fluid and the secreted proteins, each of which are likely to have different biological functions – the secretions in orchestrating the transit of the egg from the blood vessels to the lumen of the gut, the hatch fluid in protecting the miracidium and aiding shell rupture and the miracidium which transmits the parasite's genes to the next stage of the life cycle.

Previous work focussing on *S. mansoni* egg proteins has almost invariably involved homogenizing thousands of intact eggs of mixed ages to produce a standardised egg preparation known as SEA. Although some individual SEA proteins have been described on a paper-by-paper basis, no overall picture of protein expression in the egg has previously emerged. Little was known about how abundant each of the egg proteins actually are, to what extent their expression levels change as the egg matures and which proteins are enriched in the different components or structures in the egg. These are important questions because the pathology in schistosomiasis can be linked to egg deposition and destruction. For example, the host's immune response changes from being of a polarised Th1-type to becoming a more balanced Th-1/Th-2 type when egg deposition begins, and it is then down-regulated at a point in time when large numbers of mature eggs that have become embolised in the liver die and disintegrate, releasing their protein content.

The work in this thesis is the first detailed characterisation of the *S. mansoni* soluble egg proteome. It achieves this by using a combination of 2-DE, software capable of comparing multiple gel images and MALDI-MSMS. Preparations were made representing eggs at different stages of development. These were then separated by 2-DE and their spot-patterns compared using the gel analysis software. Identities for the spots were sought using MALDI-MSMS and sequencing data generated by the *S. mansoni* genome project, annotated with gene predictions and ESTs representing over 90% of the transcriptome. Each of the identified proteins was then assigned to one of eleven categories, based on its molecular function. The proteomes of each of the egg preparations were then compared in terms of function by using the normalised volumes of the gel-spots as a measure of protein expression levels. Another set of preparations representing the mature egg's constituents (the miracidium, hatch fluid and the ESP) was also made, analysed in the same way and their gel spot-patterns matched back to the gel of the mature egg preparation. A picture then emerged; firstly of how the egg's proteome changed as it developed, and secondly of how the mature egg's proteome is portioned into the ESP, the hatch fluid and the miracidium. By comparing the expression levels of specific proteins or functional categories between the preparations it was possible to link the egg's biological requirements and functions to its proteome at the appropriate time-point. For example, uniquely vitelline cell proteins can now be distinguished from miracidial proteins so the former can be eliminated as potential candidates in influencing events such as the transit of eggs across the gut wall or driving particular immune responses at the point of egg disintegration. Alternatively, proteins only present in the miracidium cannot be involved in the early events of granuloma formation.

As the newly-released egg mostly contains vitelline cells, the preparation representing the earliest time-point in the egg's development was made from the vitellaria-containing section of gravid worms that had been severed just below the ventral sucker. It was anticipated that this "female, vitellaria-enriched preparation" would have many proteins in common with the preparation representing the next stage in the egg's development ("immature SEA"), but surprisingly this was not the case. Immature SEA was made from a population of eggs, 92% of which could be seen to be immature in that their embryo was undeveloped. However, despite the obviously undeveloped state of these eggs, the resulting gel was so different from the gel of the female, vitellaria-enriched preparation that spot-

matching could not be undertaken. Therefore, the shared spots remained unidentified. The extreme between-gel differences demonstrate that the vitellaria-containing region of the worm is not highly enriched in mature vitelline cells, despite the published TEM images that show the vitellaria to completely occupy the posterior two-thirds of the worm. Presumably, the production rate of eggs is so high that the mature vitelline cells are used up in egg production immediately they are produced, and therefore, the population of vitelline cells in the vitellaria at any one time consists of immature cells with a different proteome.

The eggs making up immature SEA were at the point in their development when the vitelline cells were being degraded to provide amino acids for the developing miracidium. The eggs making up mature SEA were fully developed however, with no vitelline cells remaining. It was therefore possible to link UPP activity to egg development by using the immature SEA and mature SEA preparations as the basis of a comparison. The comparison involved assaying the 20S proteasomal activity using a fluorogenic substrate and probing Western blots with antibodies recognising proteasomal subunit isoforms and ubiquitin. Taken together, the results demonstrated for the first time that the level of UPP activity decreases as the egg matures, and furthermore, that the UPP is involved in the process of vitelline cell degradation. This is an important finding, not only because the mechanisms by which vitelline cells degrade have never been studied before, but also because experiments investigating the degradation pathways used by insect nurse cells have not incorporated the UPP either.

Meanwhile, the proteomic comparison between immature SEA and mature SEA demonstrated that although both preparations mainly consisted of chaperones, cytoskeletal proteins and enzymes involved in ATP production, more subtle changes were happening in the background. In terms of the functional categories, the mature egg contained secretory proteins (whereas the immature egg had none), more defence proteins and proteins without a known function. These developmental proteomic changes could then be assigned to the miracidium, the hatch fluid or the ESP. It could be seen for example that the defence proteins were primarily in the hatch fluid, highlighting the role that hatch fluid plays in protecting the miracidium. Changes within the functional categories could also be seen in context of the biology of the egg. For example, the proteomes of both immature and mature

SEA contained a similar proportion of enzymes involved in ATP production, but immature SEA was enriched in enzymes for anaerobic respiration whilst mature SEA had more TCA cycle enzymes. This illustrates how the egg is undergoing transition from the anaerobic adult which produced it to the aerobic miracidium it releases.

ESP is the only egg preparation whose proteome has previously been studied. This is not surprising because ESP represents the interface between the live egg and the host so it is likely to be involved in both granuloma formation and the egg's escape from the host. Although the existence of ESP was first proven in the 1950s, little work was done to follow it up and it was not until 2001 that ESP was demonstrated to be a distinct subset of egg proteins, produced by the envelope located between the miracidium and the shell (Ashton *et al.*, 2001). Work in this thesis follows on from both the Ashton *et al.*, study and other research carried out in the Wilson laboratory that had shown ESP to consist of 15 proteins, all of which were unique and had no known function judging by their PMFs, but two of which exhibited proteolytic activity *in vitro* (Ashton, 2001). ESP3-6 is the most abundant ESP, making up about 80% of the total secreted protein. It is not one of the proteases, but it has been studied by two other groups, one of whom think it induces basophils to degranulate and the other who consider it to bind to and inactivate chemokines (Schramm *et al.*, 2003; Smith *et al.*, 2005). Various other proteins have been detected in egg cultures over the years, and these have also been described as "secreted", but in all of these instances the proteins in question could have leaked from damaged or dead eggs. The proteomic work of this thesis obtains the amino acid sequences of each ESP for the first time and establishes that no ESP has any homology to any known protein from another organism, apart from ESP1-2 which has homology to an RNAse (Fitzsimmons *et al.*, 2005). The amino acid sequence of another of the ESPs might contain a subtilase-like pro-protein convertase functional domain. This finding raises the question as to whether the proteolytic activity of ESP might be more indirect than previously thought. If the egg were to secrete a subtilase-like protein it could be activating pro-proteases secreted by the host cells of the inflammatory focus. Such a mechanism could be beneficial for the egg because it would enable the envelope and miracidium to be spatially separated from the active site of the protease, which might not be the case if the egg were to produce its own, active protease. A series of functional assays was therefore carried out that aimed to establish whether ESP

could induce the secretion of proteases from macrophages and furthermore, to answer the more general question of whether ESP was immunogenic to cell-types known to be present in the granuloma. An attempt was also made to fractionate crude ESP into its components using HPLC so that any functionality observed in crude ESP could potentially be attributed to a particular ESP by using the enriched fractions in place of crude ESP.

The results from the functional ESP work demonstrated that ESP3-6 binds to other ESPs, which in turn indicates that rather than having a specific affinity as proposed by Schramm *et al.*, (2003) and Smith *et al.*, (2005), ESP 3-6 is probably a fairly ubiquitous binding protein. As ESP3-6 has a *pI* at approximately pH10, it would be positively charged at physiological pH and so it is possibly its charge that mediates its ubiquitous binding characteristics. The binding might occur for reasons of protection, by binding to proteins that otherwise might enter the egg and damage the envelope of miracidium. Alternatively, ESP3-6 might bind to the proteases that enable the egg to transit the gut wall, keeping them attached to the inflammatory focus and preventing them from being solubilized and lost in the blood stream. The functional experiments also show that ESP is enriched in a factor(s) that is/are recognised by macrophages of the innate immune system. This result indicates that ESP might be involved in the early events of granuloma formation, but further experiments will be required to strengthen this hypothesis because the level of activation, as measured by IL-6 secretion and MHCII upregulation, was low. A more realistic situation could be achieved *in vitro* if five-week infected mice (at the point just before egg deposition commences) rather than uninfected mice are used as the source of the macrophages. Also, expression levels of co-stimulatory molecules such as CD80, CD86, CD54, CD40 or OX-40L might prove to be a better method of assessing macrophage stimulation. Unfortunately, the assays that were intended to establish whether ESP induced protease secretion from macrophages were unsuccessful in that an ESP component (likely to be ESP3-6) bound to the substrate's fluorophor and hindered its operation. However, the protease assay could be repeated with ESP fractions, purified using the HPLC purification protocol that was established in this thesis and described in the Addendum to Chapter 3. The leukocyte protease assay could also be applied to cultures of $CD4^+$ cells obtained from infected mice or indeed from cells obtained from granulomata themselves.

Unlike ESP, the miracidial and hatch fluid proteomes have never previously been studied. It was evident that most of the proteins in mature SEA were miracidial and these principally consisted of cytoskeletal proteins, chaperones and enzymes involved in ATP production. The cytoskeletal proteins were mostly tubulin, likely to make up the locomotory cilia that cover the miracidium and actin, which would form cytoskeletal microfilaments and muscle fibres used by the miracidium to change direction while swimming, extract itself from the ruptured shell and aid its penetration into a snail. The most abundant protein in the miracidial preparation (making up fifteen percent of the soluble proteome) is Sm-p40, which is a non-ATP-requiring chaperone and a major T cell antigen (Hernandez & Stadecker, 1999). Sm-p40 production begins fairly early in miracidial development (it makes up four percent of immature SEA) but by the time the egg has matured its expression levels have increased such that ten percent of mature SEA is Sm-p40. The localisation of Sm-p40 to the miracidium demonstrates that it is not going to be presented to host cells until the egg has died and ruptured, so consequently it cannot be involved in creating the T cell-rich inflammatory focus that initially forms around the live egg. It is not known why Sm-p40 is so enriched in the miracidium, but its high level of expression is indicative of it being a protein of vital importance. I propose that Sm-p40 is a vital part of an energy-conservation strategy adopted by the miracidium. The miracidium is quiescent whilst it is in the egg but once hatched it is very active, short-lived and non-feeding. Its likelihood of finding a snail will depend upon its lifespan, which in turn will depend upon how quickly its glycogen reserves are exhausted. So, by having high intracellular concentrations of Sm-p40, the miracidium can quarantine its damaged proteins without expending ATP, rather than having to degrade them via the UPP, which is an ATP-expensive business. The low utilisation of the UPP by the miracidium was also demonstrated by probing Western Blots with the same anti-proteasomal subunit isoform and anti-ubiquitin antibodies discussed previously in relation to the developing egg. It was found that compared with hatch fluid, the miracidium expressed few proteasome subunit isoforms, consistent with its reduced utilization of the UPP.

The reason why the hatch fluid blot contained more proteasome subunit isoforms than the miracidial blot is likely to be because the hatch fluid contains intracellular envelope proteins, and the envelope will have to use the UPP to degrade misfolded ESPs. In addition

to containing proteins involved in protein turnover, the hatch fluid proteome was also found to contain most of the mature egg's compliment of defence proteins, its proteins of unknown function plus some proteins that the egg had taken up from the host. The defence proteins are most likely to be located in the liquid between the miracidium and the envelope. Here they would be able to protect the miracidium from damage from toxins produced by the cells of the granuloma. The reason why there are so many proteins of unknown function in the hatch fluid is less obvious, but presumably relates to its unstudied nature and the lack of similar material in other animals. The most highly expressed protein of unknown function is Smp170410, which is a large, acidic, glycosylated protein that makes up over 18% of hatch fluid. Smp170410 is not a remnant of degraded vitelline cells and nor is it secreted by the egg, but it is produced by the egg in increasing quantities as it matures. It is quite possibly located in the egg's vesicles and involved in the hatching process. Localisation studies and gene silencing could be used to address these hypotheses. Finding host proteins of up to 70kDa in the hatch fluid was surprising because it demonstrates that the egg shell is more porous than previously thought. Some of the host proteins probably have value to the egg (such as albumin, which can bind to and transport fatty-acids) but others are potentially hazardous (such as haemoglobin, which contains a potentially toxic haem group). Albumin is currently a topical subject with schistosome researchers because it has recently been claimed that an albumin gene was acquired by *S. mansoni* from its host by lateral gene transfer (Williams *et al.*, 2006). Chapter 2 includes a proteomic analysis of hamster albumin which demonstrates that the claimed "schistosome albumin" is identical at the amino acid level to hamster albumin and so is probably a laboratory artefact.

The work of this thesis is also of value with regard to the processes of drug design and vaccine development. Chemotherapy using the drug praziquantel is the mainstay of schistosomiasis control programs because an effective vaccine has yet to be developed (Fenwick & Webster, 2006). Praziquantel is used because it is easy to store and administer, it has a long shelf life, is well tolerated and is effective against all schistosome species. Also, as the patent on the drug has expired, cheap generic variants are available for as little as US$0.065 per tablet (WHO, 2002). However, reliance on praziquantel raises concerns as to whether schistosome resistance to it has or will evolve. Low cure rates in Senegal have

largely been explained in terms of high transmission rather than resistance (Danso-Appiah & De Vlas, 2002), but laboratory-maintained parasite strains originally obtained from patients with low cure rates appear to have some resistance to praziquantel (Ismail *et al.*, 1996). Other reports of resistant parasites emerge from time to time, such as one where a traveller returning from Kenya had a *S. mansoni* infection which resisted three consecutive regimens of praziquantel treatment (Lawn *et al.*, 2003). Thus, the discovery that the anti-malarial drug artemisinin also has anti-schistosomal activity is generating considerable interest in the schistosome-research community. Studies into the mechanisms by which artemisinin compounds operate have shown that it reacts with heme to produce toxic free radicals (Meshnick, 2002). The work of Chapter 2 demonstrates that host haemoglobin is present inside the egg, so this raises the possibility that artemisinin might have an anti-egg activity. This hypothesis is supported by a study demonstrating that the livers of infected mice treated with artemisinin contained no eggs, that the granulomata had dissipated and no liver pathology was observable (Botros *et al.*, 2007). If artemisinin kills eggs, and if its efficacy at the different stages of egg development can be established, then knowing how the egg's proteome alters over time will provide indications as to which proteins are targeted by artemisinin. The dead egg will then leak its contents, so studies looking at the immunogenicity of the egg's proteome at that point in the egg's development can also be facilitated.

The concept of a schistosomiasis vaccine is attractive because protective immunity develops naturally in some individuals (Butterworth *et al.*, 1985) and can be induced in mice by infecting them with irradiated cercariae (Smythies *et al.*, 1996). The WHO has designated seven proteins as vaccine candidates, but none have proved to be effective. The work in this thesis demonstrates that five out of these seven proteins are highly expressed in the egg. This finding is important because vaccinating with a protein found in the egg could induce sensitisation, so any vaccinated individuals who later become infected could find themselves facing severe immune responses to disintegrating eggs. Alternatively, any individuals who were already infected with *S. mansoni* before vaccination took place may fail to respond to the vaccine because their immune systems had already become anergic to the vaccine's epitopes. The author therefore proposes that the egg proteins characterised in

this thesis should form an exclusion list, from which any prospective vaccine candidates should not be taken.

Appendix 1. The proteome of the *Schistosoma mansoni* egg. Spot numbers correspond to those annotated in Figs 2.1 – 2.6 and the peptides were identified by MSMS utilizing the Mascot search engine.

Spot no.[1]	Prep[2]	Protein name	Accession no.[3]	Pep. count	Total Ion Score (protein)	C.I. (%)	Calculated Mass (Da)	Observed Mass (Da)	Match Error (Da)	Sequence	Ion Score (pep)	Mods.[4]
1	ESP	Omega 1	Sm19482	3	145	100	980.56	980.52	-0.04	FGIKLMQK	31	Ox (M)[6]
							1624.80	1624.80	0	QYDTINLMNVLER	40	Ox (M)[8]
							2272.05	2272.05	0	HGLCAVEDPQVFNQYGY	75	Carb (C)[4]
2	ESP	IPSE	gi73765569*	4	317	100	1287.64	1287.63	-0.01	DGKVECINQPK	46	Carb(C)[6]
							1634.78	1634.78	-0.01	ITGLGHGTCIDDFTK	68	Carb (C)[9]
							1652.73	1652.72	-0.01	YCLQLYDETYER	92	Carb (C)[2]
							2092.99	2092.97	-0.02	ERPYWYLFDNVNYTGR	112	
3	ESP	IPSE	gi73765569*	2	85	100	1595.70	1595.70	0.00	YCLQLYDETYER	79	
							1652.73	1652.73	0.00	YCLQLYDETYER	85	Carbl (C)[2]
4	ESP	IPSE	gi73765569*	2	129	100	1634.78	1634.85	0.06	ITGLGHGTCIDDFTK	56	Carb (C)[9]
							1652.73	1652.79	0.06	YCLQLYDETYER	73	Carbl (C)[2]
5	ESP	IPSE	gi73765569*	2	154	100	1634.78	1634.79	0.00	ITGLGHGTCIDDFTK	85	Carb (C)[9]
							1652.73	1652.73	0.00	YCLQLYDETYER	68	Carb (C)[2]
6	ESP	IPSE	gi73765569*	2	128	100	1634.78	1634.84	0.06	ITGLGHGTCIDDFTK	78	Carb (C)[9]
							1652.73	1652.78	0.06	YCLQLYDETYER	50	Carb (C)[2]
7	ESP	IPSE	gi73765569*	1	66	99.91	1652.73	1652.77	0.04	YCLQLYDETYER	66	Carbl (C)[2]
8	ESP	ESP12	Snap 42294	1	48	99.9	1023.57	1023.57	0.00	KFIFPPFQ	48	
9	ESP	ESP15	Sm00193	1	121	100	2015.99	2015.99	0.00	DGCPIPSTPDLLLGNYQR	121	Carb (C)[3]
10	ESP	ESP13	Sm11845	2	186	100	1378.58	1378.58	0.00	HCEGNNEYVTR	100	Carb (C)[2]
							1506.68	1506.68	0.00	KHCEGNNEYVTR	86	Carb (C)[3]
11	ESP	ESP14	Sm11845	2	91	100	1378.58	1378.58	0.00	HCEGNNEYVTR	41	Carb (C)[2]
							1506.68	1506.68	0.00	KHCEGNNEYVTR	49	Carb (C)[3]
12	ESP	ESP17	Sm12949	2	217	100	1329.58	1329.58	0.00	HCGGHNEYVTR	87	Carb (C)[2]
							2069.81	2069.79	-0.01	CNGSPQLTESSCQNDCG	131	Carb (C)[1,12,16]
13	ESP	ESP19	Sm12949	1	99.986	60	1329.58	1329.58	0.01	HCGGHNEYVTR	60	Carb (C)[2]
14	ESP	ESP15	Sm00193	1	100	121	2015.99	2015.99	0.00	DGCPIPSTPDLLLGNYQR	121	Carb (C)[3]

Spot no.[1]	Prep[2]	Protein name	Accession no.[3]	Pep. count	Total Ion Score (protein)	C.I. (%)	Calculated Mass (Da)	Observed Mass (Da)	Match Error (Da)	Sequence	Ion Score (pep)	Mods.[4]
50	vit	14-3-3 protein	Sm12452	1	71	100	1592.84	1592.84	0.00	ATTAAENLPTTHPIR	71	
51C	vit	actin	Sm00900	4	308	100	976.45	976.39	-0.06	AGFAGDDAPR	65	
							1132.53	1132.46	-0.07	GYSFTTTAER	54	
							1486.69	1486.61	-0.08	QEYDESGPGIVHR	79	
							1790.89	1790.80	-0.09	SYELPDGQVITIGNER	110	
51L	vit	actin	Sm00900	2	152	100	1198.71	1198.71	0.01	AVFPSIVGRPR	57	
							1790.89	1790.91	0.02	SYELPDGQVITIGNER	95	
51R	vit	actin	Sm00900	1	84	100	1790.89	1790.89	0.00	SYELPDGQVITIGNER	84	
52CL	vit	aldehyde dehydrogenase	Sm01315	5	374	100	1249.64	1249.64	0.00	FNTLEEVIER	73	
							1637.82	1637.83	0.01	LADLIEMNAEYIAR	32	Ox (M)[7]
							1696.86	1696.86	0.00	IFVQAPIYDQMVEK	43	Ox (M)[11]
							1812.91	1812.91	0.00	TVESALGDVFFAAQTTR	139	
							2004.99	2004.98	-0.01	YTQLFIGNEFVDSESKK	86	
52CR	vit	aldehyde dehydrogenase	Sm01315	4	320	100	1249.64	1249.64	0.00	FNTLEEVIER	88	
							1696.86	1696.87	0.01	IFVQAPIYDQMVEK	42	Ox (M)[11]
							1812.91	1812.92	0.00	TVESALGDVFFAAQTTR	124	
							2004.99	2004.99	0.00	YTQLFIGNEFVDSESKK	67	
52L	vit	aldehyde dehydrogenase	Sm01315	2	106	100	1249.64	1249.63	-0.01	FNTLEEVIER	37	
							1812.91	1812.89	-0.02	TVESALGDVFFAAQTTR	69	
52R	vit	aldehyde dehydrogenase	Sm01315	2	209.17	100	1249.64	1249.65	0.01	FNTLEEVIER	70	
							1812.91	1812.92	0.01	TVESALGDVFFAAQTTR	139	
53	vit	ATP synthase	Sm00685	2	73.620	100	975.56	975.58	0.02	IGLFGGAGVGK	35	
							2001.03	2001.10	0.07	AIAELGIYPAVDPLDSNSR	39	
54	vit	ATP synthase	Sm01126	4	295.466	100	1026.59	1026.59	0.00	AVDSLVPIGR	57	
							1405.70	1405.68	-0.01	AGAPEFSSILEER	54	
							1564.91	1564.89	-0.02	AGAIVDVPVGVELLGR	90	
							1672.89	1672.87	-0.02	ILGQTLQTNLEETGR	95	

Spot no.[1]	Prep[2]	Protein name	Accession no.[3]	Pep. count	Total Ion Score (protein)	C.I. (%)	Calculated Mass (Da)	Observed Mass (Da)	Match Error (Da)	Sequence	Ion Score (pep)	Mods.[4]
55	vit	bovine apolipoprotein	gi74268269*	3	170	100	1195.72	1195.74	0.01	QGLLPVLESLK	41	
							1305.64	1305.65	0.00	QQLAPYSDDLR	62	
							1398.69	1398.69	0.00	DYVAQFEASALGK	67	
56	vit	BSA	gi30794280*	3	231	100	1479.80	1479.78	-0.01	LGEYGFQNALIVR	76	
							1567.74	1567.72	-0.02	DAFLGSFLYEYSR	80	
							1639.94	1639.92	-0.01	KVPQVSTPTLVEVSR	75	
57	vit	BSA	gi74267962*	5	363	100	1163.63	1163.63	0.00	LVNELTEFAK	49	
							1439.81	1439.81	0.00	RHPEYAVSVLLR	56	
							1537.80	1537.80	0.00	LGEYGFQNELIVR	64	
							1567.74	1567.75	0.00	DAFLGSFLYEYSR	81	
							1639.94	1639.94	0.00	KVPQVSTPTLVEVSR	113	
58	vit	chaperonin	Sm00296	1	67	99.99	1543.78	1543.77	-0.01	VVLDENEYFLFR	67	
59	vit	superoxide dismutase	Sm11433	2	95	100	1366.78	1366.79	0.01	LISLNGSHSIIGR	39	
							2213.06	2213.08	0.02	FTQETDNGPVHVHAEFSGLK	56	
60	vit	cytosol aminopeptidase	Sm11876	3	156	100	1180.58	1180.59	0.01	GITFDTGGADVK	34	
							1836.93	1836.93	-0.01	NSIGSESYVADEIIIAR	75	
							1971.00	1970.99	-0.01	FSDEVSVIPFPEHPSKR	47	
61	vit	disulphide isomerase	Sm08285	2	93	100	1168.64	1168.63	-0.01	GFPTIYFVPK	55	
							1295.61	1295.60	-0.01	EATEELIGYDR	38	
62	vit	enolase	Sm12193	1	50	99.91	1188.64	1188.65	0.01	AGAAEAGLPLYR	50	
63	vit	exportin 7	Sm04735	1	60	99.94	1732.92	1732.92	0.00	QLNQFLTNEIKQEK	60	
64	vit	ferritin	Sm12942	3	138	100	1207.67	1207.66	-0.01	LSDYITNLIR	52	
							1299.59	1299.58	0.00	FFLNESEEER	47	
							1688.90	1688.89	-0.01	KVNQSLMELVAVGER	40	Ox (M)[7]

Spot no.[1]	Prep[2]	Protein name	Accession no.[3]	Pep. count	Total Ion Score (protein)	C.I. (%)	Calculated Mass (Da)	Observed Mass (Da)	Match Error (Da)	Sequence	Ion Score (pep)	Mods.[4]
65	vit	fructose bisphosphate aldolase	Sm05684	5	290	100	1515.80	1515.79	-0.02	SDDGKTLPTLLAER	42	
							1542.75	1542.74	-0.01	LQQIGVENNEENR	33	
							1698.85	1698.84	-0.01	LQQIGVENNEENRR	60	
							1879.93	1879.92	-0.01	FQPYLTEAQENDLRR	46	
							2330.15	2330.14	-0.01	GVVPLAGTDNETTTQGLDDLASR	112	
66	vit	fructose bisphosphate aldolase	Sm05684	6	359	100	1296.72	1296.72	0.00	VTEQVLAFVYK	56	
							1433.74	1433.74	0.00	AYTPQENALATVR	55	
							1698.85	1698.84	-0.01	LQQIGVENNEENRR	47	
							1879.93	1879.93	0.00	FQPYLTEAQENDLRR	47	
							2285.20	2285.19	-0.01	TVPPAVPGITFLSGGQSELDATK	30	
							2330.15	2330.12	-0.03	GVVPLAGTDNETTTQGLDDLASR	124	
67L	vit	HSP60	Sm01537	1	86	100	1623.91	1623.89	-0.01	AAIEEGIVPGGGTALLR	86	
67R	vit	HSP60	Sm01537	3	163	100	1285.67	1285.68	0.01	LEDVQLQDLGR	56	
							1431.72	1431.71	0.00	GYISPYFLNTEK	45	
							1623.91	1623.91	0.00	AAIEEGIVPGGGTALLR	62	
68	vit	HSP60	Sm01537	1	80	100	2560.25	2560.22	-0.02	LVQDVANNTNEEAGDGTTTATVLAR	80	
69	vit	HSP70	Sm00325	3	152	100	1199.68	1199.68	0.00	FDLTGIPPALR	63	
							1288.61	1288.60	0.00	NEFESSAYTLK	36	
							2538.25	2538.24	-0.01	SQIFSTAADNQPTVTIQVFEGER	53	
70	vit	HSP70	Sm00325	4	354	100	1199.68	1199.68	0.00	FDLTGIPPALR	88	
							1213.69	1213.69	0.00	DAGTIAGLNILR	55	
							1566.78	1566.77	-0.01	ITPSYVAFTPEGER	91	
							2538.25	2538.24	-0.01	SQIFSTAADNQPTVTIQVFEGER	120	
71	vit	HSP70	Sm09042	3	133	100	1081.57	1081.56	0.00	LLQDFFNGK	41	
							1253.62	1253.61	-0.01	FEELNADLFR	58	
							1480.75	1480.74	-0.01	ARFEELNADLFR	35	

Spot no.[1]	Prep[2]	Protein name	Accession no.[3]	Pep. count	Total Ion Score (protein)	C.I. (%)	Calculated Mass (Da)	Observed Mass (Da)	Match Error (Da)	Sequence	Ion Score (pep)	Mods.[4]
72	vit	HSP70	Sm09042	5	273	100	1169.66	1169.66	0.00	DAGAIAGLNVLR	59	
							1473.69	1473.68	-0.01	TTPSYVAFTDSER	35	
							1691.73	1691.72	-0.01	STAGDTHLGGEDFDNR	33	
							1787.99	1787.99	0.00	IINEPTAAAIAYGLDKK	68	
							1982.98	1982.98	-0.01	TVSDAVITVPAYFNDSQR	78	
73	vit	14-3-3 epsilon	Sm11575	1	67	99.99	1336.65	1336.65	0.00	VFSAVEQTEGNR	67	
74	vit	myosin heavy chain	Sm12294	7	516	100	1084.61	1084.61	0.00	LQGELQQLR	33	
							1286.70	1286.69	0.00	ATVLAGELDELR	50	
							1494.68	1494.69	0.01	YADSQAELENAQR	48	
							1532.77	1532.77	0.00	FEDEQGLVAQLQR	101	
							1661.81	1661.81	0.01	LQGELEDLMVDVER	35	Ox(M)[9]
							1982.94	1982.94	0.00	NLSDEIHDLTEQLGEGGR	125	
							2043.04	2043.04	0.00	KLEQDINELEVSLDGANR	124	
75	vit	myosin light chain	Sm01066	4	171	100	1192.60	1192.60	0.00	EAFSLIDQNR	50	
							1296.68	1296.68	0.00	LDYDGFVNLIK	51	
							2073.98	2073.97	-0.01	DGFIDIEDLKDMYASLGR	32	Ox (M)[12]
							2102.00	2102.00	-0.01	ATSNVFGMFPQNQIQEFK	39	Ox (M)[8]
76	vit	Sm14	Sm04779	2	125	100	1232.68	1232.68	0.00	TTVTVGDVTAIR	83	
							1940.93	1940.93	0.00	QIGNTVTPTVTFTMDGDK	43	Ox (M)[14]
77	vit	Sm20.8	Sm00101	1	110	100	1906.04	1906.03	-0.01	LHPDVVVIYEQLPLDR	111	
78C	vit	BSA	gi 76445989*	3	219	100	1479.80	1479.78	-0.01	LGEYGFQNALIVR	58	
							1567.74	1567.73	-0.01	DAFLGSFLYEYSR	77	
							1639.94	1639.93	-0.01	KVPQVSTPTLVEVSR	83	
78L	vit	BSA	gi 76445989*	3	206	100	1479.80	1479.80	0.01	LGEYGFQNALIVR	54	
							1567.74	1567.75	0.00	DAFLGSFLYEYSR	87	
							1639.94	1639.95	0.01	KVPQVSTPTLVEVSR	65	

Spot no.[1]	Prep[2]	Protein name	Accession no.[3]	Pep. count	Total Ion Score (protein)	C.I. (%)	Calculated Mass (Da)	Observed Mass (Da)	Match Error (Da)	Sequence	Ion Score (pep)	Mods.[4]
78R	vit	BSA	gi76445989*	2	109	100	1567.74	1567.74	0.00	DAFLGSFLYEYSR	63	
							1639.94	1639.93	0.00	KVPQVSTPTLVEVSR	46	
79	vit	BSA	gi74267962*	1	101	100	1639.94	1639.94	0.00	KVPQVSTPTLVEVSR	101	
100	mat	unknown function	Sm00115	2	205	100	1484.73	1484.73	0.00	TEFDEEFVSLLR	77	
							1812.90	1812.91	0.00	AEKTEFDEEFVSLLR	127	
101	mat	IPSE/ESP3-6	gi28894857*	4	166	100	958.49	958.48	0.00	GSYIEVYK	40	
							1595.70	1595.70	-0.01	YCLQLYDETYER	46	
							1634.78	1634.78	-0.01	ITGLGHGTCIDDFTK	61	Carb (C)[9]
							1652.73	1652.71	-0.13	YCLQLYDETYER	65	Carb (C)[2]
102	mat	IPSE/ESP3-6	gi28894857*	3	174	100	958.49	958.48	0.00	GSYIEVYK	40	
							1634.78	1634.78	0.00	ITGLGHGTCIDDFTK	64	Carb (C)[9]
							1652.73	1652.72	-0.01	YCLQLYDETYER	71	Carb (C)[2]
103	mat	IPSE/ESP3-6	gi28894857*	1	65	99.90	1652.73	1652.73	0.00	YCLQLYDETYER	65	Carb (C)[2]
104	mat	IPSE/ESP3-6	gi28894857*	1	67	99.94	1652.73	1652.72	-0.01	YCLQLYDETYER	67	Carb (C)[2]
105	mat	SmE16	Phat12638	3	314	100	1320.72	1320.71	0.00	ISLEEYLNALR	91	
							1704.78	1704.77	-0.01	DGELDYDEFLAYVR	109	
							1946.91	1946.90	-0.02	NKDGELDYDEFLAYVR	115	
106	mat	GST 26kDa	Sm00145	3	230	100	1390.74	1390.73	-0.01	VDFLNQLPGMLK	41	Ox (M)[10]
							1597.81	1597.80	-0.01	LLLEYLGEAYEER	94	
							1938.98	1938.99	0.00	LGLDFPNLPYYIDGDVK	96	
107	mat	lactate dehydrogenase	Sm00165	5	377	100	1291.70	1291.70	0.00	QVVQSAYDIIR	51	
							1536.80	1536.80	0.00	YSANSDIVVITAGAR	85	
							1730.86	1730.87	0.01	GEVLDLQHGQQFFGR	100	
							1958.02	1958.03	0.00	VKGEVLDLQHGQQFFGR	38	
							2031.13	2031.13	0.00	CIIVVVSNPVDILTYVAR	102	Carb (C)[1]

Spot no.[1]	Prep[2]	Protein name	Accession no.[3]	Pep. count	Total Ion Score (protein)	C.I. (%)	Calculated Mass (Da)	Observed Mass (Da)	Match Error (Da)	Sequence	Ion Score (pep)	Mods.[4]
108	mat	ESP15	Sm00193	1	68	99.99	2015.99	2016.05	0.07	DGCPIPSTPDLLLGNYQR	68	Carb (C)[3]
109	mat	Phosphoenolpyruvate carboxykinase	Sm00203	1	54	99.92	1667.83	1667.83	0.00	DLPDVIQNELNNQR	54	
110	mat	HSP10	Sm00296	2	114	100	1110.58	1110.53	-0.05	VFLPEYGGTK	35	
							1543.78	1543.71	-0.07	VVLDENEYFLFR	79	
111	mat	HSP70	Sm00325	7	569	100	975.59	975.60	0.01	LNIDLFLK	62	
							1199.68	1199.69	0.02	FDLTGIPPALR	76	
							1566.78	1566.80	0.02	ITPSYVAFTPEGER	84	
							1705.84	1705.88	0.04	NQLTSNPENTVFDVK	44	
							1887.97	1888.00	0.03	VTHAVVTVPAYFNDAQR	104	
							1999.09	1999.13	0.04	GVPQIEVTFEIDVNGILR	81	
							2538.25	2538.30	0.05	SQIFSTAADNQPTVTIQVFEGER	118	
112	mat	HSP70	Sm00325	7	704	100	975.59	975.58	0.00	LNIDLFLK	61	
							1199.68	1199.68	0.00	FDLTGIPPALR	79	
							1566.78	1566.78	0.00	ITPSYVAFTPEGER	97	
							1705.84	1705.85	0.01	NQLTSNPENTVFDVK	51	
							1887.97	1887.97	0.00	VTHAVVTVPAYFNDAQR	161	
							1999.09	1999.09	0.00	GVPQIEVTFEIDVNGILR	97	
							2538.25	2538.25	0.00	SQIFSTAADNQPTVTIQVFEGER	158	
113	mat	malate dehydrogenase	Sm00407	3	157	100	1292.72	1292.72	0.00	DVIFSFPVQIK	39	
							1435.74	1435.74	0.00	FAITAEELKEER	76	
							1726.95	1726.95	0.00	VVVVGNPANTNALALMK	42	Ox (M)[16]
114	mat	malate dehydrogenase	Sm00407	6	283	100	937.47	937.47	0.00	ENFSALTR	32	
							1021.56	1021.56	0.00	FAITAEELK	40	
							1292.72	1292.72	0.00	DVIFSFPVQIK	72	
							1435.74	1435.74	-0.01	FAITAEELKEER	52	
							1726.95	1726.96	0.00	VVVVGNPANTNALALMK	55	Ox (M)[16]
							1964.06	1964.07	0.00	VLLTGAAGQIGYSLAGMVAR	32	Ox (M)[17]

Spot no.[1]	Prep[2]	Protein name	Accession no.[3]	Pep. count	Total Ion Score (protein)	C.I. (%)	Calculated Mass (Da)	Observed Mass (Da)	Match Error (Da)	Sequence	Ion Score (pep)	Mods.[4]
115	mat	dihydrolipoamide dehydrogenase	Sm00414	2	140	100	1426.79	1426.79	-0.01	AVSSLTGGIAYLFK	88	
							1603.88	1603.88	0.00	RPYTSGLGLENVGIK	51	
116	mat	succinate-CoA-ligase	Sm00415	1	83	100	1595.93	1595.94	0.02	KPVVSFIAGVTAPPGR	83	
119	mat	calreticulin	Sm00636	4	253	100	1077.57	1077.57	0.00	KISEPFSNR	61	
							1092.55	1092.55	0.01	KFHGESPYK	35	
							1282.69	1282.70	0.01	SPVDPIEDLGLK	81	
							1526.83	1526.84	0.01	THLYTLIVNPNNK	77	
120	mat	calreticulin	Sm00636	3	212	100	1077.57	1077.57	0.00	KISEPFSNR	54	
							1282.69	1282.69	0.00	SPVDPIEDLGLK	79	
							1526.83	1526.83	0.00	THLYTLIVNPNNK	79	
124	mat	ATP synthase	Sm00685	3	272	100	1038.59	1038.60	0.00	IPVGPETLGR	83	
							1435.75	1435.75	0.00	FTQAGSEVSALLGR	96	
							2001.03	2001.04	0.01	AIAELGIYPAVDPLDSNSR	93	
126	mat	actin	Sm00900	5	443	100	976.45	976.45	0.00	AGFAGDDAPR	46	
							1132.53	1132.53	0.00	GYSFTTTAER	57	
							1486.69	1486.69	0.00	QEYDESGPGIVHR	107	
							1790.89	1790.89	0.00	SYELPDGQVITIGNER	130	
							1954.06	1954.06	0.00	VAPEEHPVLLTEAPLNPK	104	
127	mat	actin	Sm00900	7	445	100	976.45	976.47	0.02	AGFAGDDAPR	34	
							1132.53	1132.55	0.03	GYSFTTTAER	50	
							1198.71	1198.74	0.03	AVFPSIVGRPR	33	
							1486.69	1486.73	0.04	QEYDESGPGIVHR	65	
							1790.89	1790.93	0.04	SYELPDGQVITIGNER	122	
							1954.06	1954.12	0.06	VAPEEHPVLLTEAPLNPK	94	
							2233.04	2233.12	0.07	DLYSNTVLSGGSTMYPGIADR	47	Ox (M)[14]

Spot no.[1]	Prep[2]	Protein name	Accession no.[3]	Pep. count	Total Ion Score (protein)	C.I. (%)	Calculated Mass (Da)	Observed Mass (Da)	Match Error (Da)	Sequence	Ion Score (pep)	Mods.[4]
128	mat	actin	Sm00900	5	395	100	1132.53	1132.52	0.00	GYSFTTTAER	41	
							1198.71	1198.70	0.00	AVFPSIVGRPR	34	
							1486.69	1486.69	-0.01	QEYDESGPGIVHR	84	
							1790.89	1790.88	-0.01	SYELPDGQVITIGNER	115	
							1954.06	1954.06	0.00	VAPEEHPVLLTEAPLNPK	122	
130	mat	disulphide isomerase	Sm00980	5	419	100	1039.58	1039.60	0.02	VLEFFGLSK	65	
							1059.66	1059.68	0.02	ANIAILGFIK	52	
							1261.58	1261.60	0.02	NEQPIDFGGER	77	
							1797.95	1797.98	0.03	LHVIYVDVDVENNLR	151	
							1974.03	1974.08	0.05	HFIQVESVPLVSEFSQK	73	
131	mat	triose phosphate isomerase	Sm00999	1	53	99.91	1737.90	1737.89	-0.01	VATPQQAQEVHNFLR	53	
134	mat	GAPDH	Sm01185	4	235	100	1176.64	1176.64	0.00	AGISLNNNFVK	53	
							1208.65	1208.64	0.00	VVDLITHMHK	55	Ox (M)[8]
							1557.79	1557.80	0.00	VPTPDVSVVDLTCR	73	Carb (C)[13]
							1795.77	1795.78	0.00	LVSWYDNEFGYSCR	54	Carb (C)[13]
135	mat	aldehyde dehydrogenase	Sm01315	9	796	100	1249.64	1249.64	0.00	FNTLEEVIER	90	
							1397.79	1397.79	0.00	SPLIILADADIEK	99	
							1432.75	1432.75	0.00	EEIFGPVQCILK	40	
							1507.76	1507.76	0.00	QLPVDGNMITFTR	42	
							1637.82	1637.82	0.00	LADLIEMNAEYIAR	51	
							1696.86	1696.87	0.00	IFVQAPIYDQMVEK	52	
							1812.91	1812.91	0.00	TVESALGDVFFAAQTTR	151	
							1970.89	1970.90	0.01	ANATHYGLGAGVFTSDMDK	156	
							2004.99	2005.00	0.01	YTQLFIGNEFVDSESKK	113	

Spot no.[1]	Prep[2]	Protein name	Accession no.[3]	Pep. count	Total Ion Score (protein)	C.I. (%)	Calculated Mass (Da)	Observed Mass (Da)	Match Error (Da)	Sequence	Ion Score (pep)	Mods.[4]
136	mat	phosphoglycerate kinase	Sm01343	3	200	100	1634.79	1634.80	0.01	LGDVYVNDAFGTAHR	79	
							1741.92	1741.93	0.01	VNELIIGGGMAYTFLK	50	Ox (M)[10]
							1796.01	1796.02	0.01	ALENPERPFLAILGGAK	72	
138	mat	HSP60	Sm01537	6	539	100	1285.67	1285.69	0.01	LEDVQLQDLGR	83	
							1431.72	1431.72	0.00	GYISPYFLNTEK	39	
							1623.91	1623.91	0.01	AAIEEGIVPGGGTALLR	107	
							2405.38	2405.38	0.00	RPLLIIAEDVEGEALTA LVLNR	64	
							2456.35	2456.34	-0.01	TALVDAAGVASLLTTAE TVVTDLPK	65	
							2560.25	2560.25	0.00	LVQDVANNTNEEAGDG TTTATVLAR	182	
140	mat	citrate synthase	Sm01548	1	57	99.90	1701.90	1701.85	-0.05	GLVTETSVLDVNEGIR	57	
141	mat	cysteine protease inhibitor	Sm01636	1	86	100	2204.17	2204.09	-0.08	SFEIVQITSQVVAGTNHFVK	86	
142	mat	HSP70	Sm01676	2	90	100	1673.89	1673.88	-0.01	VINEPTAAALAYGLDR	57	
							1722.88	1722.87	-0.01	NVVITVPAYFNDSQR	33	
143	mat	elongation factor 1 alpha	Sm01686	1	44	99.56	975.55	975.56	0.01	IPLQDVK	44	
144	mat	GST (28kDa)	Sm02267	4	220	100	869.45	869.45	0.00	VIYFDGR	35	
							986.53	986.53	0.00	ENLLASSPR	54	
							1165.60	1165.60	0.00	YLSNRPATPF	39	
							1667.80	1667.80	0.00	LIGQAEDVEHEYHK	92	
146	mat	proteasome α7 subunit	Sm02321	3	179	100	1091.61	1091.61	0.01	IPLYSLTER	62	
							1170.57	1170.58	0.01	LFDEAETFAK	39	
							1298.66	1298.67	0.01	KLFDEAETFAK	78	
147	mat	aldo keto reductase	Sm03515	3	167	100	1196.55	1196.57	0.02	HLDCAYVYR	40	Carb (C)[4]
							1672.82	1672.86	0.04	IEENFGVFDFQLSK	79	
							1828.92	1828.95	0.03	RIEENFGVFDFQLSK	49	
149	mat	calmodulin	Sm03962	2	156	100	1738.88	1738.86	-0.02	VFDKDGNGFISAAELR	85	
							1844.89	1844.88	-0.01	EAFSLFDKDGDGTITTK	71	

Spot no.[1]	Prep[2]	Protein name	Accession no.[3]	Pep. count	Total Ion Score (protein)	C.I. (%)	Calculated Mass (Da)	Observed Mass (Da)	Match Error (Da)	Sequence	Ion Score (pep)	Mods.[4]
151	mat	unknown function	Sm05001	2	164	100	1794.00	1794.05	0.05	YVLFQIIDNEISVIK	77	
							1979.02	1979.07	0.05	GANLIYFSLVSDSAPPTAR	88	
154	mat	tubulin β chain	Sm06624	4	317	100	1053.61	1053.61	0.00	YLTVAAIFR	48	
							1130.60	1130.59	0.00	FPGQLNADLR	81	
							1901.97	1901.96	-0.01	MSVTFIGNSTAIQELFK	78	Ox (M)[1]
							1958.98	1958.96	-0.02	GHYTEGAELVDSVLDVVR	110	
155	mat	Tubulin β chain	Sm06624	4	334	100	1053.61	1053.62	0.01	YLTVAAIFR	66	
							1130.60	1130.60	0.01	FPGQLNADLR	79	
							1314.63	1314.64	0.01	INVYYNEASGGK	43	
							1958.98	1958.99	0.01	GHYTEGAELVDSVLDVVR	147	
157	mat	α-N-acetylgalactosaminidase	Sm06626	1	67	100	1766.86	1766.86	0.00	VDGGPINFTTNLDEFK	67	
159	mat	p40	Sm07196	7	835	100	1234.67	1234.66	-0.01	QHNAVSIPVNR	76	
							1432.73	1432.73	0.00	DLLTGLEHGGGAHR	124	
							1603.78	1603.78	-0.01	GVHGLSYVDDGSGGKR	45	
							1782.86	1782.86	0.00	MGSLDVPSTGSVNDFLK	111	Ox (M)[1]
							2095.97	2095.95	-0.02	FDAQGFAPQDINVTSSE NR	170	
							2183.14	2183.13	-0.01	VDQNQSLTLNESGQVAVRPK	181	
							2780.43	2780.40	-0.02	LHVEVPVDPVYKPEDLFVNVDSNR	127	
160	mat	p40	Sm07196	2	174	100	1234.67	1234.65	-0.02	QHNAVSIPVNR	57	
							2095.97	2095.93	-0.03	FDAQGFAPQDINVTSSENR	117	
161	mat	p40	Sm07196	8	966	100	1054.63	1054.62	0.00	AVPASQALVAK	47	
							1234.67	1234.65	-0.01	QHNAVSIPVNR	98	
							1432.73	1432.71	-0.02	DLLTGLEHGGGAHR	151	
							1603.78	1603.76	-0.02	GVHGLSYVDDGSGGKR	88	
							1782.86	1782.85	-0.01	MGSLDVPSTGSVNDFLK	96	Ox (M)[1]
							2095.97	2095.93	-0.04	FDAQGFAPQDINVTSSENR	170	
							2183.14	2183.11	-0.03	VDQNQSLTLNESGQVAVRPK	182	
							2780.43	2780.39	-0.03	LHVEVPVDPVYKPEDLFVNVDSNR	133	

Spot no.[1]	Prep[2]	Protein name	Accession no.[3]	Pep. count	Total Ion Score (protein)	C.I. (%)	Calculated Mass (Da)	Observed Mass (Da)	Match Error (Da)	Sequence	Ion Score (pep)	Mods.[4]
162	mat	p40	Sm07196	7	887	100	1234.67	1234.67	0.00	QHNAVSIPVNR	85	
							1432.73	1432.73	0.00	DLLTGLEHGGGAHR	122	
							1603.78	1603.79	0.01	GVHGLSYVDDGSGGKR	104	
							1782.86	1782.88	0.02	MGSLDVPSTGSVNDFLK	98	Ox (M)[1]
							2095.97	2095.97	0.01	FDAQGFAPQDINVTSSENR	169	
							2183.14	2183.15	0.01	VDQNQSLTLNESGQVAVRPK	191	
							2780.43	2780.46	0.04	LHVEVPVDPVYKPEDLFVNVDSNR	119	
163	mat	p40	Sm07196	7	853	100	1234.67	1234.66	0.00	QHNAVSIPVNR	94	
							1432.73	1432.72	0.00	DLLTGLEHGGGAHR	146	
							1603.78	1603.78	0.00	GVHGLSYVDDGSGGKR	64	
							1782.86	1782.86	0.00	MGSLDVPSTGSVNDFLK	76	
							2095.97	2095.95	-0.02	FDAQGFAPQDINVTSSENR	181	
							2183.14	2183.13	-0.02	VDQNQSLTLNESGQVAVRPK	187	
							2780.43	2780.40	-0.03	LHVEVPVDPVYKPEDLFVNVDSNR	106	
165	mat	p40	Sm07598	1	100	100	1675.83	1675.83	0.00	DNQVHSIGSISDYLK	100	
166	mat	unknown function	Sm07933	2	141	100	1125.59	1125.58	-0.01	FLSLEPYTR	61	
							1465.68	1465.67	-0.01	EQYYEAYSTLAK	80	
167	mat	unknown function	Sm07933	3	223	100	1125.59	1125.60	0.00	FLSLEPYTR	49	
							1415.67	1415.68	0.01	APQIYHEECLR	80	
							2288.06	2288.07	0.01	NGATDITLLQSYENEYEEAK	94	
169	mat	disulphide isomerase	Sm08285	6	389	100	986.52	986.52	0.01	HGQGLVGYR	54	
							1168.64	1168.65	0.01	GFPTIYFVPK	44	
							1295.61	1295.62	0.01	EATEELIGYDR	73	
							1362.66	1362.67	0.01	TKFEDDFAVYK	45	
							1403.68	1403.69	0.01	FSLDAFSDFLNK	91	
							1532.83	1532.84	0.01	LAPEFTSAAQIISGK	82	

Spot no.[1]	Prep[2]	Protein name	Accession no.[3]	Pep. count	Total Ion Score (protein)	C.I. (%)	Calculated Mass (Da)	Observed Mass (Da)	Match Error (Da)	Sequence	Ion Score (pep)	Mods.[4]
170	mat	disulphide isomerase	Sm08285	4	268	100	1168.64	1168.65	0.01	GFPTIYFVPK	45	
							1295.61	1295.62	0.01	EATEELIGYDR	57	
							1403.68	1403.68	0.00	FSLDAFSDFLNK	96	
							1532.83	1532.83	0.00	LAPEFTSAAQIISGK	70	
171	mat	proteasome α6	Sm08991	2	163	100	1612.89	1612.89	0.00	ALNSTLPNEVSLNIK	68	
							1730.82	1730.81	0.00	FTIFEDDDIDPYLK	95	
172L	mat	HSP70	Sm09042	7	633	100	1081.57	1081.57	0.00	LLQDFFNGK	37	
							1169.66	1169.67	0.00	DAGAIAGLNVLR	64	
							1253.62	1253.62	0.00	FEELNADLFR	76	
							1480.75	1480.76	0.00	ARFEELNADLFR	45	
							1787.99	1787.99	0.00	IINEPTAAAIAYGLDKK	106	
							1982.98	1982.98	0.00	TVSDAVITVPAYFNDSQR	128	
							2758.33	2758.33	0.00	QTQTFTTYSDNQPGVLIQVFEGER	177	
172R	mat	HSP70	Sm09042	8	757	100	1081.57	1081.56	0.00	LLQDFFNGK	45	
							1169.66	1169.67	0.01	DAGAIAGLNVLR	93	
							1253.62	1253.62	0.00	FEELNADLFR	80	
							1480.75	1480.76	0.01	ARFEELNADLFR	33	
							1787.99	1788.00	0.01	IINEPTAAAIAYGLDKK	107	
							1982.98	1982.98	0.00	TVSDAVITVPAYFNDSQR	138	
							2516.29	2516.28	-0.01	GTPQIEVTFDIDANGILNVSAVDK	127	
							2758.33	2758.32	-0.01	QTQTFTTYSDNQPGVLIQVFEGER	134	
173	mat	HSP70	Sm09042	7	632	100	1081.57	1081.57	0.00	LLQDFFNGK	68	
							1169.66	1169.66	0.00	DAGAIAGLNVLR	82	
							1253.62	1253.61	0.00	FEELNADLFR	76	
							1481.81	1481.79	-0.02	SQIHDIVLVGGSTR	34	
							1691.73	1691.71	-0.01	STAGDTHLGGEDFDNR	67	
							1982.98	1982.96	-0.02	TVSDAVITVPAYFNDSQR	147	
							2758.33	2758.29	-0.04	QTQTFTTYSDNQPGVLIQVFEGER	157	

Spot no.[1]	Prep[2]	Protein name	Accession no.[3]	Pep. count	Total Ion Score (protein)	C.I. (%)	Calculated Mass (Da)	Observed Mass (Da)	Match Error (Da)	Sequence	Ion Score (pep)	Mods.[4]
174	mat	HSP70	Sm09042	8	766	100	1081.57	1081.57	0.00	LLQDFFNGK	61	
							1169.66	1169.67	0.01	DAGAIAGLNVLR	96	
							1253.62	1253.62	0.00	FEELNADLFR	89	
							1473.69	1473.69	0.00	TTPSYVAFTDSER	49	
							1691.73	1691.72	0.00	STAGDTHLGGEDFDNR	96	
							1787.99	1787.99	0.00	IINEPTAAAIAYGLDKK	64	
							1982.98	1982.98	-0.01	TVSDAVITVPAYFNDSQR	152	
							2758.33	2758.33	0.00	QTQTFTTYSDNQPGVLIQVFEGER	159	
175	mat	HSP70	Sm09042	7	705	100	1081.57	1081.57	0.00	LLQDFFNGK	65	
							1169.66	1169.67	0.01	DAGAIAGLNVLR	86	
							1253.62	1253.62	0.00	FEELNADLFR	69	
							1691.73	1691.73	0.00	STAGDTHLGGEDFDNR	87	
							1787.99	1787.99	0.00	IINEPTAAAIAYGLDKK	86	
							1982.98	1982.98	0.00	TVSDAVITVPAYFNDSQR	148	
							2758.33	2758.31	-0.03	QTQTFTTYSDNQPGVLIQVFEGER	164	
177	mat	tubulin β chain	Sm10465	2	105	100	1053.61	1053.63	0.02	YLTVAAIFR	39	
							1130.60	1130.61	0.02	FPGQLNADLR	65	
178	mat	paramyosin	Sm11278	3	206	100	1327.72	1327.72	0.00	LQLANEIEEIR	37	
							1493.75	1493.74	0.00	VKDLETFLDEER	36	
							2075.05	2075.04	-0.01	DLQSEIESLSLENSELIR	133	
180	mat	translationally-controlled tumour protein	Sm11405	1	94	100	1446.69	1446.70	0.01	VVADFFYEVDSR	94	
180	mat	translationally-controlled tumour protein	Sm11405	4	274	100	971.57	971.58	0.01	AHLNLYLK	60	
							1182.58	1182.60	0.03	FTTVSSNVDGR	37	
							1446.69	1446.72	0.03	VVADFFYEVDSR	73	
							1999.06	1999.13	0.06	VIDLVHANGFISVPFDQK	105	
181	mat	superoxide dismutase	Sm11433	2	87	100	1366.78	1366.82	0.04	LISLNGSHSIIGR	30	
							2213.06	2213.14	0.08	FTQETDNGPVHVHAEFSGLK	58	

Spot no.[1]	Prep[2]	Protein name	Accession no.[3]	Pep. count	Total Ion Score (protein)	C.I. (%)	Calculated Mass (Da)	Observed Mass (Da)	Match Error (Da)	Sequence	Ion Score (pep)	Mods.[4]
184	mat	enolase	Sm12193	3	238	100	1113.65	1113.65	0.00	GLQLLEEAIK	46	
							1188.64	1188.64	0.01	AGAAEAGLPLYR	72	
							1764.92	1764.91	-0.01	AAVPSGASTGVHEALELR	120	
185	mat	enolase	Sm12193	5	433	100	952.62	952.56	-0.06	IIAPALINK	33	
							1113.65	1113.65	0.00	GLQLLEEAIK	64	
							1188.64	1188.63	0.00	AGAAEAGLPLYR	65	
							1764.92	1764.91	-0.02	AAVPSGASTGVHEALELR	141	
							2116.11	2116.11	-0.01	LTSSTNIQIVGDDLTVTNPK	132	
186	mat	enolase	Sm12193	3	251	100	1113.65	1113.65	0.00	GLQLLEEAIK	61	
							1188.64	1188.64	0.00	AGAAEAGLPLYR	79	
							1764.92	1764.91	-0.01	AAVPSGASTGVHEALELR	112	
188	mat	thioredoxin peroxidase	Sm12448	5	326	100	1209.65	1209.64	-0.01	LLDAFQFVEK	68	
							1240.70	1240.69	-0.01	QITINDKPVGR	60	
							1327.77	1327.77	-0.01	GLFIIDPNGILR	48	
							1380.80	1380.79	-0.01	VLLPNRPAPEFK	43	
							1589.69	1589.68	-0.01	AYGVFDEEDGNAFR	107	
189	mat	valosin-containing protein	Sm12453	2	102	100	1298.70	1298.70	0.01	EIEIGIPDSIGR	42	
							1742.93	1742.93	0.00	LDQLIYPLPDEASR	59	
190L	mat	peptidyl prolyl cis trans isomerase	Sm12777	1	96	100	1679.86	1679.86	-0.01	IIFELFNDVPDTTR	96	
190R	mat	peptidyl prolyl cis trans isomerase	Sm12777	2	148	100	915.55	915.55	0.00	VVSGIDVVK	38	
							1679.86	1679.88	0.01	IIFELFNDVPDTTR	110	
191	mat	nucleoside diphosphate kinase	Sm12959	2	86	100	970.57	970.55	-0.02	GLVGEVIQR	53	
							1970.97	1970.97	0.00	LVAYMSSGPVVPMVFEGR	33	Ox (M)[5,13]
192	mat	unknown function	Snap04600	3	218	100	948.51	948.50	-0.01	ELMELIGK	33	
							1236.67	1236.67	0.01	QALHLGNEINK	93	
							2057.98	2057.99	0.01	NASPEDLEAIFPEFHDVK	93	
193	mat	unknown function	Snap15963	2	177	100	1099.62	1099.63	0.00	GAQVSLVVNGR	49	
							1929.90	1929.89	-0.01	GTDDYSVFLLHEGSYAR	128	

Spot no.[1]	Prep[2]	Protein name	Accession no.[3]	Pep. count	Total Ion Score (protein)	C.I. (%)	Calculated Mass (Da)	Observed Mass (Da)	Match Error (Da)	Sequence	Ion Score (pep)	Mods.[4]
194	mat	HSP90	Snap28164	4	201	100	1275.60	1275.60	0.00	FASEFQQQYK	47	
							1695.95	1695.96	0.01	QIVLLQHGAFTLEAR	52	
							1744.93	1744.93	0.00	TPFVPEQILAIQMNK	44	Ox (M)[13]
							1938.98	1938.98	0.00	VVDVVVNVPTYYTDAER	57	
196	mat	α-N-acetylgalactosaminidase	Snap35009	3	245	100	986.51	986.50	0.00	GGHQAEFIK	41	
							1135.61	1135.61	0.00	VDQFSASLLR	95	
							1723.83	1723.83	0.00	GDGGPINFTTNLNEFK	110	
197	mat	α-N-acetylgalactosaminidase	Snap35009	2	163	100	1135.61	1135.61	0.00	VDQFSASLLR	51	
							1723.83	1723.83	0.00	GDGGPINFTTNLNEFK	111	
198	mat	plant pathogenesis family (PR1)	Snap41543	3	177	100	978.43	978.43	0.00	NYDFYTR	38	
							1309.69	1309.69	0.00	NELLTLHNEAR	55	
							1810.06	1810.06	0.00	NGQLFGQPIAVSIKPLK	85	
206	imm	HSP70	Sm00325	4	340	100	1199.68	1199.68	0.00	FDLTGIPPALR	70	
							1213.69	1213.69	0.00	DAGTIAGLNILR	78	
							1566.78	1566.77	-0.01	ITPSYVAFTPEGER	96	
							1861.94	1861.94	0.00	NQLTSNPENTVFDVKR	96	
210	imm	chaperonin	Sm00497	2	107	100	1213.75	1213.75	0.00	TAIETAILLLR	69	
							1434.72	1434.72	0.01	TIGDEYFTFITK	39	
220	imm	actin	Sm00900	1	61	99.96	976.45	976.42	-0.03	AGFAGDDAPR	61	
224	imm	unknown function	Sm01135	2	134	100	1299.67	1299.67	0.01	ENPNLVASSNVR	63	
							1833.92	1833.93	0.01	NLFDTVSGDLNVPVESK	71	
226	imm	aldehyde dehydrogenase	Sm01315	2	88	100	1249.64	1249.65	0.01	FNTLEEVIER	35	
							1812.91	1812.92	0.01	TVESALGDVFFAAQTTR	53	
227	imm	phosphoglycerate kinase	Sm01343	2	125	100	1634.79	1634.78	-0.01	LGDVYVNDAFGTAHR	51	
							1796.01	1795.99	-0.01	ALENPERPFLAILGGAK	73	

Spot no.[1]	Prep[2]	Protein name	Accession no.[3]	Pep. count	Total Ion Score (protein)	C.I. (%)	Calculated Mass (Da)	Observed Mass (Da)	Match Error (Da)	Sequence	Ion Score (pep)	Mods.[4]
229	imm	HSP86	Sm01524	5	293	100	948.45	948.45	0.00	FYEQFSK	35	
							1184.66	1184.67	0.01	EVLQQNNVLK	37	
							1348.66	1348.67	0.01	HFSVEGQLEFR	63	
							1513.79	1513.80	0.01	GVVDSEDLPLNISR	68	
							1848.82	1848.84	0.02	NPEDITTEEYAEFYK	90	
230	imm	HSP86	Sm01524	7	511	100	948.45	948.44	0.00	FYEQFSK	40	
							1205.63	1205.63	0.00	HSSFINYPIK	82	
							1348.66	1348.66	0.00	HFSVEGQLEFR	89	
							1513.79	1513.78	0.00	GVVDSEDLPLNISR	70	
							1848.82	1848.82	0.00	NPEDITTEEYAEFYK	105	
							1945.92	1945.92	0.00	MKPEQQDIYYITGESK	78	Ox (M)[1]
							2383.16	2383.16	0.00	GFEVLYMVDPIDEYAVTHLR	48	Ox (M)[7]
232	imm	HSP60	Sm01537	1	75	100	1623.91	1623.90	-0.01	AAIEEGIVPGGGTALLR	75	
245	imm	Sm14 fatty acid binding protein	Sm04779	1	78	100	1232.68	1232.71	0.03	TTVTVGDVTAIR	78	
249	imm	fructose bisphosphate aldolase	Sm05684	7	482	100	1296.72	1296.72	0.00	VTEQVLAFVYK	59	
							1433.74	1433.74	0.00	AYTPQENALATVR	85	
							1698.85	1698.85	0.00	LQQIGVENNEENRR	46	
							1879.93	1879.92	-0.01	FQPYLTEAQENDLRR	34	
							2041.10	2041.09	-0.01	LAENISGVILFEETLHQK	106	
							2285.20	2285.19	-0.01	TVPPAVPGITFLSGGQSELDATK	38	
							2330.15	2330.14	-0.01	GVVPLAGTDNETTTQGLDDLASR	115	
254	imm	p40	Sm07196	1	125	100	2095.97	2096.04	0.07	FDAQGFAPQDINVTSSENR	125	
255	imm	p40	Sm07196	2	199	100	1234.67	1234.65	-0.01	QHNAVSIPVNR	61	
							2095.97	2095.95	-0.02	FDAQGFAPQDINVTSSENR	138	
256	imm	p40	Sm07196	4	482	100	1234.67	1234.66	0.00	QHNAVSIPVNR	66	
							1432.73	1432.72	-0.01	DLLTGLEHGGGAHR	79	
							2095.97	2095.95	-0.02	FDAQGFAPQDINVTSSENR	170	
							2183.14	2183.13	-0.01	VDQNQSLTLNESGQVAVRPK	168	

Spot no.[1]	Prep[2]	Protein name	Accession no.[3]	Pep. count	Total Ion Score (protein)	C.I. (%)	Calculated Mass (Da)	Observed Mass (Da)	Match Error (Da)	Sequence	Ion Score (pep)	Mods.[4]
264	imm	HSP70	Sm09042	2	112	100	1169.66	1169.65	-0.01	DAGAIAGLNVLR	55	
							1253.62	1253.60	-0.02	FEELNADLFR	57	
265	imm	HSP70	Sm09042	3	215	100	1169.66	1169.67	0.00	DAGAIAGLNVLR	59	
							1253.62	1253.62	0.00	FEELNADLFR	55	
							1982.98	1982.97	-0.01	TVSDAVITVPAYFNDSQR	100	
266	imm	HSP70	Sm09042	3	129	100	1253.62	1253.62	0.00	FEELNADLFR	51	
							1480.75	1480.76	0.01	ARFEELNADLFR	41	
							1982.98	1982.99	0.01	TVSDAVITVPAYFNDSQR	37	
276	imm	enolase	Sm12193	3	207	100	1113.65	1113.65	0.00	GLQLLEEAIK	53	
							1188.64	1188.65	0.01	AGAAEAGLPLYR	59	
							1764.92	1764.93	0.01	AAVPSGASTGVHEALELR	96	
281	imm	valosin-containing protein	Sm12453	1	59	99.95	1742.93	1742.93	0.00	LDQLIYIPLPDEASR	59	
283	imm	ferritin heavy chain	Sm12942	4	204	100.00	1207.67	1207.67	0.00	LSDYITNLIR	60	
							1299.59	1299.59	0.00	FFLNESEEER	71	
							1560.80	1560.80	0.00	VNQSLMELVAVGER	33	Ox (M)[6]
							1688.90	1688.90	0.00	KVNQSLMELVAVGER	41	Ox (M)[7]
301	mira	SmE16	Phat12638	3	232	100.00	1320.72	1320.71	-0.01	ISLEEYLNALR	65	
							1704.78	1704.77	-0.01	DGELDYDEFLAYVR	75	
							1946.91	1946.90	-0.01	NKDGELDYDEFLAYVR	94	
302	mira	SmE16	Phat12638	3	248	100.00	1320.72	1320.70	-0.02	ISLEEYLNALR	68	
							1704.78	1704.77	-0.01	DGELDYDEFLAYVR	87	
							1946.91	1946.89	-0.02	NKDGELDYDEFLAYVR	94	
307	mira	HSP10	Sm00296	2	130	100	1392.76	1392.76	0.00	VLEATVVAHGPGSR	54	
							1543.78	1543.78	0.00	VVLDENEYFLFR	78	

Spot no.[1]	Prep[2]	Protein name	Accession no.[3]	Pep. count	Total Ion Score (protein)	C.I. (%)	Calculated Mass (Da)	Observed Mass (Da)	Match Error (Da)	Sequence	Ion Score (pep)	Mods.[4]
308	mira	HSP70	Sm00325	6	299	100	975.59	975.59	0.00	LNIDLFLK	40	
							1199.68	1199.69	0.01	FDLTGIPPALR	60	
							1213.69	1213.69	0.00	DAGTIAGLNILR	41	
							1566.78	1566.78	0.00	ITPSYVAFTPEGER	41	
							1887.97	1887.96	-0.01	VTHAVVTVPAYFNDAQR	57	
							2538.25	2538.22	-0.03	SQIFSTAADNQPTVTIQVFEGER	60	
310	mira	malate dehydrogenase	Sm00407	2	109	100	1292.72	1292.72	0.00	DVIFSFPVQIK	61	
							1435.74	1435.74	0.00	FAITAEELKEER	48	
314	mira	malate dehydrogenase	Sm00493	2	58	99.50	1219.71	1218.70	0.00	LFGVTTLDVVR	49	
							1296.66	1295.65	0.00	FAVSLLEAMSGR	19	
317	mira	tubulin α chain	Sm00654	1	65	99.98	1687.89	1687.89	0.00	AVFVDLEPTVVDEVR	65	
318	mira	Tubulin α chain	Sm00654	3	218	100	1071.60	1071.60	0.00	EIVDLVLDR	34	
							1687.89	1687.88	-0.01	AVFVDLEPTVVDEVR	101	
							2409.21	2409.22	0.01	FDGALNVDLTEFQTNLVPYPR	82	
319	mira	thioredoxin peroxidase	Sm00674	3	228	100	1225.69	1225.69	0.00	QITINDLPVGR	64	
							1274.75	1274.75	0.00	GLFIISADGIIR	75	
							1570.82	1570.82	-0.01	DYGVLHEELGVALR	89	
320	mira	ATP synthase	Sm00685	4	313	100	1038.59	1038.58	-0.01	IPVGPETLGR	58	
							1435.75	1435.73	-0.02	FTQAGSEVSALLGR	105	
							1907.95	1907.92	-0.03	DQEGQDVLLFVDNIFR	97	
							2001.03	2001.00	-0.03	AIAELGIYPAVDPLDSNSR	55	
321	mira	α-N-acetylgalactosaminidase	Snap35009	2	146	100	1135.61	1135.62	0.00	VDQFSASLLR	51	
							1723.83	1723.82	0.00	GDGGPINFTTNLNEFK	95	
322	mira	actin	Sm00900	2	110	100	1198.71	1198.73	0.02	AVFPSIVGRPR	36	
							1790.89	1790.91	0.02	SYELPDGQVITIGNER	74	
323	mira	tropomodulin	Sm08082	1	48	99.52	1253.72	1253.72	-0.01	NLTELILANPR	48	
323	mira	actin	Sm00900	1	47	99.54	1790.89	1790.88	-0.01	SYELPDGQVITIGNER	47	

Spot no.[1]	Prep[2]	Protein name	Accession no.[3]	Pep. count	Total Ion Score (protein)	C.I. (%)	Calculated Mass (Da)	Observed Mass (Da)	Match Error (Da)	Sequence	Ion Score (pep)	Mods.[4]
324	mira	actin	Sm00900	3	217	100	1486.69	1486.69	0.00	QEYDESGPGIVHR	52	
							1790.89	1790.88	-0.01	SYELPDGQVITIGNER	109	
							1954.06	1954.05	-0.01	VAPEEHPVLLTEAPLNPK	55	
325	mira	actin	Sm00900	1	70	99.99	1790.89	1790.88	-0.01	SYELPDGQVITIGNER	70	
327	mira	triose phosphate isomerase	Sm00999	2	144	100	1464.72	1464.73	0.01	NIFGESDELIAEK	73	
							1737.90	1737.90	0.00	VATPQQAQEVHNFLR	71	
328	mira	triose phosphate isomerase	Sm00999	2	139	100	1464.72	1464.73	0.01	NIFGESDELIAEK	89	
							1737.90	1737.91	0.00	VATPQQAQEVHNFLR	50	
329	mira	unknown function	Sm01135	1	71	99.99	1299.67	1299.67	0.00	ENPNLVASSNVR	71	
333	mira	phosphoglycerate kinase	Sm01343	1	53	99.59	1796.01	1796.00	-0.01	ALENPERPFLAILGGAK	53	
334	mira	phosphoglycerate kinase	Sm01343	1	71	100	1796.01	1796.02	0.01	ALENPERPFLAILGGAK	71	
335	mira	phosphoglycerate kinase	Sm01343	2	79	100	1634.79	1634.79	0.00	LGDVYVNDAFGTAHR	35	
							1796.01	1796.00	-0.01	ALENPERPFLAILGGAK	45	
337	mira	HSP60	Sm01537	2	147	100	1285.67	1285.72	0.04	LEDVQLQDLGR	50	
							1623.91	1623.96	0.06	AAIEEGIVPGGGTALLR	97	
338	mira	HSP60	Sm01537	4	309	100	1024.51	1024.51	0.00	YTDALNATR	37	
							1285.67	1285.67	0.00	LEDVQLQDLGR	69	
							1623.91	1623.90	-0.01	AAIEEGIVPGGGTALLR	93	
							2560.25	2560.25	0.00	LVQDVANNTNEEAGDGTTTATVLAR	110	
339	mira	HSP60	Sm01537	1	70	100	1623.91	1623.91	0.00	AAIEEGIVPGGGTALLR	70	
342	mira	HSP70	Sm01676	2	150	100	1673.89	1673.89	0.01	VINEPTAAALAYGLDR	78	
							1722.88	1722.89	0.01	NVVITVPAYFNDSQR	72	
347	mira	unknown function (p25 family)	Sm03155	2	96	100	1113.52	1113.52	0.00	EVDFSDFVR	47	
							1241.62	1241.62	0.00	KEVDFSDFVR	49	
349	mira	Sm21.7	Sm03938	3	189	100	1091.61	1091.61	0.00	QVEVTQLFK	42	
							1267.74	1267.75	0.01	FIQTYLTLLR	75	
							2028.07	2028.08	0.01	EQSLPEGVSIIASTMPKPK	73	Ox (M)[15]

Spot no.[1]	Prep[2]	Protein name	Accession no.[3]	Pep. count	Total Ion Score (protein)	C.I. (%)	Calculated Mass (Da)	Observed Mass (Da)	Match Error (Da)	Sequence	Ion Score (pep)	Mods.[4]
350	mira	Sm14 fatty acid binding protein	Sm04779	1	61	99.98	1232.68	1232.69	0.00	TTVTVGDVTAIR	61	
352	mira	tubulin β chain	Sm06624	3	139	100	1053.61	1053.61	0.01	YLTVAAIFR	43	
							1130.60	1130.60	0.00	FPGQLNADLR	36	
							1958.98	1958.98	0.00	GHYTEGAELVDSVLDVVR	59	
353	mira	tubulin β chain	Sm06624	2	119	100	1130.60	1130.59	-0.01	FPGQLNADLR	46	
							1958.98	1958.98	0.00	GHYTEGAELVDSVLDVVR	72	
354	mira	tubulin β chain	Sm06624	4	263	100	1053.61	1053.62	0.01	YLTVAAIFR	48	
							1130.60	1130.60	0.01	FPGQLNADLR	59	
							1901.97	1901.98	0.01	MSVTFIGNSTAIQELFK	64	Ox (M)[1]
							1958.98	1958.98	0.00	GHYTEGAELVDSVLDVVR	91	
355	mira	tubulin β chain	Sm06624	5	193	100	1053.61	1053.61	0.00	YLTVAAIFR	34	
							1130.60	1130.60	0.00	FPGQLNADLR	46	
							1723.86	1723.86	0.00	SLTVPELTQQMFDAK	36	Ox (M)[11]
							1901.97	1901.97	0.00	MSVTFIGNSTAIQELFK	39	Ox (M)[1]
							1958.98	1958.98	0.00	GHYTEGAELVDSVLDVVR	38	
356	mira	tubulin β chain	Sm06624	3	207	100	1053.61	1053.61	0.00	YLTVAAIFR	49	
							1130.60	1130.59	0.00	FPGQLNADLR	66	
							1958.98	1958.96	-0.02	GHYTEGAELVDSVLDVVR	92	
357	mira	α-N-acetylgalactosaminidase	Sm06626	2	123	100	1766.86	1766.86	0.00	VDGGPINFTTNLDEFK	84	
							2438.15	2438.15	0.00	SQMYTISGDKFELLDVFTGDR	38	Ox (M)[3]
358	mira	aconitase	Sm07278	1	55	99.90	1509.77	1509.74	-0.03	SQFFITPGSEQIR	55	
359	mira	adenylate kinase	Sm06837	2	108	100	1492.93	1492.93	0.00	GELVPLEVVLALLK	63	
							1664.87	1664.87	0.00	VITIDASGTVDAIFDK	44	
360	mira	adenylate kinase	Sm06837	3	184	100	1492.93	1492.93	0.00	GELVPLEVVLALLK	85	
							1542.78	1542.77	-0.01	FHFNHLSSGDLLR	54	
							1664.87	1664.87	0.00	VITIDASGTVDAIFDK	45	

Spot no.[1]	Prep[2]	Protein name	Accession no.[3]	Pep. count	Total Ion Score (protein)	C.I. (%)	Calculated Mass (Da)	Observed Mass (Da)	Match Error (Da)	Sequence	Ion Score (pep)	Mods.[4]
361	mira	adenylate kinase	Sm06837	4	241	100	1130.66	1130.64	-0.01	VIFVLGGPGSGK	36	
							1492.93	1492.93	-0.01	GELVPLEVVLALLK	74	
							1542.78	1542.77	-0.01	FHFNHLSSGDLLR	65	
							1664.87	1664.87	-0.01	VITIDASGTVDAIFDK	66	
367	mira	p40	Sm07196	1	172	100	2095.97	2095.88	-0.09	FDAQGFAPQDINVTSSENR	172	
368	mira	p40	Sm07196	2	175	100	1234.67	1234.61	-0.06	QHNAVSIPVNR	63	
							1432.73	1432.66	-0.07	DLLTGLEHGGGAHR	112	
369	mira	p40	Sm07196	2	159	100	2095.97	2095.97	0.00	FDAQGFAPQDINVTSSENR	115	
							2183.14	2183.14	-0.01	VDQNQSLTLNESGQVAVRPK	44	
370	mira	p40	Sm07196	2	159	100	2095.97	2095.97	0.00	FDAQGFAPQDINVTSSENR	126	
							2183.14	2183.14	0.00	VDQNQSLTLNESGQVAVRPK	33	
371	mira	p40	Sm07196	3	243	100	1234.67	1234.66	0.00	QHNAVSIPVNR	37	
							2095.97	2095.95	-0.01	FDAQGFAPQDINVTSSENR	111	
							2183.14	2183.13	-0.01	VDQNQSLTLNESGQVAVRPK	94	
376	mira	HSP70	Sm09042	2	95	100	1253.62	1253.61	0.00	FEELNADLFR	56	
							1982.98	1982.97	-0.01	TVSDAVITVPAYFNDSQR	39	
377	mira	HSP70	Sm09042	4	291	100	1169.66	1169.67	0.00	DAGAIAGLNVLR	69	
							1253.62	1253.62	0.00	FEELNADLFR	77	
							1473.69	1473.69	0.01	TTPSYVAFTDSER	57	
							1982.98	1982.99	0.01	TVSDAVITVPAYFNDSQR	88	
378L	mira	HSP70	Sm09042	4	259	100	1169.66	1169.70	0.03	DAGAIAGLNVLR	65	
							1253.62	1253.65	0.03	FEELNADLFR	75	
							1473.69	1473.73	0.05	TTPSYVAFTDSER	66	
							1982.98	1983.05	0.06	TVSDAVITVPAYFNDSQR	53	
378R	mira	HSP70	Sm09042	3	278	100	1169.66	1169.66	-0.01	DAGAIAGLNVLR	56	
							1253.62	1253.60	-0.01	FEELNADLFR	89	
							1473.69	1473.68	-0.01	TTPSYVAFTDSER	39	

Spot no.[1]	Prep[2]	Protein name	Accession no.[3]	Pep. count	Total Ion Score (protein)	C.I. (%)	Calculated Mass (Da)	Observed Mass (Da)	Match Error (Da)	Sequence	Ion Score (pep)	Mods.[4]
379	mira	HSP70	Sm09042	3	210	100	1169.66	1169.67	0.01	DAGAIAGLNVLR	49	
							1253.62	1253.62	0.00	FEELNADLFR	71	
							1982.98	1982.98	0.00	TVSDAVITVPAYFNDSQR	90	
382	mira	paramyosin	Sm11278	1	60	99.51	2075.05	2075.04	-0.01	DLQSEIESLSLENSELIR	60	
385	mira	superoxide dismutase	Sm11433	3	127	100	1238.58	1238.57	-0.01	QEHGAPEDSIR	56	
							1366.78	1366.78	0.00	LISLNGSHSIIGR	38	
							2213.06	2213.10	0.03	FTQETDNGPVHVHAEFSGLK	33	
387	mira	thioredoxin	Sm11767	3	173	100	1274.66	1274.66	0.00	VDVDKLEETAR	64	
							1441.76	1441.75	0.00	ELSEKYDAIFVK	79	
							1612.88	1612.88	0.00	KYNISAMPTFIAIK	30	Ox (M)[7]
388	mira	enolase	Sm12193	4	269	100	1113.65	1113.65	0.00	GLQLLEEAIK	39	
							1188.64	1188.65	0.01	AGAAEAGLPLYR	52	
							1764.92	1764.93	0.01	AAVPSGASTGVHEALELR	95	
							2116.11	2116.11	0.00	LTSSTNIQIVGDDLTVTNPK	84	
389	mira	enolase	Sm12193	3	140	100	1113.65	1113.65	0.00	GLQLLEEAIK	42	
							1188.64	1188.64	0.00	AGAAEAGLPLYR	51	
							1764.92	1764.92	0.00	AAVPSGASTGVHEALELR	48	
390	mira	enolase	Sm12193	3	195	100	1113.65	1113.64	-0.01	GLQLLEEAIK	54	
							1188.64	1188.63	0.00	AGAAEAGLPLYR	51	
							1764.92	1764.91	-0.01	AAVPSGASTGVHEALELR	91	
391	mira	enolase	Sm12193	3	165	100	1113.65	1113.65	0.00	GLQLLEEAIK	43	
							1188.64	1188.64	0.00	AGAAEAGLPLYR	50	
							1764.92	1764.92	0.00	AAVPSGASTGVHEALELR	72	
393	mira	valosin-containing protein	Sm12453	2	114	100	1298.70	1298.69	0.00	EIEIGIPDSIGR	43	
							1742.93	1742.91	-0.02	LDQLIYIPLPDEASR	71	
394	mira	peptidyl prolyl cis trans isomerase	Sm12777	1	96	100	1679.86	1679.85	-0.01	IIFELFNDVPDTTR	96	
395	mira	peptidyl prolyl cis trans isomerase	Sm12777	1	101	100	1679.86	1679.85	-0.02	IIFELFNDVPDTTR	101	
400	mira	universal stress	Sm05431	1	61	99.97	1598.89	1598.90	0.01	AFLHVDTKPGSSLVK	61	

Spot no.[1]	Prep[2]	protein Protein name	Accession no.[3]	Pep. count	Total Ion Score (protein)	C.I. (%)	Calculated Mass (Da)	Observed Mass (Da)	Match Error (Da)	Sequence	Ion Score (pep)	Mods.[4]
401	mira	tubulin β chain	Snap30454	6	324	100	1053.61	1053.61	0.00	YLTVAAIFR	46	
							1130.60	1130.60	0.00	FPGQLNADLR	65	
							1258.69	1258.69	0.00	FPGQLNADLRK	35	
							1723.86	1723.86	0.00	SLTVPELTQQMFDAK	45	Ox (M)[11]
							1901.97	1901.97	0.00	MSVTFIGNSTAIQELFK	58	Ox (M)[1]
							1958.98	1958.98	-0.01	GHYTEGAELVDSVLDVVR	77	
402	mira	tubulin β chain	Snap30454	4	224	100	1053.61	1053.61	0.00	YLTVAAIFR	46	
							1130.60	1130.60	0.00	FPGQLNADLR	65	
							1328.65	1328.64	0.00	INVYYNEATGGK	34	
							1958.98	1958.97	-0.01	GHYTEGAELVDSVLDVVR	79	
504	Hf	mouse haemoglobin α subunit	gi122385*	4	195	100	1045.50	1045.51	0.01	MFASFPTTK	39	Ox (M)[1]
							1252.71	1252.71	0.00	FLASVSTVLTSK	46	
							1529.73	1529.73	0.00	IGGHGAEYGAEALER	66	
							1819.88	1819.88	0.00	TYFPHFDVSHGSAQVK	45	
505	Hf	mouse hsc70	gi1661134*	4	153	99.98	1981.98	1980.99	-0.02	TVTNAVVTVPAYFNDSQR	73	
							1199.67	1198.67	0.00	DAGTIAGLNVLR	14	
							1691.72	1690.71	-0.01	STAGDTHLGGEDFDNR	36	
							1081.56	1080.56	0.00	LLQDFFNGK	30	
506	Hf	mouse albumin	gi29612571*	2	115	100	1250.58	1250.58	0.00	YNDLGEQHFK	46	
							1439.79	1439.79	0.00	APQVSTPTLVEAAR	70	
507	Hf	mouse albumin	gi29612571*	1	127	100	1439.79	1439.78	-0.01	APQVSTPTLVEAAR	127	
508	Hf	mouse albumin	gi29612571*	6	179	100	1479.80	1479.79	0.00	LGEYGFQNAILVR	79	
							1479.80	1479.79	0.00	LGEYGFQNAILVR	79	
							1681.84	1681.83	-0.01	LSQTFPNADFAEITK	44	
							1681.84	1681.83	-0.01	LSQTFPNADFAEITK	44	
							1960.05	1960.03	-0.02	YTQKAPQVSTPTLVEAAR	56	
							1960.05	1960.03	-0.02	YTQKAPQVSTPTLVEAAR	56	

Spot no.[1]	Prep[2]	Protein name	Accession no.[3]	Pep. count	Total Ion Score (protein)	C.I. (%)	Calculated Mass (Da)	Observed Mass (Da)	Match Error (Da)	Sequence	Ion Score (pep)	Mods.[4]
509	Hf	mouse albumin	gi29612571*	4	297	100	1439.79	1439.78	0.00	APQVSTPTLVEAAR	81	
							1479.80	1479.79	0.00	LGEYGFQNAILVR	71	
							1609.79	1609.78	-0.01	DVFLGTFLYEYSR	88	
							1681.84	1681.83	-0.01	LSQTFPNADFAEITK	59	
510	Hf	mouse albumin	gi29612571*	3	221	100	1439.79	1439.78	0.00	APQVSTPTLVEAAR	97	
							1479.78	1479.80	0.00	LGEYGFQNAILVR	52	
							1681.84	1681.84	0.00	LSQTFPNADFAEITK	75	
511	Hf	mouse albumin	gi29612571*	4	245	100	1439.79	1439.79	0.00	APQVSTPLTLVEAAR	76	
							1479.80	1479.80	0.00	LGEYGFQNAILVR	68	
							1609.79	1609.79	0.00	DVFLGTFLYEYSR	60	
							1681.84	1681.85	0.00	LSQTFPNADFAEITK	43	
512	Hf	mouse haemoglobin β subunit	gi31982300*	2	183	100	1756.92	1756.93	0.01	VITAFNDGLNHLDSLK	104	
							1996.90	1996.92	0.02	YFDSFGDLSSASAIMGNAK	80	Ox (M)[15]
515	Hf	GST 26kDa	Sm00145	3	153	100	1390.74	1390.73	-0.01	VDFLNQLPGMLK	35	Ox (M)[10]
							1597.81	1597.80	-0.01	LLLEYLGEAYEER	63	
							1938.98	1938.98	0.00	LGLDFPNLPYYIDGDVK	54	
519L	Hf	unknown function	Snap25404	1	83	100	1878.04	1878.03	-0.01	GQLKPESPPLNLTQLSR	83	
519R	Hf	unknown function	Snap25404	1	105	100	1344.69	1344.69	0.00	FGIQAYGGVFASK	105	
525	Hf	ubiquitin	Sm01509	2	97	100	1081.55	1081.55	0.00	TLSDYNIQK	35	
							1787.93	1787.93	0.00	TITLEVEPSDTIENVK	64	
526	Hf	GST (28kDa)	Sm02267	4	267	100	986.53	986.53	0.01	ENLLASSPR	60	
							1165.60	1165.61	0.01	YLSNRPATPF	37	
							1584.72	1584.72	0.00	MTLVAAGVDYEDER	76	Ox (M)[1]
							1667.80	1667.81	0.00	LIGQAEDVEHEYHK	94	

Spot no.[1]	Prep[2]	Protein name	Accession no.[3]	Pep. count	Total Ion Score (protein)	C.I. (%)	Calculated Mass (Da)	Observed Mass (Da)	Match Error (Da)	Sequence	Ion Score (pep)	Mods.[4]
527	Hf	GST (28kDa)	Sm02267	4	182	100	869.45	869.45	-0.01	VIYFDGR	41	
							986.53	986.52	0.00	ENLLASSPR	39	
							1165.60	1165.59	-0.01	YLSNRPATPF	42	
							1584.72	1584.72	0.00	MTLVAAGVDYEDER	60	Ox (M)[1]
528	Hf	GST (28kDa)	Sm02267	4	208	100	869.45	869.45	0.00	VIYFDGR	38	
							1165.60	1165.60	0.00	YLSNRPATPF	46	
							1584.72	1584.72	0.00	MTLVAAGVDYEDER	52	Ox (M)[1]
							1667.80	1667.80	0.00	LIGQAEDVEHEYHK	72	
530	Hf	Sm14 fatty acid binding protein	Sm04779	2	96	100	1232.68	1232.69	0.00	TTVTVGDVTAIR	50	
							1940.93	1940.93	0.00	QIGNTVTPTVTFTMDGDK	46	Ox (M)[14]
531	Hf	fructose bisphosphate aldolase	Sm05684	6	309	100	1296.72	1296.72	0.00	VTEQVLAFVYK	65	
							1433.74	1433.74	0.00	AYTPQENALATVR	41	
							1698.85	1698.86	0.00	LQQIGVENNEENRR	36	
							1879.93	1879.92	-0.01	FQPYLTEAQENDLRR	38	
							2041.10	2041.09	0.00	LAENISGVILFEETLHQK	69	
							2330.15	2330.13	-0.02	GVVPLAGTDNETTTQGLDDLASR	61	
532	Hf	fructose bisphosphate aldolase	Sm05684	2	92	100	1296.72	1296.73	0.01	VTEQVLAFVYK	51	
							1879.93	1879.94	0.01	FQPYLTEAQENDLRR	42	
533	Hf	fructose bisphosphate aldolase	Sm05684	2	92	100	1296.72	1296.73	0.01	VTEQVLAFVYK	51	
							1879.93	1879.94	0.01	FQPYLTEAQENDLRR	42	
538	Hf	superoxide dismutase	Sm11433	4	197	100	1238.58	1238.58	0.00	QEHGAPEDSIR	63	
							1366.78	1366.79	0.01	LISLNGSHSIIGR	57	
							1544.70	1544.71	0.01	TMVIHENEDDLGR	30	Ox (M)[2]
							2213.06	2213.07	0.01	FTQETDNGPVHVHAEFSGLK	47	
539	Hf	thioredoxin	Sm11767	4	290	100	1274.66	1274.66	0.00	VDVDKLEETAR	78	
							1484.78	1484.79	0.01	YNISAMPTFIAIK	47	Ox (M)[6]
							1511.73	1511.74	0.00	QDGDLESLLEQHK	86	
							1612.88	1612.88	0.00	KYNISAMPTFIAIK	79	Ox (M)[7]

Spot no.[1]	Prep[2]	Protein name	Accession no.[3]	Pep. count	Total Ion Score (protein)	C.I. (%)	Calculated Mass (Da)	Observed Mass (Da)	Match Error (Da)	Sequence	Ion Score (pep)	Mods.[4]
540	Hf	thioredoxin	Sm11767	1	81	100	1274.66	1274.66	0.00	VDVDKLEETAR	81	
544	Hf	thioredoxin peroxidase	Sm12448	5	326	100	1209.65	1209.65	-0.01	LLDAFQFVEK	63	
							1240.70	1240.70	-0.01	QITINDKPVGR	62	
							1327.77	1327.77	0.00	GLFIIDPNGILR	48	
							1380.80	1380.80	0.00	VLLPNRPAPEFK	52	
							1589.69	1589.68	-0.01	AYGVFDEEDGNAFR	101	
546	Hf	unknown function	Sm14608	1	57	99.56	1498.75	1498.74	0.00	IDSLSARASSFFPT	57	
550	Hf	plant pathogenesis family (PR1)	Snap41543	2	141	100	1309.69	1309.68	0.00	NELLTLHNEAR	74	
							1810.06	1810.05	-0.01	NGQLFGQPIAVSIKPLK	67	
551	Hf	plant pathogenesis family (PR1)	Snap41543	2	112	100	978.43	978.43	0.00	NYDFYTR	45	
							1309.69	1309.68	0.00	NELLTLHNEAR	68	
552	Hf	plant pathogenesis family (PR1)	Snap41543	3	197	100	978.43	978.43	0.00	NYDFYTR	35	
							1309.69	1309.70	0.02	NELLTLHNEAR	84	
							1810.06	1810.06	0.00	NGQLFGQPIAVSIKPLK	78	
554	Hf	unknown function	Sm05341	2	84	100	1413.73	1413.71	-0.01	SLILSDSEFFQK	61	
							1643.85	1643.83	-0.02	FIITYDELSSQISK	84	
555	Hf	mouse regucalcin	gi6677739*	7	388	100	989.51	989.50	0.00	QPDAGNIFK	65	
							1175.58	1175.58	0.00	FNDGKVDPAGR	53	
							1207.67	1207.66	0.00	QLGGYVATIGTK	51	
							1283.73	1283.73	0.00	VAVDAPVSSVALR	59	
							1714.85	1714.85	-0.01	HQGSSLYSLFPDHSVK	76	
							1871.88	1871.88	-0.01	YFAGTMAEETAPAVLER	53	Ox (M)[6]
							914.48	915.49	0.00	LDPETGKR	30	

[1] when more than one spot have the same Spot Number, then C = centre spot, R = right spot, L = left spot, CR = centre right spot etc.
[2] vit = female, vitellaria-enriched preparation: imm = immature SEA: mat = mature SEA: mira = miracidia preparation: Hf = hatch fluid.

[3] accession numbers are CDS, unless *, which denotes NCBI. [4] Ox (M) = oxidation of methionine. Carb (C) = carbamidomethylation of cysteine. The number inside [] denotes the amino acid to which the modification refers to.

Appendix 2: *Mesocricetus auratus* albumin: the listed peptides were separated by nano-LC and then fragmented by Electrospray-MSMS. When a listed peptide was fragmented more than once the data is for the peptide with the largest ion score.

Sequence	Residue nos. (start/end)	No. times peptide fragmented	Observed m/z (Da)	Experimental m/z (Da)	Calculated m/z (Da)	Charge	Error (Da)	e-value	Ion score
SEIAHR	29-34	4	356.69	711.37	711.37	2	0.00	24	24
DLGEQHFK	37-44	2	487.31	972.47	972.60	2	0.13	12	29
GLVLIAFSQFLQK	45-57	2	732.49	1462.96	1462.85	2	0.10	0.13	46
LVNEVTDFAK	66-75	4	568.39	1134.75	1134.59	2	0.16	0.04	53
TCVADESAENCDK	76-88	2	749.84	1497.66	1497.57	2	0.09	2.8E+02	13
SLHTLFGDK	89-97	5	509.31	1016.61	1016.53	2	0.08	0.54	42
LCAIPTLR	98-105	5	472.33	942.64	942.53	2	0.11	2	36
RHPYFYAPELLYYAEK	169-184	6	687.38	2059.12	2059.02	3	0.10	5.7	29
HPYFYAPELLYYAEK	170-184	3	635.41	1903.21	1902.92	3	0.29	0.27	42
YSAIMTECCGEADK	185-198	5	817.91	1633.80	1633.64	2	0.16	5.9	30
AACITPK	199-205	2	380.72	759.42	759.39	2	0.03	0.21	47
CSSLQR	224-229	2	375.69	749.36	749.35	2	0.01	5.6	31
AWAVAR	237-242	2	337.20	672.38	672.37	2	0.01	6.1	33
LTEECCHGDLLECADDR	265-281	2	698.30	2091.88	2091.83	3	0.05	10	26
YMCENQASISSK	287-298	9	709.31	1416.61	1416.60	2	0.01	0.0075	49
LQACCDKPVLK	299-309	2	666.42	1330.83	1330.67	2	0.16	0.28	44
SHCLSEVENDDLPAD LPSLAADFVEDK	311-337	2	996.30	2985.89	2985.35	3	0.54	0.00084	67
SHCLSEVENDDLPADL PSLAADFVEDKEVCK	311-341	1	876.54	3502.13	3501.59	4	0.54	1.7E+02	14
DVFLGTFLYEYAR	348-360	12	797.48	1592.95	1592.79	2	0.16	4.6	31
RHPDYSVALLLR	361-372	6	480.64	1438.90	1438.80	3	0.10	0.6	40
HPDYSVALLLR	362-372	4	642.36	1282.71	1282.70	2	0.01	0.087	49
VLDEFQPLVEEPK	397-409	11	771.95	1541.89	1541.80	2	0.09	2.8E-05	83

Sequence	Residue nos. (start/end)	No. times peptide fragmented	Observed m/z (Da)	Experimental m/z (Da)	Calculated m/z (Da)	Charge	Error (Da)	e-value	Ion score
ANCELFEK	414-421	2	505.81	1009.61	1009.45	2	0.15	2.4E+02	14
LGEYGFQNALIVR	422-434	6	740.46	1478.89	1478.79	2	0.11	0.26	44
APQVSTPTLVEAAR	439-452	13	720.38	1438.75	1438.78	2	-0.03	4.0E-06	92
CCVLPEAQR	461-469	9	566.86	1131.70	1131.52	2	0.18	23	25
LPCVEDYISAILNR	470-483	5	832.04	1662.07	1661.84	2	0.22	0.022	54
VCVLHEK	484-490	3	422.79	883.57	883.46	2	0.11	11	28
TPVSEQVTK	491-499	10	494.84	987.66	987.52	2	0.13	2.3	35
RPCFSALPVDETYVPK	509-524	5	627.07	1878.20	1877.93	3	0.26	0.015	55
AETFTFHADICSLPEK	528-543	4	622.74	1865.21	1864.87	3	0.35	10	27
AETFTFHADICSLPEKEK	528-545	4	708.37	2122.11	2122.00	3	0.11	75	18
KQAALVELVK	549-558	3	549.91	1097.80	1097.68	2	0.12	0.00014	73
QAALVELVK	550-558	6	485.86	969.71	969.59	2	0.12	0.52	38
ATGPQLR	563-569	4	371.80	741.43	741.41	2	0.01	0.33	43
TVLGEFTAFLDK	570-581	8	670.92	1339.83	1339.70	2	0.13	0.0096	58
AEDKEACFSEDGPK	585-598	3	791.89	1581.76	1581.66	2	0.10	0.67	39
LVASSQAALA	599-608	1	465.86	929.70	929.52	2	0.18	33	21

Appendix 3. Identification of HPLC-purified ESP components. The peptides were identified by MALDI-MSMS utilizing the Mascot search engine.

Fig.	Spot.	Protein name	Accession no.[1]	Total ion score	Protein CI (%)	Calculated mass	Observed mass	Match error (Da)	Sequence	Ion score (peptide)	Peptide CI (%)	Mods[4]
3.14	a	ESP13/14	Sm11845	124	100	1506.675	1506.662	-0.014	KHCEGNNEYVTR	73	99.997	Carb (C)[3]
						1378.58	1378.568	-0.012	HCEGNNEYVTR	52	99.664	Carb (C)[2]
3.14	c	thioredoxin	Sm11767	222	100	1274.659	1274.654	-0.005	VDVDKLEETAR	51	99.58	
						1484.782	1484.777	-0.005	YNISAMPTFIAIK	45	98.548	Ox (M)[6]
						1511.734	1511.727	-0.006	QDGDLESLLEQHK	59	99.931	
						1612.877	1612.872	-0.004	KYNISAMPTFIAIK	67	99.99	Ox (M)[7]
3.14	b	ubiquitin	Sm00183	63	99.97	1023.566	1023.562	-0.004	KFIFPPFQ	68	99.993	
3.16	a	ESP1-2	Smp193860	112	100	1772.821	1772.825	0.004	GMYHLEEVHVCLNR	44	98.266	Carb (C)[11] Ox (M)[2]
						2272.049	2272.063	0.014	HGLCAVEDPQVFNQYGYFK	138	100	Carb (C)[4]
3.16	b	ESP11/15	Sm00193	95	100	2015.986	2015.968	-0.017	DGCPIPSTPDLLLGNYQR	95	100	Carb (C)[3]
3.10	a (upper)	ESP1-2	Sm19482	127	100	980.5597	980.5223	-0.037	FGIKLMQK	31	75.19	Ox (M)[6]
						1608.805	1608.801	-0.004	QYDTINLMNVLER	38	95.93	
						1624.8	1624.8	0	QYDTINLMNVLER	30	73.108	Ox (M)[8]
						2272.049	2272.051	0.0019	HGLCAVEDPQVFNQYGYFK	58	99.958	Carb (C)[4]
3.10	a (lower)	ESP1-2	Sm19482	145	100	980.5597	980.5225	-0.037	FGIKLMQK	31	73.776	Ox (M)[6]
						1624.8	1624.801	0.0009	QYDTINLMNVLER	40	96.446	Ox (M)[8]
						2272.049	2272.05	0.0009	HGLCAVEDPQVFNQYGYFK	75	99.999	Carb (C)[4]
3.10	b	ESP12	Smp193860	46	99.77	1023.566	1023.566	0	KFIFPPFQ	46	99.766	
3.10	d	ESP1-2	Smp193860	24	70.74	1023.566	1023.565	-0.001	KFIFPPFQ	24	70.737	
3.10	e	ESP12	Smp193860	145	100	980.5597	980.5198	-0.04	FGIKLMQK	39	95.687	Ox (M)[6]
						2272.049	2272.054	0.0046	HGLCAVEDPQVFNQYGY	105	100	Carb (C)[4]
3.10	f (upper)	IPSE	gi|28894857*	71	99.993	1577.763	1577.757	-0.006	ITGLGHGTCIDDFTK	71	99.993	
3.10	f (lower)	IPSE	gi|28894857*	102	100	2092.988	2092.982	-0.006	ERPYWYLFDNVNYTGR	102	100	

Fig.	Spot.	Protein name	Accession no.[1]	Total ion score	Protein CI (%)	Calculated mass	Observed mass	Match error (Da)	Sequence	Ion score (peptide)	Peptide CI (%)	Mods[4]
3.10	c (lower)	IPSE	gi|28894857*	317	100	1287.636	1287.627	-0.009	DGKVECINQPK	46	93.998	Carb (C)[6]
						1634.784	1634.776	-0.009	ITGLGHGTCIDDFTK	68	99.956	Carb (C)[9]
						1652.726	1652.715	-0.011	YCLQLYDETYER	92	100	Carb (C)[2]
						2092.988	2092.968	-0.019	ERPYWYLFDNVNYTGR	112	100	
3.10	c (upper)	IPSE	gi|28894857*	85	100	1595.705	1595.7	-0.004	YCLQLYDETYER	79	99.997	
						1652.726	1652.726	0	YCLQLYDETYER	85	99.999	Carb (C)[2]

[1] accession numbers are CDS, unless *, which denotes NCBI.
[4] Ox (M) = oxidation of methionine. Carb (C) = carbamidomethylation of cysteine. The number inside [] denotes the amino acid to which the modification refers to.

Bibliographical References

Abdel-Azim, M. and Gismann, A. (1956). Bilharziasis survey in south-western Asia; covering Iraq, Israel, Jordan, Lebanon, Sa'udi Arabia, and Syria: 1950-51. *Bull World Health Organ* **14**,(3) 403-56.

Abouel-Nour, M. F., Lotfy, M., Attallah, A. M. and Doughty, B. L. (2006). Schistosoma mansoni major egg antigen Smp40: molecular modeling and potential immunoreactivity for anti-pathology vaccine development. *Mem Inst Oswaldo Cruz* **101**,(4) 365-72.

Ahlberg, J., Marzella, L. and Glaumann, H. (1982). Uptake and degradation of proteins by isolated rat liver lysosomes. Suggestion of a microautophagic pathway of proteolysis. *Lab Invest* **47**,(6) 523-32.

Akarsu, E., Pirim, I., Capoglu, I., Deniz, O., Akcay, G. *et al.* (2001). Relationship between electroneurographic changes and serum ubiquitin levels in patients with type 2 diabetes. *Diabetes Care* **24**,(1) 100-3.

Akira, S. and Takeda, K. (2004). Toll-like receptor signalling. *Nat Rev Immunol* **4**,(7) 499-511.

Aksoy, E., Zouain, C. S., Vanhoutte, F., Fontaine, J., Pavelka, N. *et al.* (2005). Double-stranded RNAs from the helminth parasite Schistosoma activate TLR3 in dendritic cells. *J Biol Chem* **280**,(1) 277-83.

Al-Adhami, B. H., Thornhill, J., Akhkha, A., Doenhoff, M. J. and Kusel, J. R. (2003). The properties of acidic compartments in developing schistosomula of Schistosoma mansoni. *Parasitology* **127**,(Pt 3) 253-64.

Albert, P. S. and Riddle, D. L. (1988). Mutants of Caenorhabditis elegans that form dauer-like larvae. *Dev Biol* **126**,(2) 270-93.

Alger, H. M., Sayed, A. A., Stadecker, M. J. and Williams, D. L. (2002). Molecular and enzymatic characterisation of Schistosoma mansoni thioredoxin. *Int J Parasitol* **32**,(10) 1285-92.

Andrade, Z. A. (2004). Schistosomal hepatopathy. *Mem Inst Oswaldo Cruz* **99**,(5: Suppl 1) 51-7.

Angelini, G., Gardella, S., Ardy, M., Ciriolo, M. R., Filomeni, G. *et al.* (2002). Antigen-presenting dendritic cells provide the reducing extracellular microenvironment required for T lymphocyte activation. *Proc Natl Acad Sci U S A* **99**,(3) 1491-6.

Asahi, H., Hernandez, H. J. and Stadecker, M. J. (1999). A novel 62-kilodalton egg antigen from Schistosoma mansoni induces a potent CD4(+) T helper cell response in the C57BL/6 mouse. *Infect Immun* **67**,(4) 1729-35.

Asahi, H., Osman, A., Cook, R. M., LoVerde, P. T. and Stadecker, M. J. (2000). Schistosoma mansoni phosphoenolpyruvate carboxykinase, a novel egg antigen: immunological properties of the recombinant protein and identification of a T-cell epitope. *Infect Immun* **68**,(6) 3385-93.

Asahi, H. and Stadecker, M. J. (2003). Analysis of egg antigens inducing hepatic lesions in schistosome infection. *Parasitol Int* **52**,(4) 361-7.

Asch, H. L. and Dresden, M. H. (1979). Acidic thiol proteinase activity of Schistosoma mansoni egg extracts. *J Parasitol* **65**,(4) 543-9.

Ashton, P. D. (2001). Characterisation of the Egg Secretions of *Schistosoma mansoni*. Ph.D thesis. University of York, York

Ashton, P. D., Harrop, R., Shah, B. and Wilson, R. A. (2001). The schistosome egg: development and secretions. *Parasitology* **122**,(Pt 3) 329-38.

Asojo, O. A., Loukas, A., Inan, M., Barent, R., Huang, J. *et al.* (2005). Crystallization and preliminary X-ray analysis of Na-ASP-1, a multi-domain pathogenesis-related-1 protein from the human hookworm parasite Necator americanus. *Acta Crystallograph Sect F Struct Biol Cryst Commun* **61**,(Pt 4) 391-4.

Asseman, C., Pancre, V., Delanoye, A., Capron, A. and Auriault, C. (1994). A radioimmunoassay for the quantification of human ubiquitin in biological fluids: application to parasitic and allergic diseases. *J Immunol Methods* **173**,(1) 93-101.

Bahia, D., Avelar, L. G., Vigorosi, F., Cioli, D., Oliveira, G. C. *et al.* (2006). The distribution of motor proteins in the muscles and flame cells of the Schistosoma mansoni miracidium and primary sporocyst. *Parasitology* **133**,(Pt 3) 321-9.

Baum, J. S., St George, J. P. and McCall, K. (2005). Programmed cell death in the germline. *Semin Cell Dev Biol* **16**,(2) 245-59.

Baumeister, W., Walz, J., Zuhl, F. and Seemuller, E. (1998). The proteasome: paradigm of a self-compartmentalizing protease. *Cell* **92**,(3) 367-80.

Baumgart, M., Tompkins, F., Leng, J. and Hesse, M. (2006). Naturally occurring CD4+Foxp3+ regulatory T cells are an essential, IL-10-independent part of the immunoregulatory network in Schistosoma mansoni egg-induced inflammation. *J Immunol* **176**,(9) 5374-87.

Benaroudj, N., Zwickl, P., Seemuller, E., Baumeister, W. and Goldberg, A. L. (2003). ATP hydrolysis by the proteasome regulatory complex PAN serves multiple functions in protein degradation. *Mol Cell* **11**,(1) 69-78.

Benitez, L., Harrison, L. J., Parkhouse, R. M. and Garate, T. (1998). Sequence and preliminary characterisation of a Taenia saginata oncosphere gene homologue of the small heat-shock protein family. *Parasitol Res* **84**,(5) 423-5.

Bercovich, B., Stancovski, I., Mayer, A., Blumenfeld, N., Laszlo, A. *et al.* (1997). Ubiquitin-dependent degradation of certain protein substrates in vitro requires the molecular chaperone Hsc70. *J Biol Chem* **272**,(14) 9002-10.

Bergmann, A., Yang, A. Y. and Srivastava, M. (2003). Regulators of IAP function: coming to grips with the grim reaper. *Curr Opin Cell Biol* **15**,(6) 717-24.

Bergquist, R., Al-Sherbiny, M., Barakat, R. and Olds, R. (2002). Blueprint for schistosomiasis vaccine development. *Acta Trop* **82**,(2) 183-92.

Bertini, R., Howard, O. M., Dong, H. F., Oppenheim, J. J., Bizzarri, C. *et al.* (1999). Thioredoxin, a redox enzyme released in infection and inflammation, is a unique chemoattractant for neutrophils, monocytes, and T cells. *J Exp Med* **189**,(11) 1783-9.

Bertolaet, B. L., Clarke, D. J., Wolff, M., Watson, M. H., Henze, M. *et al.* (2001). UBA domains of DNA damage-inducible proteins interact with ubiquitin. *Nat Struct Biol* **8**,(5) 417-22.

Bjellqvist, B., Ek, K., Righetti, P. G., Gianazza, E., Gorg, A. *et al.* (1982). Isoelectric focusing in immobilized pH gradients: principle, methodology and some applications. *J Biochem Biophys Methods* **6**,(4) 317-39.

Blackstock, W. P. and Weir, M. P. (1999). Proteomics: quantitative and physical mapping of cellular proteins. *Trends Biotechnol* **17**,(3) 121-7.

Bogitsh, B. J. (1975). Cytochemistry of gastrodermal autophagy following starvation in Schistosoma mansoni. *J Parasitol* **61**,(2) 237-48.

Boros, D. L., Pelley, R. P. and Warren, K. S. (1975). Spontaneous modulation of granulomatous hypersensitivity in schistosomiasis mansoni. *J Immunol* **114**,(5) 1437-41.

Boros, D. L. and Warren, K. S. (1970). Delayed hypersensitivity-type granuloma formation and dermal reaction induced and elicited by a soluble factor isolated from Schistosoma mansoni eggs. *J Exp Med* **132**,(3) 488-507.

Boros, D. L. and Whitfield, J. R. (1999). Enhanced Th1 and dampened Th2 responses synergize to inhibit acute granulomatous and fibrotic responses in murine schistosomiasis mansoni. *Infect Immun* **67**,(3) 1187-93.

Botros, S. S., Mahmoud, M. R., Moussa, M. M. and Nosseir, M. M. (2007). Immunohistopathological and biochemical changes in Schistosoma mansoni-infected mice treated with artemether. *J Infect* **55**,(5) 470-7.

Brouwers, J. F., Smeenk, I. M., van Golde, L. M. and Tielens, A. G. (1997). The incorporation, modification and turnover of fatty acids in adult Schistosoma mansoni. *Mol Biochem Parasitol* **88**,(1-2) 175-85.

Bruckner, D. A. and Schiller, E. L. (1974). Some biological characteristics of Liberian and Puerto Rican strains of Schistosoma mansoni. *J Parasitol* **60**,(3) 551-2.

Brunet, L. R., Finkelman, F. D., Cheever, A. W., Kopf, M. A. and Pearce, E. J. (1997). IL-4 protects against TNF-alpha-mediated cachexia and death during acute schistosomiasis. *J Immunol* **159**,(2) 777-85.

Burnell, A. M., Houthoofd, K., O'Hanlon, K. and Vanfleteren, J. R. (2005). Alternate metabolism during the dauer stage of the nematode Caenorhabditis elegans. *Exp Gerontol* **40**,(11) 850-6.

Butterworth, A. E., Capron, M., Cordingley, J. S., Dalton, P. R., Dunne, D. W. *et al.* (1985). Immunity after treatment of human schistosomiasis mansoni. II. Identification of resistant individuals, and analysis of their immune responses. *Trans R Soc Trop Med Hyg* **79**,(3) 393-408.

Byram, J. E., Doenhoff, M. J., Musallam, R., Brink, L. H. and von Lichtenberg, F. (1979). Schistosoma mansoni infections in T-cell deprived mice, and the ameliorating effect of administering homologous chronic infection serum. II. Pathology. *Am J Trop Med Hyg* **28**,(2) 274-85.

Canty, E. G. and Kadler, K. E. (2005). Procollagen trafficking, processing and fibrillogenesis. *J Cell Sci* **118**,(Pt 7) 1341-53.

Cass, C. L., Johnson, J. R., Califf, L. L., Xu, T., Hernandez, H. J. *et al.* (2007). Proteomic analysis of Schistosoma mansoni egg secretions. *Mol Biochem Parasitol* **155**,(2) 84-93.

Cassada, R. C. and Russell, R. L. (1975). The dauerlarva, a post-embryonic developmental variant of the nematode Caenorhabditis elegans. *Dev Biol* **46**,(2) 326-42.

Castro-Borges, W., Cartwright, J., Ashton, P. D., Braschi, S., Guerra Sa, R. *et al.* (2007). The 20S proteasome of Schistosoma mansoni: a proteomic analysis. *Proteomics* **7**,(7) 1065-75.

Cavanaugh, J. E. (2004). Role of extracellular signal regulated kinase 5 in neuronal survival. *Eur J Biochem* **271**,(11) 2056-9.

Chandu, D. and Nandi, D. (2004). Comparative genomics and functional roles of the ATP-dependent proteases Lon and Clp during cytosolic protein degradation. *Res Microbiol* **155**,(9) 710-9.

Chang, C. and Werb, Z. (2001). The many faces of metalloproteases: cell growth, invasion, angiogenesis and metastasis. *Trends Cell Biol* **11**,(11) S37-43.

Chang, T. S., Cho, C. S., Park, S., Yu, S., Kang, S. W. *et al.* (2004). Peroxiredoxin III, a mitochondrion-specific peroxidase, regulates apoptotic signaling by mitochondria. *J Biol Chem* **279**,(40) 41975-84.

Cheever, A. W. and Anderson, L. A. (1971). Rate of destruction of Schistosoma mansoni eggs in the tissues of mice. *Am J Trop Med Hyg* **20**,(1) 62-8.

Cheever, A. W. and Duvall, R. H. (1974). Single and repeated infections of grivet monkeys with Schistosoma mansoni: parasitological and pathological observations over a 31-month period. *Am J Trop Med Hyg* **23**,(5) 884-94.

Cheever, A. W., Kamel, I. A., Elwi, A. M., Mosimann, J. E. and Danner, R. (1977). Schistosoma mansoni and S. haematobium infections in Egypt. II. Quantitative parasitological findings at necropsy. *Am J Trop Med Hyg* **26**,(4) 702-16.

Chen, Y. and Boros, D. L. (1998). Identification of the immunodominant T cell epitope of p38, a major egg antigen, and characterization of the epitope-specific Th responsiveness during murine schistosomiasis mansoni. *J Immunol* **160**,(11) 5420-7.

Chensue, S. W., Kunkel, S. L., Ward, P. A. and Higashi, G. I. (1983). Exogenously administered prostaglandins modulate pulmonary granulomas induced by Schistosoma mansoni eggs. *Am J Pathol* **111**,(1) 78-87.

Clayton, A., Turkes, A., Navabi, H., Mason, M. D. and Tabi, Z. (2005). Induction of heat shock proteins in B-cell exosomes. *J Cell Sci* **118**,(Pt 16) 3631-8.

Clough, K. A., Drew, A. C. and Brindley, P. J. (1996). Host-like sequences in the schistosome genome. *Parasitol Today* **12**,(7) 283-6.

Clurman, B. E., Sheaff, R. J., Thress, K., Groudine, M. and Roberts, J. M. (1996). Turnover of cyclin E by the ubiquitin-proteasome pathway is regulated by cdk2 binding and cyclin phosphorylation. *Genes Dev* **10**,(16) 1979-90.

Co, D. O., Hogan, L. H., Il-Kim, S. and Sandor, M. (2004). T cell contributions to the different phases of granuloma formation. *Immunol Lett* **92**,(1-2) 135-42.

Coles, G. C. (1970). A comparison of some isoenzymes of Schistosoma mansoni and Schistosoma haematobium. *Comp Biochem Physiol* **33**,(3) 549-58.

Connell, P., Ballinger, C. A., Jiang, J., Wu, Y., Thompson, L. J. *et al.* (2001). The co-chaperone CHIP regulates protein triage decisions mediated by heat-shock proteins. *Nat Cell Biol* **3**,(1) 93-6.

Cordingley, J. S. (1987). Trematode eggshells: Novel protein biopolymers. *Parasitol Today* **3**,(11) 341-4.

Cottrell, J. S. (1994). Protein identification by peptide mass fingerprinting. *Pept Res* **7**,(3) 115-24.

Cuervo, A. M. and Dice, J. F. (1996). A receptor for the selective uptake and degradation of proteins by lysosomes. *Science* **273**,(5274) 501-3.

Curtis, R. H. C. (1991). Characterization of some *Schistosoma mansoni* hydrolases and other surface antigens. Ph.D thesis. London School of Hygiene and Tropical Medicine, University of London, London

Curwen, R. S., Ashton, P. D., Johnston, D. A. and Wilson, R. A. (2004). The Schistosoma mansoni soluble proteome: a comparison across four life-cycle stages. *Mol Biochem Parasitol* **138**,(1) 57-66.

Curwen, R. S., Ashton, P. D., Sundaralingam, S. and Wilson, R. A. (2006). Identification of novel proteases and immunomodulators in the secretions of schistosome cercariae that facilitate host entry. *Mol Cell Proteomics* **5**,(5) 835-44.

Cyr, D. M., Hohfeld, J. and Patterson, C. (2002). Protein quality control: U-box-containing E3 ubiquitin ligases join the fold. *Trends Biochem Sci* **27**,(7) 368-75.

Dalton, J. P., Lewis, S. A., Aronstein, W. S. and Strand, M. (1987). Schistosoma mansoni: immunogenic glycoproteins of the cercarial glycocalyx. *Exp Parasitol* **63**,(2) 215-26.

Damian, R. T. and Chapman, R. W. (1983). The fecundity of Schistosoma mansoni in baboons, with evidence for a sex ratio effect. *J Parasitol* **69**,(5) 987-9.

Danso-Appiah, A. and De Vlas, S. J. (2002). Interpreting low praziquantel cure rates of Schistosoma mansoni infections in Senegal. *Trends Parasitol* **18**,(3) 125-9.

de Diego, J. L., Katz, J. M., Marshall, P., Gutierrez, B., Manning, J. E. *et al.* (2001). The ubiquitin-proteasome pathway plays an essential role in proteolysis during Trypanosoma cruzi remodeling. *Biochemistry* **40**,(4) 1053-62.

de Waal Malefyt, R., Haanen, J., Spits, H., Roncarolo, M. G., te Velde, A. *et al.* (1991). Interleukin 10 (IL-10) and viral IL-10 strongly reduce antigen-specific human T cell proliferation by diminishing the antigen-presenting capacity of monocytes via downregulation of class II major histocompatibility complex expression. *J Exp Med* **174**,(4) 915-24.

Debatin, K. M. and Krammer, P. H. (2004). Death receptors in chemotherapy and cancer. *Oncogene* **23**,(16) 2950-66.

Delcroix, M., Sajid, M., Caffrey, C. R., Lim, K. C., Dvorak, J. *et al.* (2006). A multienzyme network functions in intestinal protein digestion by a platyhelminth parasite. *J Biol Chem* **281**,(51) 39316-29.

DeMarco, R., Mathieson, W., G.P, D. and Wilson, R. A. (2007). Schistosome albumin is of host, not parasite, origin. *International Journal for Parasitology* **in press.**

Dillon, G. P., Feltwell, T., Skelton, J. P., Ashton, P. D., Coulson, P. S. *et al.* (2006). Microarray analysis identifies genes preferentially expressed in the lung schistosomulum of Schistosoma mansoni. *Int J Parasitol* **36**,(1) 1-8.

DiScipio, R. G., Schraufstatter, I. U., Sikora, L., Zuraw, B. L. and Sriramarao, P. (2006). C5a mediates secretion and activation of matrix metalloproteinase 9 from human eosinophils and neutrophils. *Int Immunopharmacol* **6**,(7) 1109-18.

Doenhoff, M., Musallam, R., Bain, J. and McGregor, A. (1979). Schistosoma mansoni infections in T-cell deprived mice, and the ameliorating effect of administering homologous chronic infection serum. I. Pathogenesis. *Am J Trop Med Hyg* **28**,(2) 260-3.

Doenhoff, M. J., Hassounah, O., Murare, H., Bain, J. and Lucas, S. (1986). The schistosome egg granuloma: immunopathology in the cause of host protection or parasite survival? *Trans R Soc Trop Med Hyg* **80**,(4) 503-14.

Doenhoff, M. J., Pearson, S., Dunne, D. W., Bickle, Q., Lucas, S. *et al.* (1981). Immunological control of hepatotoxicity and parasite egg excretion in Schistosoma mansoni infections: stage specificity of the reactivity of immune serum in T-cell deprived mice. *Trans R Soc Trop Med Hyg* **75**,(1) 41-53.

Donnelly, S., O'Neill, S. M., Sekiya, M., Mulcahy, G. and Dalton, J. P. (2005). Thioredoxin peroxidase secreted by Fasciola hepatica induces the alternative activation of macrophages. *Infect Immun* **73**,(1) 166-73.

Doong, H., Rizzo, K., Fang, S., Kulpa, V., Weissman, A. M. *et al.* (2003). CAIR-1/BAG-3 abrogates heat shock protein-70 chaperone complex-mediated protein degradation: accumulation of poly-ubiquitinated Hsp90 client proteins. *J Biol Chem* **278**,(31) 28490-500.

Duckett, C. S. and Thompson, C. B. (1997). CD30-dependent degradation of TRAF2: implications for negative regulation of TRAF signaling and the control of cell survival. *Genes Dev* **11**,(21) 2810-21.

Dunn, W. A., Jr. (1990). Studies on the mechanisms of autophagy: formation of the autophagic vacuole. *J Cell Biol* **110**,(6) 1923-33.

Dunne, D. W., Hassounah, O., Musallam, R., Lucas, S., Pepys, M. B. *et al.* (1983). Mechanisms of Schistosoma mansoni egg excretion: parasitological observations in immunosuppressed mice reconstituted with immune serum. *Parasite Immunol* **5**,(1) 47-60.

Dunne, D. W., Hillyer, G. V. and Vazquez, G. (1988). Schistosoma mansoni cationic egg antigens (CEF6): immunoserology with oxamniquine-treated patients and involvement of CEF6 in the circumoval precipitin reaction. *Am J Trop Med Hyg* **38**,(3) 508-14.

Dunne, D. W., Jones, F. M. and Doenhoff, M. J. (1991). The purification, characterization, serological activity and hepatotoxic properties of two cationic glycoproteins (alpha 1 and omega 1) from Schistosoma mansoni eggs. *Parasitology* **103 Pt** 2225-36.

Dunne, D. W., Lucas, S., Bickle, Q., Pearson, S., Madgwick, L. *et al.* (1981). Identification and partial purification of an antigen (omega 1) from Schistosoma mansoni eggs which is putatively hepatotoxic in T-cell deprived mice. *Trans R Soc Trop Med Hyg* **75**,(1) 54-71.

Eberl, M., Langermans, J. A., Frost, P. A., Vervenne, R. A., van Dam, G. J. *et al.* (2001a). Cellular and humoral immune responses and protection against schistosomes induced by a radiation-attenuated vaccine in chimpanzees. *Infect Immun* **69**,(9) 5352-62.

Eberl, M., Langermans, J. A., Vervenne, R. A., Nyame, A. K., Cummings, R. D. *et al.* (2001b). Antibodies to glycans dominate the host response to schistosome larvae and eggs: is their role protective or subversive? *J Infect Dis* **183**,(8) 1238-47.

Eberle, H. B., Serrano, R. L., Fullekrug, J., Schlosser, A., Lehmann, W. D. *et al.* (2002). Identification and characterization of a novel human plant pathogenesis-related protein that localizes to lipid-enriched microdomains in the Golgi complex. *J Cell Sci* **115**,(Pt 4) 827-38.

Ebersberger, I., Knobloch, J. and Kunz, W. (2005). Cracks in the shell--zooming in on eggshell formation in the human parasite Schistosoma mansoni. *Dev Genes Evol* **215**,(5) 261-7.

Edman, P. (1949). A method for the determination of the amino acid sequence in peptides. *Archives of Biochemistry* **22**,(3) 475-476.

El-Gindy, M. S. (1951). Post-cercarial development of *Schistosomatium douthitti* (Cort, 1914) Price 1931 in mice, with special reference to the genital system (schistosomatidae-Trematoda). *Journal of Morphology* **89**,(1) 151-185.

El Ridi, R., Velupillai, P. and Harn, D. A. (1996). Regulation of schistosome egg granuloma formation: host-soluble L-selectin enters tissue-trapped eggs and binds to carbohydrate antigens on surface membranes of miracidia. *Infect Immun* **64**,(11) 4700-5.

Erasmus, D. A. (1973). A comparative study of the reproductive system of mature, immature and "unisexual" female Schistosoma mansoni. *Parasitology* **67**,(2) 165-83.

Erasmus, D. A. (1975). Schistosoma mansoni: development of the vitelline cell, its role in drug sequestration, and changes induced by Astiban. *Exp Parasitol* **38**,(2) 240-56.

Erasmus, D. A. (1987). The Adult Schistosome: Structure and Reproductive Biology. In *The Biology of Schistosomes from Genes to Latrines*. (eds D. Rollinson and A. J. G. Simpson), pp. 51 - 82. London: Academic Press.

Eskelinen, E. L. (2005). Maturation of autophagic vacuoles in Mammalian cells. *Autophagy* **1**,(1) 1-10.

Faust, E. C. (1946). The diagnosis of Schistosomiasis Japonica II. The diagnostic characteristics of the eggs of the etiologic agent *Schistosoma japonicum*. *Am J Trop Med Hyg* **26**113 - 123.

Faust, E. C., Jones, C. A. and Hoffman, W. A. (1934). Studies on schistosomiasis mansoni in Puerto Rico. III. Biological studies. 2. The mammalian phase of the life cycle. *Puerto Rico Journal of Public Health and Tropical Medicine* **10**,(2) 133-196.

Fenwick, A. and Webster, J. P. (2006). Schistosomiasis: challenges for control, treatment and drug resistance. *Curr Opin Infect Dis* **19**,(6) 577-82.

File, S. (1995). Interaction of schistosome eggs with vascular endothelium. *J Parasitol* **81**,(2) 234-8.

Finger, E., Brodeur, P. H., Hernandez, H. J. and Stadecker, M. J. (2005). Expansion of CD4 T cells expressing a highly restricted TCR structure specific for a single parasite epitope correlates with high pathology in murine schistosomiasis. *Eur J Immunol* **35**,(9) 2659-69.

Fitzsimmons, C. M., Schramm, G., Jones, F. M., Chalmers, I. W., Hoffmann, K. F. ***et al.*** (2005). Molecular characterization of omega-1: a hepatotoxic ribonuclease from Schistosoma mansoni eggs. *Mol Biochem Parasitol* **144**,(1) 123-7.

Flierman, D., Ye, Y., Dai, M., Chau, V. and Rapoport, T. A. (2003). Polyubiquitin serves as a recognition signal, rather than a ratcheting molecule, during retrotranslocation of proteins across the endoplasmic reticulum membrane. *J Biol Chem* **278**,(37) 34774-82.

Flores Villanueva, P. O., Reiser, H. and Stadecker, M. J. (1994). Regulation of T helper cell responses in experimental murine schistosomiasis by IL-10. Effect on expression of B7 and B7-2 costimulatory molecules by macrophages. *J Immunol* **153**,(11) 5190-9.

Foley, K. and Cooley, L. (1998). Apoptosis in late stage Drosophila nurse cells does not require genes within the H99 deficiency. *Development* **125**,(6) 1075-82.

Friedman, J. and Xue, D. (2004). To live or die by the sword: the regulation of apoptosis by the proteasome. *Dev Cell* **6**,(4) 460-1.

Fukaya, Y. and Yamaguchi, M. (2004). Regucalcin increases superoxide dismutase activity in rat liver cytosol. *Biol Pharm Bull* **27**,(9) 1444-6.

Fulton, S. A., Reba, S. M., Pai, R. K., Pennini, M., Torres, M. *et al.* (2004). Inhibition of major histocompatibility complex II expression and antigen processing in murine alveolar macrophages by Mycobacterium bovis BCG and the 19-kilodalton mycobacterial lipoprotein. *Infect Immun* **72**,(4) 2101-10.

Gantt, S. M., Myung, J. M., Briones, M. R., Li, W. D., Corey, E. J. *et al.* (1998). Proteasome inhibitors block development of Plasmodium spp. *Antimicrob Agents Chemother* **42**,(10) 2731-8.

Gawaz, M., Langer, H. and May, A. E. (2005). Platelets in inflammation and atherogenesis. *J Clin Invest* **115**,(12) 3378-84.

Geminard, C., Nault, F., Johnstone, R. M. and Vidal, M. (2001). Characteristics of the interaction between Hsc70 and the transferrin receptor in exosomes released during reticulocyte maturation. *J Biol Chem* **276**,(13) 9910-6.

Gillece, P., Luz, J. M., Lennarz, W. J., de La Cruz, F. J. and Romisch, K. (1999). Export of a cysteine-free misfolded secretory protein from the endoplasmic reticulum for degradation requires interaction with protein disulfide isomerase. *J Cell Biol* **147**,(7) 1443-56.

Glaumann, H. (1989). Crinophagy as a means for degrading excess secretory proteins in rat liver. *Revis Biol Celular* **2097-110.**

Glickman, M. H. and Ciechanover, A. (2002). The ubiquitin-proteasome proteolytic pathway: destruction for the sake of construction. *Physiol Rev* **82**,(2) 373-428.

Goetzl, E. J., Banda, M. J. and Leppert, D. (1996). Matrix metalloproteinases in immunity. *J Immunol* **156**,(1) 1-4.

Gomez, D. E., Alonso, D. F., Yoshiji, H. and Thorgeirsson, U. P. (1997). Tissue inhibitors of metalloproteinases: structure, regulation and biological functions. *Eur J Cell Biol* **74**,(2) 111-22.

Gomez, D. E., De Lorenzo, M. S., Alonso, D. F. and Andrade, Z. A. (1999). Expression of metalloproteinases (MMP-1, MMP-2, and MMP-9) and their inhibitors (TIMP-1 and TIMP-2) in schistosomal portal fibrosis. *Am J Trop Med Hyg* **61**,(1) 9-13.

Gonzalez, E. (1989). Schistosomiasis, cercarial dermatitis, and marine dermatitis. *Dermatol Clin* **7**,(2) 291-300.

Gozuacik, D. and Kimchi, A. (2004). Autophagy as a cell death and tumor suppressor mechanism. *Oncogene* **23**,(16) 2891-906.

Green, D. R. and Evan, G. I. (2002). A matter of life and death. *Cancer Cell* **1**,(1) 19-30.

Gregory, C. D. and Devitt, A. (2004). The macrophage and the apoptotic cell: an innate immune interaction viewed simplistically? *Immunology* **113**,(1) 1-14.

Groll, M., Ditzel, L., Lowe, J., Stock, D., Bochtler, M. *et al.* (1997). Structure of 20S proteasome from yeast at 2.4 A resolution. *Nature* **386**,(6624) 463-71.

Gruden-Movsesijan, A. and Milosavljevic Lj, S. (2006). The involvement of the macrophage mannose receptor in the innate immune response to infection with parasite Trichinella spiralis. *Vet Immunol Immunopathol* **109**,(1-2) 57-67.

Guerra-Sa, R., Castro-Borges, W., Evangelista, E. A., Kettelhut, I. C. and Rodrigues, V. (2005). Schistosoma mansoni: functional proteasomes are required for development in the vertebrate host. *Exp Parasitol* **109**,(4) 228-36.

Hang, L. M., Warren, K. S. and Boros, D. L. (1974). Schistosoma mansoni: antigenic secretions and the etiology of egg granulomas in mice. *Exp Parasitol* **35**,(2) 288-98.

Hanna, J., Hathaway, N. A., Tone, Y., Crosas, B., Elsasser, S. *et al.* (2006). Deubiquitinating enzyme Ubp6 functions noncatalytically to delay proteasomal degradation. *Cell* **127**,(1) 99-111.

Harrop, R., Coulson, P. S. and Wilson, R. A. (1999). Characterization, cloning and immunogenicity of antigens released by lung-stage larvae of Schistosoma mansoni. *Parasitology* **118 (Pt 6)**583-94.

Hedstrom, R., Culpepper, J., Harrison, R. A., Agabian, N. and Newport, G. (1987). A major immunogen in Schistosoma mansoni infections is homologous to the heat-shock protein Hsp70. *J Exp Med* **165**,(5) 1430-5.

Hedstrom, R., Culpepper, J., Schinski, V., Agabian, N. and Newport, G. (1988). Schistosome heat-shock proteins are immunologically distinct host-like antigens. *Mol Biochem Parasitol* **29**,(2-3) 275-82.

Hegerl, R., Pfeifer, G., Puhler, G., Dahlmann, B. and Baumeister, W. (1991). The three-dimensional structure of proteasomes from Thermoplasma acidophilum as determined by electron microscopy using random conical tilting. *FEBS Lett* **283**,(1) 117-21.

Hegmans, J. P., Bard, M. P., Hemmes, A., Luider, T. M., Kleijmeer, M. J. *et al.* (2004). Proteomic analysis of exosomes secreted by human mesothelioma cells. *Am J Pathol* **164**,(5) 1807-15.

Hengartner, M. O. (2000). The biochemistry of apoptosis. *Nature* **407**,(6805) 770-6.

Hernandez, H. J., Edson, C. M., Harn, D. A., Ianelli, C. J. and Stadecker, M. J. (1998). Schistosoma mansoni: genetic restriction and cytokine profile of the CD4 + T helper cell response to dominant epitope peptide of major egg antigen Sm-p40. *Exp Parasitol* **90**,(1) 122-30.

Hernandez, H. J. and Stadecker, M. J. (1999). Elucidation and role of critical residues of immunodominant peptide associated with T cell-mediated parasitic disease. *J Immunol* **163**,(7) 3877-82.

Hernandez, H. J., Trzyna, W. C., Cordingley, J. S., Brodeur, P. H. and Stadecker, M. J. (1997). Differential antigen recognition by T cell populations from strains of mice developing polar forms of granulomatous inflammation in response to eggs of Schistosoma mansoni. *Eur J Immunol* **27**,(3) 666-70.

Hertz-Fowler, C., Peacock, C. S., Wood, V., Aslett, M., Kerhornou, A. *et al.* (2004). GeneDB: a resource for prokaryotic and eukaryotic organisms. *Nucleic Acids Res* **32**,(Database issue) D339-43.

Hesse, M., Piccirillo, C. A., Belkaid, Y., Prufer, J., Mentink-Kane, M. *et al.* (2004). The pathogenesis of schistosomiasis is controlled by cooperating IL-10-producing innate effector and regulatory T cells. *J Immunol* **172**,(5) 3157-66.

Hicke, L. (2001). Protein regulation by monoubiquitin. *Nat Rev Mol Cell Biol* **2**,(3) 195-201.

Hirano, Y., Yoshinaga, S., Ogura, K., Yokochi, M., Noda, Y. *et al.* (2004). Solution structure of atypical protein kinase C PB1 domain and its mode of interaction with ZIP/p62 and MEK5. *J Biol Chem* **279**,(30) 31883-90.

Hofmann, K. and Bucher, P. (1996). The UBA domain: a sequence motif present in multiple enzyme classes of the ubiquitination pathway. *Trends Biochem Sci* **21**,(5) 172-3.

Hoppe, T. (2005). Multiubiquitylation by E4 enzymes: 'one size' doesn't fit all. *Trends Biochem Sci* **30**,(4) 183-7.

Hunt, C. R., Parsian, A. J., Goswami, P. C. and Kozak, C. A. (1999). Characterization and expression of the mouse Hsc70 gene. *Biochim Biophys Acta* **1444**,(3) 315-25.

Hutchins, M. U., Veenhuis, M. and Klionsky, D. J. (1999). Peroxisome degradation in Saccharomyces cerevisiae is dependent on machinery of macroautophagy and the Cvt pathway. *J Cell Sci* **112 (Pt 22)**4079-87.

Iacomini, J., Ricklan, D. E. and Stadecker, M. J. (1995). T cells expressing the gamma delta T cell receptor are not required for egg granuloma formation in schistosomiasis. *Eur J Immunol* **25**,(4) 884-8.

Imase, A., Matsuda, H., Irie, Y. and Iwamura, Y. (2003). Existence of host DNA sequences in schistosomes--horizontal and vertical transmission. *Parasitol Int* **52**,(4) 369-73.

Irie, Y., Tanaka, M. and Yasuraoka, K. (1987). Degenerative changes in the reproductive organs of female schistosomes during maintenance in vitro. *J Parasitol* **73**,(4) 829-35.

Ismail, M., Metwally, A., Farghaly, A., Bruce, J., Tao, L. F. *et al.* (1996). Characterization of isolates of Schistosoma mansoni from Egyptian villagers that tolerate high doses of praziquantel. *Am J Trop Med Hyg* **55**,(2) 214-8.

Isogai, M., Oishi, K. and Yamaguchi, M. (1994a). Serum release of hepatic calcium-binding protein regucalcin by liver injury with galactosamine administration in rats. *Mol Cell Biochem* **136**,(1) 85-90.

Isogai, M., Shimokawa, N. and Yamaguchi, M. (1994b). Hepatic calcium-binding protein regucalcin in released into the serum of rats administered orally carbon tetrachloride. *Mol Cell Biochem* **131**,(2) 173-9.

Janeway, C. A., Jr. and Medzhitov, R. (2002). Innate immune recognition. *Annu Rev Immunol* **20**197-216.

Jang-Lee, J., Curwen, R. S., Ashton, P. D., Tissot, B., Mathieson, W. *et al.* (2007). Glycomic analysis of Schistosoma mansoni egg and cercarial secretions. *Mol Cell Proteomics*.

Jarosch, E., Taxis, C., Volkwein, C., Bordallo, J., Finley, D. *et al.* (2002). Protein dislocation from the ER requires polyubiquitination and the AAA-ATPase Cdc48. *Nat Cell Biol* **4**,(2) 134-9.

Jensen-Smith, H. C., Luduena, R. F. and Hallworth, R. (2003). Requirement for the betaI and betaIV tubulin isotypes in mammalian cilia. *Cell Motil Cytoskeleton* **55**,(3) 213-20.

Johnson, R. S., Martin, S. A., Biemann, K., Stults, J. T. and Watson, J. T. (1987). Novel fragmentation process of peptides by collision-induced decomposition in a tandem mass spectrometer: differentiation of leucine and isoleucine. *Anal Chem* **59**,(21) 2621-5.

Jourdane, J. and Theron, A. (1987). Larval Development: Eggs to Cercariae. In *The Biology of Schistosomes. From Genes to Latrienes.* (eds D. Rollinson and A. J. G. Simpson), pp. 83 - 113. London: Academic Press.

Kallestrup, P., Zinyama, R., Gomo, E., Butterworth, A. E., van Dam, G. J. *et al.* (2005). Schistosomiasis and HIV-1 infection in rural Zimbabwe: implications of coinfection for excretion of eggs. *J Infect Dis* **191**,(8) 1311-20.

Kanamura, H. Y., Hancock, K., Rodrigues, V. and Damian, R. T. (2002). Schistosoma mansoni heat shock protein 70 elicits an early humoral immune response in S. mansoni infected baboons. *Mem Inst Oswaldo Cruz* **97**,(5) 711-6.

Kanse, S. M., Liang, O., Schubert, U., Haas, H., Preissner, K. T. *et al.* (2005). Characterisation and partial purification of Schistosoma mansoni egg-derived pro-angiogenic factor. *Mol Biochem Parasitol* **144**,(1) 76-85.

Kappe, G., Aquilina, J. A., Wunderink, L., Kamps, B., Robinson, C. V. *et al.* (2004). Tsp36, a tapeworm small heat-shock protein with a duplicated alpha-crystallin domain, forms dimers and tetramers with good chaperone-like activity. *Proteins* **57**,(1) 109-17.

Karanja, D. M., Colley, D. G., Nahlen, B. L., Ouma, J. H. and Secor, W. E. (1997). Studies on schistosomiasis in western Kenya: I. Evidence for immune-facilitated excretion of schistosome eggs from patients with Schistosoma mansoni and human immunodeficiency virus coinfections. *Am J Trop Med Hyg* **56**,(5) 515-21.

Kassim, O. and Gibertson, D. E. (1976). Hatching of Schistosoma mansoni eggs and observations on motility of miracidia. *J Parasitol* **62**,(5) 715-20.

Khoo, K. H., Chatterjee, D., Caulfield, J. P., Morris, H. R. and Dell, A. (1997). Structural mapping of the glycans from the egg glycoproteins of Schistosoma mansoni and Schistosoma japonicum: identification of novel core structures and terminal sequences. *Glycobiology* **7**,(5) 663-77.

Kim, T. Y., Joo, I. J., Kang, S. Y., Cho, S. Y. and Hong, S. J. (2002). Paragonimus westermani: molecular cloning, expression, and characterization of a recombinant yolk ferritin. *Exp Parasitol* **102**,(3-4) 194-200.

Kimura, Y., Takaoka, M., Tanaka, S., Sassa, H., Tanaka, K. *et al.* (2000). N(alpha)-acetylation and proteolytic activity of the yeast 20 S proteasome. *J Biol Chem* **275**,(7) 4635-9.

King, C. (2001). Epidemiology of Schistosomiasis: Determinants of Transmission of Infection In *Schistosomiasis*. (eds A. Mahmoud), pp. 115 - 212. London: Imperial College Press.

King, C. H., Dickman, K. and Tisch, D. J. (2005). Reassessment of the cost of chronic helmintic infection: a meta-analysis of disability-related outcomes in endemic schistosomiasis. *Lancet* **365**,(9470) 1561-9.

Klionsky, D. J. (2005). The molecular machinery of autophagy: unanswered questions. *J Cell Sci* **118**,(Pt 1) 7-18.

Klionsky, D. J. and Emr, S. D. (2000). Autophagy as a regulated pathway of cellular degradation. *Science* **290**,(5497) 1717-21.

Kloetzel, K. (1967). Egg and pigment production in Schistosoma mansoni infections of the white mouse. *Am J Trop Med Hyg* **16**,(3) 293-9.

Kloetzel, K. (1968). A collagenaselike substance produced by eggs of Schistosoma mansoni. *J Parasitol* **54**,(1) 177-8.

Klose, J. (1975). Protein mapping by combined isoelectric focusing and electrophoresis of mouse tissues. A novel approach to testing for induced point mutations in mammals. *Humangenetik* **26**,(3) 231-43.

Koegl, M., Hoppe, T., Schlenker, S., Ulrich, H. D., Mayer, T. U. *et al.* (1999). A novel ubiquitination factor, E4, is involved in multiubiquitin chain assembly. *Cell* **96**,(5) 635-44.

Kopp, F., Dahlmann, B. and Hendil, K. B. (1993). Evidence indicating that the human proteasome is a complex dimer. *J Mol Biol* **229**,(1) 14-9.

Koster, B., Dargatz, H., Schroder, J., Hirzmann, J., Haarmann, C. *et al.* (1988). Identification and localisation of the products of a putative eggshell precursor gene in the vitellarium of Schistosoma mansoni. *Mol Biochem Parasitol* **31**,(2) 183-98.

Kouoh, F., Gressier, B., Luyckx, M., Brunet, C., Dine, T. *et al.* (1999). Antioxidant properties of albumin: effect on oxidative metabolism of human neutrophil granulocytes. *Farmaco* **54**,(10) 695-9.

Koura, M. (1970). The relation between egg production and worm burden in experimental Schistosomiasis. I. Worm burden. *J Egypt Med Assoc* **53**,(7) 598-602.

Kuhlbrodt, K., Mouysset, J. and Hoppe, T. (2005). Orchestra for assembly and fate of polyubiquitin chains. *Essays Biochem* **411**-14.

Kusel, J. R. (1970). Studies on the structure and hatching of the eggs of Schistosoma mansoni. *Parasitology* **60**,(1) 79-88.

La Flamme, A. C., Patton, E. A., Bauman, B. and Pearce, E. J. (2001). IL-4 plays a crucial role in regulating oxidative damage in the liver during schistosomiasis. *J Immunol* **166**,(3) 1903-11.

Lacraz, S., Isler, P., Vey, E., Welgus, H. G. and Dayer, J. M. (1994). Direct contact between T lymphocytes and monocytes is a major pathway for induction of metalloproteinase expression. *J Biol Chem* **269**,(35) 22027-33.

Lanar, D. E., Pearce, E. J. and Sher, A. (1985). Expression in Escherichia coli of two Schistosoma mansoni genes that encode major antigens recognized by immune mice. *Mol Biochem Parasitol* **17**,(1) 45-60.

Lawn, S. D., Lucas, S. B. and Chiodini, P. L. (2003). Case report: Schistosoma mansoni infection: failure of standard treatment with praziquantel in a returned traveller. *Trans R Soc Trop Med Hyg* **97**,(1) 100-1.

Lawson, J. R. and Wilson, R. A. (1980). Metabolic changes associated with the migration of the schistosomulum of Schistosoma mansoni in the mammal host. *Parasitology* **81**,(2) 325-36.

Lee, D. H. and Goldberg, A. L. (1998). Proteasome inhibitors cause induction of heat shock proteins and trehalose, which together confer thermotolerance in Saccharomyces cerevisiae. *Mol Cell Biol* **18**,(1) 30-8.

Lee, H. F. (1962). Life history of Heterobilharzia americana Price 1929, a schistosome of the raccoon and other mammals in southeastern United States. *J Parasitol* **48**728-39.

Leitch, B. and Probert, A. J. (1984). Schistosoma haematobium: amoscanate and adult worm ultrastructure. *Exp Parasitol* **58**,(3) 278-89.

Lemasters, J. J., Qian, T., Elmore, S. P., Trost, L. C., Nishimura, Y. *et al.* (1998). Confocal microscopy of the mitochondrial permeability transition in necrotic cell killing, apoptosis and autophagy. *Biofactors* **8**,(3-4) 283-5.

Leroux, M. R., Ma, B. J., Batelier, G., Melki, R. and Candido, E. P. (1997). Unique structural features of a novel class of small heat shock proteins. *J Biol Chem* **272**,(19) 12847-53.

Levine, B. and Klionsky, D. J. (2004). Development by self-digestion: molecular mechanisms and biological functions of autophagy. *Dev Cell* **6**,(4) 463-77.

Li, M., Carpio, D. F., Zheng, Y., Bruzzo, P., Singh, V. *et al.* (2001). An essential role of the NF-kappa B/Toll-like receptor pathway in induction of inflammatory and tissue-repair gene expression by necrotic cells. *J Immunol* **166**,(12) 7128-35.

Lijnen, P., Saavedra, A. and Petrov, V. (1997). In vitro proliferative response of human peripheral blood mononuclear cells to concanavalin A. *Clin Chim Acta* **264**,(1) 91-101.

Lilley, B. N. and Ploegh, H. L. (2004). A membrane protein required for dislocation of misfolded proteins from the ER. *Nature* **429**,(6994) 834-40.

Linder, E. (1986). Identification of schistosomal eggs. Description of an immunological spot assay for hatch fluid antigen. *J Immunol Methods* **88**,(1) 137-40.

Liu, F., Lu, J., Hu, W., Wang, S. Y., Cui, S. J. *et al.* (2006). New perspectives on host-parasite interplay by comparative transcriptomic and proteomic analyses of Schistosoma japonicum. *PLoS Pathog* **2**,(4) e29.

Lu, G., Villalba, M., Coscia, M. R., Hoffman, D. R. and King, T. P. (1993). Sequence analysis and antigenic cross-reactivity of a venom allergen, antigen 5, from hornets, wasps, and yellow jackets. *J Immunol* **150**,(7) 2823-30.

Luduena, R. F., Banerjee, A. and Khan, I. A. (1992). Tubulin structure and biochemistry. *Curr Opin Cell Biol* **4**,(1) 53-7.

MacDonald, A. S., Straw, A. D., Bauman, B. and Pearce, E. J. (2001). CD8- dendritic cell activation status plays an integral role in influencing Th2 response development. *J Immunol* **167**,(4) 1982-8.

Mahajan-Miklos, S. and Cooley, L. (1994). Intercellular cytoplasm transport during Drosophila oogenesis. *Dev Biol* **165**,(2) 336-51.

Makioka, A., Kumagai, M., Ohtomo, H., Kobayashi, S. and Takeuchi, T. (2002). Effect of proteasome inhibitors on the growth, encystation, and excystation of Entamoeba histolytica and Entamoeba invadens. *Parasitol Res* **88**,(5) 454-9.

Mason, G. G., Murray, R. Z., Pappin, D. and Rivett, A. J. (1998). Phosphorylation of ATPase subunits of the 26S proteasome. *FEBS Lett* **430**,(3) 269-74.

Mayer, M. P. and Bukau, B. (2005). Hsp70 chaperones: cellular functions and molecular mechanism. *Cell Mol Life Sci* **62**,(6) 670-84.

McCall, K. (2004). Eggs over easy: cell death in the Drosophila ovary. *Dev Biol* **274**,(1) 3-14.

McClellan, A. J. and Frydman, J. (2001). Molecular chaperones and the art of recognizing a lost cause. *Nat Cell Biol* **3**,(2) E51-3.

McLaren, M. L., Lillywhite, J. E., Dunne, D. W. and Doenhoff, M. J. (1981). Serodiagnosis of human Schistosoma mansoni infections: enhanced sensitivity and specificity in ELISA using a fraction containing S. mansoni egg antigens omega 1 and alpha 1. *Trans R Soc Trop Med Hyg* **75**,(1) 72-9.

McMullen, D. B. and Beaver, P. C. (1945). Studies on schistosome dermatitis. IX. The life cycles of three dermatitis-producing schistosomes from birds and a discussion of the subfamily Bilharziellinae (Trematoda: Schistosomatidae). *american Journal of Hygiene* **42**128-154.

Melamed, P., Chong, K. L. and Johansen, M. V. (2004). Evidence for lateral gene transfer from salmonids to two Schistosome species. *Nat Genet* **36**,(8) 786-7.

Mentink-Kane, M. M., Cheever, A. W., Thompson, R. W., Hari, D. M., Kabatereine, N. B. *et al.* (2004). IL-13 receptor alpha 2 down-modulates granulomatous inflammation and prolongs host survival in schistosomiasis. *Proc Natl Acad Sci U S A* **101**,(2) 586-90.

Merckelbach, A., Wager, M. and Lucius, R. (2003). Analysis of cDNAs coding for immunologically dominant antigens from an oncosphere-specific cDNA library of Echinococcus multilocularis. *Parasitol Res* **90**,(6) 493-501.

Merrick, B. A., Bruno, M. E., Madenspacher, J. H., Wetmore, B. A., Foley, J. *et al.* (2006). Alterations in the rat serum proteome during liver injury from acetaminophen exposure. *J Pharmacol Exp Ther* **318**,(2) 792-802.

Meshnick, S. R. (2002). Artemisinin: mechanisms of action, resistance and toxicity. *Int J Parasitol* **32**,(13) 1655-60.

Misawa, H. and Yamaguchi, M. (2000). The gene of Ca2+-binding protein regucalcin is highly conserved in vertebrate species. *Int J Mol Med* **6**,(2) 191-6.

Mochizuki, S. and Okada, Y. (2007). ADAMs in cancer cell proliferation and progression. *Cancer Sci* **98**,(5) 621-8.

Moczon, T. and Swiderski, Z. (1983). Schistosoma haematobium: oxidoreductase histochemistry and ultrastructure of niridazole-treated females. *Int J Parasitol* **13**,(2) 225-32.

Molinari, M. and Sitia, R. (2005). The secretory capacity of a cell depends on the efficiency of endoplasmic reticulum-associated degradation. *Curr Top Microbiol Immunol* **3001**-15.

Moore, D. V. and Sandground, J. H. (1956). The relative egg producing capacity of Schistosoma mansoni and Schistosoma japonicum. *Am J Trop Med Hyg* **5**,(5) 831-40.

Moser, D., Doenhoff, M. J. and Klinkert, M. Q. (1992). A stage-specific calcium-binding protein expressed in eggs of Schistosoma mansoni. *Mol Biochem Parasitol* **51**,(2) 229-38.

Mpakou, V. E., Nezis, I. P., Stravopodis, D. J., Margaritis, L. H. and Papassideri, I. S. (2006). Programmed cell death of the ovarian nurse cells during oogenesis of the silkmoth Bombyx mori. *Dev Growth Differ* **48**,(7) 419-28.

Muratani, M. and Tansey, W. P. (2003). How the ubiquitin-proteasome system controls transcription. *Nat Rev Mol Cell Biol* **4**,(3) 192-201.

Muratori, M., Marchiani, S., Forti, G. and Baldi, E. (2005). Sperm ubiquitination positively correlates to normal morphology in human semen. *Hum Reprod* **20**,(4) 1035-43.

Nabhan, J. F., Hamdan, F. F. and Ribeiro, P. (2001). A Schistosoma mansoni Pad1 homologue stabilizes c-Jun. *Mol Biochem Parasitol* **116**,(2) 209-18.

Nagase, H. (1997). Activation mechanisms of matrix metalloproteinases. *Biol Chem* **378**,(3-4) 151-60.

Nassar, N., Horn, G., Herrmann, C., Scherer, A., McCormick, F. *et al.* (1995). The 2.2 A crystal structure of the Ras-binding domain of the serine/threonine kinase c-Raf1 in complex with Rap1A and a GTP analogue. *Nature* **375**,(6532) 554-60.

Nauta, A. J., Daha, M. R., van Kooten, C. and Roos, A. (2003). Recognition and clearance of apoptotic cells: a role for complement and pentraxins. *Trends Immunol* **24**,(3) 148-54.

Neill, P. J., Smith, J. H., Doughty, B. L. and Kemp, M. (1988). The ultrastructure of the Schistosoma mansoni egg. *Am J Trop Med Hyg* **39**,(1) 52-65.

Nelson, G. S. and Saoud, M. F. A. (1966). The daily egg output of *Schistosoma mansoni* in rhesus monkeys. *Transactions of the Royal Society of Hygiene and Tropical Medicine* **60**429-430.

Nene, V., Dunne, D. W., Johnson, K. S., Taylor, D. W. and Cordingley, J. S. (1986). Sequence and expression of a major egg antigen from Schistosoma mansoni. Homologies to heat shock proteins and alpha-crystallins. *Mol Biochem Parasitol* **21**,(2) 179-88.

Neumann, S., Ziv, E., Lantner, F. and Schechter, I. (1993). Regulation of HSP70 gene expression during the life cycle of the parasitic helminth Schistosoma mansoni. *Eur J Biochem* **212**,(2) 589-96.

Neves, R. H., de Lamare Biolchini, C., Machado-Silva, J. R., Carvalho, J. J., Branquinho, T. B. *et al.* (2005). A new description of the reproductive system of Schistosoma mansoni (Trematoda: Schistosomatidae) analyzed by confocal laser scanning microscopy. *Parasitol Res* **95**,(1) 43-9.

Nez, M. M. and Short, R. B. (1957). Gametogenesis in Schistosomatium douthitti (Cort) (Schistosomatidae: Trematoda). *J Parasitol* **43**,(2) 167-82.

Nezis, I. P., Stravopodis, D. J., Papassideri, I., Robert-Nicoud, M. and Margaritis, L. H. (2000). Stage-specific apoptotic patterns during Drosophila oogenesis. *Eur J Cell Biol* **79**,(9) 610-20.

Ngaiza, J. R. and Doenhoff, M. J. (1990). Blood platelets and schistosome egg excretion. *Proc Soc Exp Biol Med* **193**,(1) 73-9.

Ngaiza, J. R., Doenhoff, M. J. and Jaffe, E. A. (1993). Schistosoma mansoni egg attachment to cultured human umbilical vein endothelial cells: an in vitro model of an early step of parasite egg excretion. *J Infect Dis* **168**,(6) 1576-80.

Nijhawan, D., Fang, M., Traer, E., Zhong, Q., Gao, W. *et al.* (2003). Elimination of Mcl-1 is required for the initiation of apoptosis following ultraviolet irradiation. *Genes Dev* **17**,(12) 1475-86.

Nkemngu, N. J., Rosenkranz, V., Wink, M. and Steverding, D. (2002). Antitrypanosomal activities of proteasome inhibitors. *Antimicrob Agents Chemother* **46**,(6) 2038-40.

Nyame, A. K., Pilcher, J. B., Tsang, V. C. and Cummings, R. D. (1997). Rodents infected with Schistosoma mansoni produce cytolytic IgG and IgM antibodies to the Lewis x antigen. *Glycobiology* **7**,(2) 207-15.

O'Farrell, P. H. (1975). High resolution two-dimensional electrophoresis of proteins. *J Biol Chem* **250**,(10) 4007-21.

Okada, S., Kita, H., George, T. J., Gleich, G. J. and Leiferman, K. M. (1997). Migration of eosinophils through basement membrane components in vitro: role of matrix metalloproteinase-9. *Am J Respir Cell Mol Biol* **17**,(4) 519-28.

Okano, M., Satoskar, A. R., Nishizaki, K., Abe, M. and Harn, D. A., Jr. (1999). Induction of Th2 responses and IgE is largely due to carbohydrates functioning as adjuvants on Schistosoma mansoni egg antigens. *J Immunol* **163**,(12) 6712-7.

Okano, M., Satoskar, A. R., Nishizaki, K. and Harn, D. A., Jr. (2001). Lacto-N-fucopentaose III found on Schistosoma mansoni egg antigens functions as adjuvant for proteins by inducing Th2-type response. *J Immunol* **167**,(1) 442-50.

Oliveira, M. F., d'Avila, J. C., Tempone, A. J., Soares, J. B., Rumjanek, F. D. *et al.* (2004). Inhibition of heme aggregation by chloroquine reduces Schistosoma mansoni infection. *J Infect Dis* **190**,(4) 843-52.

Oliver-González, J. (1954). Anti-egg precipitins in the serum of humans infected with Schistosoma mansoni. *J Infect Dis* **95**,(1) 86-91.

Onodera, J. and Ohsumi, Y. (2004). Ald6p is a preferred target for autophagy in yeast, Saccharomyces cerevisiae. *J Biol Chem* **279**,(16) 16071-6.

Orlowski, M. and Wilk, S. (2000). Catalytic activities of the 20 S proteasome, a multicatalytic proteinase complex. *Arch Biochem Biophys* **383**,(1) 1-16.

Ozkan, E., Yu, H. and Deisenhofer, J. (2005). Mechanistic insight into the allosteric activation of a ubiquitin-conjugating enzyme by RING-type ubiquitin ligases. *Proc Natl Acad Sci U S A* **102**,(52) 18890-5.

Pan, S. C. (1980). The fine structure of the miracidium of Schistosoma mansoni. *J Invertebr Pathol* **36**,(3) 307-72.

Pappin, D. J., Hojrup, P. and Bleasby, A. J. (1993). Rapid identification of proteins by peptide-mass fingerprinting. *Curr Biol* **3**,(6) 327-32.

Pearce, E. J. (2003). Progress towards a vaccine for schistosomiasis. *Acta Trop* **86**,(2-3) 309-13.

Pearce, E. J., Caspar, P., Grzych, J. M., Lewis, F. A. and Sher, A. (1991). Downregulation of Th1 cytokine production accompanies induction of Th2 responses by a parasitic helminth, Schistosoma mansoni. *J Exp Med* **173**,(1) 159-66.

Pearce, E. J. and MacDonald, A. S. (2002). The immunobiology of schistosomiasis. *Nat Rev Immunol* **2**,(7) 499-511.

Pellegrino, J. and Coelho, P. M. (1978). Schistosoma mansoni: wandering capacity of a worm couple. *J Parasitol* **64**,(1) 181-2.

Pelley, R. P., Pelley, R. J., Hamburger, J., Peters, P. A. and Warren, K. S. (1976). Schistosoma mansoni soluble egg antigens. I. Identification and purification of three major antigens, and the employment of radioimmunoassay for their further characterization. *J Immunol* **117**,(5 Pt 1) 1553-60.

Peng, J., Schwartz, D., Elias, J. E., Thoreen, C. C., Cheng, D. ***et al.*** (2003). A proteomics approach to understanding protein ubiquitination. *Nat Biotechnol* **21**,(8) 921-6.

Pickart, C. M. and Cohen, R. E. (2004). Proteasomes and their kin: proteases in the machine age. *Nat Rev Mol Cell Biol* **5**,(3) 177-87.

Pilon, M., Schekman, R. and Romisch, K. (1997). Sec61p mediates export of a misfolded secretory protein from the endoplasmic reticulum to the cytosol for degradation. *Embo J* **16**,(15) 4540-8.

Price, E. W. (1929). A synopsis of the trematode family Schistosomidae, with descriptions of new genera and species. *Proceedings of the U.S. National Museum* **75**,(Article 18) 1-39.

Quinlan, G. J., Martin, G. S. and Evans, T. W. (2005). Albumin: biochemical properties and therapeutic potential. *Hepatology* **41**,(6) 1211-9.

Rabello, A. (1995). Acute human schistosomiasis mansoni. *Mem Inst Oswaldo Cruz* **90**,(2) 277-80.

Race, G. J., Martin, J. H., Moore, D. V. and Larsh, J. E., Jr. (1971). Scanning and transmission electronmicroscopy of Schistosoma mansoni eggs, cercariae, and adults. *Am J Trop Med Hyg* **20**,(6) 914-24.

Race, G. J., Michaels, R. M., Martin, J. H., Larsh, J. E., Jr. and Matthews, J. L. (1969). Schistosoma mansoni eggs: an electron microscopic study of shell pores and microbarbs. *Proc Soc Exp Biol Med* **130**,(3) 990-2.

Rappocciolo, G., Jenkins, F. J., Hensler, H. R., Piazza, P., Jais, M. *et al.* (2006). DC-SIGN is a receptor for human herpesvirus 8 on dendritic cells and macrophages. *J Immunol* **176**,(3) 1741-9.

Rathore, A., Sacristan, C., Ricklan, D. E., Flores Villanueva, P. O. and Stadecker, M. J. (1996). In situ analysis of B7-2 costimulatory, major histocompatibility complex class II, and adhesion molecule expression in schistosomal egg granulomas. *Am J Pathol* **149**,(1) 187-94.

Renthal, R., Schneider, B. G., Miller, M. M. and Luduena, R. F. (1993). Beta IV is the major beta-tubulin isotype in bovine cilia. *Cell Motil Cytoskeleton* **25**,(1) 19-29.

Rivett, A. J., Bose, S., Brooks, P. and Broadfoot, K. I. (2001). Regulation of proteasome complexes by gamma-interferon and phosphorylation. *Biochimie* **83**,(3-4) 363-6.

Roach, M. C., Boucher, V. L., Walss, C., Ravdin, P. M. and Luduena, R. F. (1998). Preparation of a monoclonal antibody specific for the class I isotype of beta-tubulin: the beta isotypes of tubulin differ in their cellular distributions within human tissues. *Cell Motil Cytoskeleton* **39**,(4) 273-85.

Robertson, C. D. (1999). The Leishmania mexicana proteasome. *Mol Biochem Parasitol* **103**,(1) 49-60.

Robijn, M. L., Wuhrer, M., Kornelis, D., Deelder, A. M., Geyer, R. ***et al.*** (2005). Mapping fucosylated epitopes on glycoproteins and glycolipids of Schistosoma mansoni cercariae, adult worms and eggs. *Parasitology* **130**,(Pt 1) 67-77.

Romisch, K. (2005). Endoplasmic reticulum-associated degradation. *Annu Rev Cell Dev Biol* **21**435-56.

Sadler, C. H., Rutitzky, L. I., Stadecker, M. J. and Wilson, R. A. (2003). IL-10 is crucial for the transition from acute to chronic disease state during infection of mice with Schistosoma mansoni. *Eur J Immunol* **33**,(4) 880-8.

Sakamoto, K. and Ishii, Y. (1977). Scanning electron microscope observations on adult Schistosoma japonicum. *J Parasitol* **63**,(3) 407-12.

Samuelson, J. C., Quinn, J. J. and Caulfield, J. P. (1984). Hatching, chemokinesis, and transformation of miracidia of Schistosoma mansoni. *J Parasitol* **70**,(3) 321-31.

Savill, J. and Fadok, V. (2000). Corpse clearance defines the meaning of cell death. *Nature* **407**,(6805) 784-8.

Savioli, L., Albonico, M., Engels, D. and Montresor, A. (2004). Progress in the prevention and control of schistosomiasis and soil-transmitted helminthiasis. *Parasitol Int* **53**,(2) 103-13.

Sayed, A. A., Cook, S. K. and Williams, D. L. (2006). Redox balance mechanisms in Schistosoma mansoni rely on peroxiredoxins and albumin and implicate peroxiredoxins as novel drug targets. *J Biol Chem* **281**,(25) 17001-10.

Sayed, A. A. and Williams, D. L. (2004). Biochemical characterization of 2-Cys peroxiredoxins from Schistosoma mansoni. *J Biol Chem* **279**,(25) 26159-66.

Schramm, G., Falcone, F. H., Gronow, A., Haisch, K., Mamat, U. ***et al.*** (2003). Molecular characterization of an interleukin-4-inducing factor from Schistosoma mansoni eggs. *J Biol Chem* **278**,(20) 18384-92.

Schramm, G., Gronow, A., Knobloch, J., Wippersteg, V., Grevelding, C. G. ***et al.*** (2006). IPSE/alpha-1: a major immunogenic component secreted from Schistosoma mansoni eggs. *Mol Biochem Parasitol* **147**,(1) 9-19.

Schubert, U., Anton, L. C., Gibbs, J., Norbury, C. C., Yewdell, J. W. ***et al.*** (2000). Rapid degradation of a large fraction of newly synthesized proteins by proteasomes. *Nature* **404**,(6779) 770-4.

Schussler, P., Potters, E., Winnen, R., Bottke, W. and Kunz, W. (1995). An isoform of ferritin as a component of protein yolk platelets in Schistosoma mansoni. *Mol Reprod Dev* **41**,(3) 325-30.

Schwertassek, U., Balmer, Y., Gutscher, M., Weingarten, L., Preuss, M. *et al.* (2007). Selective redox regulation of cytokine receptor signaling by extracellular thioredoxin-1. *Embo J.*

Shamu, C. E., Flierman, D., Ploegh, H. L., Rapoport, T. A. and Chau, V. (2001). Polyubiquitination is required for US11-dependent movement of MHC class I heavy chain from endoplasmic reticulum into cytosol. *Mol Biol Cell* **12**,(8) 2546-55.

Shaw, M. K., He, C. Y., Roos, D. S. and Tilney, L. G. (2000). Proteasome inhibitors block intracellular growth and replication of Toxoplasma gondii. *Parasitology* **121 (Pt 1)**35-47.

Shibue, T. and Taniguchi, T. (2006). BH3-only proteins: integrated control point of apoptosis. *Int J Cancer* **119**,(9) 2036-43.

Shiratsuchi, A., Watanabe, I., Takeuchi, O., Akira, S. and Nakanishi, Y. (2004). Inhibitory effect of Toll-like receptor 4 on fusion between phagosomes and endosomes/lysosomes in macrophages. *J Immunol* **172**,(4) 2039-47.

Simard, J. R., Zunszain, P. A., Ha, C. E., Yang, J. S., Bhagavan, N. V. *et al.* (2005). Locating high-affinity fatty acid-binding sites on albumin by x-ray crystallography and NMR spectroscopy. *Proc Natl Acad Sci U S A* **102**,(50) 17958-63.

Simpson, A. J. and Pena, S. D. (1991). Host-related DNA sequences in the schistosome genome? *Parasitol Today* **7**,(10) 266.

Singh, K. P., Gerard, H. C., Hudson, A. P. and Boros, D. L. (2004). Dynamics of collagen, MMP and TIMP gene expression during the granulomatous, fibrotic process induced by Schistosoma mansoni eggs. *Ann Trop Med Parasitol* **98**,(6) 581-93.

Singh, K. P., Gerard, H. C., Hudson, A. P. and Boros, D. L. (2006). Differential expression of collagen, MMP, TIMP and fibrogenic-cytokine genes in the granulomatous colon of Schistosoma mansoni-infected mice. *Ann Trop Med Parasitol* **100**,(7) 611-20.

Skelly, P. J., Stein, L. D. and Shoemaker, C. B. (1993). Expression of Schistosoma mansoni genes involved in anaerobic and oxidative glucose metabolism during the cercaria to adult transformation. *Mol Biochem Parasitol* **60**,(1) 93-104.

Skelly, P. J., Tielens, A. G. and Shoemaker, C. B. (1998). Glucose Transport and Metabolism in Mammalian-stage Schistosomes. *Parasitol Today* **14**,(10) 402-6.

Smith, P., Fallon, R. E., Mangan, N. E., Walsh, C. M., Saraiva, M. *et al.* (2005). Schistosoma mansoni secretes a chemokine binding protein with antiinflammatory activity. *J Exp Med* **202**,(10) 1319-25.

Smithers, S. R. and Terry, R. J. (1965). The infection of laboratory hosts with cercariae of *Schistosoma mansoni* and the recovery of adult worms. *Parasitology* **55** 695-700.

Smyth, J. D. and Halton, D. W. (1983). The Physiology of Trematodes.2nd Edition. Cambridge: Cambridge University Press.

Smythies, L. E., Betts, C., Coulson, P. S., Dowling, M. A. and Wilson, R. A. (1996). Kinetics and mechanism of effector focus formation in the lungs of mice vaccinated with irradiated cercariae of Schistosoma mansoni. *Parasite Immunol* **18**,(7) 359-69.

Soilleux, E. J., Morris, L. S., Leslie, G., Chehimi, J., Luo, Q. *et al.* (2002). Constitutive and induced expression of DC-SIGN on dendritic cell and macrophage subpopulations in situ and in vitro. *J Leukoc Biol* **71**,(3) 445-57.

Spence, I. M. and Silk, M. H. (1971). Ultrastructural studies of the blood fluke--Schistosoma mansoni. V. The female reproductive system--a preliminary report. *S Afr J Med Sci* **36**,(3) 41-50.

Stadecker, M. J., Hernandez, H. J. and Asahi, H. (2001). The identification and characterization of new immunogenic egg components: implications for evaluation and control of the immunopathogenic T cell response in schistosomiasis. *Mem Inst Oswaldo Cruz* **96 Suppl**29-33.

Stamler, R., Kappe, G., Boelens, W. and Slingsby, C. (2005). Wrapping the alpha-crystallin domain fold in a chaperone assembly. *J Mol Biol* **353**,(1) 68-79.

Standen, O. D. (1951). The effects of temperature, light and salinity upon the hatching of the ova of Schistosoma mansoni. *Trans R Soc Trop Med Hyg* **45**,(2) 225-41.

Steen, H. and Mann, M. (2004). The ABC's (and XYZ's) of peptide sequencing. *Nat Rev Mol Cell Biol* **5**,(9) 699-711.

Stein, R. L., Melandri, F. and Dick, L. (1996). Kinetic characterization of the chymotryptic activity of the 20S proteasome. *Biochemistry* **35**,(13) 3899-908.

Sumegi, M., Hunyadi-Gulyas, E., Medzihradszky, K. F. and Udvardy, A. (2003). 26S proteasome subunits are O-linked N-acetylglucosamine-modified in Drosophila melanogaster. *Biochem Biophys Res Commun* **312**,(4) 1284-9.

Sun, Y. and MacRae, T. H. (2005). Small heat shock proteins: molecular structure and chaperone function. *Cell Mol Life Sci* **62**,(21) 2460-76.

Swartz, J. M., Dyer, K. D., Cheever, A. W., Ramalingam, T., Pesnicak, L. *et al.* (2006). Schistosoma mansoni infection in eosinophil lineage-ablated mice. *Blood* **In Press**.

Takagi, M., Yamauchi, M., Toda, G., Takada, K., Hirakawa, T. *et al.* (1999). Serum ubiquitin levels in patients with alcoholic liver disease. *Alcohol Clin Exp Res* **23**,(4 Suppl) 76S-80S.

Takeda, K. and Akira, S. (2004). TLR signaling pathways. *Semin Immunol* **16**,(1) 3-9.

Tanahashi, N., Murakami, Y., Minami, Y., Shimbara, N., Hendil, K. B. ***et al.*** (2000). Hybrid proteasomes. Induction by interferon-gamma and contribution to ATP-dependent proteolysis. *J Biol Chem* **275**,(19) 14336-45.

Tanaka, K., Yoshimura, T. and Ichihara, A. (1989). Role of substrate in reversible activation of proteasomes (multi-protease complexes) by sodium dodecyl sulfate. *J Biochem (Tokyo)* **106**,(3) 495-500.

Tang, Y., Cho, P. Y., Kim, T. I. and Hong, S. J. (2006). Clonorchis sinensis: molecular cloning, enzymatic activity, and localization of yolk ferritin. *J Parasitol* **92**,(6) 1275-80.

Taylor, J. J., Mohrs, M. and Pearce, E. J. (2006a). Regulatory T cell responses develop in parallel to Th responses and control the magnitude and phenotype of the Th effector population. *J Immunol* **176**,(10) 5839-47.

Taylor, J. L., Hattle, J. M., Dreitz, S. A., Troudt, J. M., Izzo, L. S. ***et al.*** (2006b). Role for matrix metalloproteinase 9 in granuloma formation during pulmonary Mycobacterium tuberculosis infection. *Infect Immun* **74**,(11) 6135-44.

Thery, C., Boussac, M., Veron, P., Ricciardi-Castagnoli, P., Raposo, G. ***et al.*** (2001). Proteomic analysis of dendritic cell-derived exosomes: a secreted subcellular compartment distinct from apoptotic vesicles. *J Immunol* **166**,(12) 7309-18.

Thorburn, A. (2004). Death receptor-induced cell killing. *Cell Signal* **16**,(2) 139-44.

Thornberry, N. A., Rano, T. A., Peterson, E. P., Rasper, D. M., Timkey, T. ***et al.*** (1997). A combinatorial approach defines specificities of members of the caspase family and granzyme B. Functional relationships established for key mediators of apoptosis. *J Biol Chem* **272**,(29) 17907-11.

Thrower, J. S., Hoffman, L., Rechsteiner, M. and Pickart, C. M. (2000). Recognition of the polyubiquitin proteolytic signal. *Embo J* **19**,(1) 94-102.

Tielens, A. G., Horemans, A. M., Dunnewijk, R., van der Meer, P. and van den Bergh, S. G. (1992). The facultative anaerobic energy metabolism of Schistosoma mansoni sporocysts. *Mol Biochem Parasitol* **56**,(1) 49-57.

Tielens, A. G., van de Pas, F. A., van den Heuvel, J. M. and van den Bergh, S. G. (1991). The aerobic energy metabolism of Schistosoma mansoni miracidia. *Mol Biochem Parasitol* **46**,(1) 181-4.

Treves, A. J., Yagoda, D., Haimovitz, A., Ramu, N., Rachmilewitz, D. *et al.* (1980). The isolation and purification of human peripheral blood monocytes in cell suspension. *J Immunol Methods* **39**,(1-2) 71-80.

Trottein, F., Pavelka, N., Vizzardelli, C., Angeli, V., Zouain, C. S. *et al.* (2004). A type I IFN-dependent pathway induced by Schistosoma mansoni eggs in mouse myeloid dendritic cells generates an inflammatory signature. *J Immunol* **172**,(5) 3011-7.

Truden, J. L. and Boros, D. L. (1985). Collagenase, elastase, and nonspecific protease production by vigorous or immunomodulated liver granulomas and granuloma macrophages/eosinophils of S mansoni-infected mice. *Am J Pathol* **121**,(1) 166-75.

Tyas, L., Brophy, V. A., Pope, A., Rivett, A. J. and Tavare, J. M. (2000). Rapid caspase-3 activation during apoptosis revealed using fluorescence-resonance energy transfer. *EMBO Rep* **1**,(3) 266-70.

Ulmer, M. J. and van de Vusse, F. J. (1970). Morphology of Dendritobilharzia pulverulenta (Braun, 1901) Skrjabin, 1924 (Trematoda: Schistosomatidae) with notes on secondary hermaphroditism in males. *J Parasitol* **56**,(1) 67-74.

Van der Kleij, D., Latz, E., Brouwers, J. F., Kruize, Y. C., Schmitz, M. *et al.* (2002). A novel host-parasite lipid cross-talk. Schistosomal lyso-phosphatidylserine activates toll-like receptor 2 and affects immune polarization. *J Biol Chem* **277**,(50) 48122-9.

Van der Werf, M. J., de Vlas, S. J., Brooker, S., Looman, C. W., Nagelkerke, N. J. *et al.* (2003). Quantification of clinical morbidity associated with schistosome infection in sub-Saharan Africa. *Acta Trop* **86**,(2-3) 125-39.

van Die, I., van Vliet, S. J., Nyame, A. K., Cummings, R. D., Bank, C. M. *et al.* (2003). The dendritic cell-specific C-type lectin DC-SIGN is a receptor for Schistosoma mansoni egg antigens and recognizes the glycan antigen Lewis x. *Glycobiology* **13**,(6) 471-8.

van Liempt, E., van Vliet, S. J., Engering, A., Garcia Vallejo, J. J., Bank, C. M. *et al.* (2007). Schistosoma mansoni soluble egg antigens are internalized by human dendritic cells through multiple C-type lectins and suppress TLR-induced dendritic cell activation. *Mol Immunol* **44**,(10) 2605-15.

Van Oordt, B. E., Tielens, A. G. and Van den Bergh, S. G. (1989). Aerobic to anaerobic transition in the carbohydrate metabolism of Schistosoma mansoni cercariae during transformation in vitro. *Parasitology* **98 Pt 3**409-15.

Van Remoortere, A., Bank, C. M., Nyame, A. K., Cummings, R. D., Deelder, A. M. *et al.* (2003). Schistosoma mansoni-infected mice produce antibodies that cross-react with plant, insect, and mammalian glycoproteins and recognize the truncated biantennaryN-glycan Man3GlcNAc2-R. *Glycobiology* **13**,(3) 217-25.

Velentzas, A. D., Nezis, I. P., Stravopodis, D. J., Papassideri, I. S. and Margaritis, L. H. (2007). Stage-specific regulation of programmed cell death during oogenesis of the medfly Ceratitis capitata (Diptera, Tephritidae). *Int J Dev Biol* **51**,(1) 57-66.

Velupillai, P. and Harn, D. A. (1994). Oligosaccharide-specific induction of interleukin 10 production by B220+ cells from schistosome-infected mice: a mechanism for regulation of CD4+ T-cell subsets. *Proc Natl Acad Sci U S A* **91**,(1) 18-22.

Verjovski-Almeida, S., DeMarco, R., Martins, E. A., Guimaraes, P. E., Ojopi, E. P. *et al.* (2003). Transcriptome analysis of the acoelomate human parasite Schistosoma mansoni. *Nat Genet* **35**,(2) 148-57.

Verma, R., Chen, S., Feldman, R., Schieltz, D., Yates, J. *et al.* (2000). Proteasomal proteomics: identification of nucleotide-sensitive proteasome-interacting proteins by mass spectrometric analysis of affinity-purified proteasomes. *Mol Biol Cell* **11**,(10) 3425-39.

Vermeire, J. J., Taft, A. S., Hoffmann, K. F., Fitzpatrick, J. M. and Yoshino, T. P. (2006). Schistosoma mansoni: DNA microarray gene expression profiling during the miracidium-to-mother sporocyst transformation. *Mol Biochem Parasitol* **147**,(1) 39-47.

von Lampe, B., Barthel, B., Coupland, S. E., Riecken, E. O. and Rosewicz, S. (2000). Differential expression of matrix metalloproteinases and their tissue inhibitors in colon mucosa of patients with inflammatory bowel disease. *Gut* **47**,(1) 63-73.

von Lichtenberg, F. (1964). Studies on granuloma formation III. Antigen sequestration and destruction in the schistosome pseudotubercle. *Am J Pathology* **4575 - 93.**

Waite, J. H. and Rice-Ficht, A. C. (1987). Presclerotized eggshell protein from the liver fluke Fasciola hepatica. *Biochemistry* **26**,(24) 7819-25.

Waite, J. H. and Rice-Ficht, A. C. (1989). A histidine-rich protein from the vitellaria of the liver fluke Fasciola hepatica. *Biochemistry* **28**,(14) 6104-10.

Wang, Q. and Chang, A. (2003). Substrate recognition in ER-associated degradation mediated by Eps1, a member of the protein disulfide isomerase family. *Embo J* **22**,(15) 3792-802.

Warren, K. S. and Domingo, E. O. (1970). Granuloma formation around *Schistosoma mansoni, S. haematobium*, and *S. japonicum* eggs. Size and rate of development, cellular composition, cross-sensitivity, and rate of egg destruction. *Am J Trop Med Hyg* **19**,(2) 292-304.

Wasinger, V. C., Cordwell, S. J., Cerpa-Poljak, A., Yan, J. X., Gooley, A. A. *et al.* (1995). Progress with gene-product mapping of the Mollicutes: Mycoplasma genitalium. *Electrophoresis* **16**,(7) 1090-4.

Watts, T. H. (2005). TNF/TNFR family members in costimulation of T cell responses. *Annu Rev Immunol* **23**23-68.

Wegrzyn, J., Lee, J., Neveu, J. M., Lane, W. S. and Hook, V. (2007). Proteomics of neuroendocrine secretory vesicles reveal distinct functional systems for biosynthesis and exocytosis of peptide hormones and neurotransmitters. *J Proteome Res* **6**,(5) 1652-65.

Weinreb, O., Dovrat, A., Dunia, I., Benedetti, E. L. and Bloemendal, H. (2001). UV-A-related alterations of young and adult lens water-insoluble alpha-crystallin, plasma membranous and cytoskeletal proteins. *Eur J Biochem* **268**,(3) 536-43.

Weinstock, J. V. and Boros, D. L. (1983). Organ-dependent differences in composition and function observed in hepatic and intestinal granulomas isolated from mice with Schistosomiasis mansoni. *J Immunol* **130**,(1) 418-22.

Weiss, J. B., Magnani, J. L. and Strand, M. (1986). Identification of Schistosoma mansoni glycolipids that share immunogenic carbohydrate epitopes with glycoproteins. *J Immunol* **136**,(11) 4275-82.

Wells, K. E. and Cordingley, J. S. (1991). Schistosoma mansoni: eggshell formation is regulated by pH and calcium. *Exp Parasitol* **73**,(3) 295-310.

Whitfield, P. J. (1993). Parasitic Helminths. In *Modern Parasitology*, 2nd Edition. (eds F. E. G. Cox), pp. 24-52. Oxford: Blackwell Science Ltd.

WHO. (2002). Prevention and Control of Schistosomiasis and Soil-Transmitted Helminths, pp. 57. Geneva: World Health Organisation.

Wieme, R. J. (1959). An improved technique for agar-gel electrophoresis on agar gel microscopic slides. *Clinica Chemica Acta* **4**317-321.

Wiertz, E. J., Tortorella, D., Bogyo, M., Yu, J., Mothes, W. ***et al.*** (1996). Sec61-mediated transfer of a membrane protein from the endoplasmic reticulum to the proteasome for destruction. *Nature* **384**,(6608) 432-8.

Wilkinson, C. R., Seeger, M., Hartmann-Petersen, R., Stone, M., Wallace, M. ***et al.*** (2001). Proteins containing the UBA domain are able to bind to multi-ubiquitin chains. *Nat Cell Biol* **3**,(10) 939-43.

Williams, D. L., Asahi, H., Botkin, D. J. and Stadecker, M. J. (2001). Schistosome infection stimulates host CD4(+) T helper cell and B-cell responses against a novel egg antigen, thioredoxin peroxidase. *Infect Immun* **69**,(2) 1134-41.

Williams, D. L., Asahi, H., Oke, T. T., da Rosa, J. L. and Stadecker, M. J. (2005). Murine immune responses to a novel schistosome egg antigen, SmEP25. *Int J Parasitol* **35**,(8) 875-82.

Williams, D. L., Sayed, A. A., Ray, D. and McArthur, A. G. (2006). Schistosoma mansoni albumin, a major defense against oxidative damage, was acquired by lateral gene transfer from a mammalian host. *Mol Biochem Parasitol* **150**,(2) 359-63.

Wilson, R. A. (1987). Cercariae to Liver Worms: Development and Migration in the Mammalian Host. In *The Biology of Schistosomes: From Genes to Latrienes*. (eds D. Rollinson and A. J. G. Simpson), pp. 115-147. London: Academic Press.

Wilson, R. A., Ashton, P. D., Braschi, S., Dillon, G. P., Berriman, M. *et al.* (2007). 'Oming in on schistosomes: prospects and limitations for post-genomics. *Trends Parasitol* **23**,(1) 14-20.

Winnen, R., Schussler, P., Sommer, G., Bottke, W., Grevelding, C. G. *et al.* (1995). Ferretin 1 is a female-preferentially and developmentally expressed component of protein yolk in *Schistosoma mansoni*. *Biological Chemistry Hoppe Seyler* **376**S169.

Woo, K., Jensen-Smith, H. C., Luduena, R. F. and Hallworth, R. (2002). Differential synthesis of beta-tubulin isotypes in gerbil nasal epithelia. *Cell Tissue Res* **309**,(2) 331-5.

Wuhrer, M., Balog, C. I., Catalina, M. I., Jones, F. M., Schramm, G. *et al.* (2006). IPSE/alpha-1, a major secretory glycoprotein antigen from schistosome eggs, expresses the Lewis X motif on core-difucosylated N-glycans. *Febs J* **273**,(10) 2276-92.

Xu, Y. Z. and Dresden, M. H. (1986). Leucine aminopeptidase and hatching of Schistosoma mansoni eggs. *J Parasitol* **72**,(4) 507-11.

Xu, Y. Z. and Dresden, M. H. (1989). Schistosoma mansoni: egg morphology and hatchability. *J Parasitol* **75**,(3) 481-3.

Yamaguchi, M. (2005). Role of regucalcin in maintaining cell homeostasis and function (review). *Int J Mol Med* **15**,(3) 371-89.

Yamaguchi, M., Isogai, M. and Shimada, N. (1997). Potential sensitivity of hepatic specific protein regucalcin as a marker of chronic liver injury. *Mol Cell Biochem* **167**,(1-2) 187-90.

Yang, M. Y., Dong, H. F. and Jiang, M. S. (2003). Ultrastructural observation of spermatozoa and fertilization in Schistosoma japonicum. *Acta Trop* **85**,(1) 63-70.

Ye, Y., Shibata, Y., Yun, C., Ron, D. and Rapoport, T. A. (2004). A membrane protein complex mediates retro-translocation from the ER lumen into the cytosol. *Nature* **429**,(6994) 841-7.

Yuckenberg, P. D., Poupin, F. and Mansour, T. E. (1987). Schistosoma mansoni: protein composition and synthesis during early development; evidence for early synthesis of heat shock proteins. *Exp Parasitol* **63**,(3) 301-11.

Zhang, F., Su, K., Yang, X., Bowe, D. B., Paterson, A. J. *et al.* (2003). O-GlcNAc modification is an endogenous inhibitor of the proteasome. *Cell* **115**,(6) 715-25.

Zwickl, P., Grziwa, A., Puhler, G., Dahlmann, B., Lottspeich, F. *et al.* (1992). Primary structure of the Thermoplasma proteasome and its implications for the structure, function, and evolution of the multicatalytic proteinase. *Biochemistry* **31**,(4) 964-72.